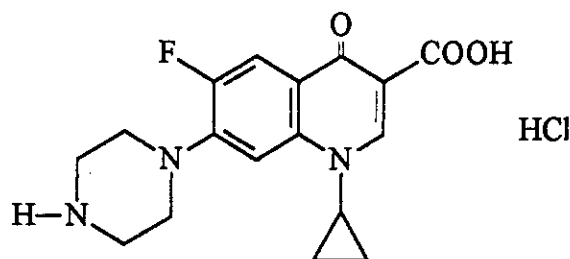


CHAPTER III

RESULTS AND DISCUSSION

3.1. Electrochemical and analytical behaviours of ciprofloxacin hydrochloride in B. R. solutions of different pH-values

Ciprofloxacin hydrochloride, is 1-cyclopropyl-6-fluoro-1, 4 dihydro-4-oxo-7-piperazinyl-3 quinolone carboxylic acid. It is the reference substance for the modern fluoroquinolones. It is considered to be the most active broad-spectrum antibiotic against gram-positive and gram-negative pathogens caused by microorganisms that are resistant or multi-resistant to other antimicrobials⁽¹⁰⁶⁾.



Ciprofloxacin HCl

This part includes studying of the electrochemical behaviour of ciprofloxacin hydrochloride using both DC-polarography and cyclic voltammetric techniques. Also the analytical determinations of ciprofloxacin hydrochloride in pure and dosage forms were performed using both square wave stripping voltammetry as well as spectrophotometric techniques.

3.1.1. Electrochemical behaviour of ciprofloxacin hydrochloride in B.R. solutions of different pH-values:

3.1.1.1. DC-Polarography:

Current-Potential Curves:

The polarographic reduction of 4×10^{-4} M of ciprofloxacin hydrochloride was investigated in B. R. buffer solutions of pH values from

2.3 to 11.2. The recorded polarograms showed only a single reduction wave in the entire pH range. This wave corresponding to the reduction of the carbonyl group, Fig. 1A. The limiting current i_l of the polarographic waves was pH independent and slightly decrease on increasing the pH of the electrolysis solution. This may be due to the increase in viscosity of the medium, Fig. 1B.

The half wave potential of the polarographic waves was pH dependent. It displayed a cathodic shift on increasing of pH values of the electrolysis solution. This behaviour indicated that H^+ ions were participating in the electrode process and the proton uptake precedes the electron transfer process⁽¹⁰⁷⁾.

Effect of pressure at mercury height:

The effect of mercury height was examined according to the relationship related the limiting current i_l and the net pressure of mercury after correction from the back pressure h_{corr} , which was given as⁽¹⁰⁸⁾:

$$i_l = k h_{corr}^x \quad \text{-----(1)}$$

$$\text{or} \quad \log i_l = \log k + x \log h_{corr} \quad \text{-----(2)}$$

Where: k is constant.

The value of x revealed the nature of the electrode reaction. For diffusion-controlled current x is equal to 0.5, and for adsorption-controlled current x is equal to 1.0, while for kinetic-controlled current x is equal to 0.05. However, x may have intermediate values between the above mentioned values if the electrode process is governed by combination of two kinds of processes.

On plotting $\log i_l$ as a function of $\log h$ at different pH values, straight lines were obtained with slope values x ranging between 0.52 and 0.64, Fig.

1C. These values indicated that the reduction process is mainly controlled by diffusion with some adsorption contribution, Table 1.

Analysis of the Polarographic Waves:

Analysis of the polarographic waves is important in determining the thermodynamic reversibility of the polarographic waves, and so in suggestion of the electrode reaction process.

The fundamental equation for the reversible polarographic wave is written in the form⁽¹⁰²⁾:

$$E_{d,e} = E_{1/2} - 0.0591 / n \log [i / (i_d - i)] \quad \text{-----}(3)$$

Where: $E_{d,e}$ is the potential of the dropping mercury electrode.

i_d : the diffusion current in μA .

$E_{1/2}$: the half wave potential in volt.

n : the number of the electrons involved in the reduction process.

In the present study, plotting of $\log [i / (i_d - i)]$ against $E_{d,e}$ for ciprofloxacin hydrochloride at different pH values gave straight lines, Fig. 1D. The reciprocal slope values S_1 of the straight lines obtained were in conflict with that predicted from the previous equation pertaining to reversible wave. Thus, the fundamental equation concerning the irreversible waves should be considered.

The equation for irreversible polarographic wave is:

$$E_{d,e} = E_{1/2} - 0.0591 / \alpha n_a \log [i / (i_d - i)] \quad \text{-----}(4)$$

Where, α is the transfer coefficient.

n_a : the number of electrons involved in the rate determining step.

and other terms have their usual significances.

From the reciprocal slopes S_1 of logarithmic analysis plots, values of the transfer coefficient α were evaluated for the probable values of n_a by considering the number of electrons involved in the rate-determining step n_a to be one or two, Table 1. Inspection of the listed data revealed that the most probable values of α are obtained at n_a equals to two, which indicated that the rate-determining step of the reduction process should involve two electrons.

Half-Wave Potential-pH Curve:

The half-wave potential $E_{1/2}$ of the polarographic wave of ciprofloxacin hydrochloride was shifted to more negative potentials on increasing the pH of the electrolysis solution, denoting that H^+ ions were consumed in the reduction process.

On plotting of $E_{1/2}$ against pH, a straight line with slope value S_2 was obtained, Fig. 1E. The number of hydrogen ions Z^+_H involved in the rate determining step was determined by using the following relationship⁽¹⁰⁹⁾:

$$\begin{aligned} Z^+_H &= [\delta E_{1/2} / \delta pH] / [0.0591 / \alpha n_a] \\ &= S_2 / S_1 \end{aligned} \quad \text{-----(5)}$$

The number of hydrogen ions Z^+_H was found to equal unity within the entire pH range. Furthermore, the values of α were determined considering the probable values of the ratio (Z^+_H / n_a) as in the relationship:

$$\begin{aligned} \delta E_{1/2} / \delta pH &= (0.0591 / \alpha) \cdot (Z^+_H / n_a) \\ \text{i.e.} \quad \alpha &= (0.0591 / S_2) \cdot (Z^+_H / n_a) \end{aligned} \quad \text{-----(6)}$$

The ratio of Z^+_H / n_a may have the values 2.0, 1.0 or 0.5 depending if one or two electrons and one or two protons are involved in the rate determining step. From the data obtained in this work, the most probable α values correspond to a ratio of Z^+_H / n_a equals 0.5 which indicates that the rate determining step involves one proton and two electrons.

Table 1:

DC-Polarographic data and parameters obtained from the electrochemical behaviour of 4×10^{-4} M ciprofloxacin hydrochloride that recorded in pure aqueous buffer solutions of various pH values at 25°C.

pH	i_d μA	$-E_{1/2}$ V	$\log i_1$ $/\log h$	S_1 mV	αn_a	α		S_2 mV	Z^+_H
						$n_a=1$	$n_a=2$		
2.3	1.01	1.31		58.5	1.009	1.009	0.5.05	39	0.667
3.2	1.00	1.35		63.7	0.928	0.928	0.464	39	0.612
4.4	0.98	1.37	0.52	58.3	1.013	1.013	0.506	39	0.669
5.3	0.96	1.41		64.9	0.910	0.910	0.4551	39	0.601
6.0	0.96	1.44		65.4	0.904	0.904	0.452	39	0.596
7.0	0.95	1.50	0.64	61.6	0.959	0.959	0.479	39	0.633
8.0	0.94	1.53		53.7	1.099	1.099	0.549	39	0.726
9.0	0.93	1.57	0.64	59.5	0.993	0.993	0.496	39	0.655
10.2	0.93	1.60		50.4	1.173	1.173	0.586	39	0.774
11.2	0.93	1.64		54.5	1.083	1.083	0.542	39	0.716

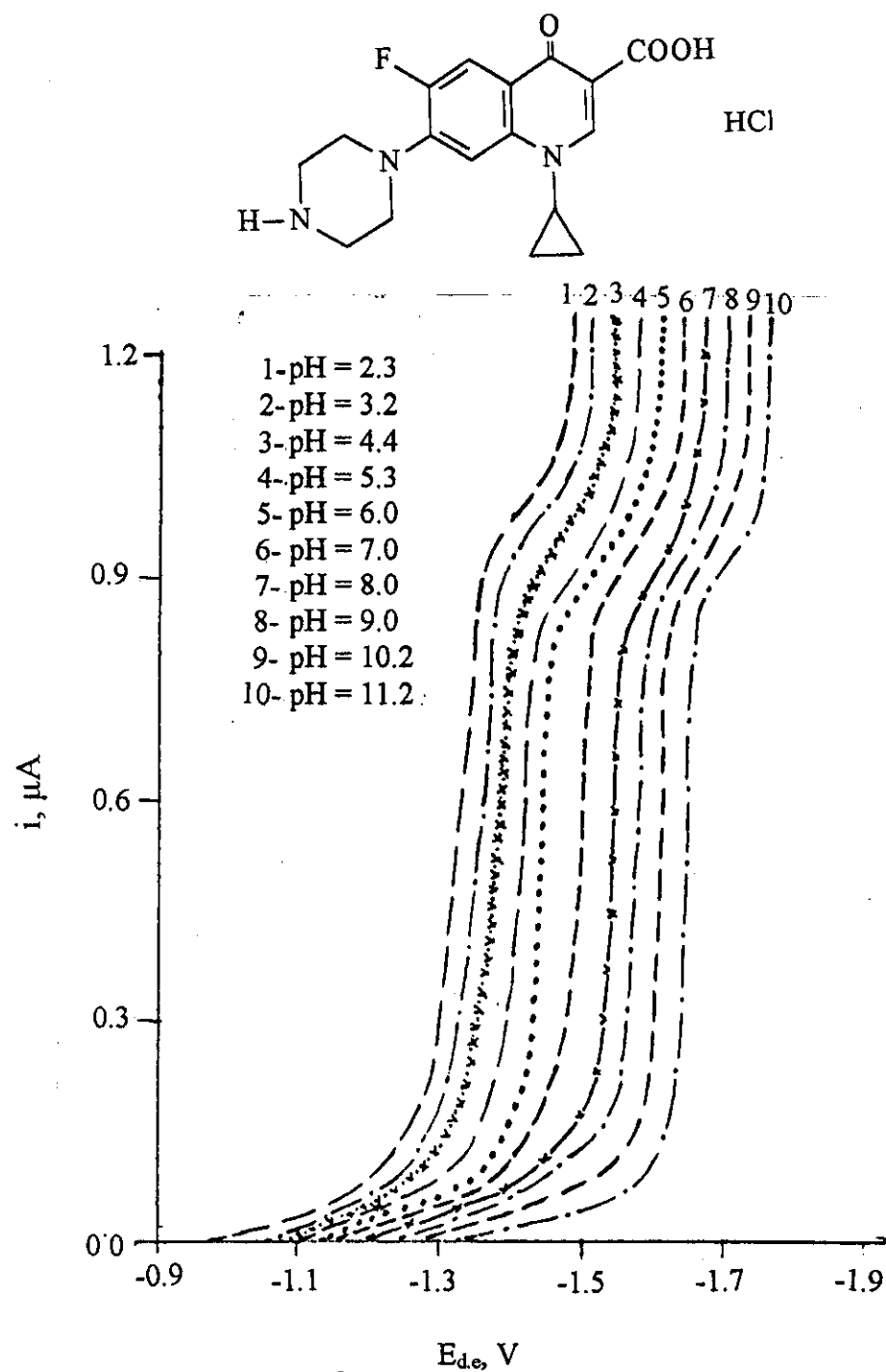


Fig. 1A: DC-polarograms of ciprofloxacin hydrochloride in B.R. buffer solutions of different pH values.

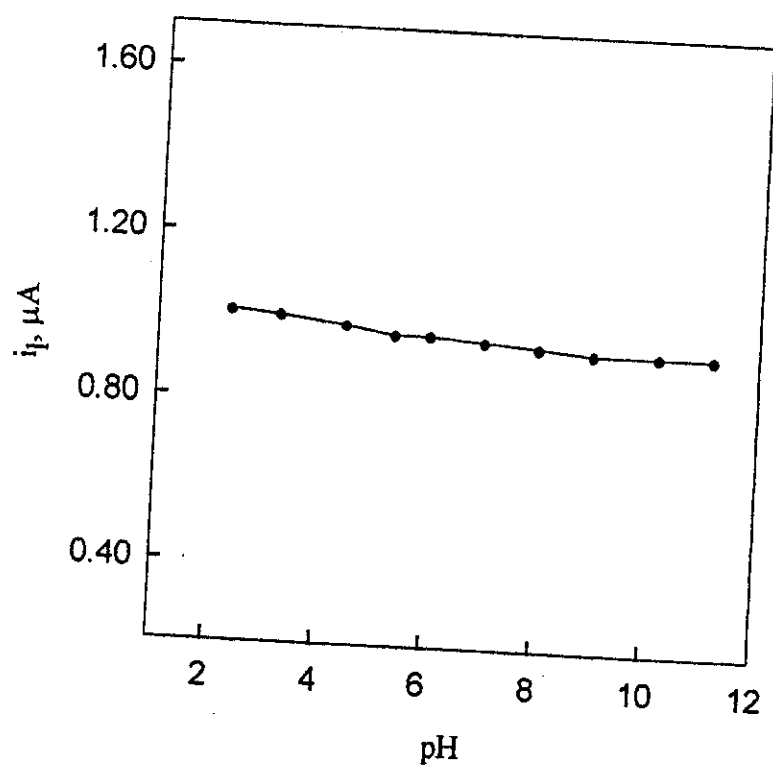


Fig. 1B: i_p -pH plot of ciprofloxacin hydrochloride

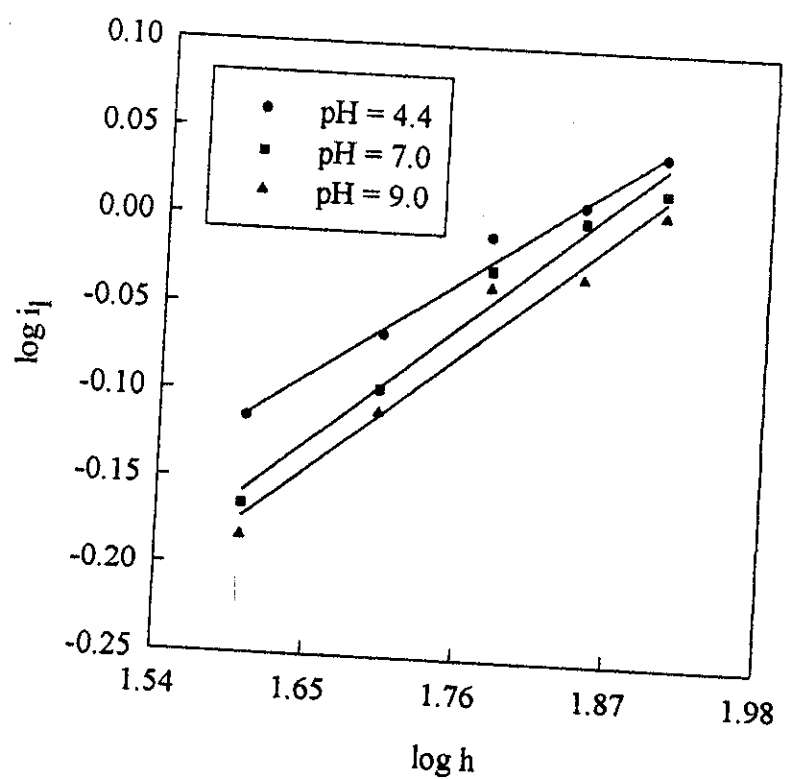


Fig. 1C: $\log i_p$ - $\log h$ plots of ciprofloxacin hydrochloride at different pH values

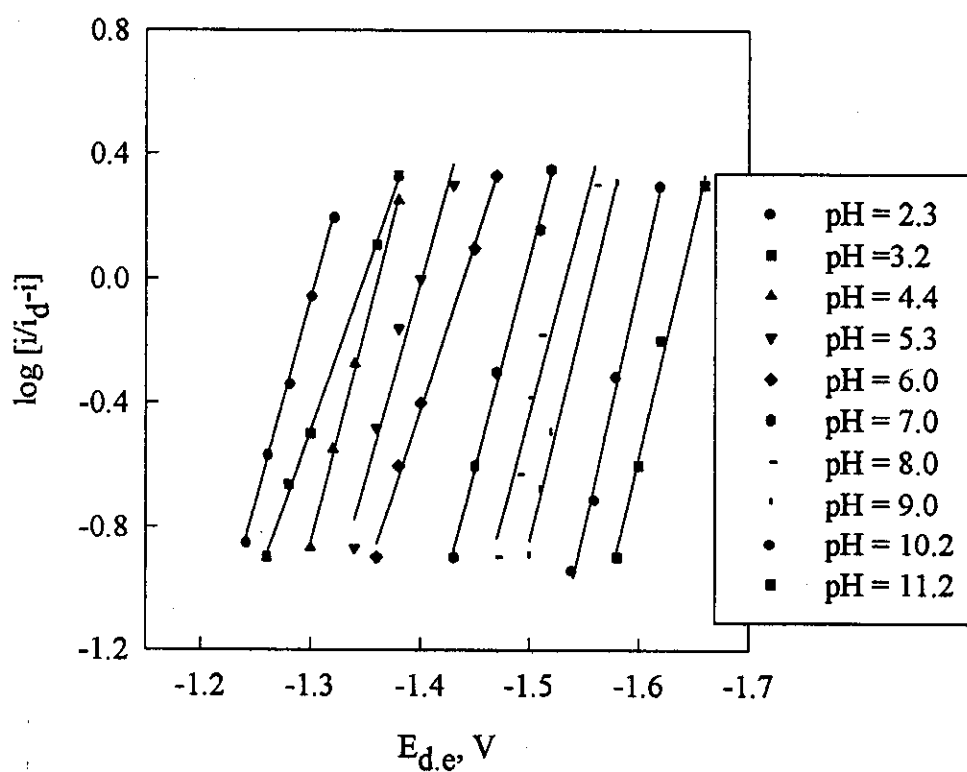


Fig. 1D: $\log [i/i_d-i] - E_{d,e}$ plots of ciprofloxacin hydrochloride at different pH values

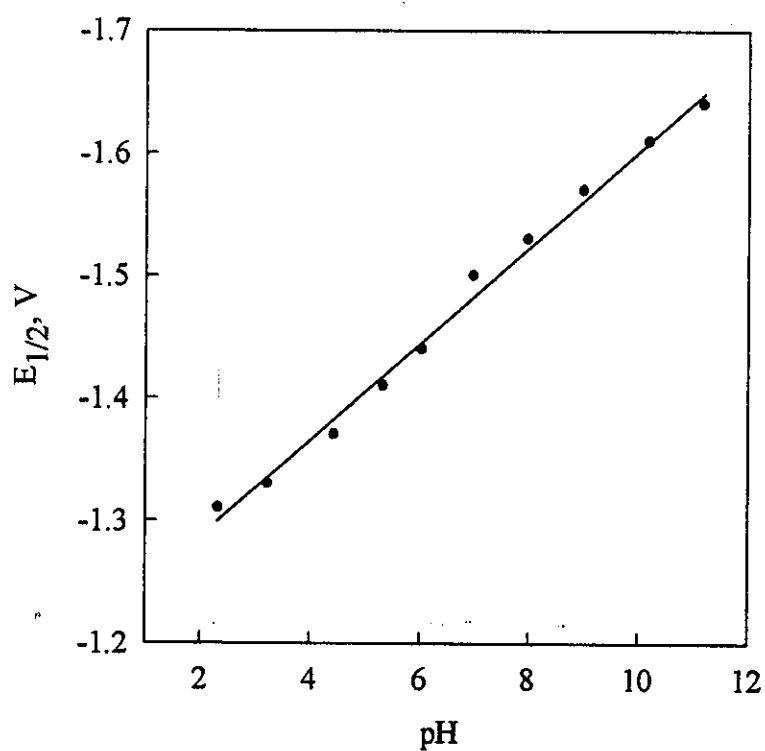


Fig. 1E: $E_{1/2}$ -pH plot of ciprofloxacin hydrochlorid.

3.1.1.2. Determination of ciprofloxacin hydrochloride by using DC-polarography

Determination of ciprofloxacin hydrochloride was performed in different media, sodium perchlorate, acetate buffer, B.R. buffer and phosphate buffer. The most obvious wave was obtained in B.R. buffer of pH 2.3. A stock solution of 1×10^{-3} M ciprofloxacin hydrochloride was prepared and different concentrations were obtained by accurate dilution. The polarograms of the final samples were recorded. The variation of wave current with concentration was represented in Fig. 2 (A-B). The concentration of ciprofloxacin hydrochloride was determined using Ilkovic equation⁽¹⁰⁸⁾:

$$i_p = 607 n D^{1/2} m^{2/3} t^{1/6} C \quad \text{-----}(7)$$

Where, i_d : the diffusion current in μA .

n : number of electrons.

D : the diffusion coefficient in cm^2/s

m : the rate of mercury flow in mg/s .

t : the drop time in seconds.

C : the concentration in $mole/cm^3$.

The precision was determined from three repeated measurements of different concentrations, Table 2. The detection limit was found to be 1×10^{-5} M (3.86 $\mu g/ml$).

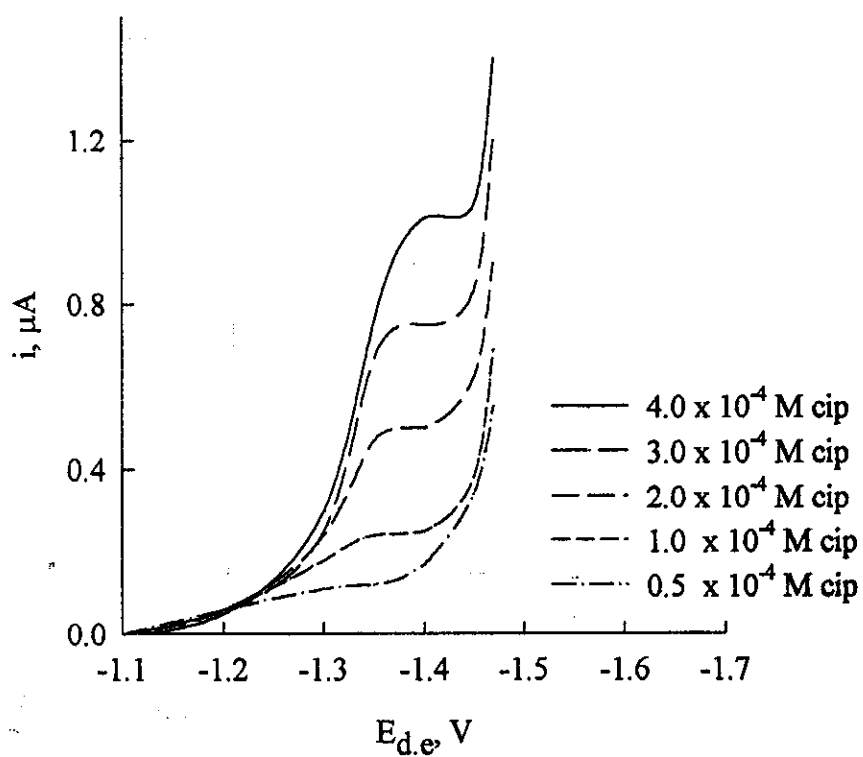


Fig. 2A: DC polarograms at different concentrations of ciprofloxacin hydrochloride

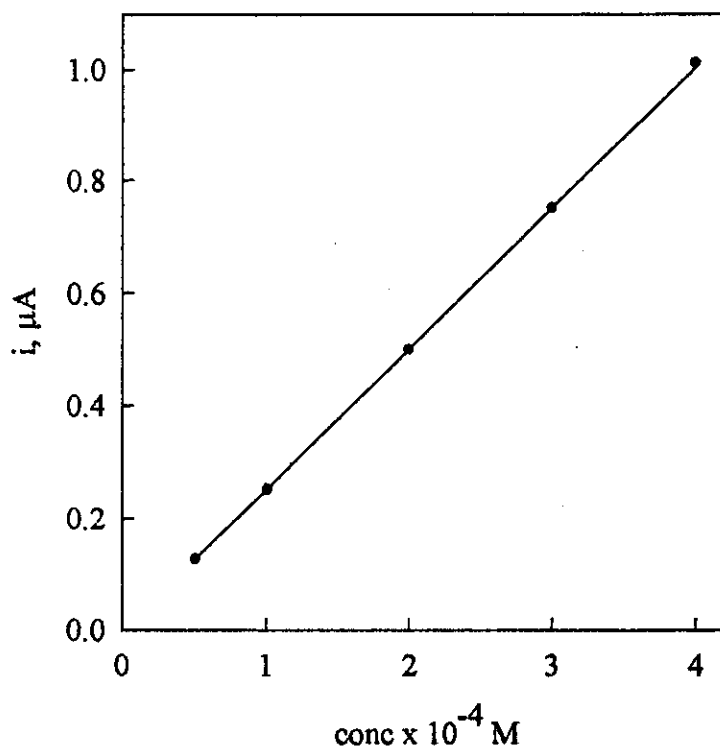


Fig. 2B: Calibration graph of ciprofloxacin hydrochloride

Table 2:

Assay of ciprofloxacin hydrochloride in B.R. buffer solution of pH 2.3 using DC polarography.

Compound Concentration M	Current (i) μ A	Conc. Found	Recovery %	S.D
0.5×10^{-4}	0.124	4.91×10^{-5}	98.20	0.462
	0.124	4.91×10^{-5}	98.20	
	0.125	4.95×10^{-5}	99.00	
1.0×10^{-4}	0.249	9.85×10^{-5}	98.50	0.173
	0.249	9.85×10^{-5}	98.50	
	0.250	9.88×10^{-5}	98.80	
2.0×10^{-4}	0.496	1.96×10^{-4}	98.19	0.395
	0.498	1.97×10^{-4}	98.59	
	0.499	1.98×10^{-4}	98.98	
3.0×10^{-4}	0.750	2.97×10^{-4}	99.00	0.774
	0.750	2.97×10^{-4}	99.00	
	0.740	2.93×10^{-4}	97.66	
4.0×10^{-4}	1.000	3.96×10^{-4}	98.98	0.990
	1.010	3.99×10^{-4}	99.97	
	0.990	3.92×10^{-4}	97.99	
Recovery = 98.6 ± 0.323				

3.1.1.3. Effect of Metal Complexes:

The effect of ciprofloxacin hydrochloride on the polarographic behaviour of Cd(II), Zn(II) ions in 0.1 M NaClO₄:

The polarographic behaviour of 2×10^{-4} M Cd(II) and Zn(II) in 0.1 M sodium perchlorate were recorded as in Fig. 3 (A-B). Logarithmic analysis of metal ion waves and calculation of the α_n values revealed the quasireversible nature. Addition of ligand within the range of concentration from 5×10^{-5} M to 8×10^{-4} M increases the irreversibility of the electrode processes, which is confirmed from the decrease of α_n values, Tables (3-4). Generally, as the concentration of ligand increases, the diffusion current of the metal decreases which is attributed to the increase in the bulk of the complexed ions. The polarographic waves showed a cathodic shift indicating complex formation.

The over all stability constants and stoichiometry of the present complexes were calculated using the following relationship⁽¹¹⁰⁾:

$$(E_{1/2})_C = (E_{1/2})_S - (0.0591 / \alpha n) \log B_{MX_j} - j (0.0591 / n) \log C_X \quad \text{--- (8)}$$

Where, $(E_{1/2})_C$: the half wave potential of the complex.

$(E_{1/2})_S$: the half wave potential of the free metal.

J: the coordination number.

C_X : the molar concentration of the ligend.

The plot of $\Delta E_{1/2} = [E_{1/2}(S) - E_{1/2}(C)]$ versus $\log C_X$ gives a linear correlation with slope equal to $j (0.0591 / \alpha n)$ from which j was found to be two with Cd(II) and also with Zn(II) Fig. 3 (C-F).

Table 3:

DC-Polarographic data obtained for Cd(II)-ciprofloxacin hydrochloride complex in 0.1 M NaClO₄.

Ligend concentration	i_d	$\Delta E_{1/2}$	αn_a	Stoichiometry Drug : Metal
Zero	0.90	0.00	0.800	2 : 1
5×10^{-5}	0.88	0.02	0.761	
1×10^{-4}	0.83	0.03	0.650	
2×10^{-4}	0.79	0.06	0.645	
4×10^{-4}	0.69	0.08	0.627	
8×10^{-4}	0.63	0.10	0.615	

Table 4:

DC-Polarographic data obtained for Zn(II)-ciprofloxacin hydrochloride complex in 0.1 M NaClO₄.

Ligend concentration	i_d	$\Delta E_{1/2}$	αn_a	Stoichiometry Drug : Metal
Zero	1.06	0.016	0.760	2 : 1
5×10^{-5}	0.95	0.034	0.708	
2×10^{-4}	0.88	0.067	0.667	
3×10^{-4}	0.83	0.085	0.661	
4×10^{-4}	0.76	0.100	0.655	
8×10^{-4}	0.72	0.105	0.650	

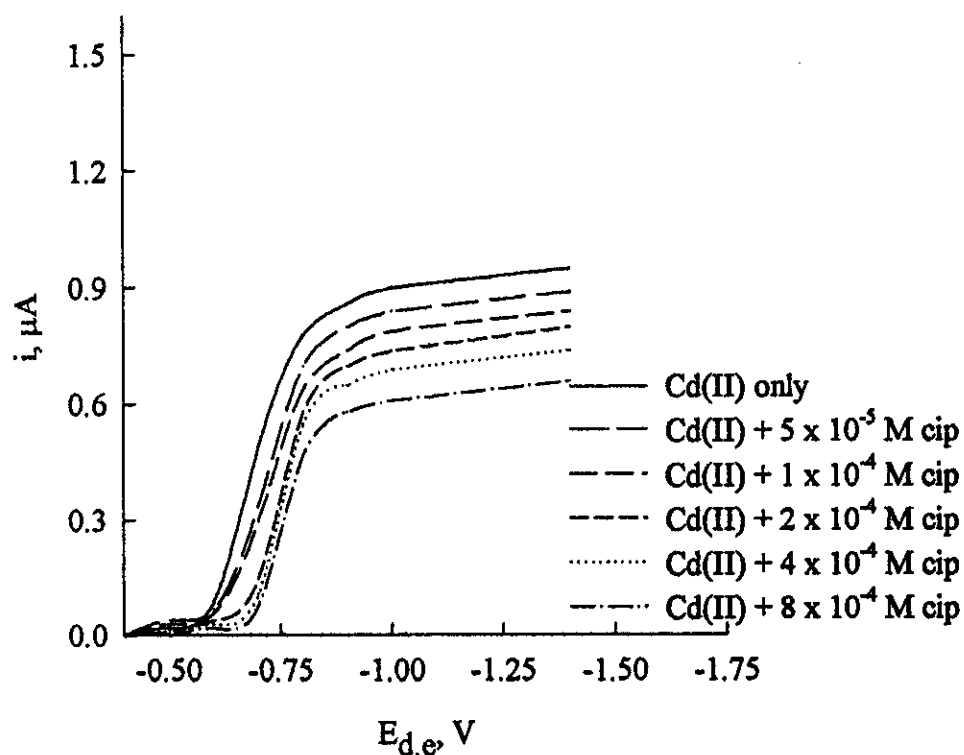


Fig. 3A: Cd(II)- ciprofloxacin hydrochloride complex in 0.1 M Sodium perchlorate.

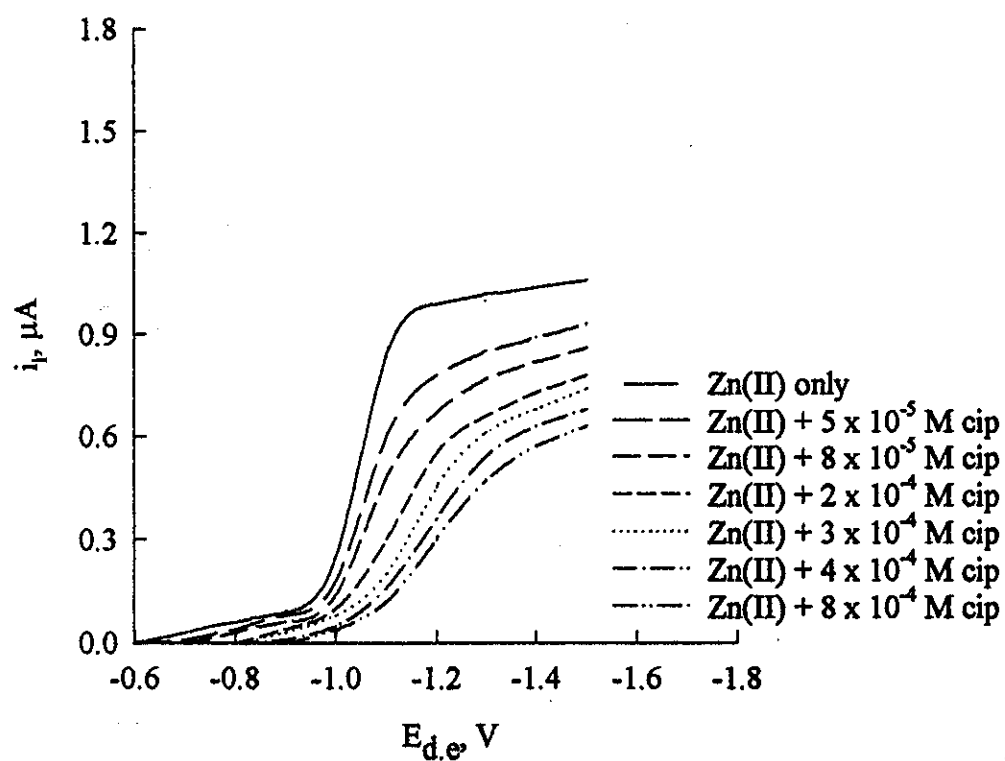


Fig. 3B: Zn(II)- ciprofloxacin hydrochloride complex in 0.1 M Sodium perchlorate.

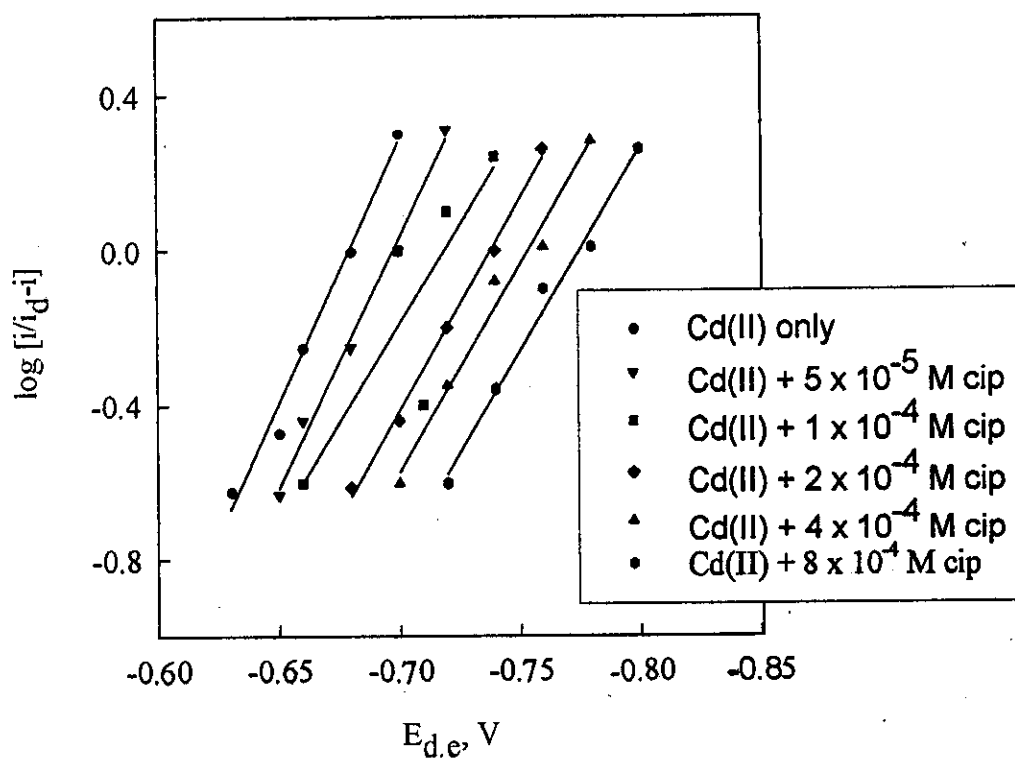


Fig. 3C: Cd(II) - ciprofloxacin hydrochloride complex

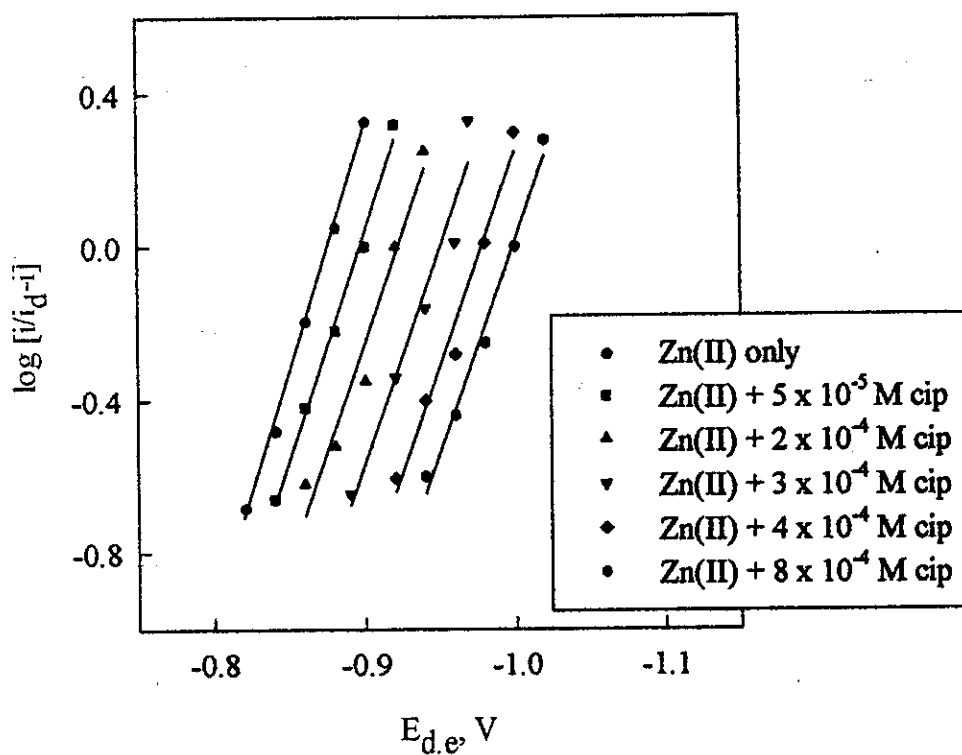


Fig. 3D: Zn(II) - ciprofloxacin hydrochloride complex.

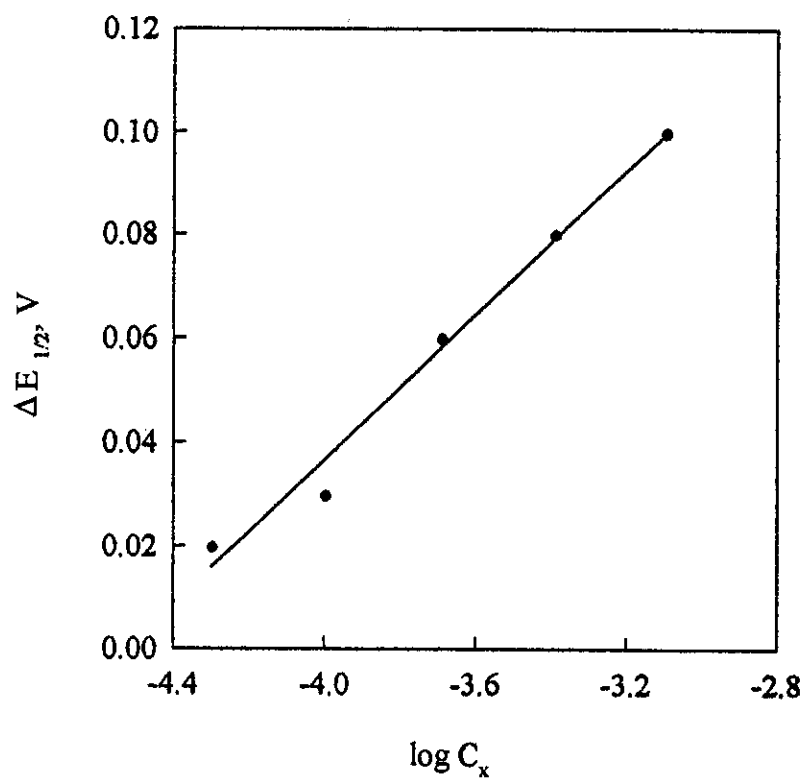


Fig. 3E: $\Delta E_{1/2}$ - $\log C_x$ plot of Cd(II)-ciprofloxacin hydrochloride

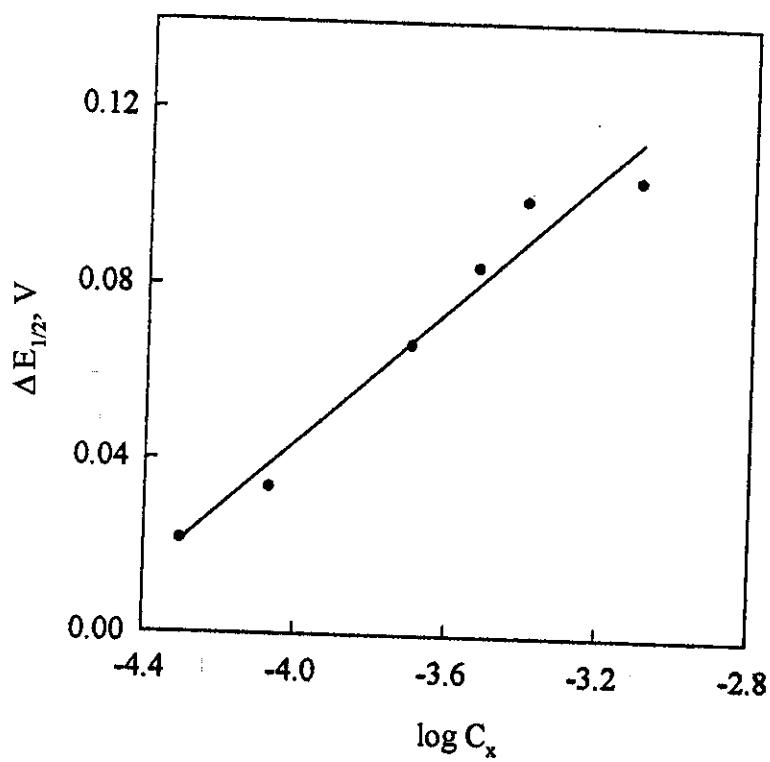


Fig. 3F: $\Delta E_{1/2}$ - $\log C_x$ plot of Zn(II)-ciprofloxacin hydrochloride

3.1.1.4. Cyclic Voltammetry:

Cyclic voltammetric behaviour of 1×10^{-4} M ciprofloxacin hydrochloride was studied at the glassy carbon electrode in B. R. buffer solutions of three different pH values 3.6, 7.0, 10.0. The voltammograms were recorded at different scan rates ranging from 20 to 500 mV/sec, Fig. 4A. The recorded voltammograms showed only one cathodic peak in all solutions and at different scan rates. The cathodic peak potential (E_p) showed a cathodic shift on increasing the scan rate (ν) which indicated the irreversible nature⁽¹¹¹⁾ of the electrode reaction. Furthermore, the absence of any peak in the reverse scan (anodic direction) denoting the irreversibility of the reduction process.

For irreversible process the peak current can be calculated from the following equation⁽¹¹²⁾:

$$i_p = 3.01 \times 10^5 n^{3/2} A (\alpha n)^{1/2} D^{1/2} C \nu^{1/2} \text{ -----(9)}$$

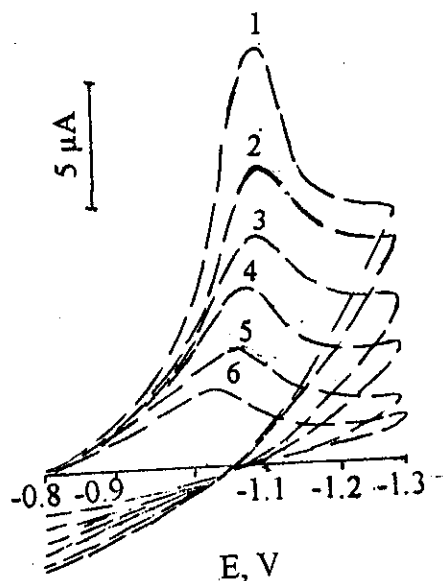
On plotting the peak current i_p against $\nu^{1/2}$ at different pH values linear correlations slightly deviated from the origin were obtained, Fig. 4B. This behaviour confirmed that the electrode process of ciprofloxacin hydrochloride is mainly controlled by diffusion with some adsorption contribution as indicated previously from DC polarographic technique.

On applying the relationship⁽¹¹³⁾ that correlates the peak potentials E_p with the logarithmic scan rate, values of αn_a parameter for the electrode reaction of the investigated compound were evaluated:

$$E_p = -1.14(RT/\alpha n_a F) + (RT/\alpha n_a F) \ln (K_{f,h}/D^{1/2}) - (RT/2\alpha n_a F) \ln (\alpha n_a \nu) \text{ --(10)}$$

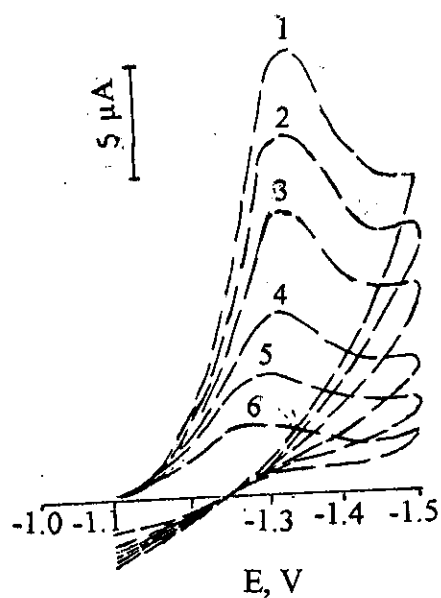
On plotting E_p versus $\ln \nu$ at the given pH, linear correlations of slope values proportional to αn_a were obtained, Fig. 4C. From these slopes, the transfer co-efficient α values were calculated for the probable values of n_a , Table 5. The values of αn_a showed that the rate determining step of the electrode process may involve two electrons.

1- pH = 3.6



1- scan rate 500 mV/s
2- scan rate 300 mV/s
3- scan rate 200 mV/s
4- scan rate 100 mV/s
5- scan rate 50 mV/s
6- scan rate 20 mV/s

2- pH = 7.0



3- pH = 10.0

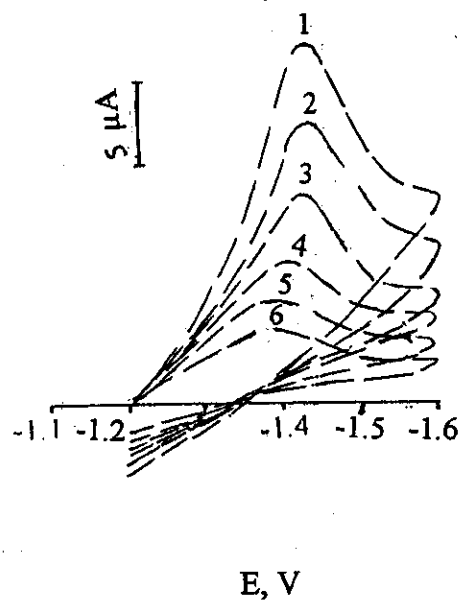


Fig. 4A: Cyclic voltammetric behaviour of ciprofloxacin hydrochloride in B.R. buffer solutions of different pH values.

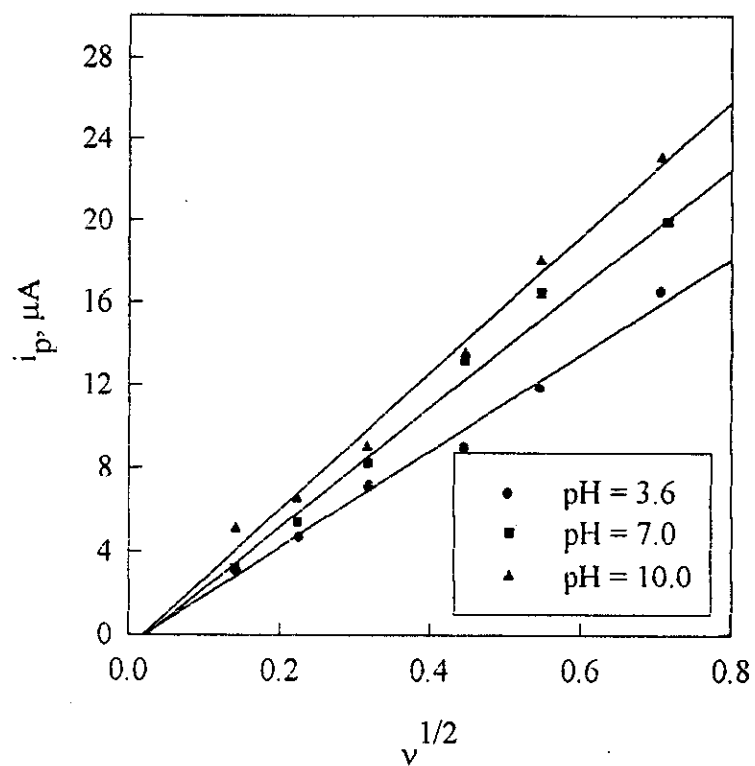


Fig. 4B: i_p - $v^{1/2}$ plots of ciprofloxacin hydrochloride at different pH values

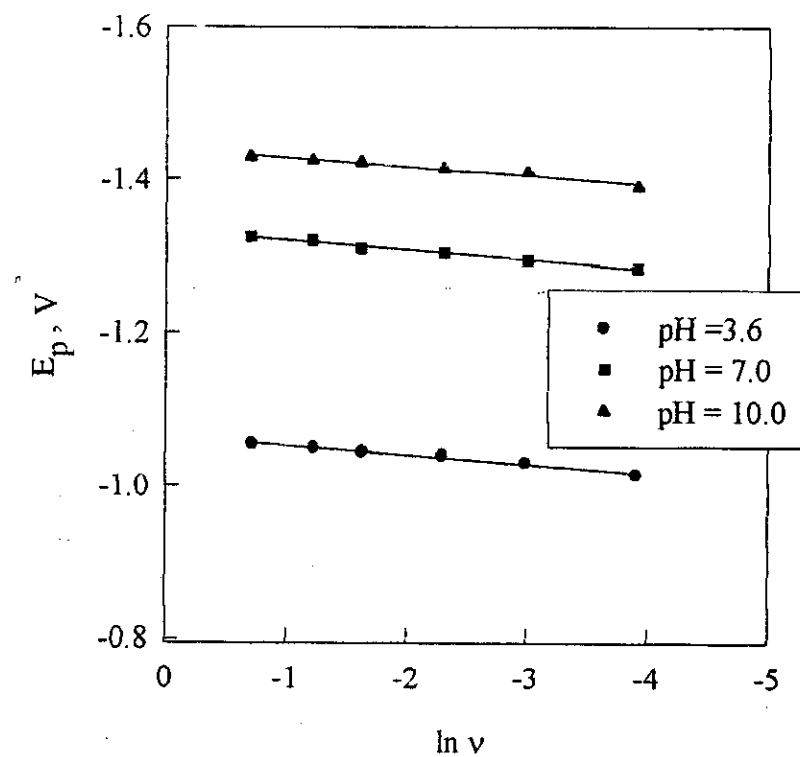


Fig. 4C: $E_{1/2}$ - $\ln v$ plots of ciprofloxacin hydrochloride at different pH values

Table 5:

Cyclic voltammetric data for 1×10^{-4} M ciprofloxacin hydrochloride in aqueous buffer solution B.R. of different pH values at 25°C.

pH	Scan rate mV/s	i_p μA	$-E_p$ V	$\delta E_p / \delta \ln v$	α	
					na=1.0	na=2.0
3.6	500	16.56	1.055	0.0121	1.062	0.531
	300	11.88	1.050			
	200	9.06	1.045			
	100	7.19	1.040			
	50	4.69	1.030			
	20	3.13	1.015			
7.0	500	19.00	1.325	0.0125	1.028	0.514
	300	16.43	1.320			
	200	13.21	1.310			
	100	8.21	1.304			
	50	5.36	1.295			
	20	3.21	1.285			
10.0	500	23.00	1.430	0.0117	1.098	0.549
	300	18.00	1.425			
	200	13.50	1.423			
	100	9.00	1.415			
	50	6.50	1.410			
	20	5.00	1.390			

3.1.1.5. The Electrode Reaction Mechanism:

Investigation of the polarographic behaviour of ciprofloxacin hydrochloride in pure aqueous buffer solutions of various pH values in the range from 2.3 to 11.2 displayed single reduction wave. Logarithmic analysis of the polarographic waves revealed the irreversibility of the reduction process. The limiting current of the polarographic waves is considered to be pH-independent confirming that the number of the electrons consumed in the overall reduction process does not altered and both the acidic and basic forms of the electroactive species are electactive at the vicinity of the electrode surface.

The half-wave potential ($E_{1/2}$) get shifted to more negative values on increasing the pH of the electrolysis medium, which confirmed the consumption of hydrogen ions participating in the rate determining step (Z_H^+) was found equal unity. On the other hand the number of electrons (n_a) involved in the rate-determining step was found to be two electrons.

The cyclic voltammograms of ciprofloxacin hydrochloride displayed only single cathodic peak from aqueous buffer solutions of pH (3.6, 7.0, 10.0) at different scan rates (20-500 mV/sec). The absence of any oxidation peaks on the anodic scan indicate the irreversibility of the reduction process. The peak potential (E_p) was shifted cathodically to more negative values on increasing the scan rate which is further confirmed the irreversibility of the electrode process.

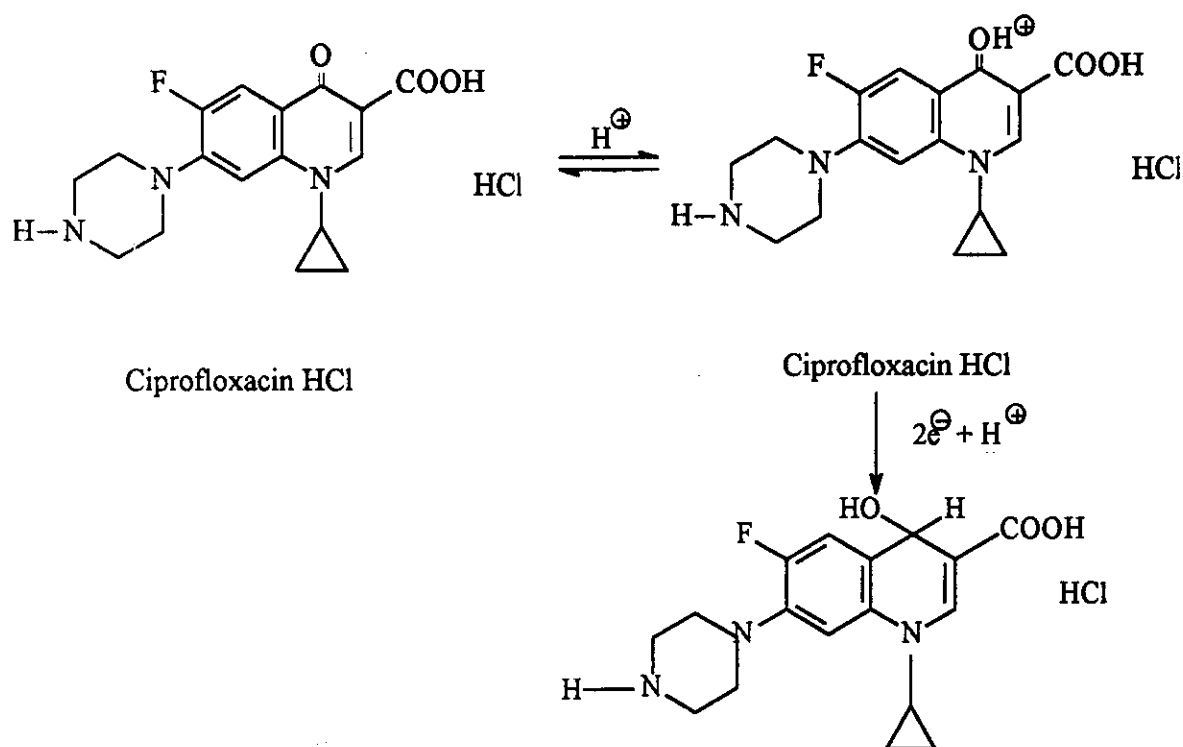
In order to through the light on the electrode reaction mechanisms it is necessary to calculate the total number of electrons consumed in the reduction process. Controlled Potential Coulometry technique (CPC) was used for determining the number of electrons (n). A coulometry system model PARC-380 with a large mercury pool cathode was used for this purpose. The amount of accumulated charge (Q) was taken directly from the digital coulometer at a

potential corresponding to the limiting current of the polarographic waves. Applying the following equation:

$$Q = \frac{nFW}{M}$$

Where, W: is the weight of the electroactive compound in grams and M: its molecular weight

The average number of electrons (n) consumed in the reduction process was amount to (2.0±0.1). Therefore, from the foregoing results the electrode mechanism could take place as following:



3.1.1.6. Cathodic Adsorption Square Wave Stripping Voltammetry (CAdSWSV) of ciprofloxacin hydrochloride

Adsorptive stripping voltammetry is based on the accumulation of the investigated compound on the electrode surface. Square wave stripping voltammetry is well known as a very sensitive technique for the determination of pharmaceutical compounds and organic substances, which of biological significance. The results of DC-polarographic studies and cyclic voltammetry at the glassy carbon electrode indicated the presence of some adsorption and association contribution of such compound under investigation at the electrode surface. Also they indicated the effective interfacial accumulation of ciprofloxacin hydrochloride. In the present study CAdSWSV is used for the electroanalytical determination of all compounds under investigation.

I. Optimization of the experimental and instrumental conditions

Both experimental conditions such as pH and supporting electrolyte and instrumental conditions such as deposition time, deposition potential, frequency, scan rate, pulse height and pulse width are optimized here for the quantitative determination of ciprofloxacin hydrochloride in its pure and dosage forms using square wave stripping voltammetry.

1- Effect of pH on the cathodic adsorption stripping peak of ciprofloxacin hydrochloride

The cathodic adsorption stripping voltammetric current of 1×10^{-6} M ciprofloxacin hydrochloride was recorded as a function of potential in Britton Robinson buffer solutions of pH 3.1-11.1, Fig. 5. The obtained peaks were due to the reduction of the adsorbed ciprofloxacin hydrochloride at the glassy carbon electrode surface. A well-defined peak was observed at pH equal to 4.2.

2- Effect of supporting electrolytes on the CAdSWSV peak of ciprofloxacin hydrochloride

The effect of supporting electrolytes such as sodium nitrate, sodium perchlorate, potassium chloride and B.R. buffer solution of pH 4.2 on the CAdSWSV peak current was studied, Fig. 6. The obtained stripping voltammograms showed that pH 4.2 was the most suitable medium for the developing of well-defined peak current for ciprofloxacin hydrochloride.

3- Effect of deposition potential

The influence of deposition potential (E_d) on the stripping peak current was recorded at -100, -200, -300, -500 and -900 mV in media containing 1×10^{-6} M of ciprofloxacin hydrochloride at pH 4.2. The deposition time (t_d) was held constant during all experiments at 300 sec. Square wave stripping voltammograms were recorded as in Fig. 7. Values of stripping peak currents at different deposition potentials revealed that -100 mV was the most suitable deposition potential, Table 6.

4- Effect of frequency

On changing the value of the frequency, the height of the formed peak is also changed. By studying the effect of different values of frequency from 100 to 5000 Hz, it was found that the most suitable value is 5000 Hz, Fig. 8.

5- Effect of pulse width

The effect of pulse width on the CAdSWSV peak height was studied in the range of 20 to 200 mV, Fig. 9. For ciprofloxacin hydrochloride, the analytical determination was performed at pulse width equal to 200 mV.

6- Effect of pulse height

The effect of pulse height on the CAdSWSV peak height is studied in the range of 10 to 200 mV. The stripping peak current was found to be directly proportional to the pulse height, Fig. 10. In the present study, a sharp peak current of ciprofloxacin hydrochloride was obtained at pulse height equal to 200 mV.

7- Effect of deposition time

In the stripping analysis, the height of the formed peak is almost proportional to the deposition time (t_d). On studying the effect of deposition time on the investigated compound, the most suitable t_d equaled 300 sec, Fig. 11. Above this value the current decreases again, this may due to the complete coverage of the electrode surface.

8- Effect of scan rate

On studying the effect of different scan rates from 1.0 to 10.0 mV/s, a scan rate of 1.0 mV/s gave a maximum response, Fig. 12.

II. Quantitative determination of ciprofloxacin hydrochloride by CAdSWSV

The applicability of the cathodic adsorptive stripping voltammetric technique as an analytical method for determination of ciprofloxacin hydrochloride is tested by measuring the CAdSWSV peak current as a function of concentration, Fig. 13.

Calibration graph

A stock solution of 1×10^{-3} M of ciprofloxacin hydrochloride was prepared and different concentrations were obtained by accurate dilution. The

CAdSWSV peaks of the final samples were recorded in quartet replicates at the optimum experimental and instrumental conditions. The optimum conditions for ciprofloxacin hydrochloride determinations are as following: deposition potential of -100 mV, frequency 5000 Hz., pulse width 200 mV, pulse height 200 mV, deposition time 300 sec and scan rate 1.0 mV/sec in B. R. buffer solution of pH = 4.2. The variation of peak current with the concentration is represented by the straight-line equation:

$$i_p = ac + b \quad \text{-----(11)}$$

Where a, b are the slope and intercept the straight line, respectively ($a = 4.6 \times 10^4$, $b = 0.071$) and c is the concentration, Fig. 14. The concentration of ciprofloxacin hydrochloride is determined using the following equation:

$$c = (i_p - b) / a \quad \text{-----(12)}$$

The precision was determined from four replicate measurements of each concentration of the compound under investigation, the mean recovery and standard deviation were calculated, Table 7.

Detection Limit

The lower detection limit (DI) of ciprofloxacin HCl is calculated using the following equation⁽¹¹⁴⁾:

$$DI = 3 \frac{S.D}{a} \quad \text{-----(13)}$$

Where S.D. = standard deviation of the blank, and a = slope of the calibration curve.

In the present study, S.D. = 3.1091×10^{-5} , $a = 4.6 \times 10^4$ and the detection limit is found to be 2.0×10^{-9} M (7.7×10^{-4} µg/ml).

Determination of ciprofloxacin hydrochloride in its dosage form:

The above proposed stripping voltammetric procedure is successfully applied for the analysis of ciprofloxacin hydrochloride in its dosage form. The precision is determined from four repeated measurements of two concentrations of each reported dosage form, Table 8. The mean recovery of ciprofloxacin hydrochloride in ciprofloxacin tablets is $101.4\% \pm 0.51$ and $100.45\% \pm 0.55$ for Rancif tablets. The agreement between the proposed procedure and the official one confirms the validity of the CAdSWSV technique in the analysis of ciprofloxacin hydrochloride in its dosage forms under the optimum experimental and instrumental conditions described before, Table 9.

Table 6:

Cathodic adsorptive square wave stripping peak current (i_p) of 1×10^{-6} M ciprofloxacin hydrochloride in B.R. buffer solution of pH 4.2 at different conditions.

Deposition time Sec	Deposition potential -E _d , mV	Scan rate mV/s	Pulse height mV	Pulse width mV	i _p μA
Effect of E _d					
300	100	1.0	20	50	0.1201
	200				0.1011
	300				0.0994
	500				0.0977
	900				0.0874
Effect of pulse width					
300	100	1.0	20	200	0.1455
				100	0.1369
				50	0.1200
				20	0.0818
				10	0.0760
Effect of pulse height					
300	100	1.0	200	200	0.1567
			100		0.1536
			50		0.1455
			20		0.0728
			10		0.4630
Effect of t _d					
360	100	1.0	200	200	0.1522
300					0.1567
240					0.1343
120					0.1403
60					0.1308
Effect of scan rate					
300	100	1.0	200	200	0.1567
		2.0			0.1550
		5.0			0.1518
		10.0			0.1371

Table 7:

Assay of ciprofloxacin hydrochloride in B.R. buffer solution of pH 4.2 using CAdSWSV at: $E_d = -100$ mV, $t_d = 300$ sec, scan rate = 1.0 mV/sec, pulse height = 200 mV, pulse width = 200 mV and frequency = 5000Hz

Conc. Taken M	i_p μA	Conc. Found M	% Recovery (%R)	Av. Conc. Found M	Mean %R	S.D
1×10^{-6}	0.1157	0.972×10^{-6}	97.2	0.99×10^{-6}	98.7	1.32
	0.1161	0.980×10^{-6}	98.0			
	0.1168	0.996×10^{-6}	99.6			
	0.1172	1.000×10^{-6}	100.0			
7×10^{-7}	0.1032	7.000×10^{-7}	100.0	6.96×10^{-7}	99.4	0.55
	0.1029	6.935×10^{-7}	99.1			
	0.1028	6.913×10^{-7}	98.8			
	0.1031	6.978×10^{-7}	99.7			
5×10^{-7}	0.0935	4.891×10^{-7}	97.8	4.96×10^{-7}	99.3	0.98
	0.0940	5.000×10^{-7}	100.0			
	0.0939	4.978×10^{-7}	99.6			
	0.0939	4.978×10^{-7}	99.6			
2×10^{-7}	0.0800	1.957×10^{-7}	97.8	1.97×10^{-7}	98.4	0.64
	0.0801	1.978×10^{-7}	98.9			
	0.0800	1.957×10^{-7}	97.8			
	0.0801	1.978×10^{-7}	98.9			
The mean recovery = 98.95 ± 0.87						
Slope = 4.6×10^4						
Intercept = 0.071						
Corr. Coeff. = 0.9776						

Table 8:

Assay of ciprofloxacin hydrochloride tablets in B.R. buffer solution of pH 4.2 using CAdSWSV V at: $E_d = -100$ mV, $t_d = 300$ sec, scan rate = 1.0 mV/sec, pulse height = 200 mV, pulse width = 200 mV and frequency = 5000 Hz

Name of tablets	Conc. Taken M	ip (μA)	Conc. Found M	%R	Av. Conc (found) M	Mean %R	S.D.
Rancif	2.5×10^{-7}	0.0825	2.500×10^{-7}	100.0	2.50×10^{-7}	100.0	0.73
		0.0826	2.522×10^{-7}	100.9			
		0.0825	2.500×10^{-7}	100.0			
		0.0824	2.478×10^{-7}	99.1			
	4.5×10^{-7}	0.0919	4.543×10^{-7}	100.9	4.54×10^{-7}	100.9	0.37
		0.0920	4.565×10^{-7}	101.4			
		0.0919	4.543×10^{-7}	100.9			
		0.0918	4.522×10^{-7}	100.5			
The mean recovery = 100.45% ± 0.55							
Ciprof-loxacin	2.8×10^{-7}	0.0840	2.826×10^{-7}	100.9	2.83×10^{-7}	100.9	0.61
		0.0841	2.848×10^{-7}	101.7			
		0.0840	2.826×10^{-7}	100.9			
		0.0839	2.804×10^{-7}	100.2			
	4.8×10^{-7}	0.0935	4.891×10^{-7}	101.9	4.87×10^{-7}	101.4	0.41
		0.0934	4.869×10^{-7}	101.4			
		0.0934	4.869×10^{-7}	101.4			
		0.0933	4.848×10^{-7}	100.9			
The mean recovery = 101.4% ± 0.51							
Slope = 4.6×10^4							
Intercept = 0.071							
Corr. Coeff = 0.9776							

Table 9:

Assay of ciprofloxacin hydrochloride in its dosage forms B.R. buffer solution of pH 4.2 using CAdSWSV at: $E_d = -100$ mV, $t_d = 300$ sec, scan rate = 1.0 mV/sec, pulse height = 200 mV and pulse width = 200 mV and frequency = 5000 Hz.

Brand Name (Producer)	Labelled Conc. (Drug)	%Recovery \pm S.D.	
		Proposed Method	Reported Method*
Rancif	500 mg/tablet	100.45% \pm 0.55 (n = 4)	100 \pm 0.76 (n = 9)
Ciprofloxacin	250 mg/tablet	101.4% \pm 0.51 (n = 4)	100 \pm 0.76 (n = 9)

* The official method⁽¹⁰⁾

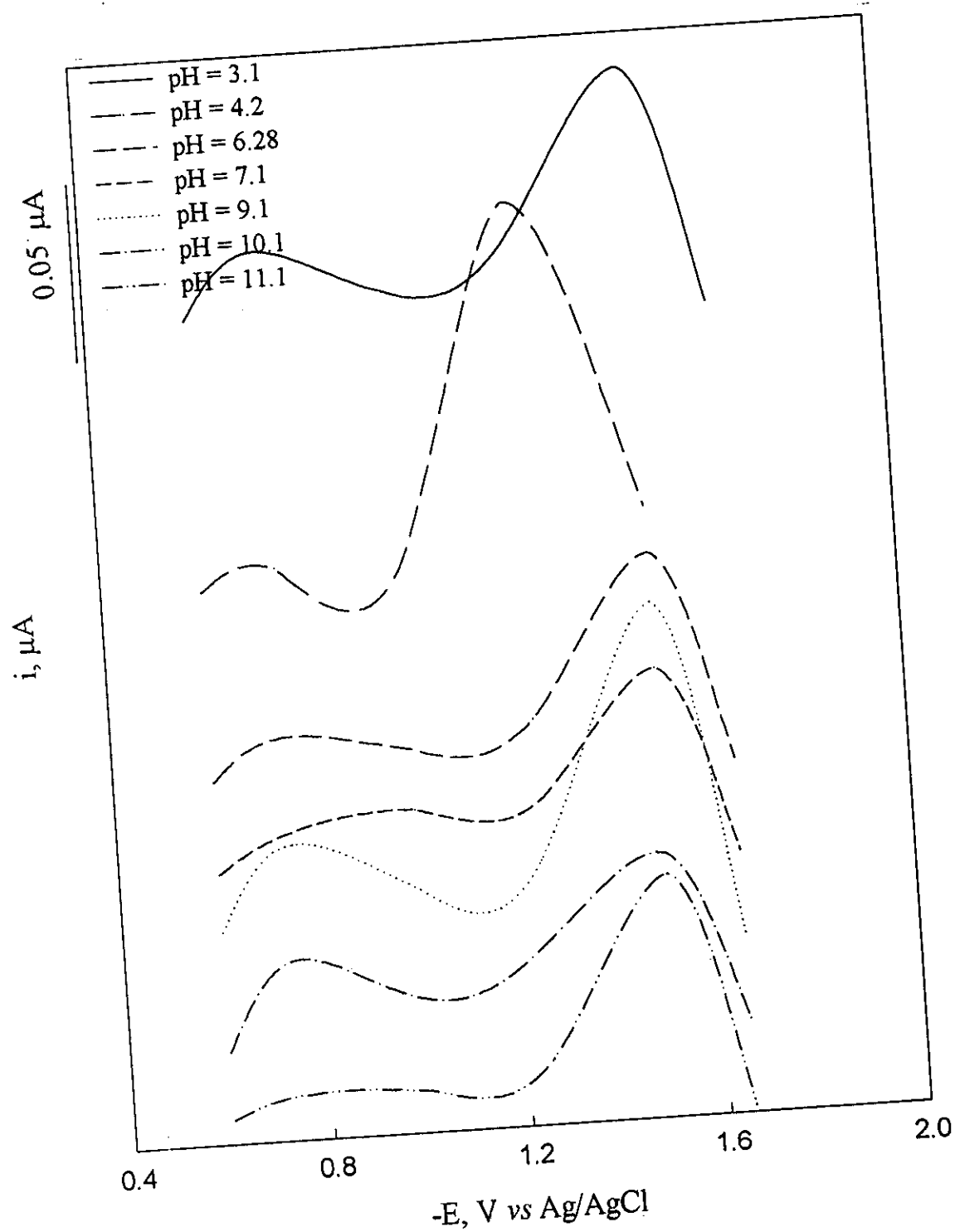


Fig. 5: Effect of pH on the CAdSWSV peak on 1×10^{-6} M of ciprofloxacin hydrochloride in B.R. buffer solution at: $t_d = 300$ sec, $E_d = -200$ mV, scan rate = 0.1 mV/s, pulse height = 20 mV and pulse width = 50 mV.

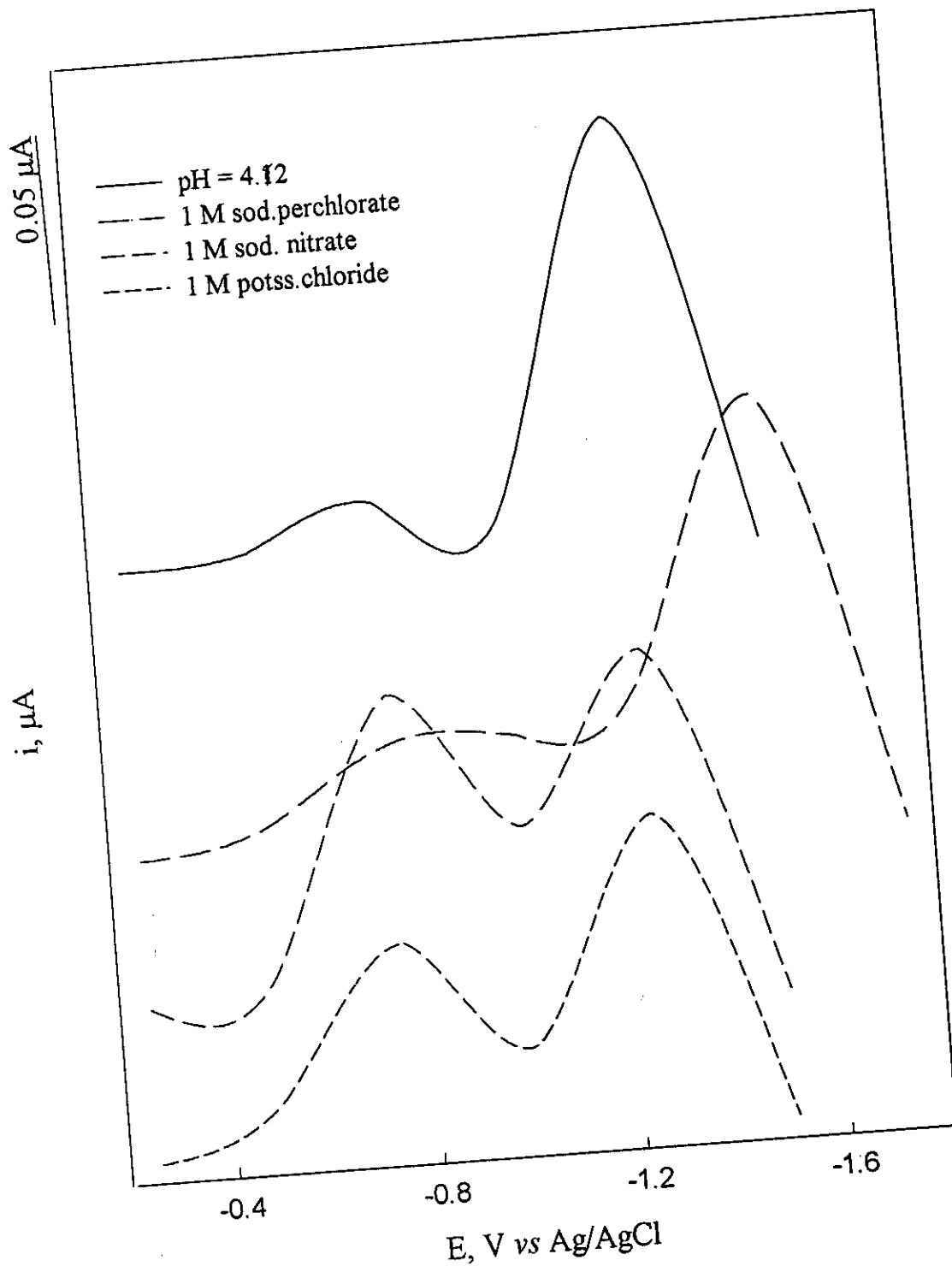


Fig. 6: Effect of supporting electrolyte solutions on the CAdSWSV peak of 1×10^{-6} M of ciprofloxacin hydrochloride in B. R buffer solution at $E_d = -200$ mV, $t_d = 300$ sec, scan rate = 0.1 mV/s pulse height = 20 mV, pulse width = 50 mV and frequency = 5000 Hz

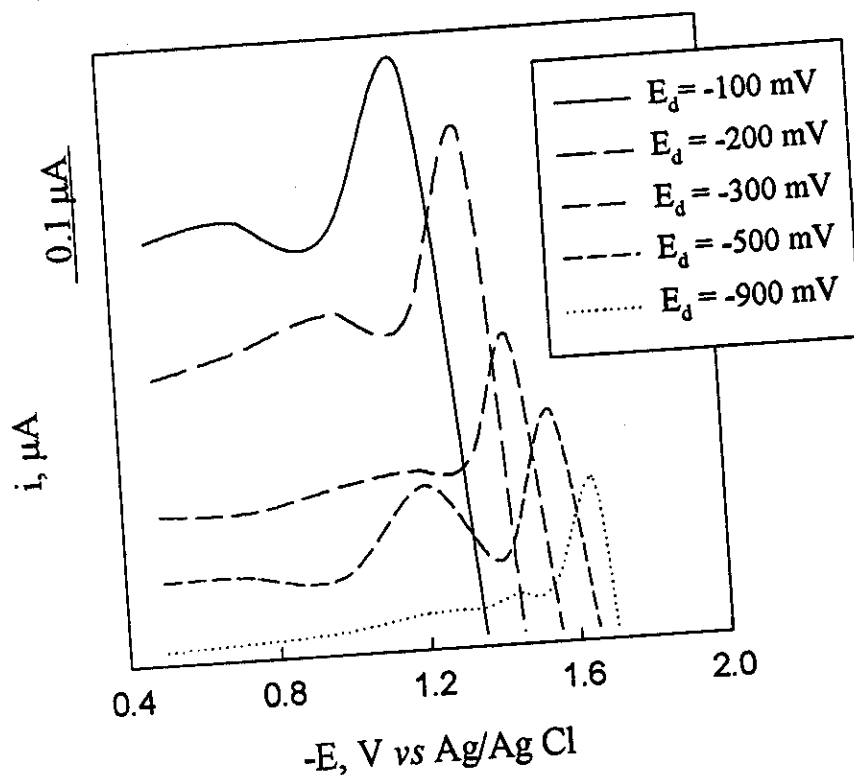


Fig. 7: Effect of E_d of 1×10^{-6} of ciprofloxacin hydrochloride in B. R. buffer solution of pH 4.2, scan rate = 0.1 mV/sec, pulse height = 20 mV, pulse width = 50 mV, t_d = 300 sec and frequency = 5000 Hz

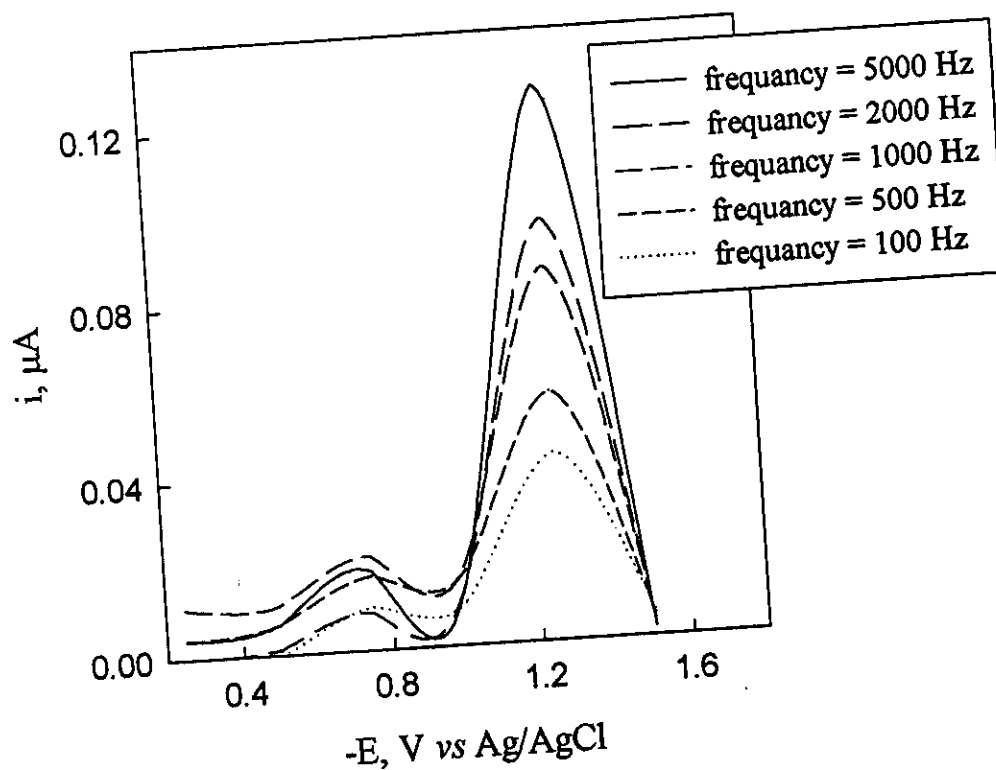


Fig. 8: Effect of frequency of 1×10^{-6} M of ciprofloxacin hydrochloride in B.R. buffer solution of pH = 4.2, scan rate = 0.1 mV/s, E_d = -100 mV, pulse height = 20 mV, pulse width = 50 mV and t_d = 300 sec

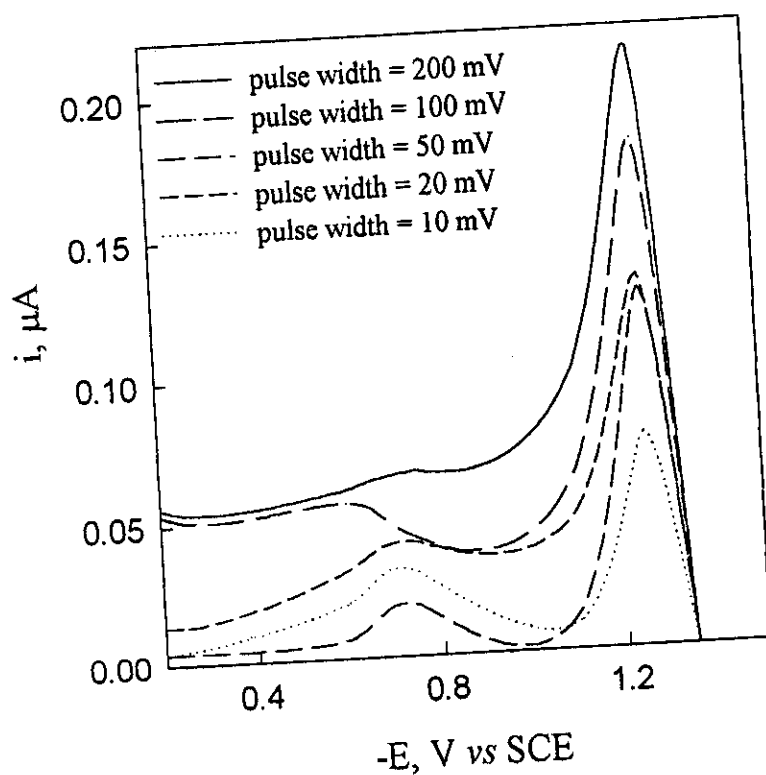


Fig. 9: Effect of pulse width of 1×10^{-6} M of ciprofloxacin HCl in B.R. buffer solution of pH = 4.2, at $E_d = -100$ mV, scan rate = 0.1 mV/s and pulse height = 20 mV, $t_d = 300$ sec and frequency = 5000 Hz.

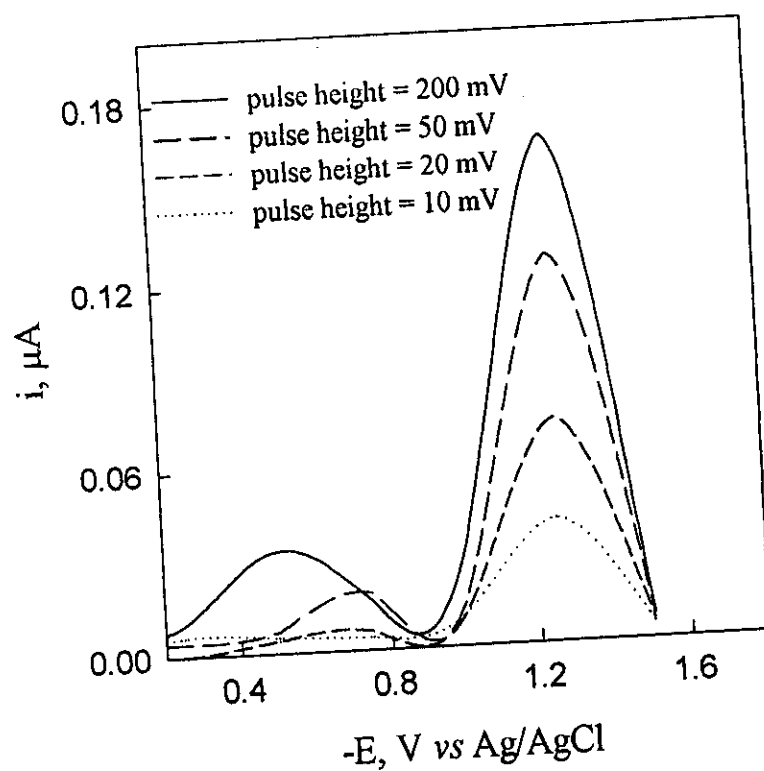


Fig. 10: Effect of pulse height of 1×10^{-6} M of ciprofloxacin HCl in B.R. buffer solution of pH = 4.2, at $E_d = -100$ mV, scan rate = 0.1 mV/s pulse width = 200 mV, $t_d = 300$ sec and frequency = 5000 Hz

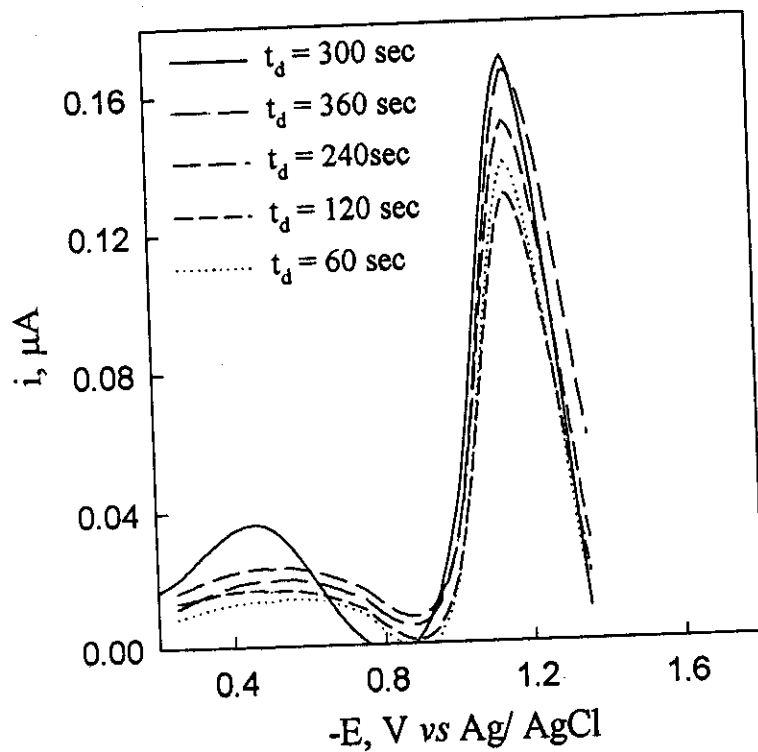


Fig. 11: Effect of t_d on 1×10^{-6} M of ciprofloxacin hydrochloride in B.R. buffer solution of pH 4.2, at $E_d = -100$ mV, scan rate = 0.1 mV/sec and pulse height = 200 mV, pulse width = 200 mV and frequency = 5000 Hz

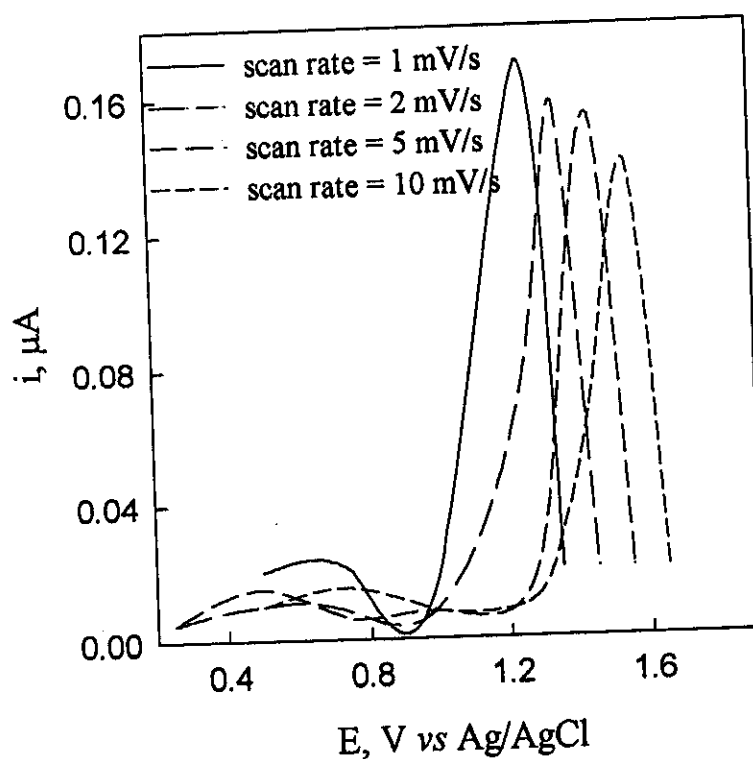


Fig. 12: Effect of scan rat on 1×10^{-6} M of ciprofloxacin hydrochloride in B.R. buffer solution of pH 4.12 at $E_d = -100$ mV, pulse height = 200 mV, pulse width = 200 mV, $t_d = 300$ sec and frequency = 5000 Hz

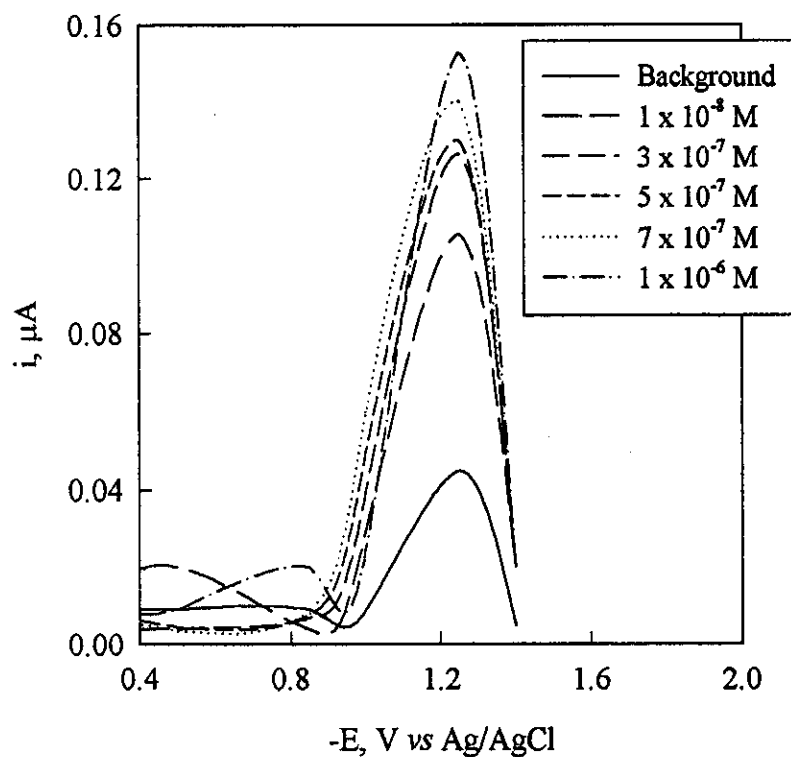


Fig. 13: Effect of concentration of ciprofloxacin hydrochloride in B.R.buffer solution of pH 4.2, $E_d = -100$ mV, $t_d = 300$ sec, pulse height = 200 mV pulse width = 200 mV, scan rate = 1.0 mV/s and frequency = 5000 Hz

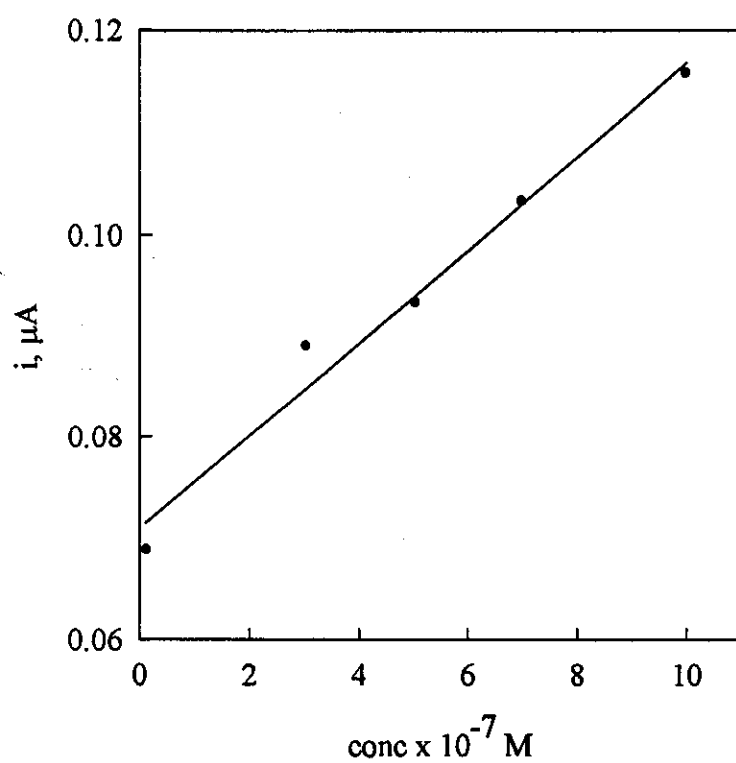


Fig. 14: Calibration curve of ciprofloxacin hydrochloride under the optimum conditions

3.1.2. Spectrophotometric studies on the drug complexes in solution

In the present study the optimum conditions for the formation of drug-reagent complexes were determined.

3.1.2.1. Determination of optimum conditions

1. Effect of pH:

The effect of pH on the formation of drug-reagent complex between ciprofloxacin hydrochloride and three analytical reagents, Sudan II (I), Congo red (II) and gentian violet (III) was studied in universal buffer solution of pH range 2.5-11.0. A series of solutions containing 1.0 ml of 1.0×10^{-3} M of reagents I, II or III, 1.0 ml of 1.0×10^{-3} M of the drug and 5 ml buffer of different pH values were added. The volume was completed to 10 ml with distilled water. The absorption spectra were recorded using a blank solution prepared by the same way without drug at the same pH value, Fig. 15–17. The optimum pH values recommended for subsequent studies of drug-reagent complexes with ciprofloxacin HCl were 5.5, 2.5 and 2.5 using reagents I, II and III, respectively as recorded in Table 10.

2. Determination of λ_{\max} of the complex species:

For determination of the optimum λ_{\max} at which each complex species was absorbed, the following sequence must be followed up:

- A) Spectrum of 1 ml of 1.0×10^{-3} M of drug at the suitable pH using the same pH as a blank.
- B) Spectrum of 1 ml of 1.0×10^{-3} M of reagent at the suitable pH value using the same pH as a blank.
- C) Spectrum of 1.0 ml of 1×10^{-3} M drug and 1.0 ml of 1.0×10^{-3} M reagent at the optimum pH using the same pH and 1.0 ml of 1.0×10^{-3} M reagent as a blank.

These curves (A-C) showed that, the maximum wavelength at which the complexes formed were 550, 517 and 585 nm with the reagents I, II and III, respectively, Fig. 15-17, as listed in Table 10.

3. Effect of time and temperature:

The effect of time on drug-reagent complexes was studied by measuring the absorbance of a solution containing 1 ml of 1×10^{-3} M of drug, 1 ml of 1×10^{-3} M reagent and 5 ml buffer of suitable pH against blank solution prepared by the same way without drug at various time intervals. Also the effect of temperature was studied for the same solution by heating the sample solution and the blank at different temperatures from 25 to 50°C. The absorbance was measured after cooling both of the sample and blank solutions to room temperature.

Experiments showed that, the complexes were formed spontaneously after mixing the drug with all reagents at room temperature and remain stable for 24 hour.

4. Effect of sequence of additions:

The effect of sequence of additions on the complex formation was studied. The absorbance of a series of solutions prepared by different sequence of additions against a blank solution prepared in the same manner was measured. Experiments showed that (reagent-drug-buffer) gave the best results for cip-I, cip-II and cip-III. Other sequences of additions gave lower absorbance values under the same experimental conditions.

5. Effect of reagent concentration:

To study the effect of the reagents concentration on the complex formation, the concentration of the drug was kept constant (1 ml of 1.0×10^{-3}

M) while that of the reagent was regularly varied. The absorption spectra of each concentration in the selected pH value were recorded against blank solution prepared at the same manner without drug. In the present study 1.0 ml of 1.0×10^{-3} M of each reagent is sufficient to produce maximum absorbance value.

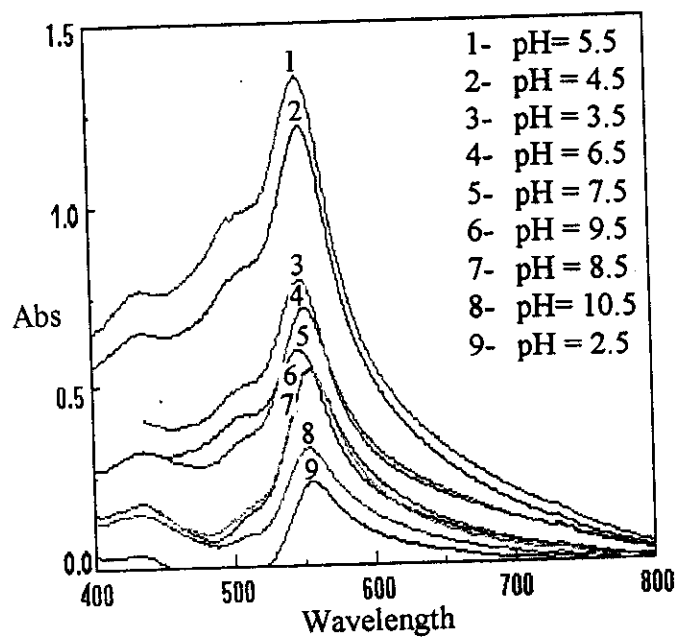
3.1.2.2. Molecular structure

1. Molar ratio method:

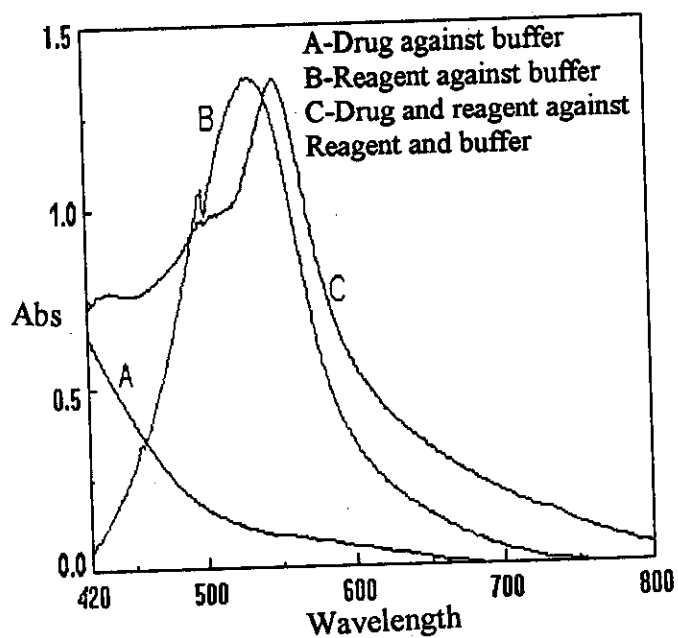
The molar ratio method described by Yoe and Jones⁽¹⁰³⁾ was used to study the stoichiometry of the complexes between ciprofloxacin HCl using studied reagents. In this method, 1.0 ml of 1.0×10^{-3} M of the drug was mixed with various concentrations of reagents (0.1, 0.2, 0.3 ...2.5 ml of 1.0×10^{-3} M), and 5 ml of the selected pH value of buffer was added. The volume was completed to 10 ml with distilled water. The absorbance was measured at the optimum wavelength against blank solution prepared in the same manner without the drug. The absorbance values were plotted against the molar ratio $[R]/[D]$. Experimental results showed that the ratio of the formed complex is 1:1 (D: R). Fig 15-17.

2. Continuous variation method:

The modification of Job's continuous variation method⁽¹⁰⁴⁾ performed by Vesburgh et al⁽¹⁰⁵⁾ is utilized for investigating the stiochiometric ratio of the reaction between the drug and reagents. Different volumes (0.2, 0.4, 0.6.....1.8 ml) of 1.0×10^{-3} M of drug and reagent were mixed while keeping the total molar concentration constant at 2.0×10^{-3} M, 5 ml of the selected pH value was added, the volume was completed to 10 ml with distilled water. The absorbance was plotted against the mole fraction of the drug. The result



Effect of pH on cip-I complex



Determination of wavelength

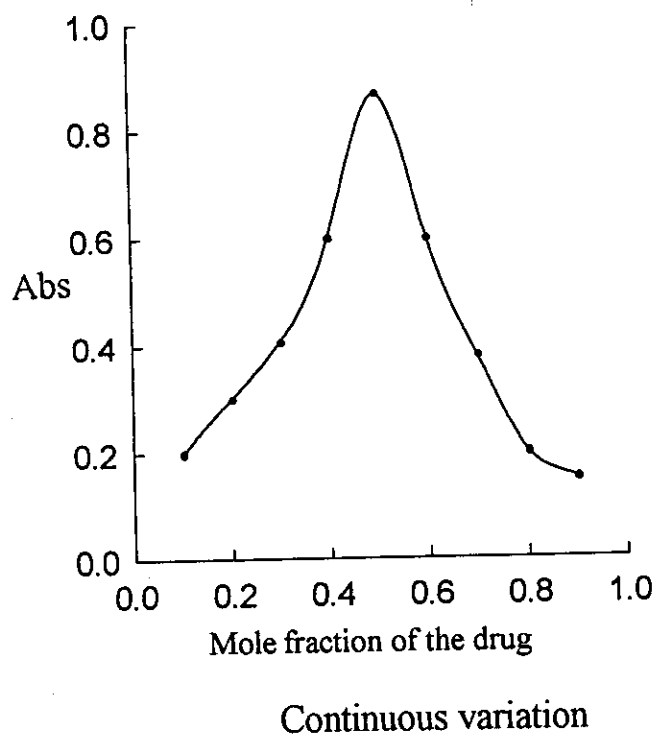
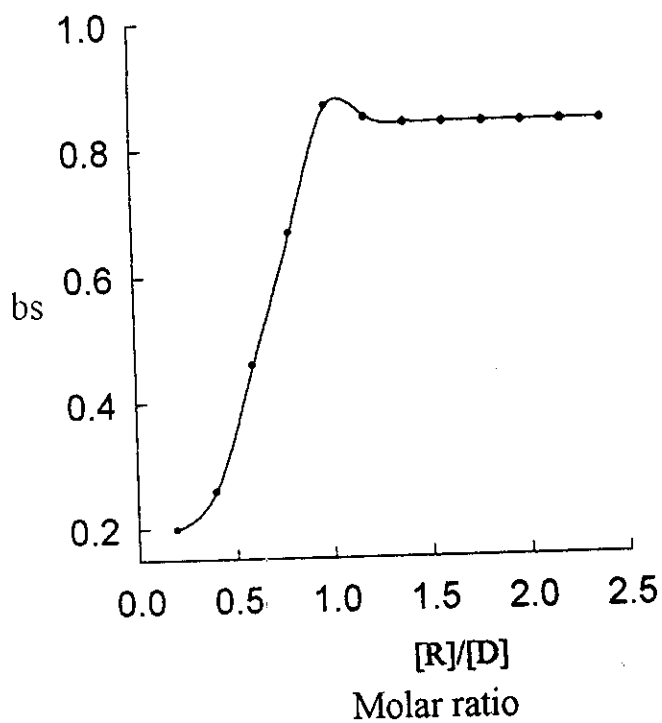
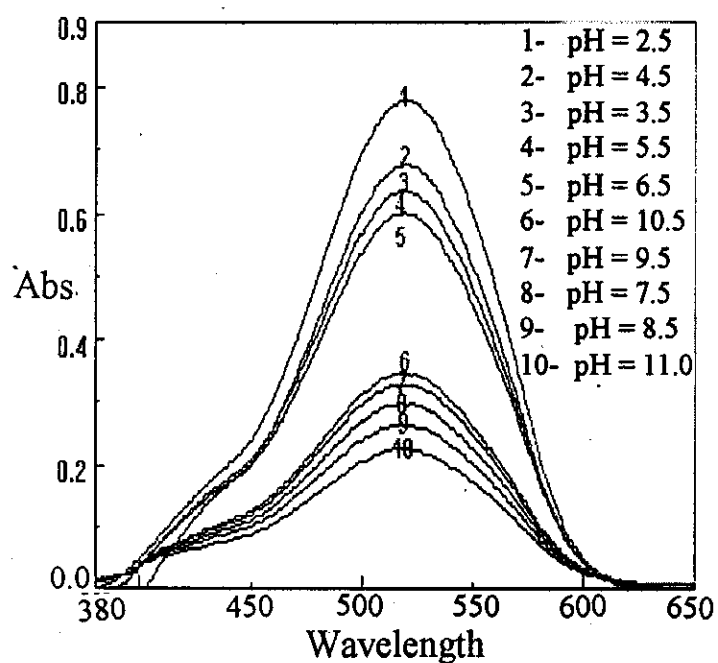
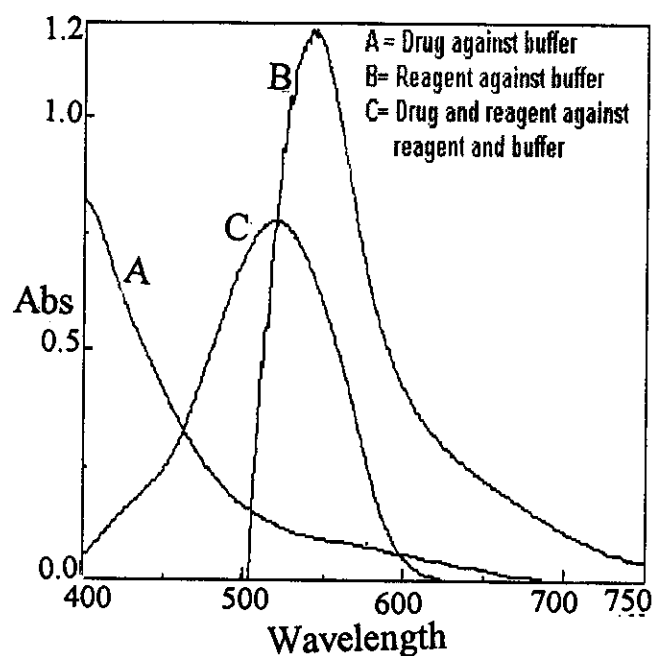


Fig. 15 ciprofloxacinhydrochloride with sudan II



Effect of pH on cip-II complex



Determination of wavelength

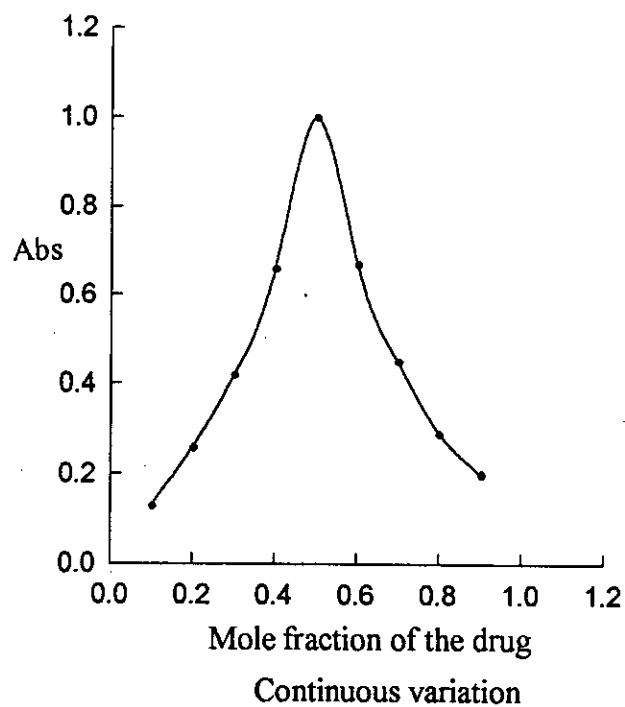
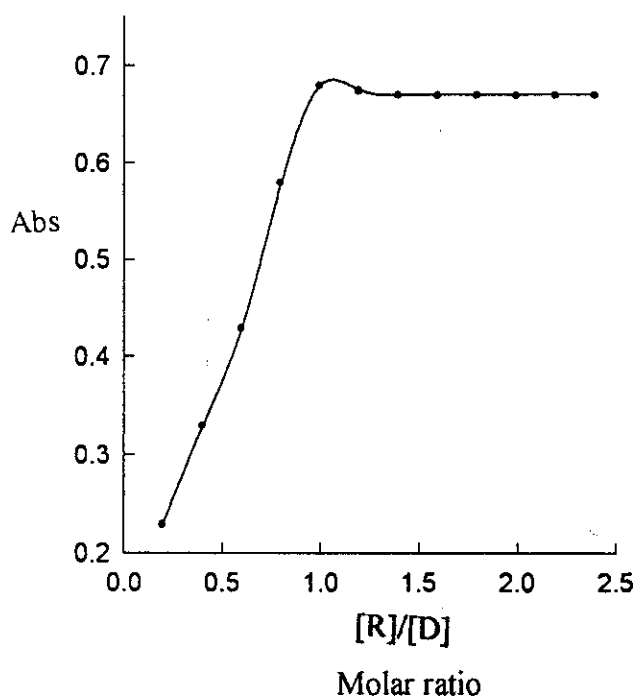
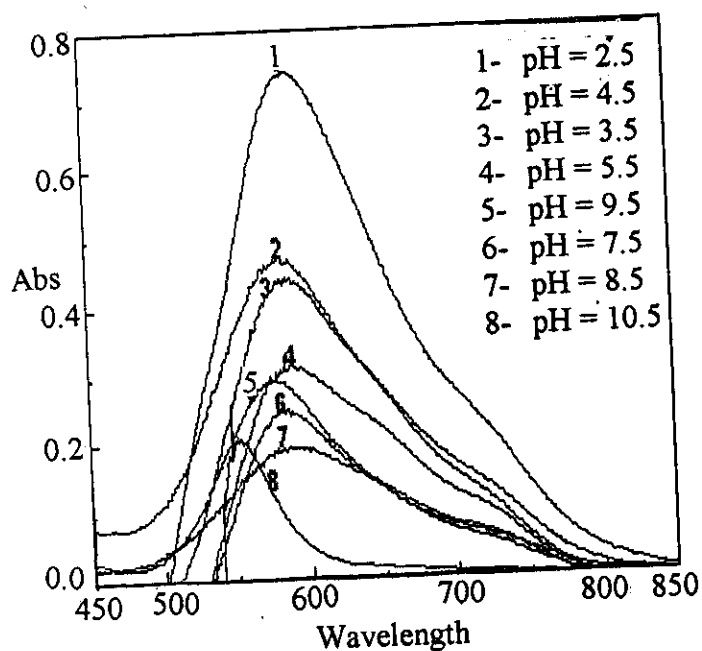
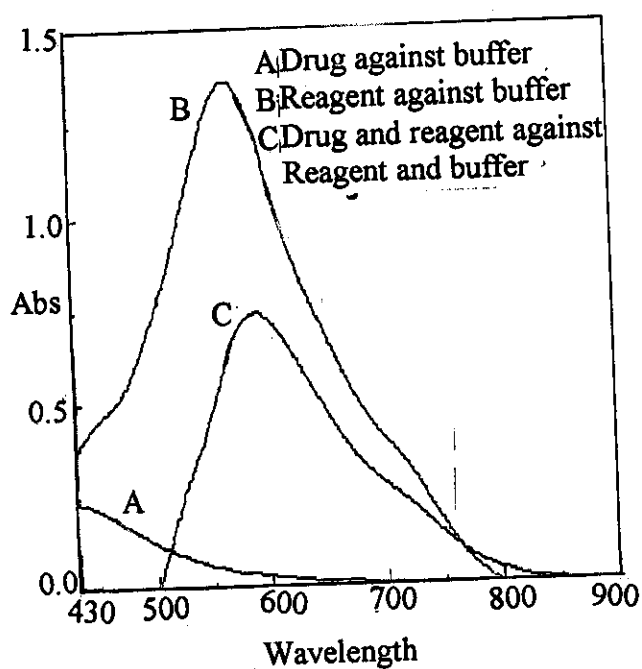


Fig. 16: Ciprofloxacin hydrochloride with congo red



Effect of pH on cip-III complex



Determination of wavelength

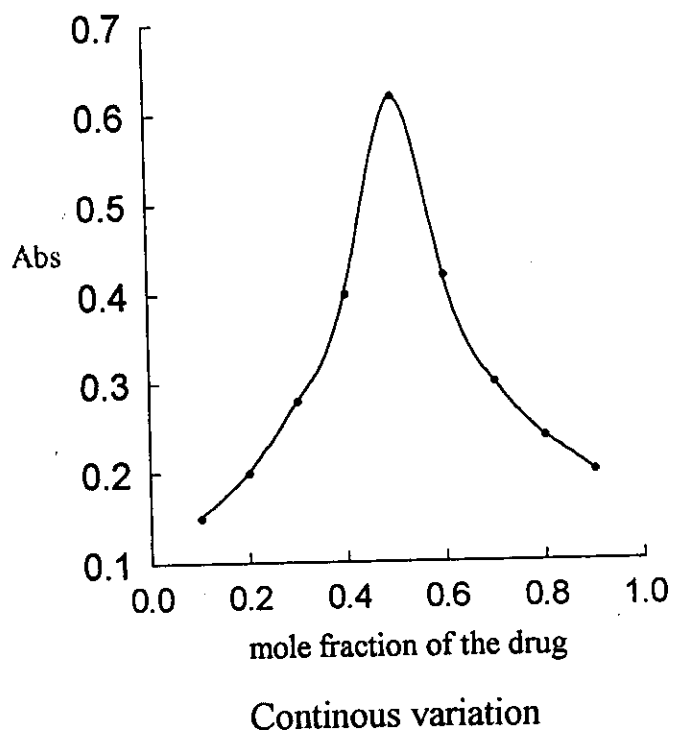
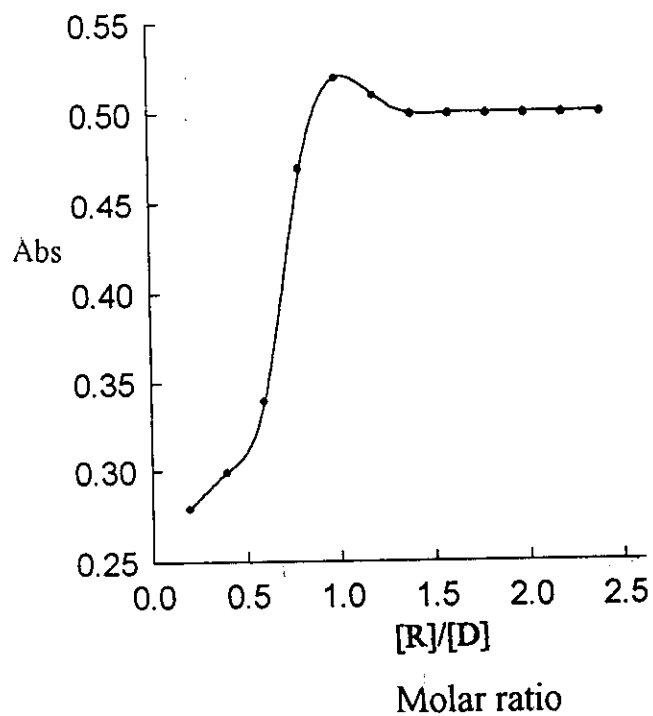


Fig. 17: Ciprofloxacin with gentian violet

3.1.2.4. Validity of Beer's law:

Under the optimum experimental conditions of pH, time, reagent concentration, sequence of addition and temperature for the formed complexes, different concentrations in $\mu\text{g/ml}$ of drug sample were transferred into 10 ml measuring flask. The suitable concentration of reagent (1 ml of $1 \times 10^{-3} \text{ M}$) and 5 ml of the optimum pH value were added. The volume was completed to the mark with distilled water. The absorbance was measured at the recommended λ_{max} . The absorbance was plotted against the concentration of the drug in $\mu\text{g/ml}$ and so the limits in which the drug obeys Beer's law were detected, Fig 18.

For more accurate analysis, **Ringbom**⁽¹¹⁶⁾ optimum concentration range is determined by calculating the transmittance percent from the following equation:

$$T \% = 10^{-A} \times 100$$

Where: T %, is transmittance percent and A, is the absorbance of the complex

Plotting $\log [D]$ in $\mu\text{g/ml}$ against T % for the formed complexes is represented in Fig. 19. The linear portion of the S-shaped curve gave an accurate range of analysis.

The range in which the drug obeys Beer's law, Ringbom optimum range, the molar absorptivity and **Sandell**⁽¹¹⁷⁾ sensitivity were calculated and listed in Table 11. Inspection of the obtained data revealed high sensitivity in micro determination of the investigated drug.

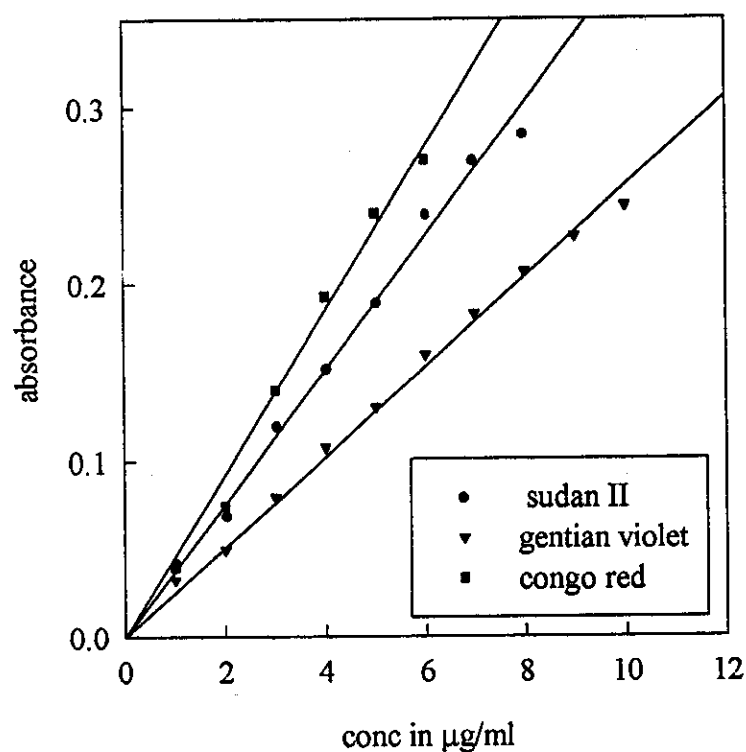


Fig. 18: Beer's law for ciprofloxacin HCl with reagents under investigation

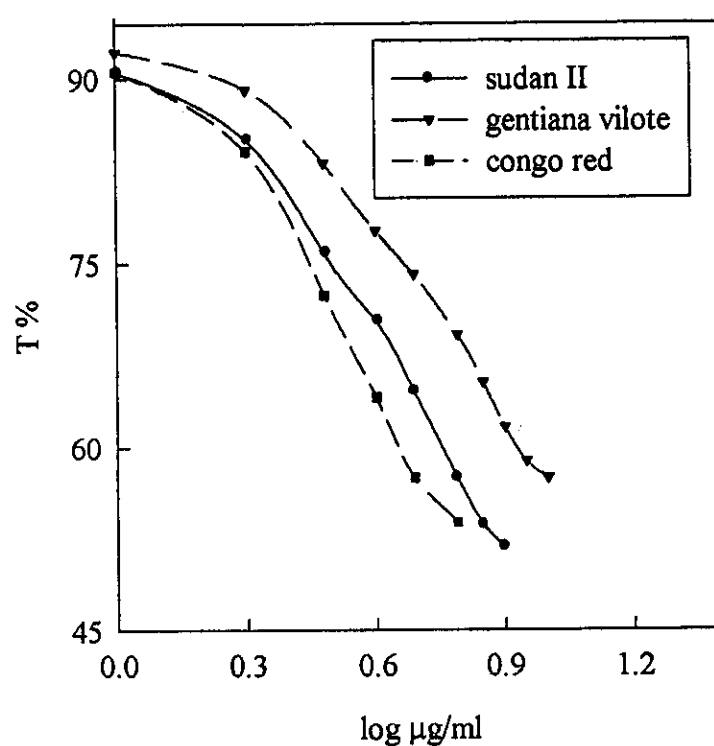


Fig. 19: Ringbom plot for the reagents complexes with ciprofloxacin HCl

Table 11:

Cumulative data of ciprofloxacin hydrochloride with reagents I, II and III
under investigation

Reagent	Ringbom optimum range $\mu\text{g/ml}$	Beer's range $\mu\text{g/ml}$	S.D	R.S.D %	Error %	*S. ng cm^{-2}	* ϵ $\text{l mol}^{-1} \text{cm}^{-1}$
I	1.44-7.1	1.0-8.0	0.025	0.037	0.91	25.72	1.5×10^4
II	1.44-5.5	1.0-6.0	0.022	0.052	0.13	22.69	1.7×10^4
III	1.44-9.6	1.0-10.0	0.034	0.077	0.19	35.07	1.1×10^4

*S.: Sandell sensitivity

* ϵ : Molar absorptivity

3.1.2.5. Interference:

The interferences of co-existing additives such as sodium acetate, starch and glucose were investigated by adding amount of these additives to a solution containing 5 µg/ml of ciprofloxacin hydrochloride and the absorbance was measured under the optimum conditions. Experiments showed that all additives didn't interfere in the determination of ciprofloxacin hydrochloride, indicating the high selectivity of the proposed method.

3.1.2.6. Analytical applications:

The proposed procedure for determination of ciprofloxacin-HCl using the analytical reagents under investigation was performed to ciprofloxacin in its tablet forms such as Ciprofloxacin and Rancif tablets. These pharmaceutical preparations was analysed by the proposed method under the optimum conditions. Results are shown in Tables 12 and 13 confirming that the proposed method is highly sensitive, therefore it could be used easily for the routine analysis of pure form and in its pharmaceutical preparations.

3.1.2.7. Accuracy and precision:

The accuracy of the proposed method for determination of ciprofloxacin hydrochloride using the analytical reagents under investigation were assessed using different concentrations. This was checked during the work by running six replicate standard samples.

In order to determine the precision of the method, solutions containing different concentrations of drug were prepared and the absorbance of the prepared solution was measured and repeated for six times. The value of standard deviation was calculated in Tables 12 and 13.

The results obtained were compared statistically by the Students t-test and the variance ratio F-test with those obtained by the HPLC⁽¹⁰⁶⁾ method which presents in the the British Pharmacopoeia procedure (1998). The Students t-test values obtained at 95 % confidence level and five degrees of freedom did not exceed the theoretical tabulated value indicating no significant difference between the methods compared.

Table 12:

Evaluation of accuracy and precision of the proposed and official methods for ciprofloxacin hydrochloride determination in ciprofloxacin tablets

Reagent	Content mg/tab	Found* (mg)		S.D	R.S.D %	Error %	Recovery %	F# value	t# value
		O	P						
I	250	244	251	0.293	0.312	0.127	102.87	4.073	0.701
II	250	244	247	0.329	0.359	0.147	101.22	3.199	0.345
III	250	244	248	0.347	0.377	0.154	101.63	2.78	0.245
t# Theoretical value = 2.57									
F# Theoretical value = 5.05									

*: Average of six determinations

O: Official method

P: Proposed method

Table 13:

Evaluation of accuracy and precision of the proposed and official methods for ciprofloxacin hydrochloride determination in Rancif tablets

Reagent	Content mg/tab	Found*		S.D	R.S.D %	Error %	Recovery %	F [#] value	t [#] value
		O	P						
I	500	490	505	0.319	0.335	0.137	101.0	2.317	0.82
II	500	490	506	0.356	0.368	0.150	101.2	1.919	0.52
III	500	490	504	0.371	0.386	0.158	100.8	1.889	0.69
t [#] Theoretical value = 2.57									
F [#] Theoretical value = 5.05									

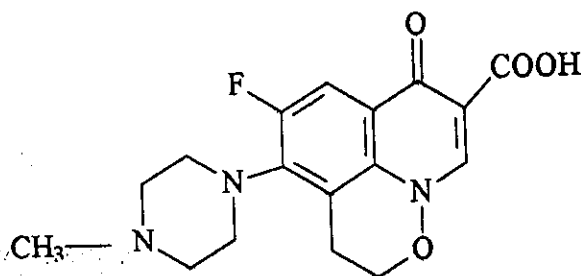
*: Average of six determinations

O: Official method

P: Proposed method

3.2. Electrochemical and analytical behaviour of ofloxacin in B.R. solutions of different pH-values containing 20% (v/v) ethanol

Ofloxacin, is [9-fluoro-3-methyl-10-(4-methyl-1-piperazinyl)-7-oxo-2,3 dihydro-7H-pyrido-(1,2,3-de)-1,4-benzoxazine-6-carboxylic acid] is broad spectrum antibacterial⁽¹¹⁸⁾. It is widely used in the treatment of respiratory and urinary tract infections and has the following chemical structure.



Ofloxacin

This part includes studying of the electrochemical behaviour of ofloxacin using both DC-polarography and cyclic voltammetric techniques. Also the analytical determinations of ofloxacin were performed using both square wave stripping voltammetry as well as spectrophotometric techniques.

3.2.1. Electrochemical behaviour of ofloxacin in B.R. solutions of different pH- values:

3.2.1.1. DC-Polarography:

Current–Potential Curves:

The polarographic reduction of 2×10^{-4} M of ofloxacin was investigated in B.R. buffer solutions of different pH values ranging from 3.5 to 10.5 containing 20% (v/v) ethanol to ensure complete solubility of the compound in the electrolysis cell. The recorded polarograms showed only a single reduction wave in the entire pH range, Fig. 20A. The polarographic wave

within the entire pH range n_a is equal to two for the ofloxacin. Values of the α obtained in the range from 0.372 to 0.724 is further confirmed the irreversibility of the electrode process.

Half-Wave Potential –pH Curves:

The plot of $E_{1/2}$ against pH of the reduction waves gives a straight line with two segments, Fig. 20E. The values of the number of hydrogen ions Z^+_H involved in the rate determining step was calculated using both slopes of $E_{1/2}$ -pH plots S_2 and those of logarithmic analysis S_1 from equation (4), Table 14. From the data obtained in the present work, the most probable values of α parameter indicated that Z^+_H is approximately unity at all pH values. From the data obtained in the present work, the most probable values of the ratio Z^+_H/n_a is equal to 0.5. This means that the number of protons Z^+_H and electrons n_a involved in the rate determining step equal to one and two; respectively.

Table 14:

DC-polarographic data and parameters obtained from electrochemical behaviour of 2×10^{-4} M ofloxacin recorded in buffer solutions of various pH values containing 20% (v/v) ethanol, at 25°C.

pH	i_d μA	$-E_{1/2}$ V	$\log i_1$ /log h	S_1 mV	α_{na}	α		S_2 mV	Z^+_H
						$na=1.0$	$na=2$		
3.5	0.74	1.23		79.48	0.744	0.744	0.372	59	0.74
4.5	0.70	1.24	0.647	63.49	0.931	0.931	0.466	59	0.93
5.5	0.69	1.27		59.52	0.993	0.993	0.497	59	0.99
6.5	0.68	1.31	0.503	63.49	0.931	0.931	0.466	59	0.93
7.5	0.68	1.34		58.52	1.019	1.019	0.509	59	1.01
8.5	0.67	1.39		42.11	1.403	1.403	0.702	24	0.57
9.5	0.69	1.47	0.652	48.19	1.226	1.226	0.613	24	0.50
10.5	0.64	1.54		40.82	1.448	1.448	0.724	24	0.59

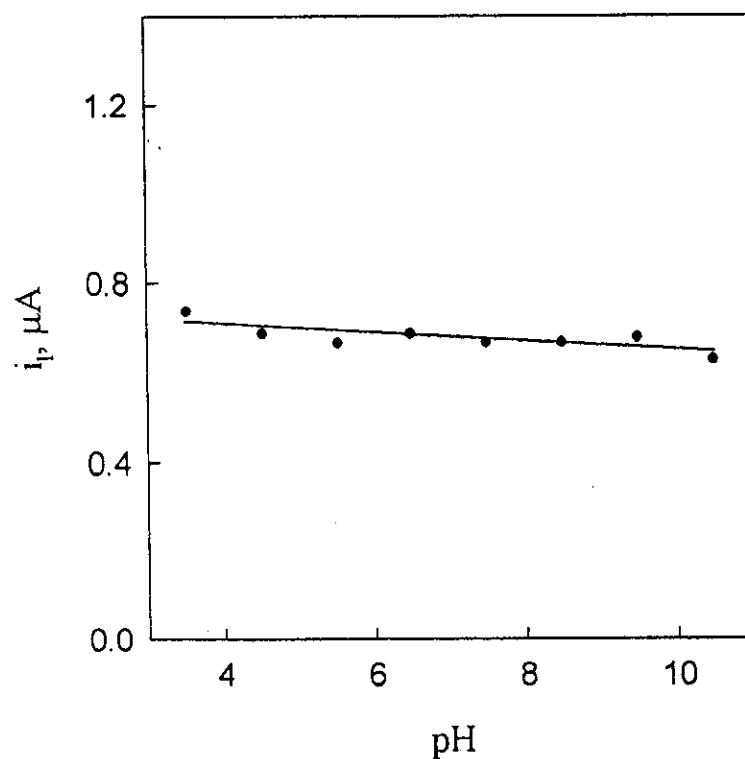


Fig. 20B: i_l -pH plot of ofloxacin.

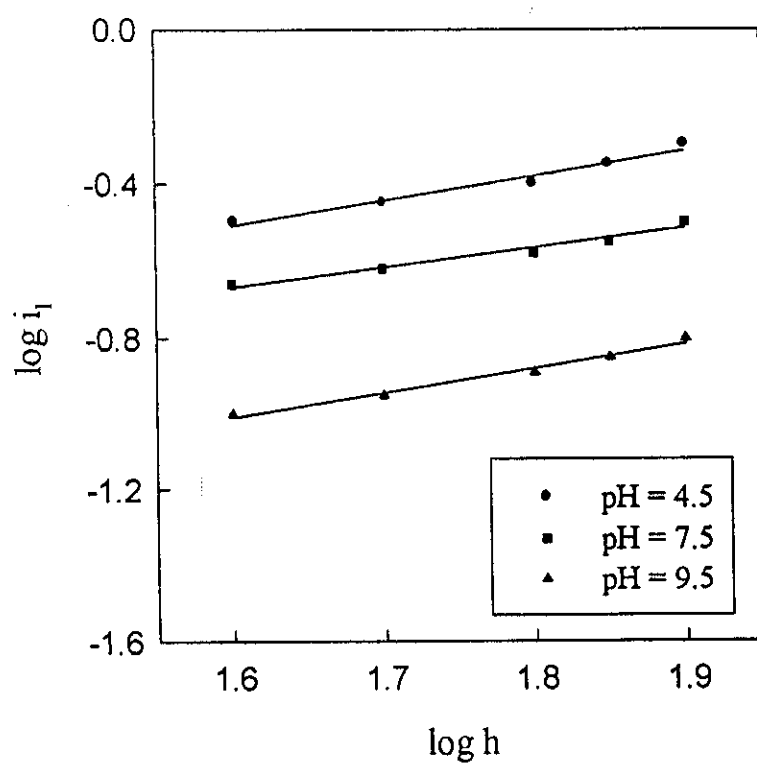


Fig. 20C: $\log h$ - $\log i_l$ plots of ofloxacin at different pH values.

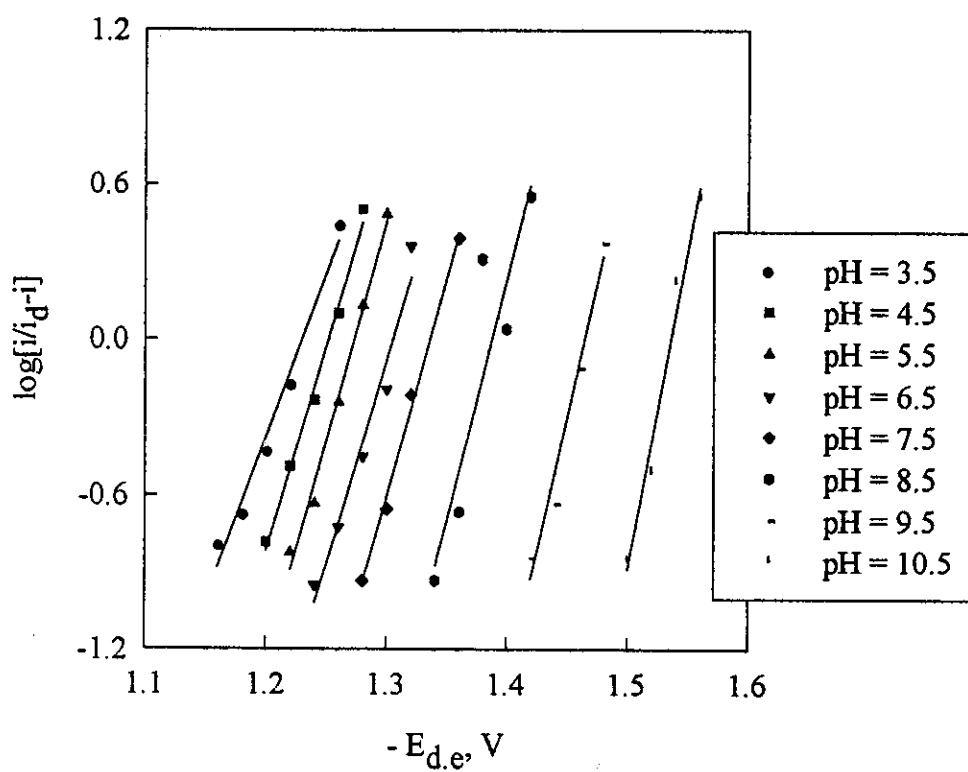


Fig. 20 D: $\log [i/i_d-i]$ - ($-E_{d,e}$) plots of ofloxacin at different pH values.

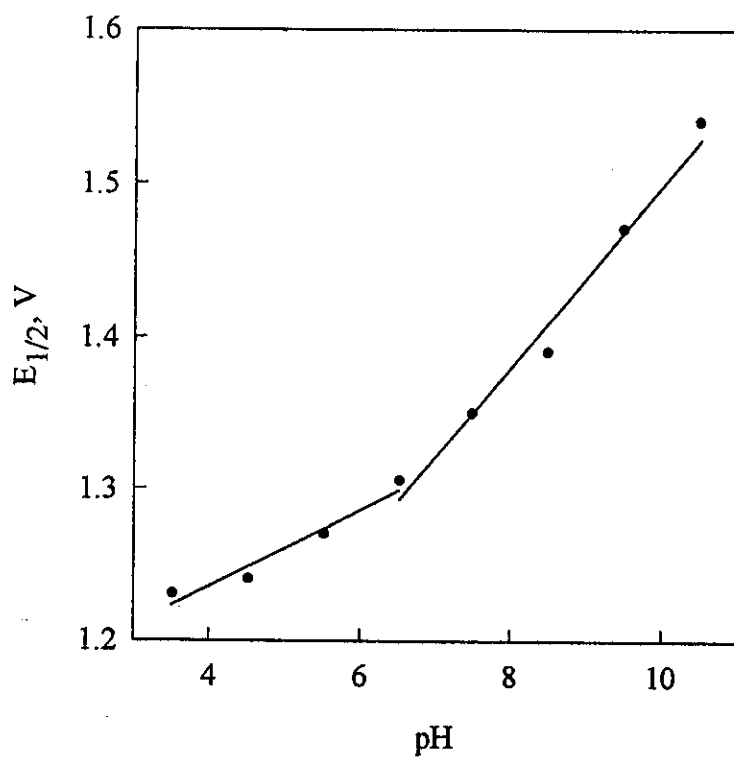


Fig. 20 E: $E_{1/2}$ -pH plot of ofloxacin.

3.2.1.2. Determination of ofloxacin by using DC-polarograph

Trials for determination of ofloxacin in different media such as sodium perchlorate, acetate buffer, B.R. buffer and phosphate buffer were performed. The most obvious wave was shown in B.R. buffer pH 3.5. A stock solution of ofloxacin 1×10^{-3} M was prepared and different concentrations were obtained by accurate dilution. The polarograms of the final samples were recorded three times for each concentration showing the variation in the wave current with concentration Fig. 21(A and B). The detection limit is 1.0×10^{-5} M (3.61 $\mu\text{g/ml}$). The recovery is calculated to be 98.63 ± 0.47 , Table 15.

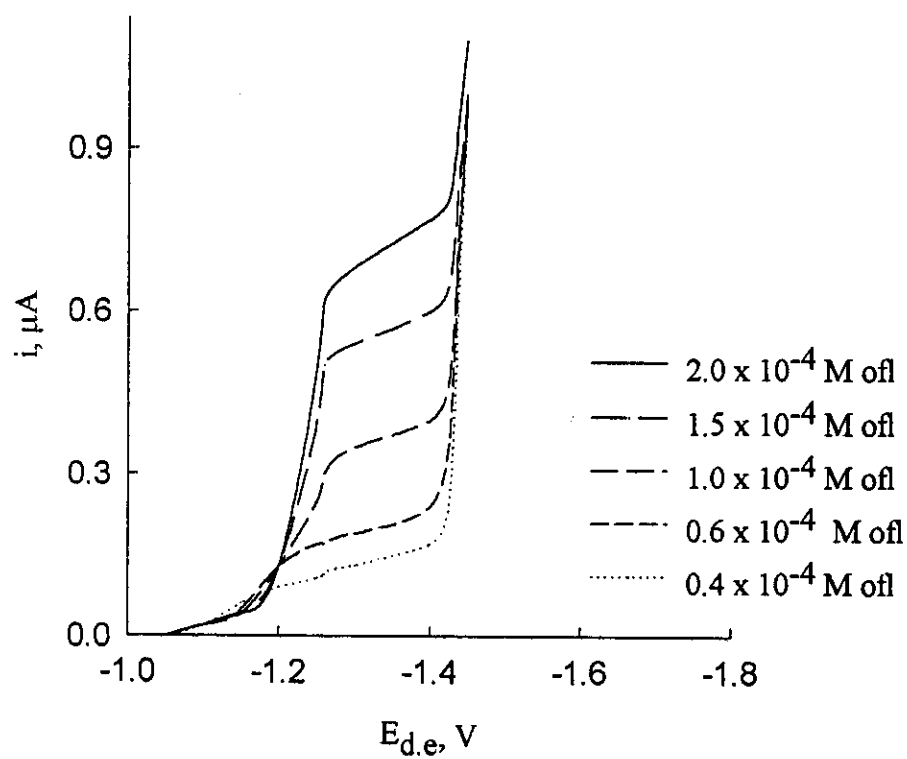


Fig. 21 A: DC polarograms of different concentrations of ofloxacin.

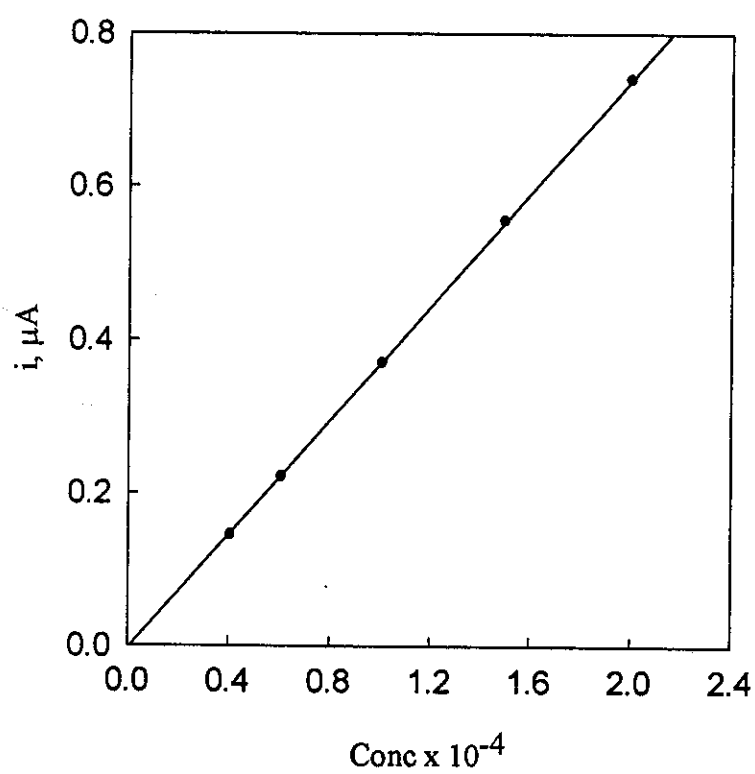


Fig. 21 B: Calibration curve of ofloxacin

Table 15:

Assay of different concentration of ofloxacin in B.R. buffer solution of pH = 3.5 using DC polarography.

Conc. Taken M	Current μA	Conc. Found M	Recovery %	S.D
0.4 x 10 ⁻⁴	0.144	3.890 x 10 ⁻⁵	97.3	0.808
	0.142	3.840 x 10 ⁻⁵	95.9	
	0.144	3.890 x 10 ⁻⁵	97.3	
0.6 x 10 ⁻⁴	0.218	5.890 x 10 ⁻⁵	98.1	0.500
	0.219	5.920 x 10 ⁻⁵	98.6	
	0.220	5.950 x 10 ⁻⁵	99.1	
1.0 x 10 ⁻⁴	0.369	0.997 x 10 ⁻⁴	99.7	0.416
	0.368	0.995 x 10 ⁻⁴	99.5	
	0.366	0.989 x 10 ⁻⁴	98.9	
1.5 x 10 ⁻⁴	0.551	1.489 x 10 ⁻⁴	99.3	0.200
	0.550	1.486 x 10 ⁻⁴	99.1	
	0.549	1.484 x 10 ⁻⁴	98.9	
2.0 x 10 ⁻⁴	0.738	1.994 x 10 ⁻⁴	99.7	0.451
	0.735	1.986 x 10 ⁻⁴	99.3	
	0.731	1.976 x 10 ⁻⁴	98.8	
Recovery = 98.63 ± 0.47				

3.2.1.3. Effect of Metal Complexes:

The effect of ofloxacin on the polarographic behaviour of Cd(II), Zn(II) ions in 0.1 M NaClO₄:

The polarographic behaviour of the simple metal of 2×10^{-4} M Cd(II) and Zn(II) in 0.1 M sodium perchlorate were recorded Fig. 22(A-B). Logarithmic analysis of metal ions waves revealed the quasereversibil nature of the electrode processes, Fig. 22(A-D). The αn_a values are determined to be 0.76 and 0.80 for Zn(II) and Cd(II) ions; respectively. Generally, as the concentration of legend increases, the diffusion current of the metal decreases which is attributed to the increased bulk of the complexed ions. Also on increasing the concentration of the ligand the irreversibility of the electrode processes increase, which is confirmed from the decrease of αn values, Table 16-17. The polarographic waves of the metal ions showed a cathodic shift indicating complex formation.

The plot of $\Delta E_{1/2} = [E_{1/2(s)} - E_{1/2(c)}]$ versus $\log C_X$ gives a linear correlation with slope equal to j ($0.0591/\alpha n$) from which j was found to be 1:2 with Cd(II) andalsowith Zn(II) Fig. 22 (E-F).

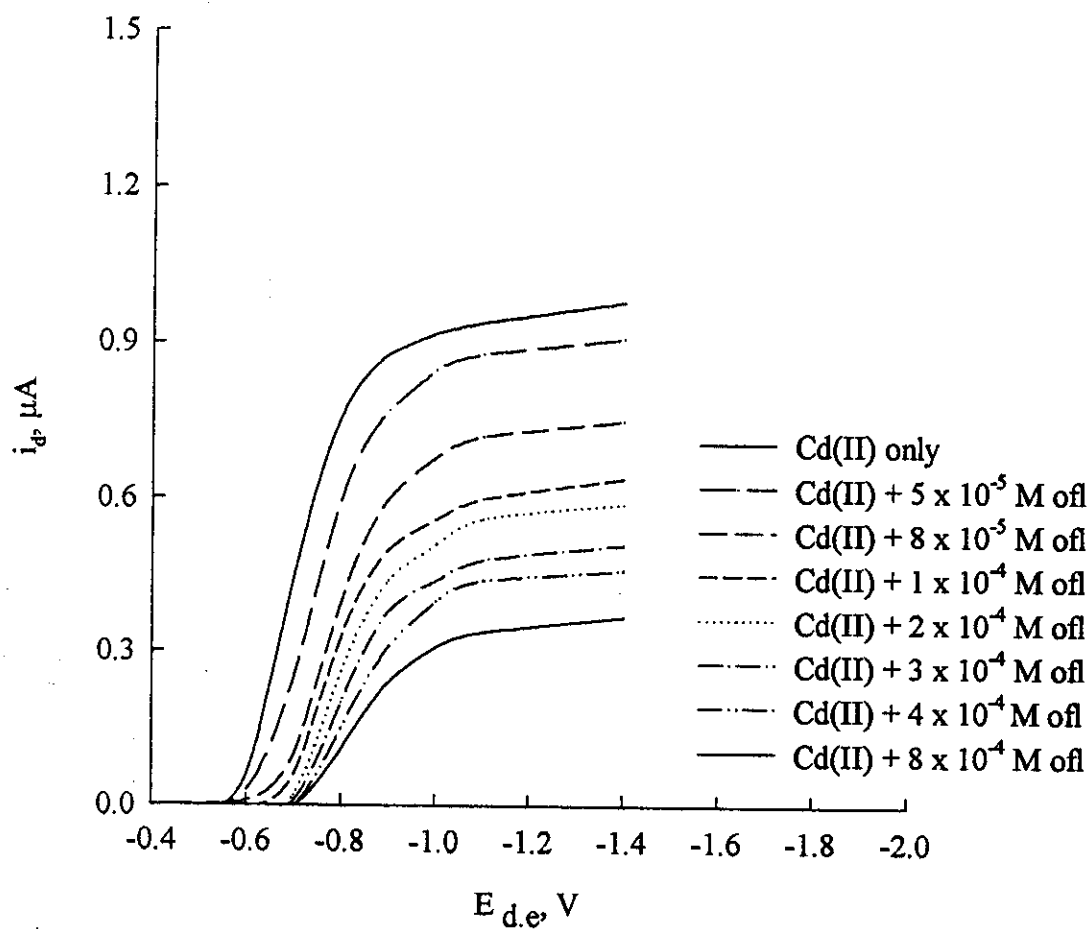


Fig. 22 A: DC polarograms of Cd(II) - ofloxacin

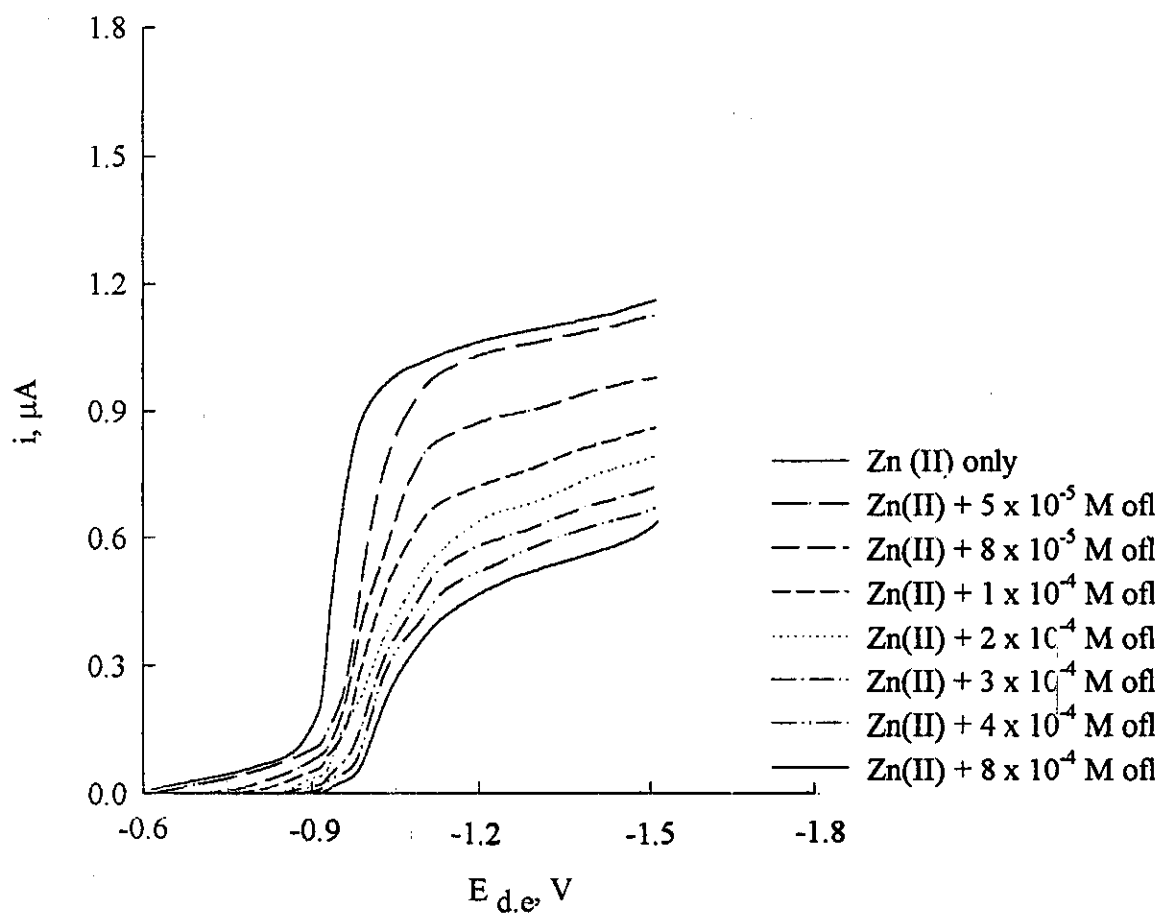


Fig. 22 B: DC polarogram of Zn (II)-ofloxacin complex.

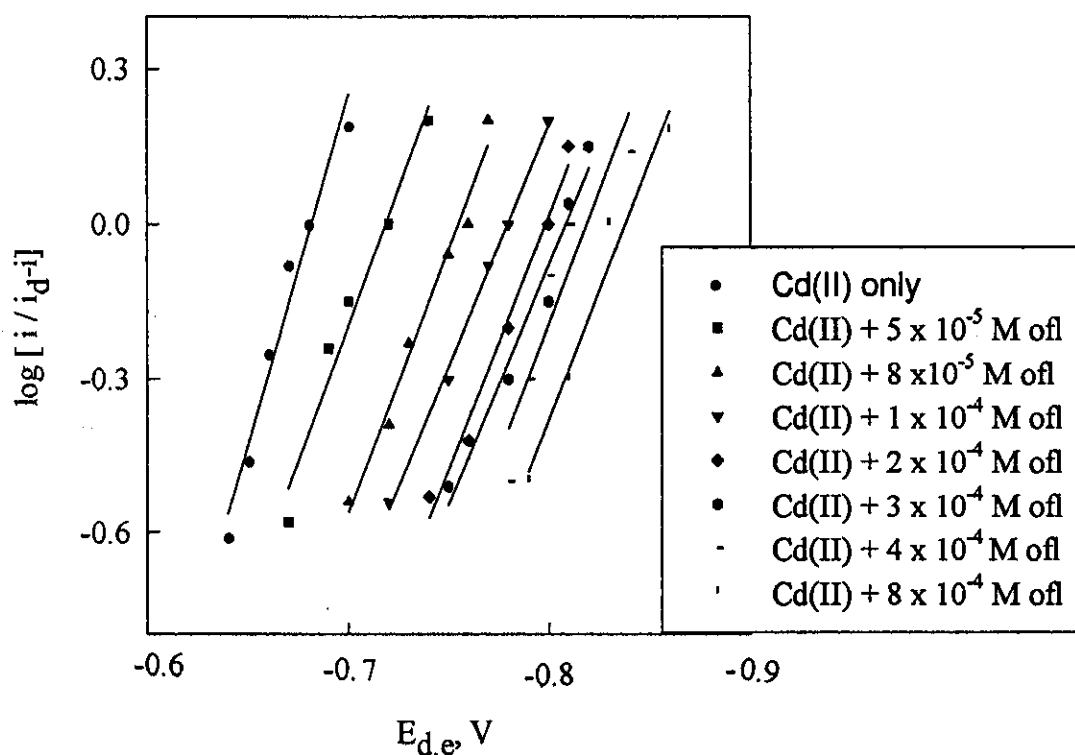


Fig. 22C: Cd II - ofloxacin complex in 0.1 M sodium berchlorate

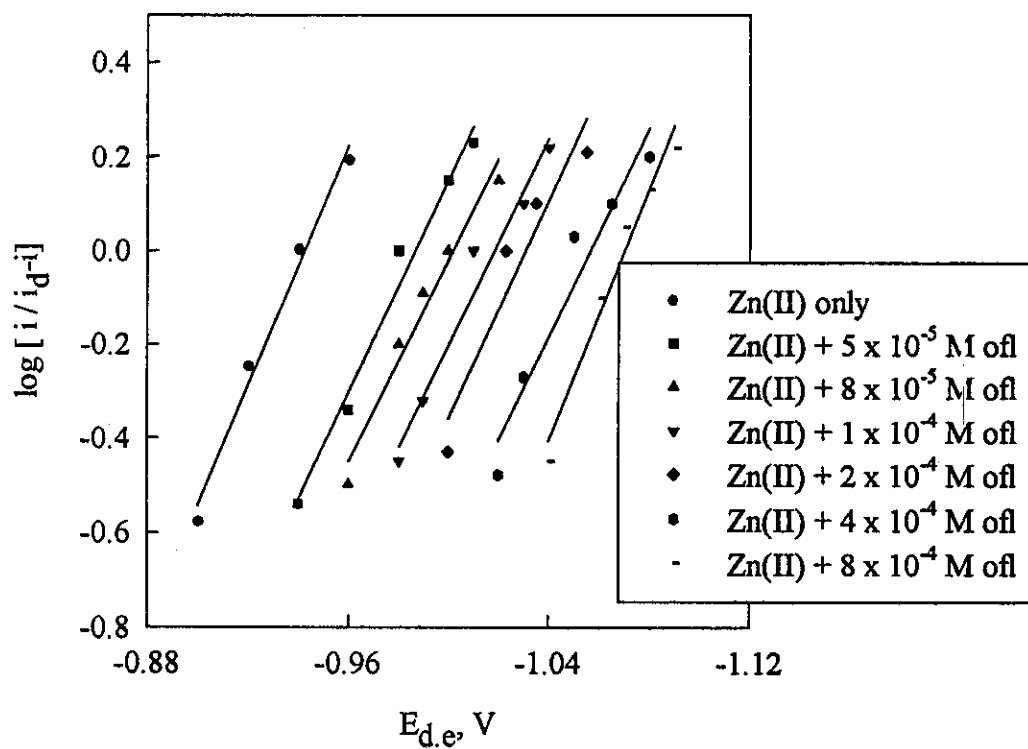


Fig. 22D: Zn(II) - ofloxacin complex in 0.1 M sodium berchlorate

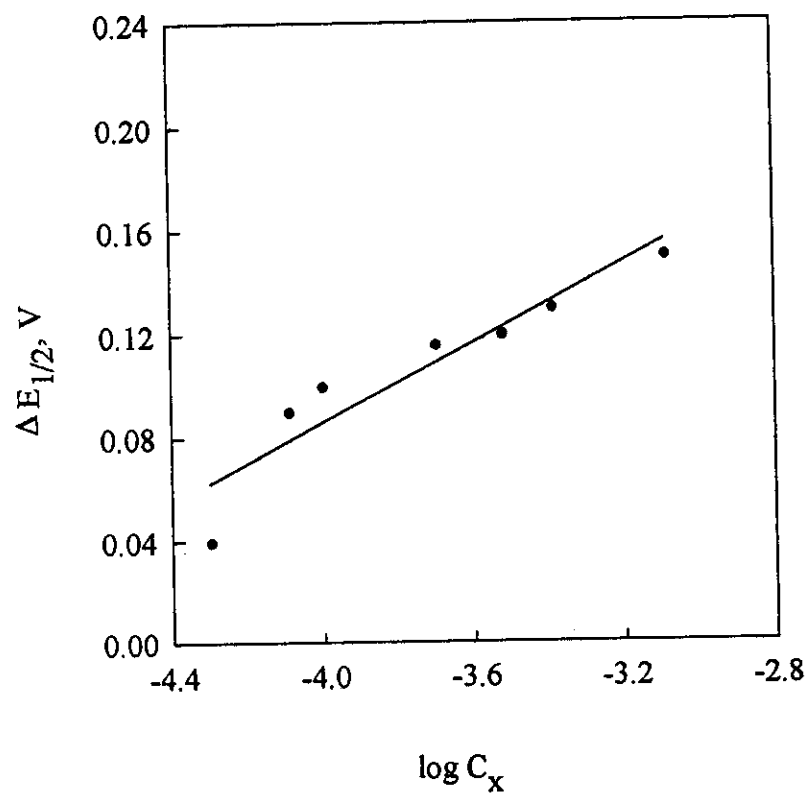


Fig. 22E: $\Delta E_{1/2}$ - $\log C_x$ plot of Cd(II)-ofloxacin complex

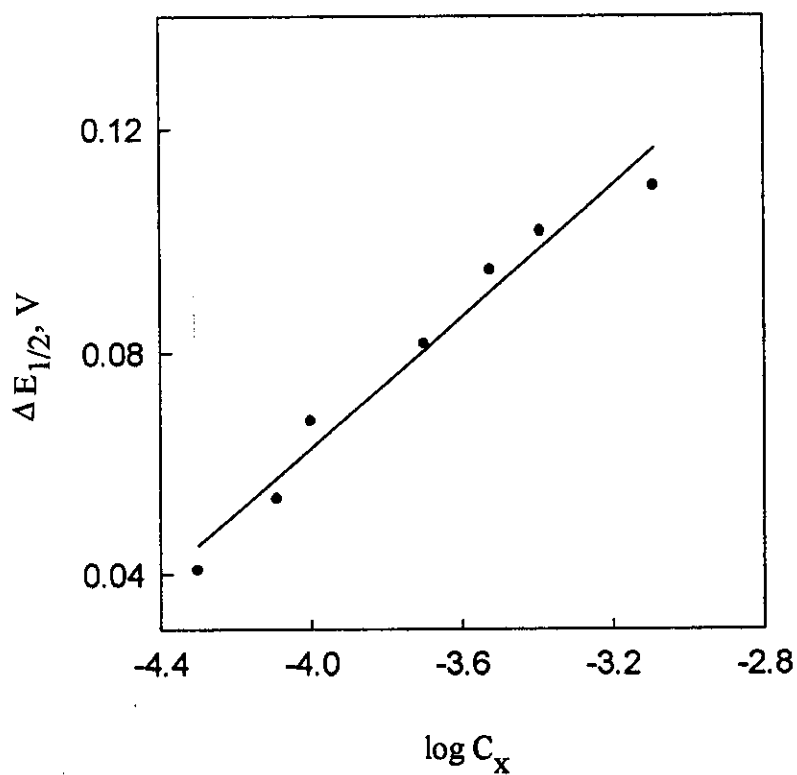


Fig. 22F: $\Delta E_{1/2}$ - $\log C_x$ plot of Zn(II)-ofloxacin complex

Table 16:

Polarographic data obtained for Cd(II)-ofloxacin complexes in 0.1 M NaClO₄

L.conc	i _d	-ΔE _{1/2}	an	stoichiometry
Zero	0.90	0.000	0.80	1 : 2
5 x 10 ⁻⁵	0.85	0.040	0.63	
8 x 10 ⁻⁵	0.68	0.090	0.60	
1 x 10 ⁻⁴	0.57	0.100	0.55	
2 x 10 ⁻⁴	0.53	0.116	0.47	
4 x 10 ⁻⁴	0.44	0.130	0.45	
8 x 10 ⁻⁴	0.31	0.145	0.44	

Table 17:

Polarographic data obtained for Zn(II)-ofloxacin complexes in 1.0 M NaClO₄

L.conc	i _d	-ΔE _{1/2}	An	stoichiometry
Zero	1.09	0.000	0.76	1 : 2
5 x 10 ⁻⁵	1.05	0.041	0.67	
8 x 10 ⁻⁵	0.91	0.054	0.63	
1 x 10 ⁻⁴	0.80	0.068	0.59	
2 x 10 ⁻⁴	0.70	0.082	0.56	
4 x 10 ⁻⁴	0.60	0.102	0.52	
8 x 10 ⁻⁴	0.53	0.109	0.47	

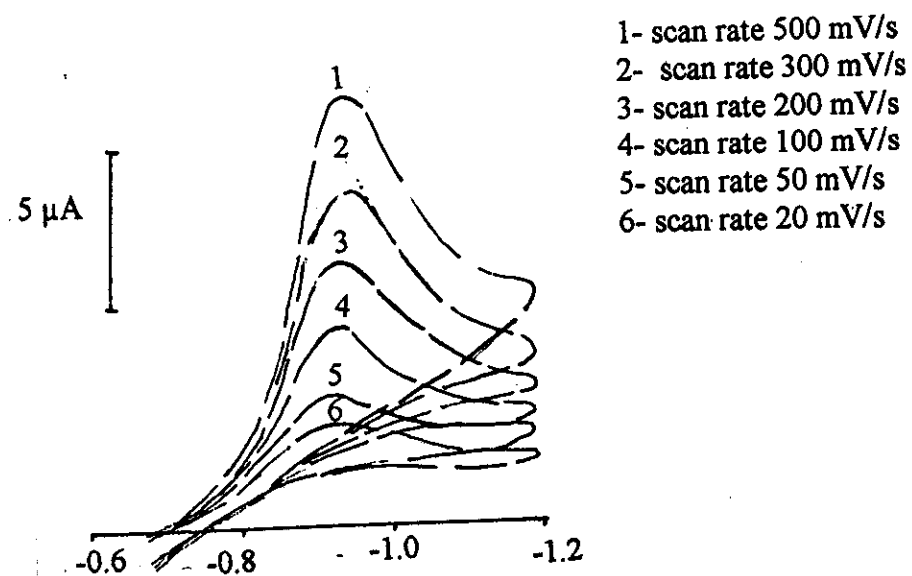
3.2.1.4. Cyclic Voltammetry:

The cyclic voltammograms of 1×10^{-4} M ofloxacin were recorded at the glassy carbon electrode in B.R. buffer solutions of pH 3.4, 7.0 and 10.0 containing 20% (v/v) ethanol at different scan rates from 20 to 500 mV/sec. The voltammograms showed one cathodic reduction peak at different pH values, Fig. 23A. The peak potential (E_p) showed cathodic shift on increasing the scan rate that indicated the irreversible nature of the electrode process. Furthermore, the irreversibility is confirmed from the absence of any oxidation peaks in the anodic scan.

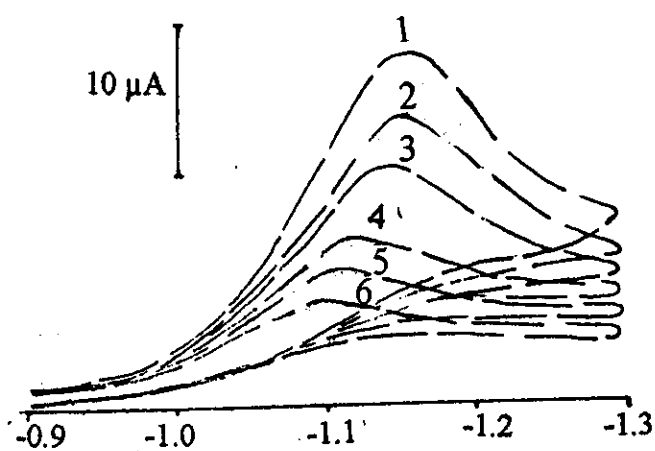
The plots of i_p as a function of square root of scan rate $v^{1/2}$ showed linear correlations slightly deviating from the origin confirming that the electrode process of ofloxacin is controlled mainly by diffusion with some adsorption contribution Fig. 23B.

Plotting of E_p against $\ln v$ at the given pH showed linear correlations with slope values proportional to (αn_a) , Fig. 23C. From these slopes, the transfer co-efficient α were calculated for the probable values of n_a , Table 18. Inspection of the data showed that n_a is equal to 2 which indicate that the rate determining step of the electrode process may involve two electrons. These results are in good agreement with those obtained from DC-polarographic technique.

1- pH = 3.4



2- pH = 7.0



3- pH = 10.0

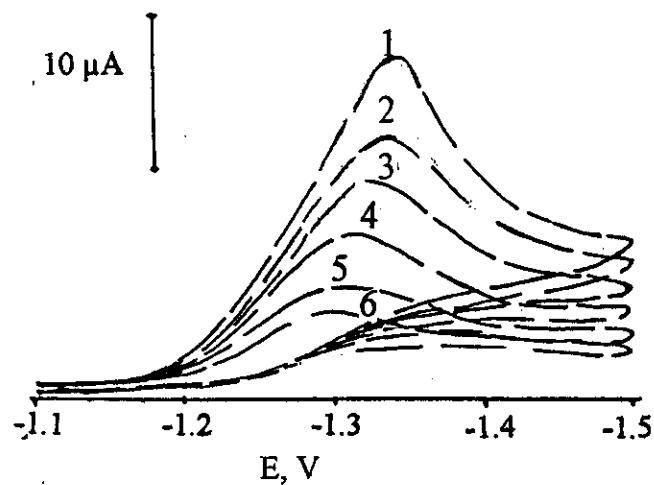


Fig. 23A : Cyclic voltammetric behaviour of ofloxacin in B.R. buffer solutions of different pH values.

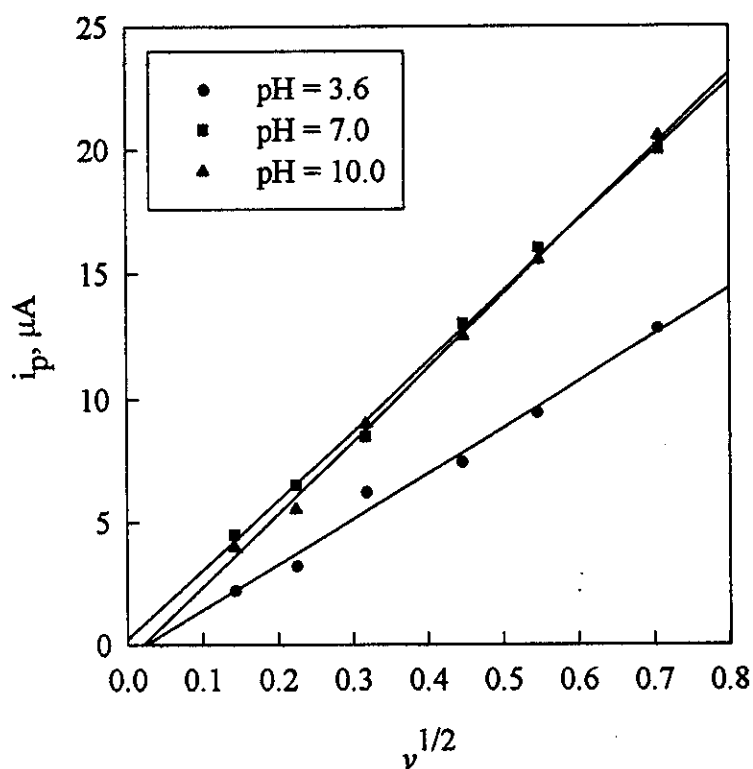


Fig. 23B: i_p - $v^{1/2}$ plots of ofloxacin at different pH values

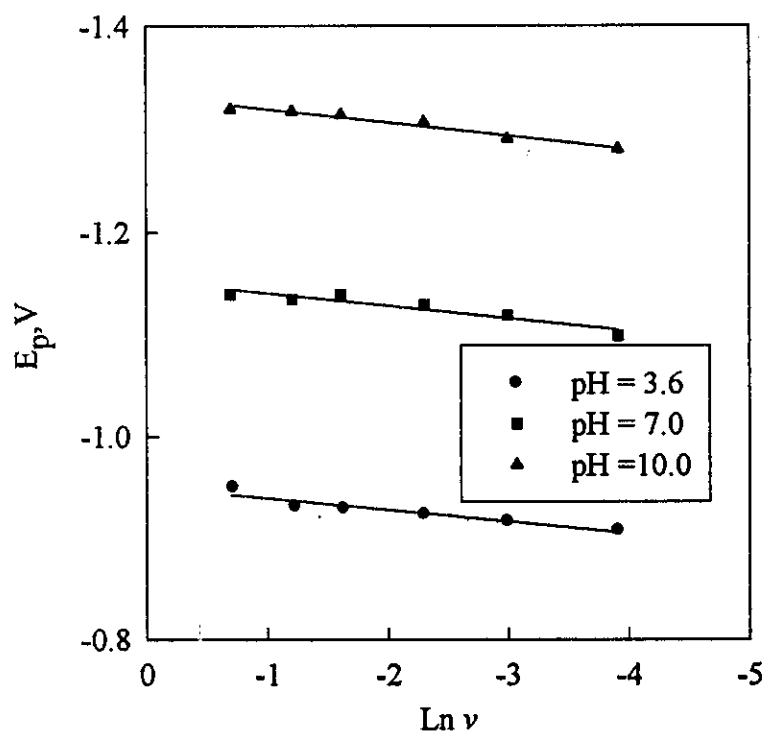


Fig. 23C: E_p - $\ln v$ plots of ofloxacin at different pH values

Table 18:

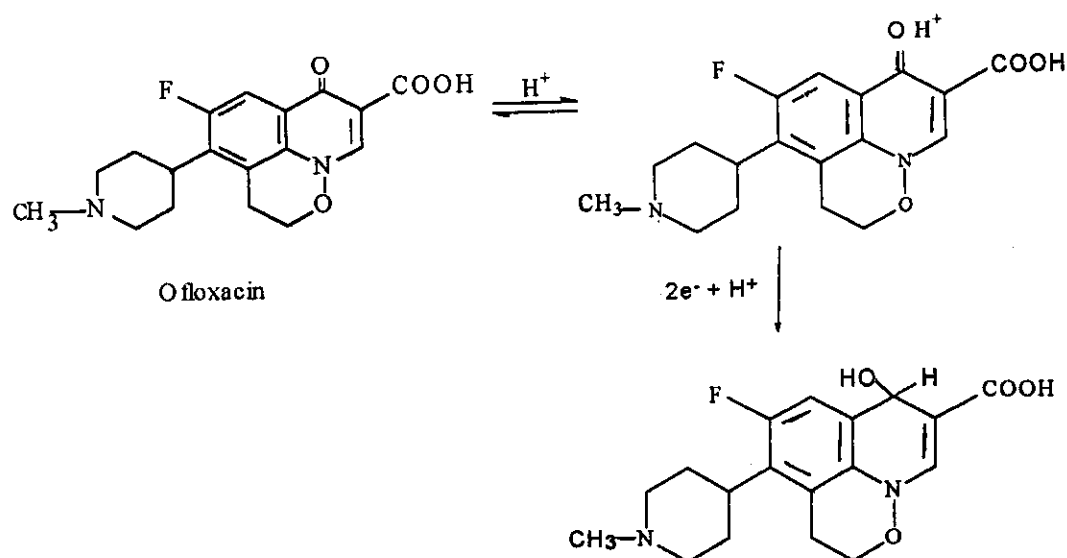
Cyclic voltammetry data for 1×10^{-4} M ofloxacin in aqueous buffer solution of different pH values containing 20% (v/v) ethanol, at 25°C.

pH	Scan rate (mV/s)	ip μA	-Ep V	$\delta E_p/\delta l$ mv	α	
					na=1.0	na=2.0
3.4	500	12.85	0.950	0.0116	1.108	0.554
	300	9.50	0.931			
	200	7.50	0.929			
	100	6.25	0.923			
	50	3.25	0.916			
	20	2.25	0.907			
7.0	500	20.00	1.140	0.0121	1.062	0.531
	300	16.00	1.135			
	200	13.00	1.140			
	100	8.50	1.130			
	50	6.50	1.120			
	20	4.50	1.100			
10.0	500	20.50	1.319	0.0131	0.981	0.490
	300	15.00	1.317			
	200	12.50	1.314			
	100	9.00	1.306			
	50	5.50	1.290			
	20	4.00	1.280			

2.2.1.5. The Electrode Reaction

The polarographic behaviour of the investigated compound was recorded in aqueous buffer solutions of different pH values containing 20 % (v/v) ethanol. The recorded polarograms displayed single irreversible reduction wave in the entire pH range. The limiting current (i_l) was found pH-independent and the half-wave potential ($E_{1/2}$) shifted to more negative potentials on increasing the pH of the electrolysis solution. The number of protons (Z_H^+) involved in the rate determining step was found to be unity whereas, the number of electrons (n_a) is two.

From controlled potential coulometry (CPC), the number of electrons was determined to be 2.0 electrons. Therefore, the electrode mechanism could take place in accordance with the only reported⁽⁶⁸⁾.



3.2.1.6. Cathodic Adsorption Square Wave Stripping Voltammetry (CAdSWSV) of ofloxacin

DC-polarographic and cyclic voltammetric studies indicated weak adsorption of ofloxacin and the effective interfacial accumulation of its film at the electrode surface. In the present study square wave stripping voltammetry is used for the electroanalytical determination of ofloxacin.

1. Optimization of the experimental and instrumental conditions

Both of the experimental and instrumental conditions are optimized here for the quantitative determination of ofloxacin using CAdSWSV.

1- Effect of pH on the cathodic adsorptive square wave stripping peak of ofloxacin

The cathodic adsorptive stripping voltammetric current of 1.0×10^{-6} M ofloxacin was recorded as a function of potential in a series of Britton Robinson buffer solutions of pH 2.0-11.5. The obtained peaks were due to the reduction of the adsorbed ofloxacin at the electrode surface. A well developed peak was observed at pH 4.2, Fig. 24.

2- Effect of supporting electrolytes on the CAdSWSV peak current

The effect of some supporting electrolytes on the CAdSWSV peak was recorded. The most suitable medium for the developing of a well peak current of ofloxacin was B.R. buffer solution of pH 4.2, Fig. 25.

3- Effect of deposition potential

The influence of deposition potential was studied over the potential range from -200 to -1000 mV. The study showed that the most suitable deposition potential is -200 mV, Fig. 26.

4- Effect of frequency

On changing the value of the frequency from 500 to 5000 Hz, the height of the formed peak is also changed. By studying the effect of frequency, 5000 Hz was found to give the maximum response, Fig. 27.

5- Effect of pulse width

The effect of pulse width on the CAdSWSV peak height was studied. On changing the value of pulse width in the range from 10 to 100 mV. For ofloxacin the analytical determination was performed at pulse width equal to 100 mV, Fig. 28.

6- Effect of pulse height

The effect of pulse height on the CAdSWSV peak height was studied in the range of 10 to 100 mV. The peak current formed was found to be directly proportional to the pulse height, Fig. 29. A sharp peak height of ofloxacin was obtained at pulse height equal to 100 mV.

7- Effect of deposition time

The peak current was recorded at different time intervals. The most suitable peak current was obtained at 300 sec, Fig. 30.

8- Effect of scan rate

On studying the effect of different scan rates in the range from 1.0 to 10.0 mV/sec, a scan rate of 10 mV/s give the maximum response as in Fig. 31.

2. Quantitative determination of ofloxacin by CAdSWSV

The applicability of the cathodic adsorptive square wave stripping voltammetric technique as an analytical method for the determination of

ofloxacin was tested by measuring the CAdSWSV peak current as a function of concentration Fig. 32.

Calibration graph

A stock solution of ofloxacin 1×10^{-3} M was prepared and the different concentrations were obtained by accurate dilution. The stripping peak current of the final samples were recorded under the optimum experimental conditions. The variation of the peak current with concentration was represented in Fig. 33. In the present study, the slope of the calibration curve, (a) is 9.9×10^4 and the intercept (b) is 0.0106, Table 20.

The precision was determined from four repeated measurements of different concentrations of ofloxacin. The mean recovery and the standard deviation were calculated.

Detection Limit

In the present study, the standard deviation of the blank S.D. is equal to 2.0×10^{-5} , $a = 9.9 \times 10^4$ and the detection limit is found to be 6.1×10^{-10} M (2.2×10^{-4} $\mu\text{g/ml}$).

Determination of ofloxacin in its dosage form:

The proposed procedure is successfully applied for the analysis of ofloxacin in its dosage form. The precision is determined from four repeated measurements of two different concentrations of each reported dosage form, Table 21. The mean recovery of ofloxacin in ofloxacin tablets is $101.38 \% \pm 0.69$ and $100.0 \% \pm 0.55$ for kiroll tablets, Table 22. The agreement between the two procedures confirms the validity of the CAdSWSV technique in the analysis of ofloxacin in its dosage forms under the suitable experimental and instrumental conditions.

Table 19:

Cathodic adsorptive square wave stripping peak current (i_p) of 1.0×10^{-6} M ofloxacin in B.R. buffer solution of pH 4.2 at different conditions.

Deposition time t_d , Sec	Deposition potential $-E_d$, mV	Scan rate mV/s	Pulse height mV	Pulse width mV	i_p μA
Effect of E_d					
300	200	1.0	20	50	0.1021
	400				0.0731
	600				0.0812
	800				0.0618
	1000				0.0787
Effect of pulse width					
300	200	1.0	20	100	0.1064
				50	0.1043
				20	0.1021
				10	0.0591
Effect of pulse height					
300	200	1.0	100	200	0.1389
			50		0.1321
			20		0.1064
			10		0.0576
Effect of t_d					
360	200	1.0	100	100	0.1149
300					0.1389
180					0.0962
60					0.0855
30					0.0294
Effect of scan rate					
300	200	0.1	100	100	0.1072
		1.0			0.1339
		2.0			0.1360
		5.0			0.1349
		10.0			0.1550

Table 20:

Assay of ofloxacin in B.R. buffer solution of pH 4.2 using square wave stripping voltammetry at: $E_d = -200$ mV, $t_d = 300$ sec, scan rate = 10 mV/sec, pulse height = 100 mV and pulse width = 100 mV.

Conc. Taken M	i _p μA	Conc. Found M	% Recovery (%R)	Av. Conc. (found) M	Mean %R	S.D
1 x 10 ⁻⁶	0.1073	9.768 x 10 ⁻⁷	97.68	9.84 x 10 ⁻⁷	98.4	0.64
	0.1078	9.818x 10 ⁻⁷	98.18			
	0.1082	9.859x 10 ⁻⁷	98.59			
	0.1088	9.919 x 10 ⁻⁷	99.19			
8 x 10 ⁻⁷	0.0899	8.010 x 10 ⁻⁷	100.10	8.01 x 10 ⁻⁷	100.10	0.13
	0.0899	8.010 x 10 ⁻⁷	100.10			
	0.0900	8.020 x 10 ⁻⁷	100.20			
	0.0897	7.989 x 10 ⁻⁷	99.90			
6 x 10 ⁻⁷	0.0700	6.000 x 10 ⁻⁷	101.00	6.00 x 10 ⁻⁷	99.93	0.29
	0.0701	6.010 x 10 ⁻⁷	101.20			
	0.0697	5.969 x 10 ⁻⁷	99.50			
	0.0700	6.000 x 10 ⁻⁷	100.00			
4 x 10 ⁻⁷	0.0500	3.979 x 10 ⁻⁷	99.49	4.07 x 10 ⁻⁷	100.18	0.66
	0.0503	4.030 x 10 ⁻⁷	100.75			
	0.0503	4.030 x 10 ⁻⁷	100.75			
	0.0501	3.989 x 10 ⁻⁷	99.75			
The mean recovery = 99.65 ± 0.34						
Slope = 9.9 x 10 ⁴						
Intercept = 0.0106						
Corr. Coeff. = 0.9808						

Table 21:

Assay of ofloxacin in B.R. buffer solution of pH 4.2 using CAdSWSV at: $E_d = -200$ mV, $t_d = 300$ sec, scan rate = 10 mV/sec, pulse height = 100 mV pulse width = 100 mV.

Name of tablets	Conc. M	ip μ A	Conc. Found M	%R	Av. Conc found M	Mean %R	S.D.
Kiroll	9.0×10^{-7}	0.0990	8.929×10^{-7}	99.21	8.98×10^{-7}	99.83	0.45
		0.0995	8.979×10^{-7}	99.78			
		0.0998	9.010×10^{-7}	100.11			
		0.0999	9.020×10^{-7}	100.22			
	3.0×10^{-7}	0.0400	2.969×10^{-7}	98.99	3.00×10^{-7}	100.17	0.88
		0.0405	3.020×10^{-7}	100.67			
		0.0403	3.000×10^{-7}	100.00			
		0.0406	3.030×10^{-7}	101.00			
The mean recovery = 100.0 % \pm 0.55							
Oflox- acin	7.0×10^{-7}	0.0790	6.909×10^{-7}	98.70	6.97×10^{-7}	99.63	0.75
		0.0795	6.959×10^{-7}	99.42			
		0.0799	7.000×10^{-7}	100.00			
		0.0802	7.030×10^{-7}	100.43			
	5.0×10^{-7}	0.0620	5.192×10^{-7}	103.84	5.16×10^{-7}	103.12	0.63
		0.0615	5.141×10^{-7}	102.83			
		0.0618	5.172×10^{-7}	103.43			
		0.0613	5.121×10^{-7}	102.42			
The mean recovery = 101.38 % \pm 0.69							
Slope = 9.9×10^4							
Intercept = 0.0106							
Corr. Coeff = 0.9808							

Table 22:

Assay of ofloxacin in its dosage forms B.R. buffer solution of pH 4.2 using CAdSWSV at: $E_d = -200$ mV, $t_d = 300$ sec, scan rate = 10 mV/sec, pulse height = 100 mV pulse width = 100 mV.

Brand Name (Producer)	Labeled Conc. (Drug)	% Recovery \pm S.D.	
		Proposed method	Reported method*
Kiroll	200 mg/tablet	100.0 % \pm 0.55 (n = 4)	100.02 \pm 0.37
Ofloxacin	200 mg/tablet	101.38 % \pm 0.69 (n = 4)	101.0 \pm 2.2

*The official method⁽⁷²⁻⁷³⁾

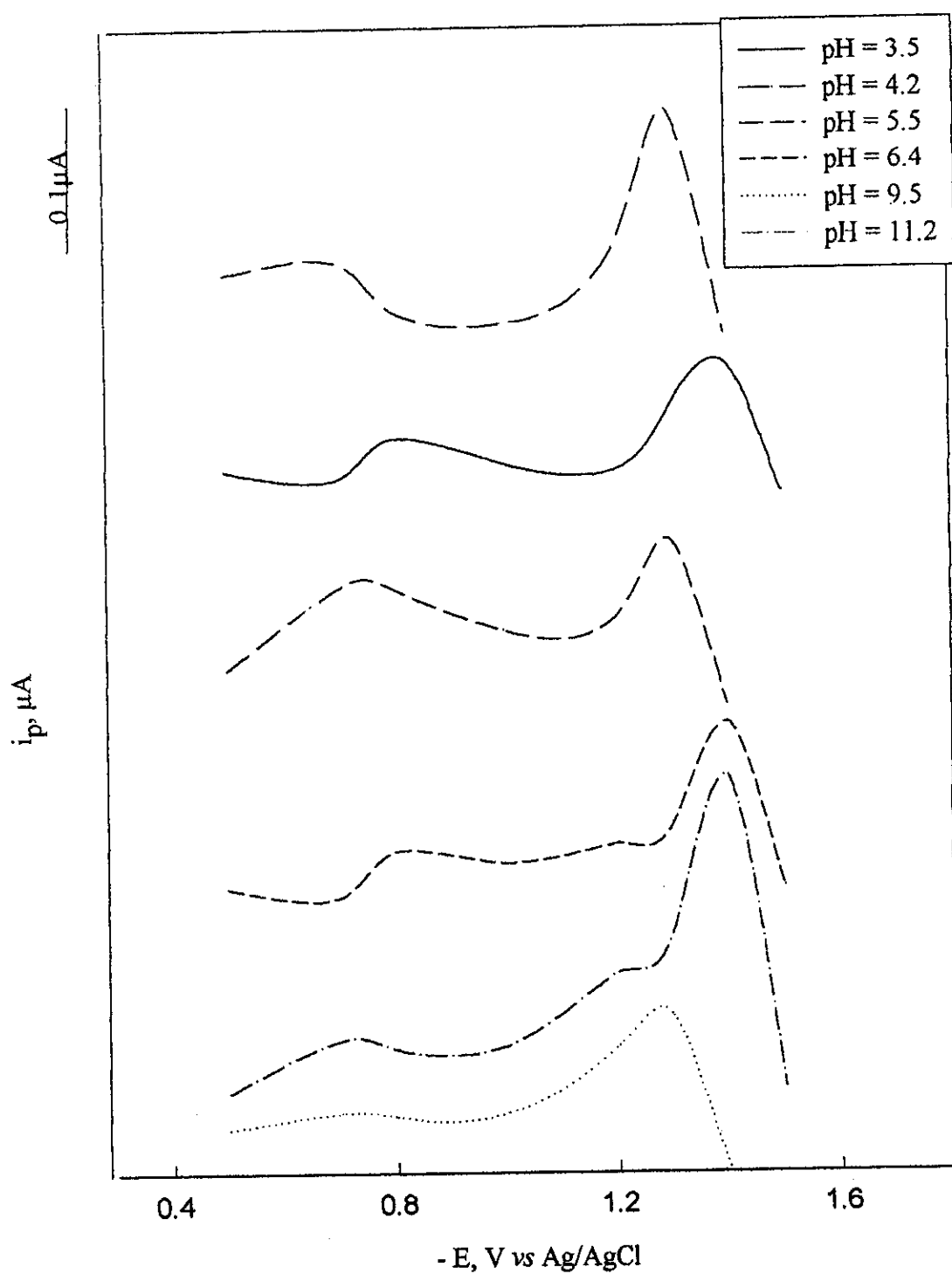


Fig. 24: Effect of pH on the CAdSWSV peak of 1×10^{-6} M of ofloxacin in B.R. buffer solutions: at $t_d = 300$ sec, $E_d = -200$ mV, scan rate = 1.0 mV/s, pulse height = 20 mV and pulse width 50 = mV.

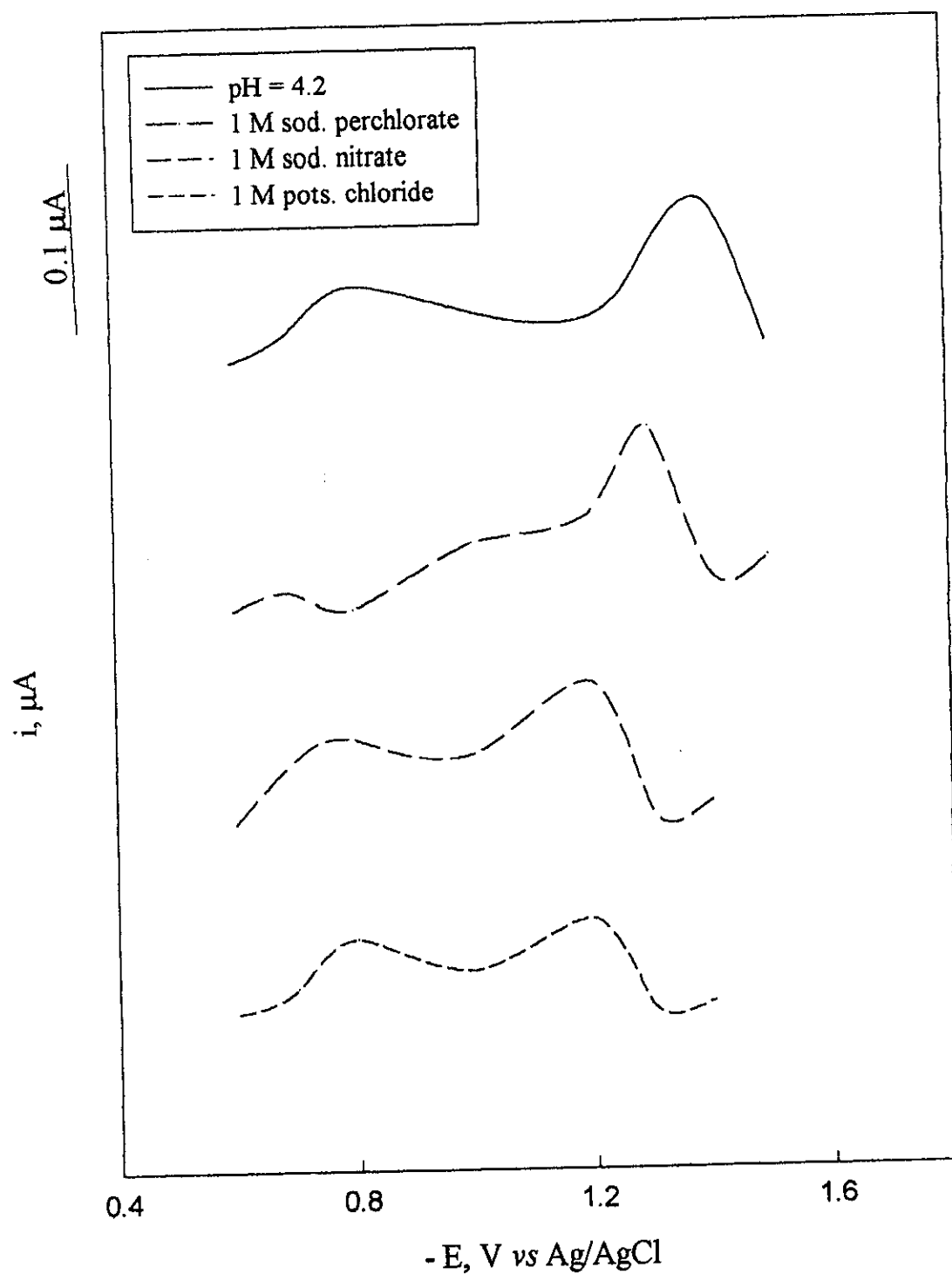


Fig. 25: Effect of supporting electrolyte solutions on the CAdSWSV peak of 1×10^{-6} M of ofloxacin in B. R buffer solution at $E_d = -200$ mV, $t_d = 300$ sec, scan rate = 1.0 mV/s pulse height = 20, pulse width = 50 and frequency = 5000 Hz.

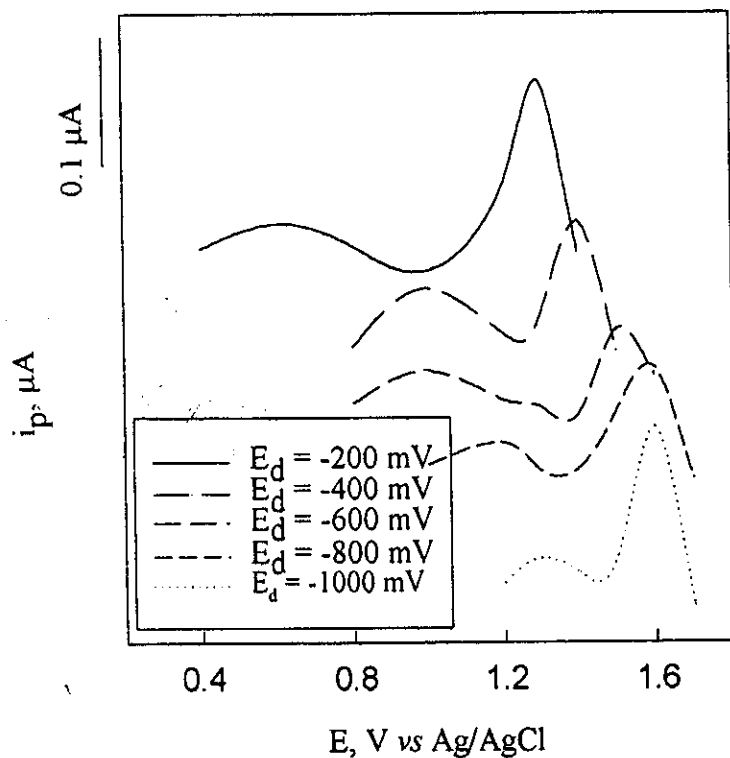


Fig. 26: Effect of E_d on 1×10^{-6} M of ofloxacin in B. R. buffer solution of pH 4.2, scan rate = 1.0 mV/sec, pulse height = 20 mV, pulse width = 50 mV, t_d = 300 sec and frequency = 5000 Hz

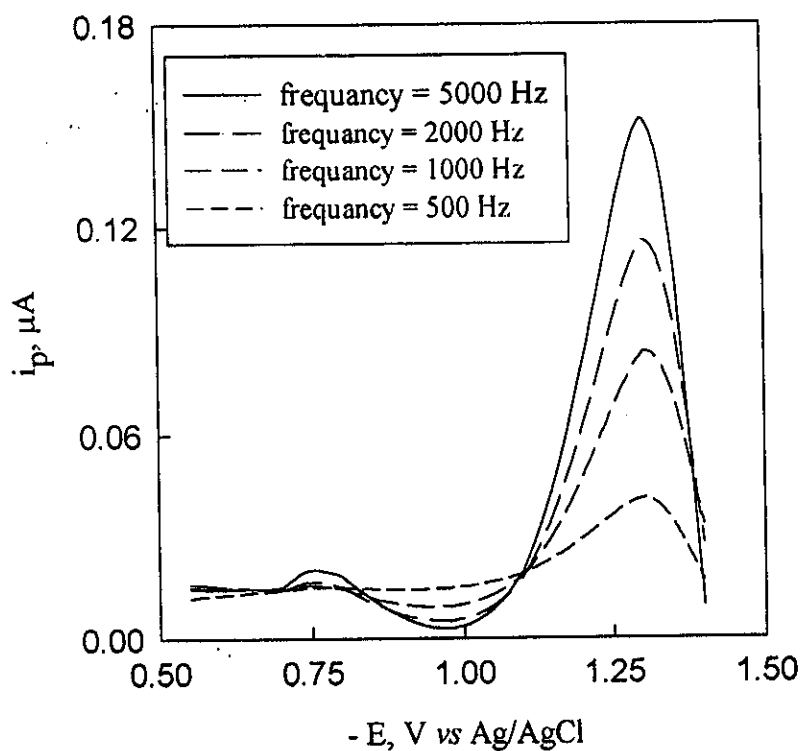


Fig. 29: Effect of frequency on 1×10^{-6} M of ofloxacin in B.R. buffer solution of pH 4.2, scan rate = 1.0 mV/s, E_d = -200 mV, pulse height = 20 mV, pulse width = 50 mV and t_d = 300 sec.

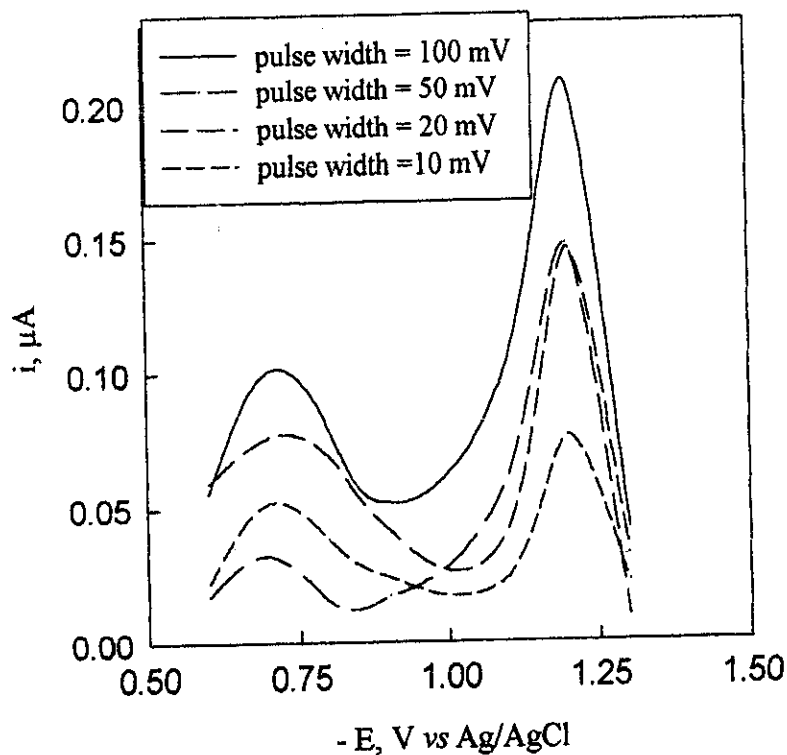


Fig. 28: Effect of pulse width of 1×10^{-6} M of ofloxacin in B.R. buffer solution of pH 4.2, at $E_d = -200$ mV, scan rate = 1.0 mV/s and pulse height = 20 mV, $t_d = 300$ sec and frequency = 5000 Hz.

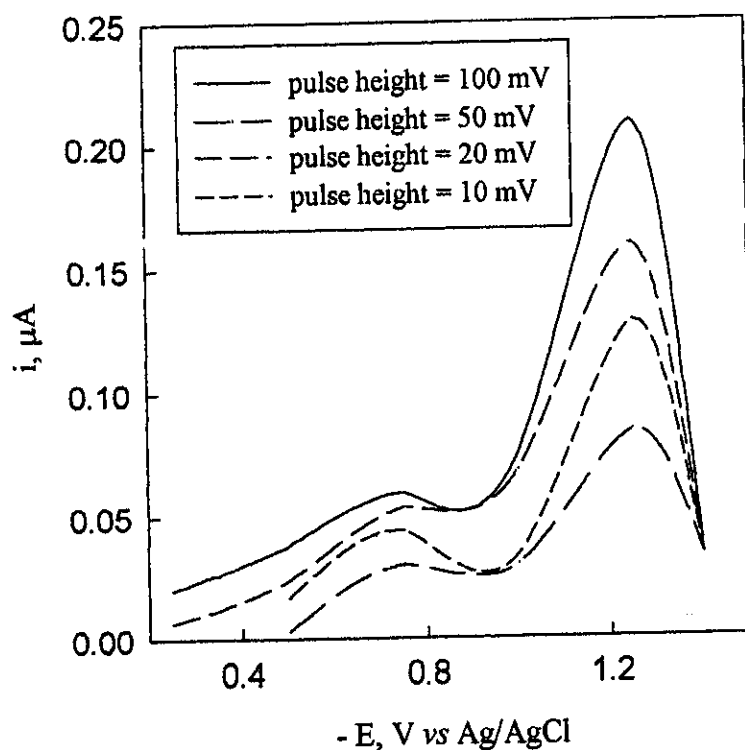


Fig. 29: Effect of pulse height on 1×10^{-6} M of ofloxacin in B.R. buffer solution of pH 4.2, at $E_d = -200$ mV, scan rate = 1.0 mV/s pulse width = 200 mV, $t_d = 300$ sec and frequency = 5000 Hz

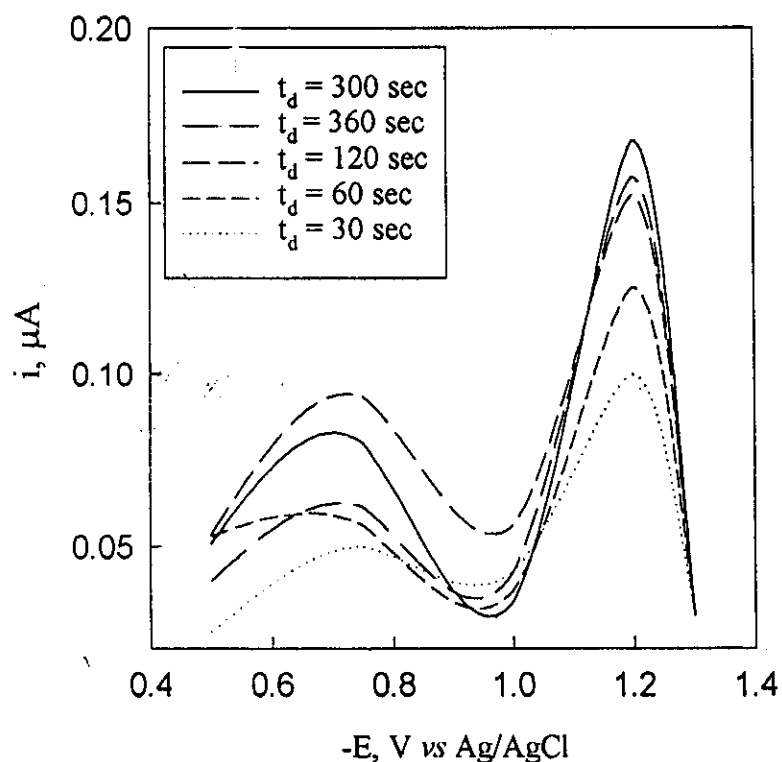


Fig. 30: Effect of t_d of 1×10^{-6} M of ofloxacin in B.R. buffer solution of pH 4.2, at $E_d = -200$ mV, scan rate = 1.0 mV/sec and pulse height = 100 mV, pulse width = 100 mV and frequency = 5000 Hz

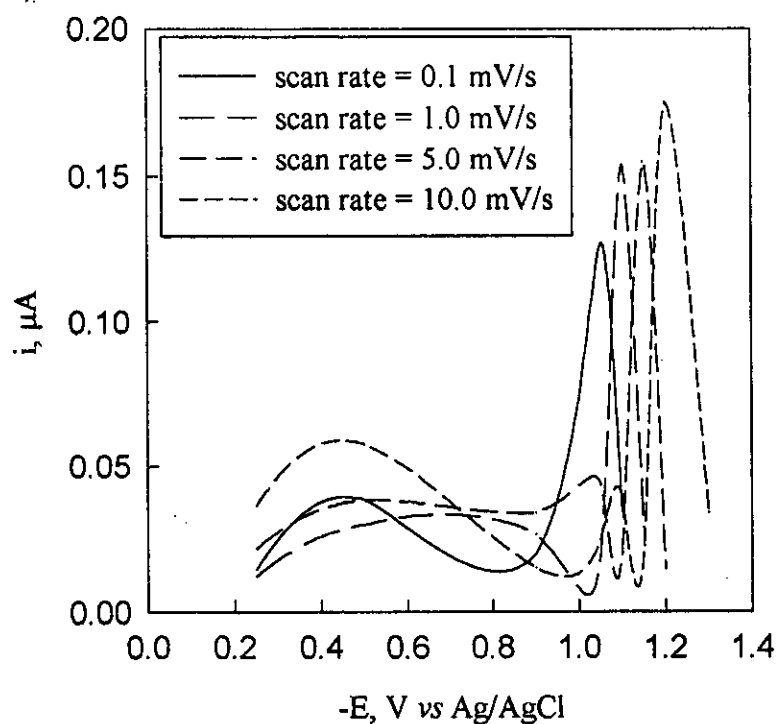


Fig. 31: Effect of scan rate of 1×10^{-6} M of ofloxacin in B.R. buffer solution of pH 4.2 at $E_d = -200$ mV, pulse height 100 mV, pulse width = 100 mV, $t_d = 300$ sec and frequency = 5000 Hz

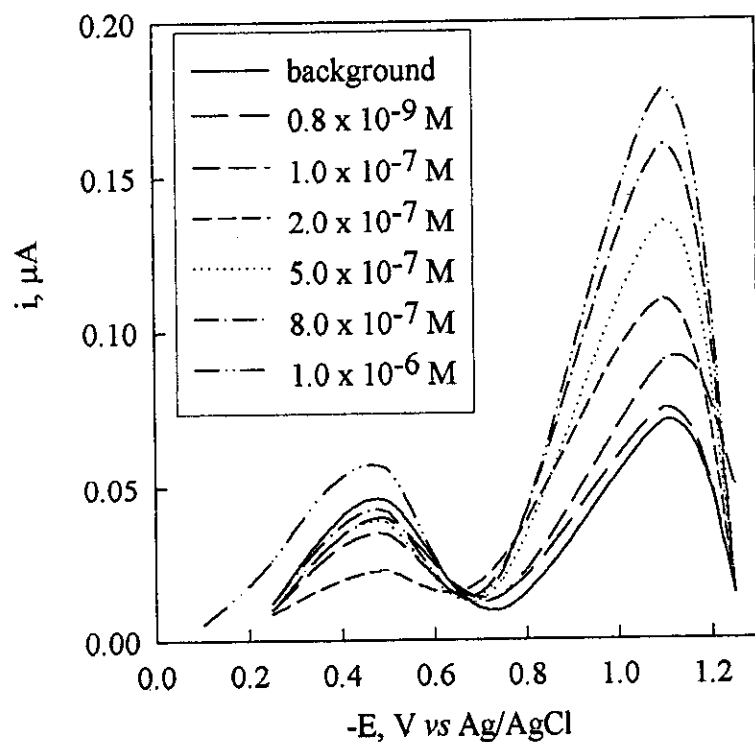


Fig. 32: Effect of concentration of ofloxacin in B.R. buffer solution of pH 4.2 at $t_d = 300$ sec, $E_d = -200$ mV, scan rate = 2.0 mV/s, pulse width = 100 mV, pulse height = 100 mV and frequency = 5000 Hz

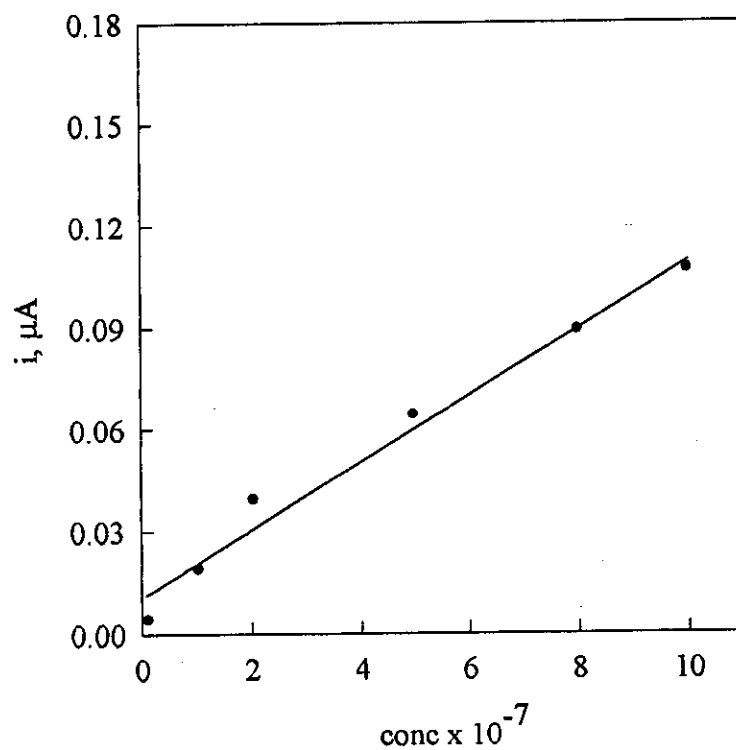


Fig. 33: Calibration curve of ofloxacin under the optimum experimental conditions.

3.2.2. Spectrophotometric studies of the drug complexes in solution

Optimization of the experimental conditions for the formation of complexes between ofloxacin and the analytical reagents under investigation is recorded.

3.2.2.1. Determination of optimum conditions

1. Effect of pH:

On studying the effect of pH on the formation of drug-reagent complex between ofloxacin and reagents, series of solutions containing 1.0 ml of 1.0×10^{-3} M reagent I, II or III, 1.0 ml of 1.0×10^{-3} M of the drug and 5 ml from universal buffer solutions of different pH in the range from 2.5 to 11.5 were mixed. The volume was completed to 10 ml with distilled water. The absorption spectra were recorded using a blank solution prepared by the same way without drug in the same pH value, Fig. 34–36. The optimum pH value were 6.0, 8.5 and 11.0 on using reagents I, II and III, respectively, Table 23.

2. Determination of λ_{\max} of the complex species:

The following sequence must be followed up for determination of the optimum value of λ_{\max} at which each complex species absorbed:

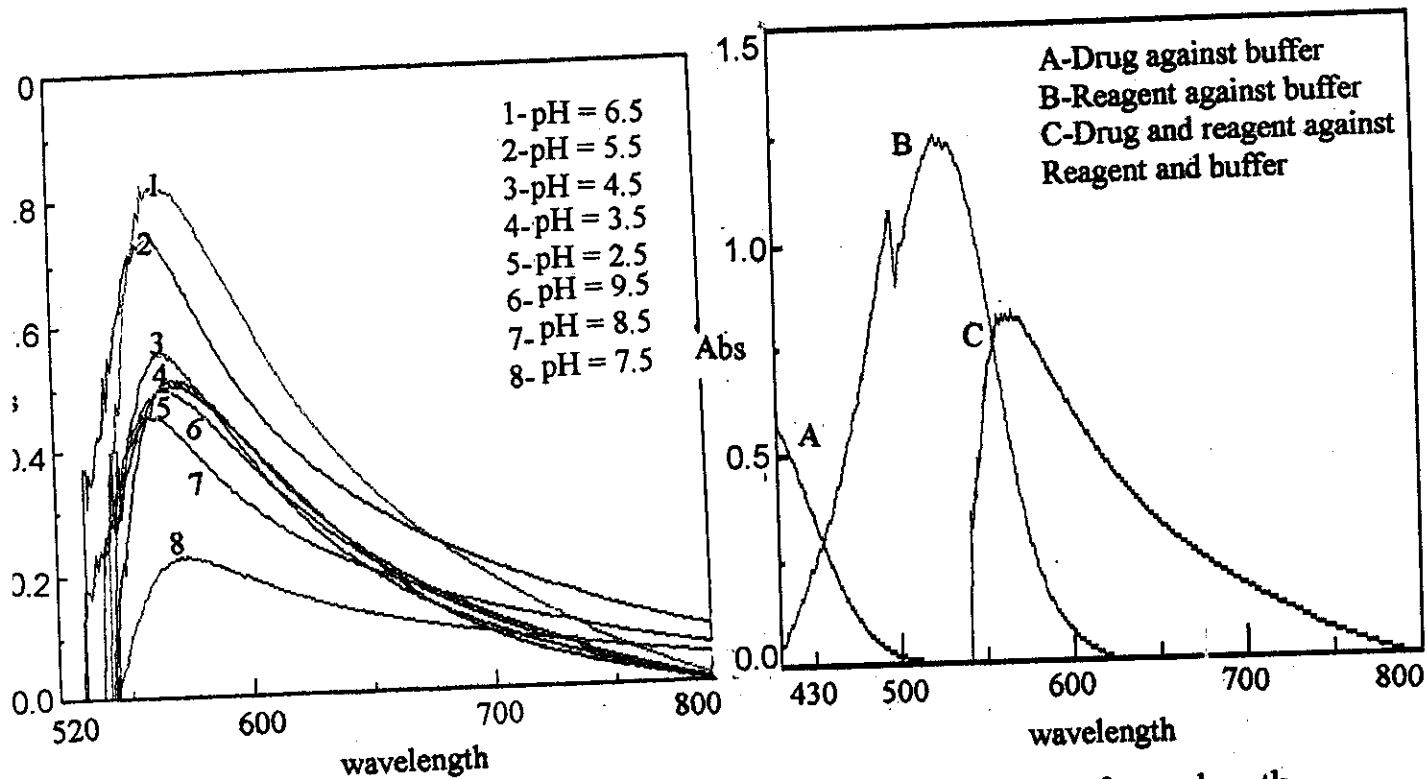
- A) Spectrum of 1.0 ml of 1×10^{-3} M of pure drug at the suitable pH using the same pH as a blank.
- B) Spectrum of 1.0 ml of 1×10^{-3} M of reagents at the same suitable pH value using the same pH as a blank
- D) Spectrum of solution 1.0 ml of 1×10^{-3} M drug and 1.0 ml of 1×10^{-3} M reagents against 1.0 ml of 1.0×10^{-3} M of reagents and buffer as blank.

The above curves (A-C) showed that, the maximum wavelength at which the complexes formed were 560, 530 and 575 nm for the reagents I, II and III, respectively, Fig. 34-36.

Table 23:

Stiochiometry and stability constant of reagent complexes obtained from different spectrophotometric methods.

Complexes	pH	λ_{max}	Molar ratio		Continuous variation	
			D:R	Log K	D:R	Log K
OfI-I	6.0	560	1:1	7.50	1:1	7.40
OfI-II	8.5	530	1:1	6.65	1:1	6.35
OfI-III	11.0	575	1:1	6.23	1:1	6.00



Effect of pH on ofl-I complex

Determination of wavelength

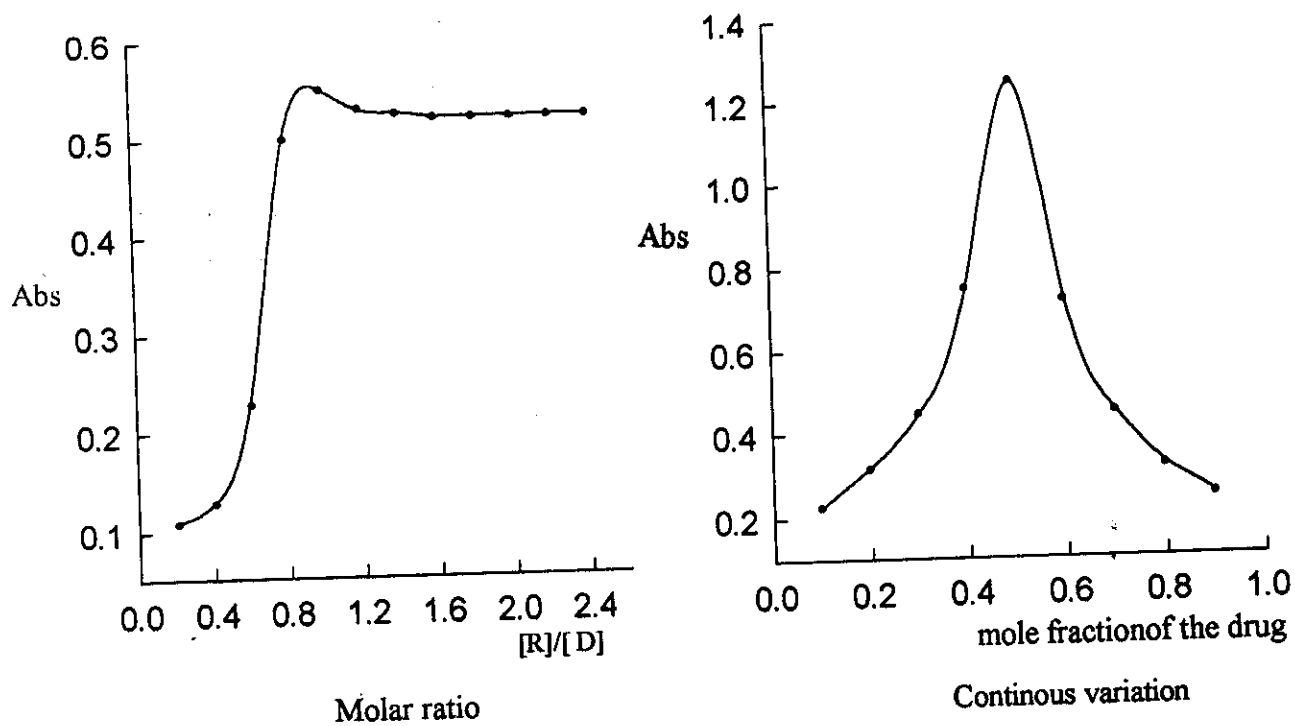
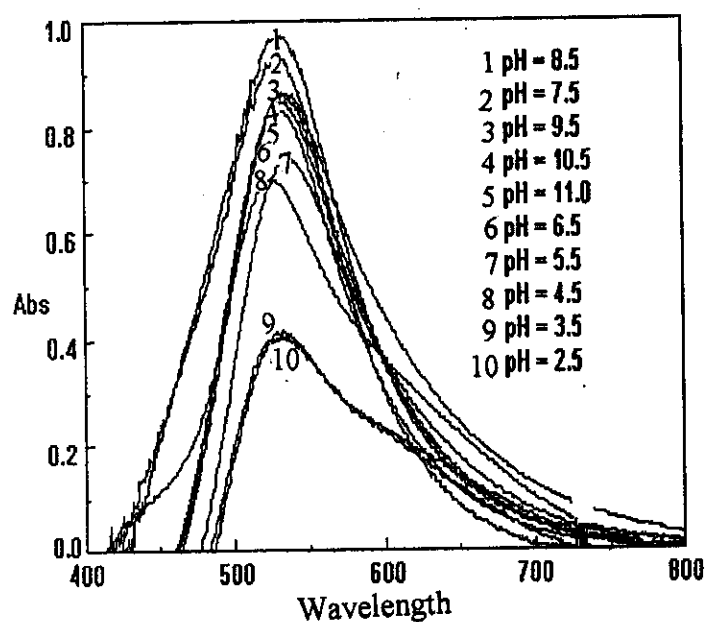
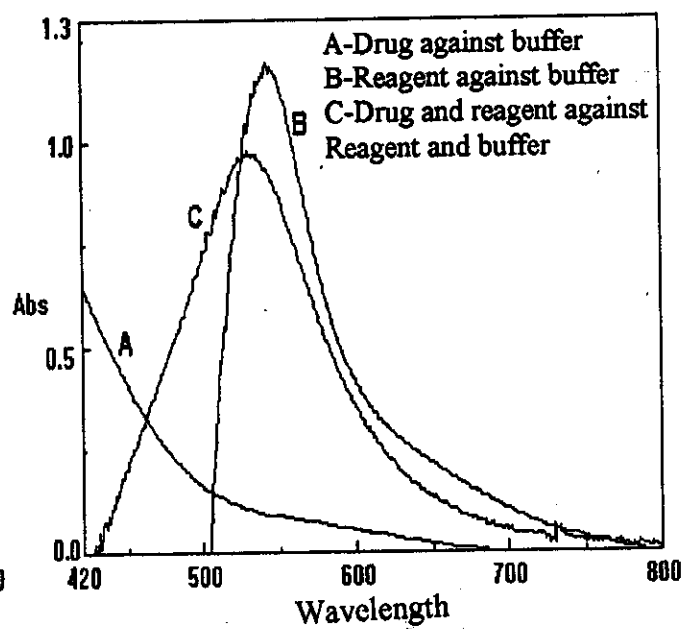


Fig. 34: Ofloxacin with sudan II



Effect of pH on ofl-II complex



Determination of wavelength

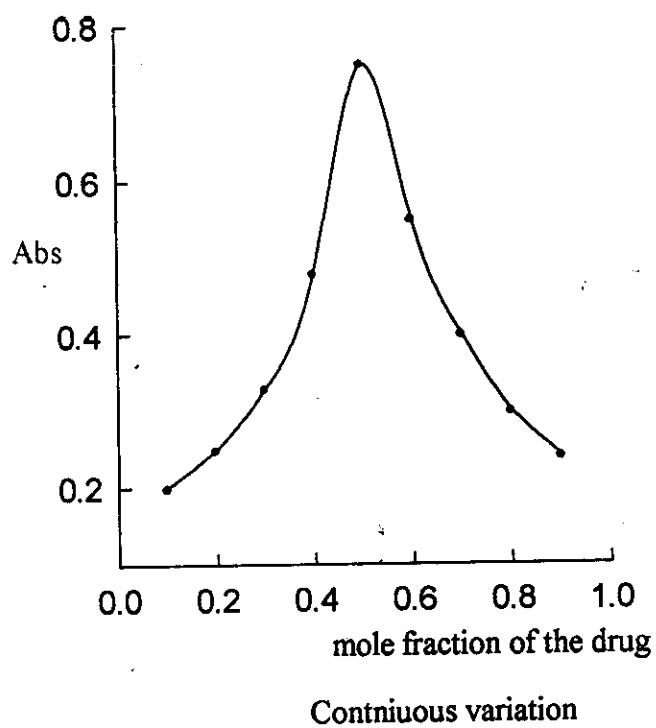
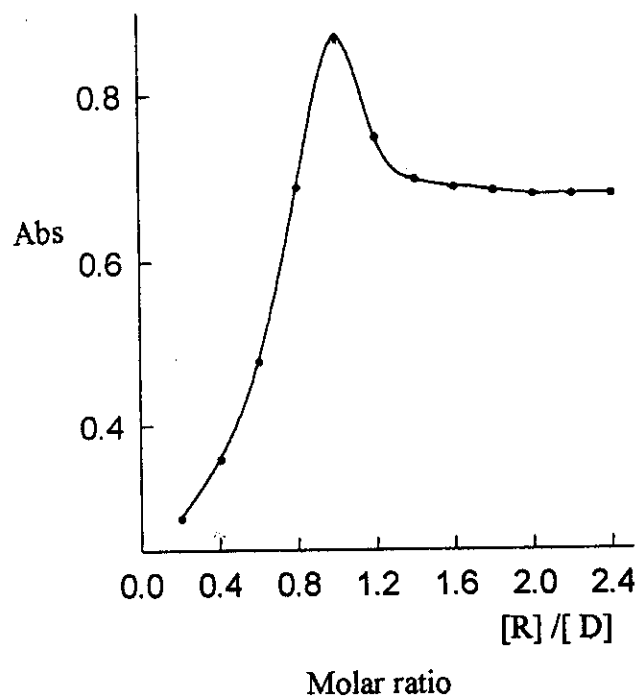
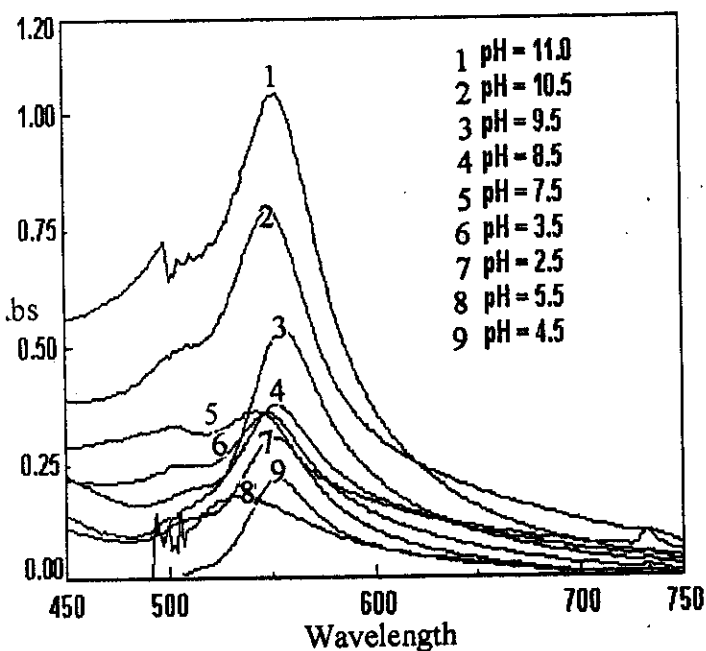
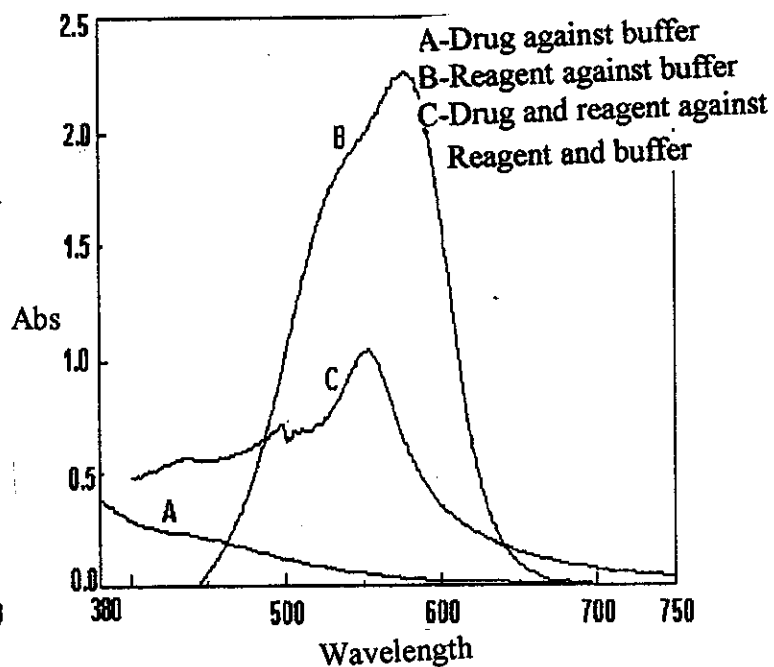


Fig. 35: Ofloxacin with congo red



Effect of pH on ofl-III complex



Determination of wavelength

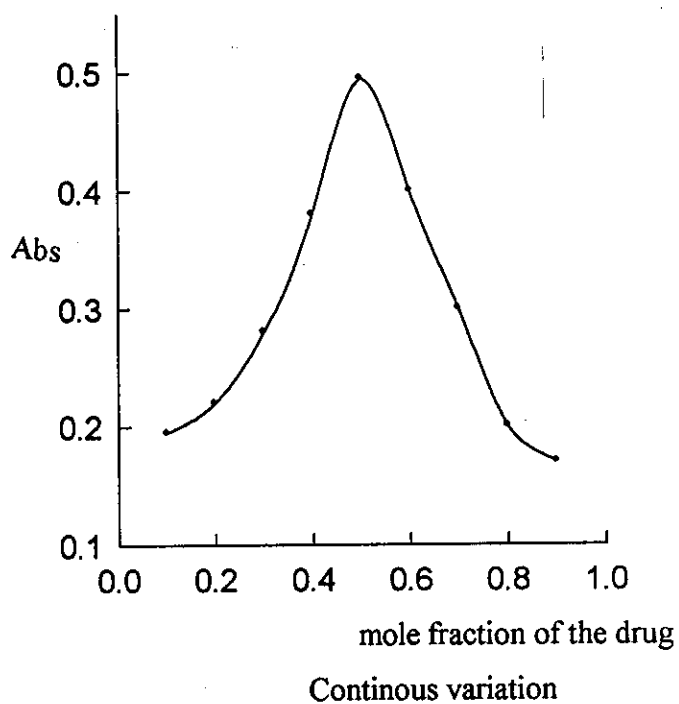
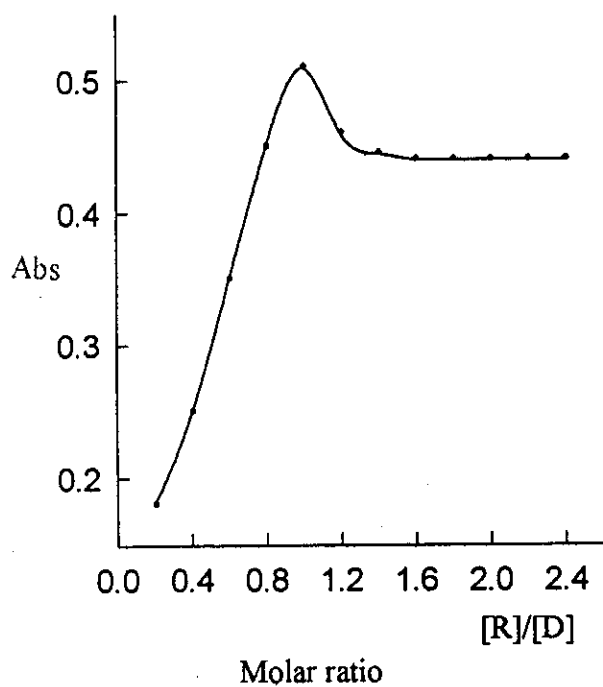


Fig. 36: Ofloxacin with gentian violet

proposed and reference HPLC⁽¹⁰⁶⁾ method which presents in the British Pharmacopoeia (1998), are compared statistically by the Students t-test and the variance ratio F-test, confirming that the proposed method is highly sensitive, therefore it could be used easily for the routine analysis of pure form and in its pharmaceutical preparations.

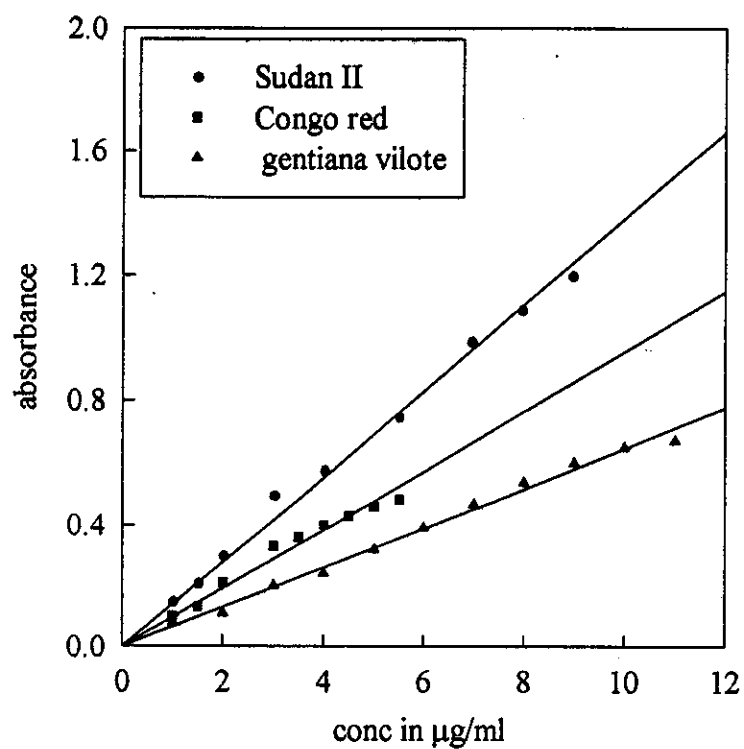


Fig. 37: Beer's law graph of ofloxacin with reagents under investigation

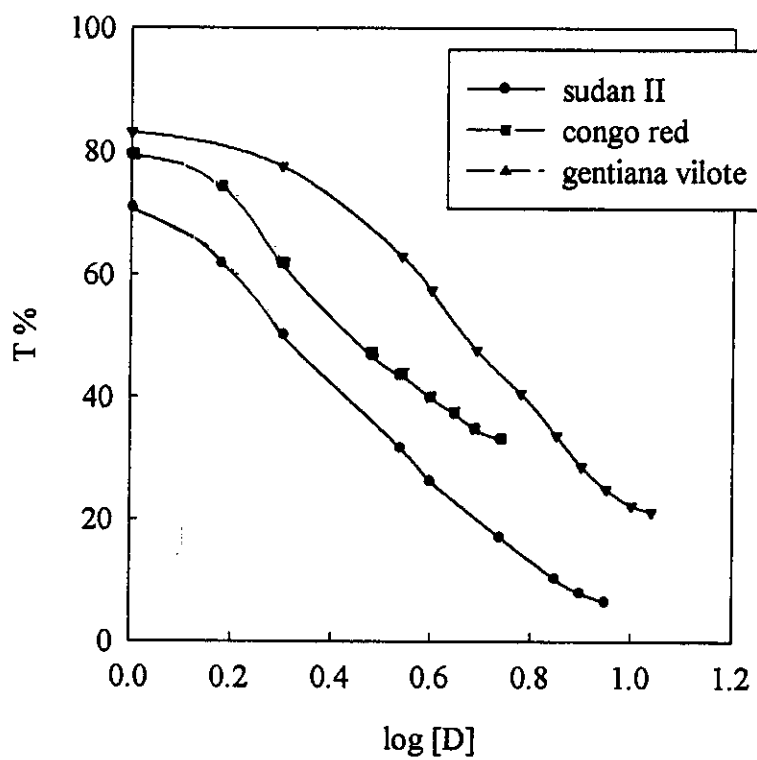


Fig. 38: Ringbom graph of ofloxacin

Table 24:

Comulative data of ofloxacin with the reagents I, II and III under investigation

Reagent	pH	λ_{\max}	Rangbom optimum range $\mu\text{g/ml}$	Beer's range $\mu\text{g/ml}$	S.D	R.S.D %	Error %	S ng cm^{-2}	ϵ $\text{l mol}^{-1} \text{cm}^{-1}$
I	11.0	560	1.4-8.38	1.0-9.0	0.023	0.045	1.07	7.83	4.6×10^4
II	5.5	630	1.5-5.10	1.0-5.5	0.026	0.084	0.89	9.72	3.7×10^4
III	11.0	575	1.7-10.73	1.0-11.0	0.031	0.057	1.28	15.65	2.3×10^4

*S: Sandell sensitivity

* ϵ : Molar absorptivity

Table 25:

Evaluation of accuracy and precision of the proposed and official methods for ofloxacin determination in ofloxacin tablets

Reagent	Content mg/tab	Found* (mg)		S.D	R.S.D %	Error %	Recovery %	F [#] value	t [#] value
		O	P						
I	200	196	201	0.317	0.335	0.137	100.5	2.292	0.75
II	200	196	202	0.393	0.451	0.184	101.0	1.491	0.56
III	200	196	205	0.451	0.482	0.197	102.5	1.132	0.26
t [#] Theoretical value = 2.57									
F [#] Theoretical value = 5.05									

*: Average of six determinations

O: Official method

P: Proposed method

Table 26:

Evaluation of accuracy and precision of the proposed and official methods
for ofloxacin determination in kiroll tablets

Reagent	Content mg/tab	Found* (mg)		S.D	R.S.D %	Error %	Recovery %	F# value	t# value
		O	P						
I	200	196	199.7	0.300	0.328	0.134	99.8	2.558	0.35
II	200	196	200.6	0.375	0.401	0.153	100.3	1.637	0.82
III	200	196	202.4	0.291	0.318	0.129	101.2	2.719	0.61
t# Theoretical value = 2.57									
F# Theoretical value = 5.05									

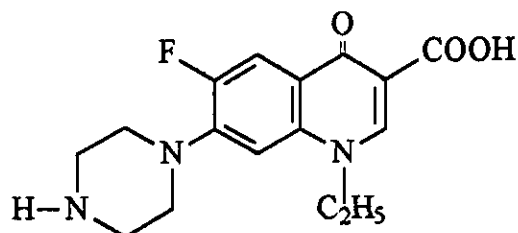
*: Average of six determinations

O: Official method

P: Proposed method

3.3. Electrochemical and analytical behaviour of norfloxacin in B.R. solutions of different pH-values:

Norfloxacin, is [1-ethyl 1-6-fluoro-1, 4 dihydro-4-oxo-7-piperazinyl -3 quinolone carboxylic acid] is a broad-spectrum antibacterial, which prescribed for the treatment of complicated urinary tract infections⁽¹¹⁹⁾.



Norfloxacin

The electrochemical behaviour of norfloxacin using DC-polarography and cyclic voltammetry techniques was studied in this part. Also the determination of norfloxacin in its pure and pharmaceutical dosage forms using square-wave adsorptive stripping voltammetric technique and spectrophotometric method using Sudan II I, Congo red II and gentian violet III as analytical reagents.

3.3.1. Electrochemical behaviour of norfloxacin in B.R. buffer solutions of different pH values:

3.3.1.1. DC-Polarography:

Current –Potential Curves:

The polarographic reduction of 4×10^{-4} M of norfloxacin was investigated in B.R. buffer solutions of various pH values from 3.2 to 10.9 containing 20 % (v/v) ethanol. The obtained polarographic waves were recorded and given in Fig. 39A. The polarograms showed single reduction

wave in the entire pH range. The wave height is pH independent but slightly decreased on increasing pH of the medium, Fig. 39B.

The half wave potential ($E_{1/2}$) of the polarographic waves of norfloxacin showed cathodic shift on increasing the pH of the electrolysis solution. This indicates that the H^+ ions are participating in the electrode process i.e. the consumption of hydrogen ions in the electroreduction of norfloxacin process and the proton uptake precedes the electron transfer process⁽¹⁰⁷⁾.

Effect of Mercury Height:

On plotting $\log i_l$ as a function of $\log h$ at different pH values straight lines were obtained, Fig. 39C. The slope values (x) were in the range from 0.62 to 0.66. The values indicating that the reduction process is mainly controlled by diffusion with some adsorption contribution, Table 27.

Analysis of the Polarographic Waves:

On plotting of $\log [i/(i_d-i)]$ against $E_{d.e}$ for norfloxacin, linear correlations were obtained, Fig. 39D. The values of the calculated slope S_1 indicating the irreversibility of the electrode process, Table 27. From the values of αn_a , the most probable values of α indicated that, within the studied pH range n_a is equal to two for the investigated compound. These values indicated the irreversibility of the polarographic waves.

Half-Wave Potential –pH Curves:

The $E_{1/2}$ - pH plot of norfloxacin showed linear relationship consists of two segments of slope values S_2 , Fig 39E. Using equation (5), the number of hydrogen ions were determined and found to equal unity at different pH values, Table 27. This means that the rate determining step involves one proton and two electrons.

Table 27:

DC-Polarographic data and parameters obtained from the reduction of 4×10^{-4} M norfloxacin in B.R. buffer solutions of various pH values containing 20% (v/v) ethanol, at 25°C.

pH	i_d μA	$-E_{1/2}$ V	$\log i_i$ $/\log h$	S_1 mV	αna	α		S_2 mV	Z^+_{H}
						$n_a=1.0$	$n_a=2$		
3.2	0.98	1.21		62.3	0.905	0.905	0.453	26	0.417
4.2	0.97	1.23	0.62	63.3	0.934	0.934	0.467	26	0.411
5.6	0.93	1.24		61.5	0.961	0.961	0.481	26	0.423
6.3	0.92	1.28	0.64	55.8	1.059	1.059	0.529	26	0.466
7.1	0.91	1.30		50.9	1.161	1.161	0.581	26	0.511
8.3	0.89	1.33		50.8	1.163	1.163	0.582	56	0.512
9.1	0.89	1.36	0.66	52.0	1.137	1.137	0.569	56	1.077
9.8	0.86	1.40		54.8	1.078	1.078	0.539	56	1.022
10.0	0.82	1.43		57.6	1.026	1.026	0.513	56	0.972
10.9	0.71	1.47		54.6	1.082	1.082	0.541	56	1.026

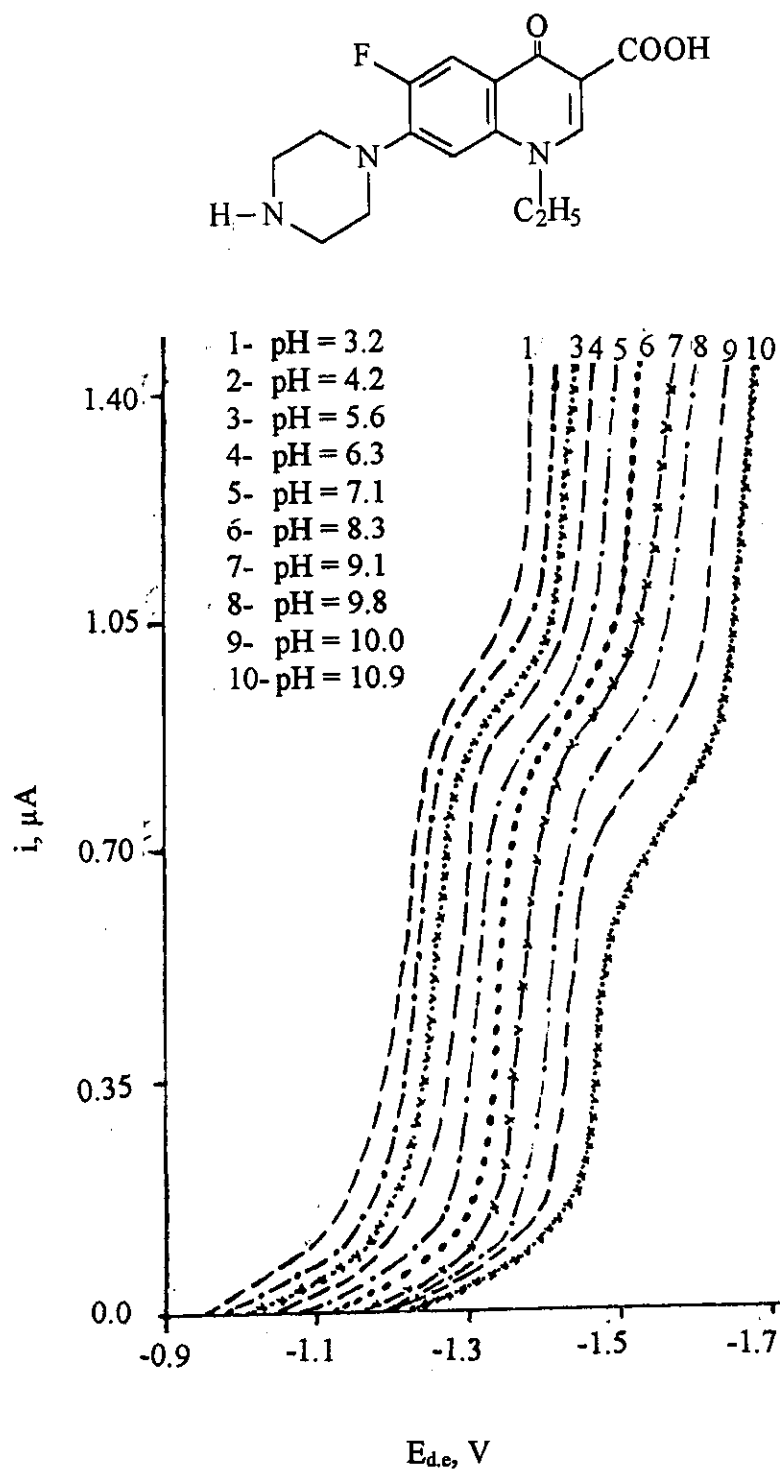


Fig. 39A: DC-polarograms of norfloxacin in B.R. buffer solutions of different pH values.

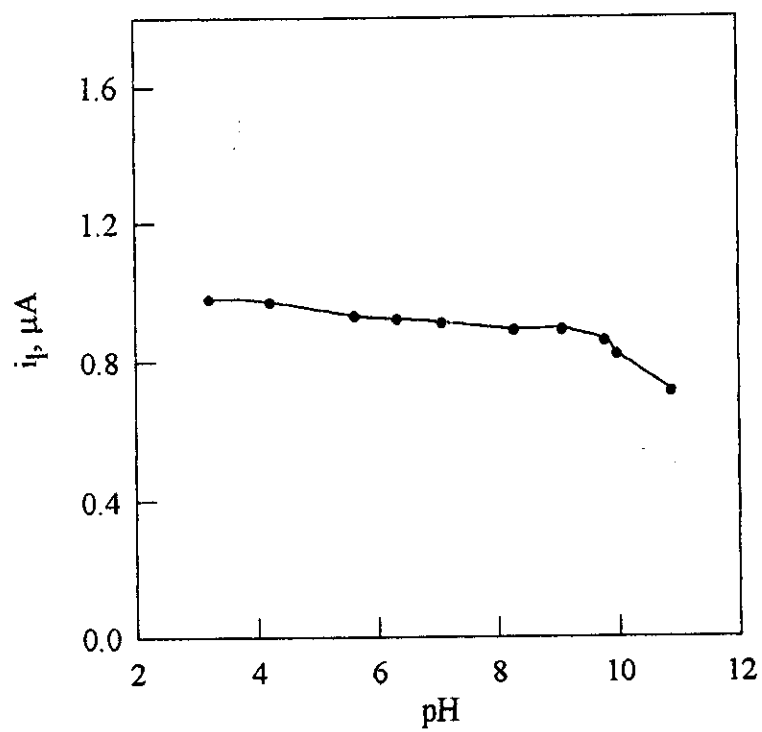


Fig. 39 B: i_l -pH plot of norfloxacin

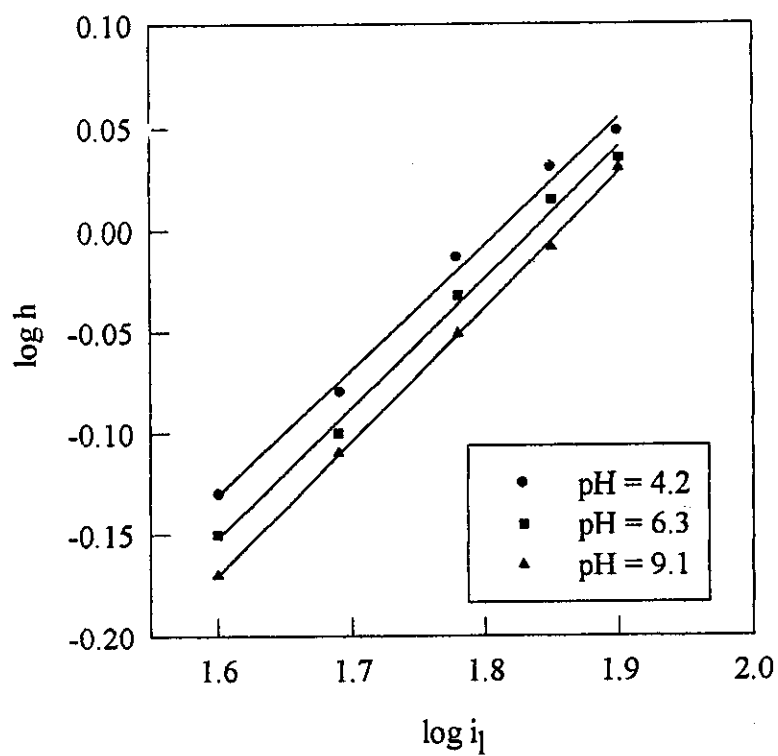


Fig. 39 C: $\log h$ - $\log i_l$ plots of norfloxacin at different pH values

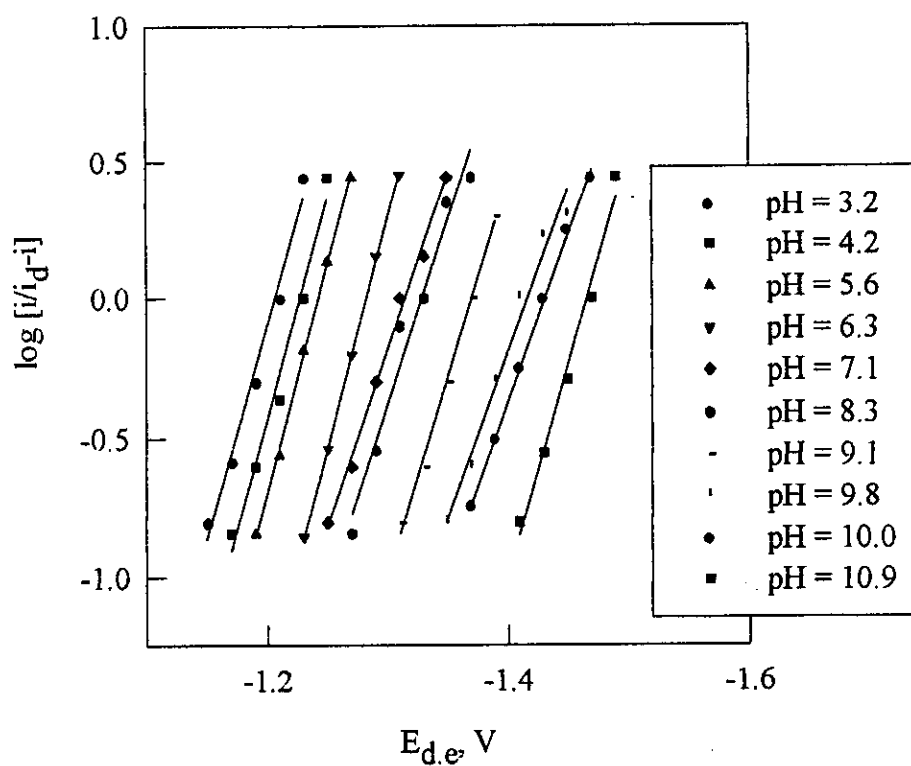


Fig. 39 D: $\log [i/i_d-i]$ - E_{dc} plots of norfloxacin at different pH values

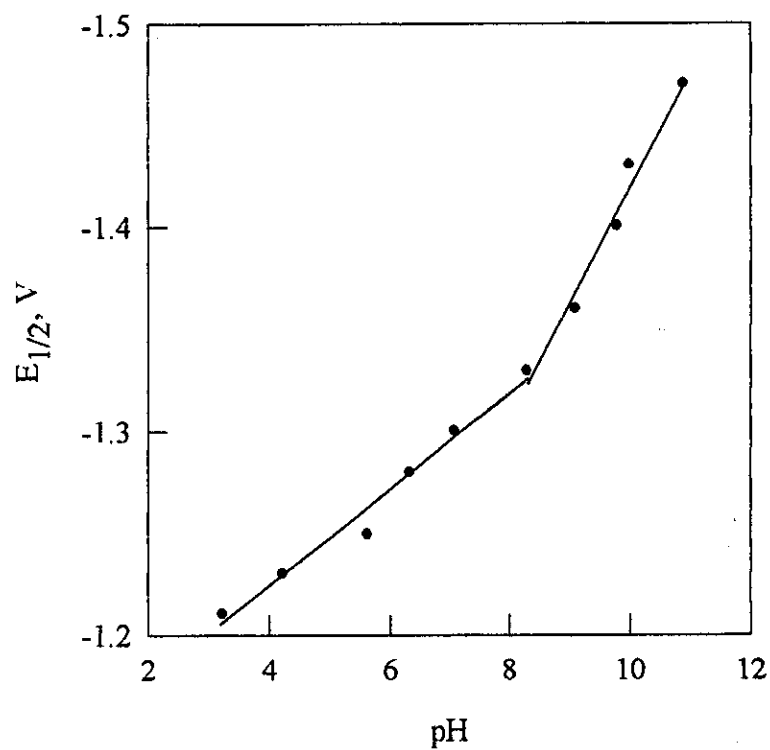


Fig. 39 E: $E_{1/2}$ -pH plot of norfloxacin

3.3.1.2. Determination of norfloxacin by using DC-polarograph

For determination of norfloxacin, many trials were occurred in different media such as sodium perchlorate, acetate buffer, B.R. buffer and phosphate buffer. The most obvious wave is shown in B.R. buffer pH 3.2. A stock solution of norfloxacin 1×10^{-3} M was prepared and different concentrations were obtained by accurate dilution. The variation of wave current with concentration is represented in, Fig. 40 (A and B). The detection limit is 1.0×10^{-5} M (3.2 $\mu\text{g/ml}$), Table 28.

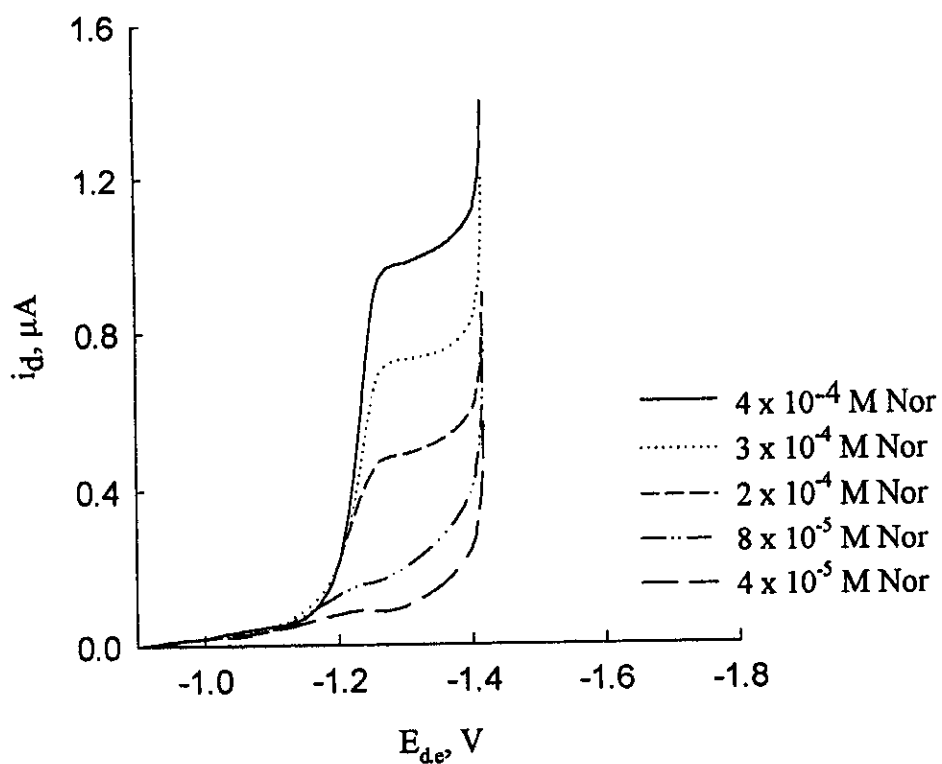


Fig. 40 A: DC polarograms of different concentrations of norfloxacin

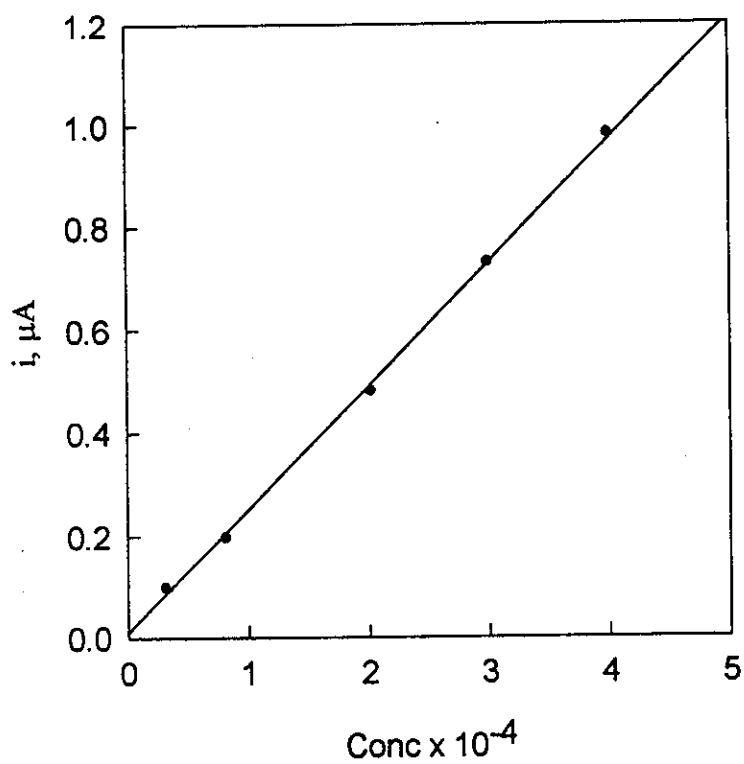


Fig. 40 B: Calibration graph of norfloxacin

Table 28:

Assay of norfloxacin in B.R. buffer solution of pH 3.2 using DC polarography.

Compound conc.	i μA	Conc. found	Recovery %	S.D
0.4 x 10 ⁻⁴	0.096	3.91 x 10 ⁻⁵	97.9	1.00
	0.094	3.84 x 10 ⁻⁵	95.9	
	0.095	3.88 x 10 ⁻⁵	96.9	
0.8 x 10 ⁻⁴	0.193	7.92 x 10 ⁻⁵	98.9	0.81
	0.195	7.96 x 10 ⁻⁵	99.5	
	0.192	7.84 x 10 ⁻⁵	97.9	
2.0 x 10 ⁻⁴	0.480	1.95 x 10 ⁻⁴	97.9	0.36
	0.482	1.96 x 10 ⁻⁴	98.4	
	0.483	1.97 x 10 ⁻⁴	98.6	
3.0 x 10 ⁻⁴	0.730	2.97 x 10 ⁻⁴	99.3	0.15
	0.731	2.98 x 10 ⁻⁴	99.5	
	0.732	2.99 x 10 ⁻⁴	99.6	
4.0 x 10 ⁻⁴	0.978	3.98 x 10 ⁻⁴	99.4	0.25
	0.979	3.99 x 10 ⁻⁴	99.9	
	0.976	0.397 x 10 ⁻⁴	99.6	
Recovery = 98.61 ± 0.51				

3.3.1.3. Effect Of Metal Complexes:

The polarographic behaviour of the simple metal of 2×10^{-4} M for Cd(II) and Zn(II) in 0.1M sodium perchlorate were recorded, Fig. 41[A-B]. Logarithmic analysis of metal ions waves revealed the quasi-reversible nature of the electrode processes. The α_n values are determined, Table (29-30). These values decrease on addition of the ligand revealed the irreversibility of the electrode processes. Generally, as the concentration of ligand increases, the diffusion current decreases which is attributed to the increased bulk of the complexed ions. The polarographic waves of the metal ions showed a cathodic shift indicating complex formation. The ratio of the formed complex is 1:2 with Zn(II) and 1: 2 with Cd(II), Fig. 41[C to F].

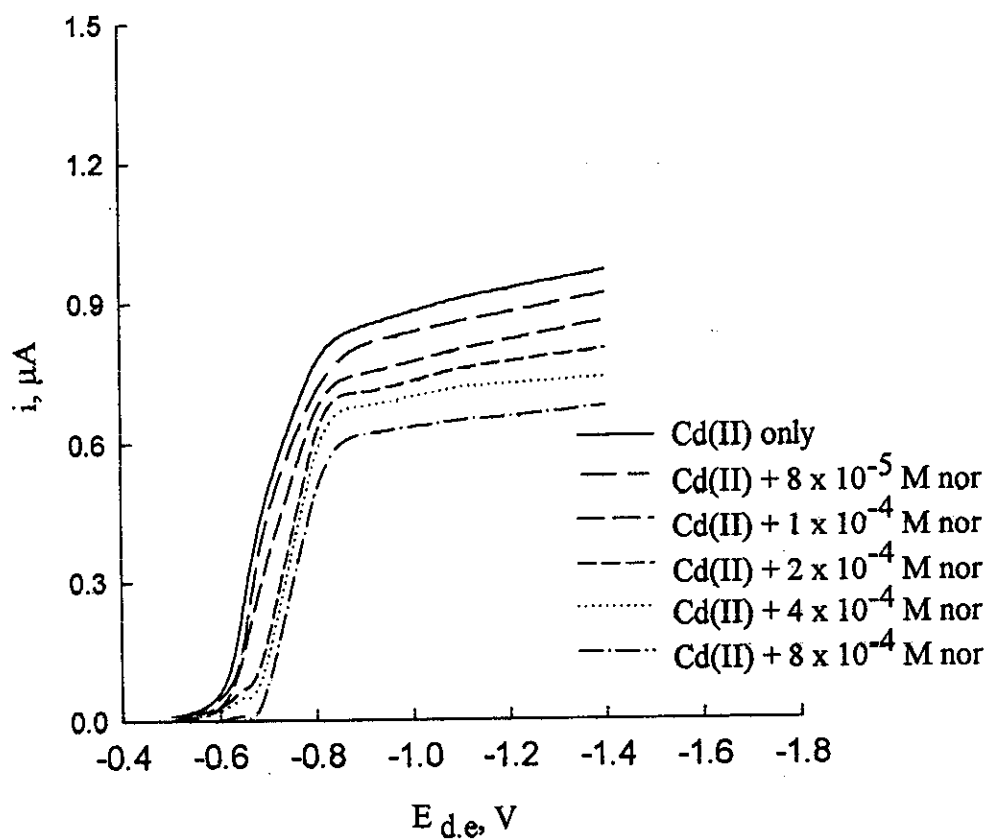


Fig. 41 A: DC-polarograms of Cd(II)- norfloxacin complex

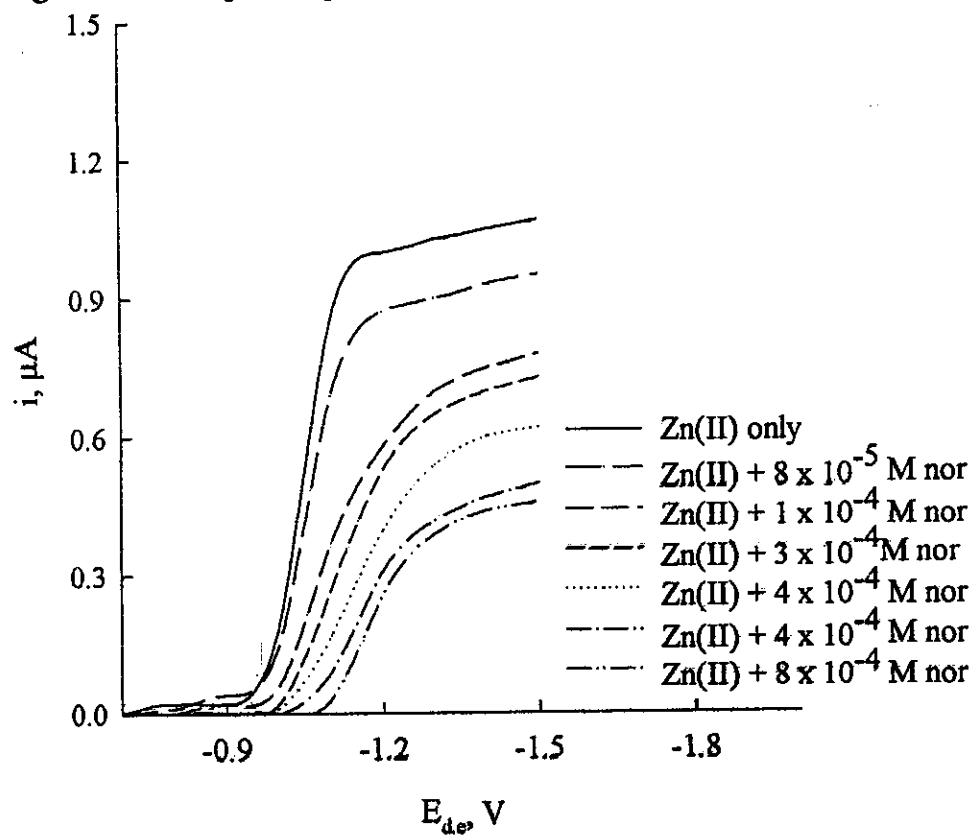


Fig. 41 B: DC-polarograms of Zn(II)-norfloxacin complex

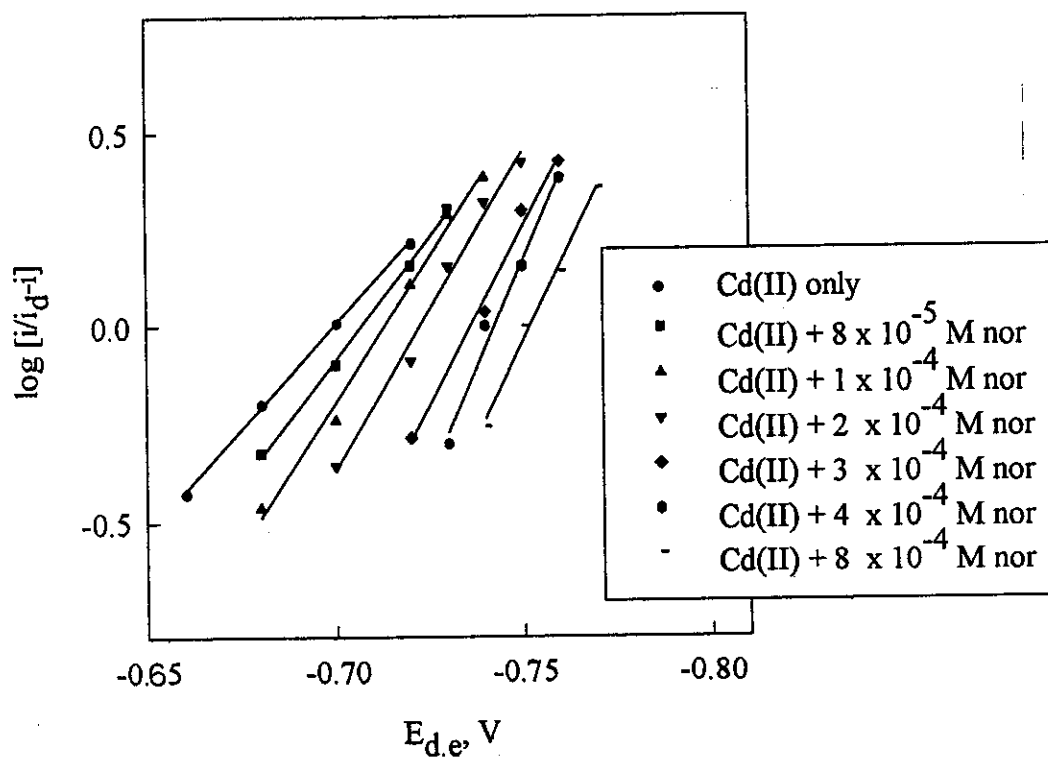


Fig. 41C: Cd(II)-norfloxacin complex

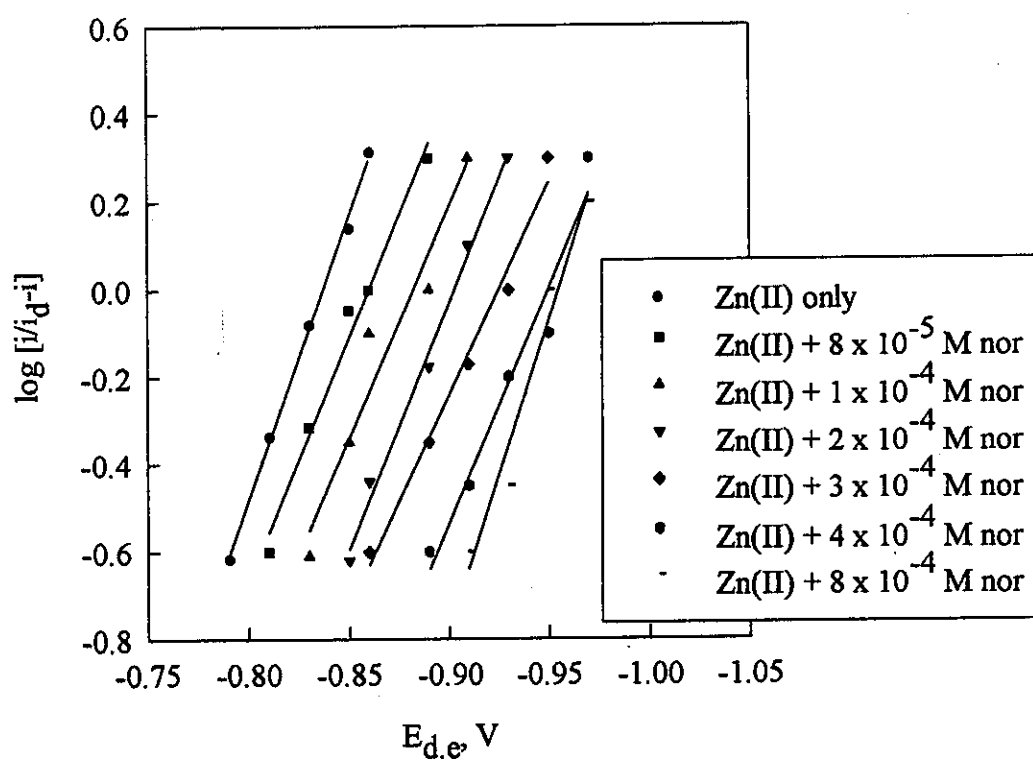


Fig. 41 D: Zn(II)-norfloxacin complex

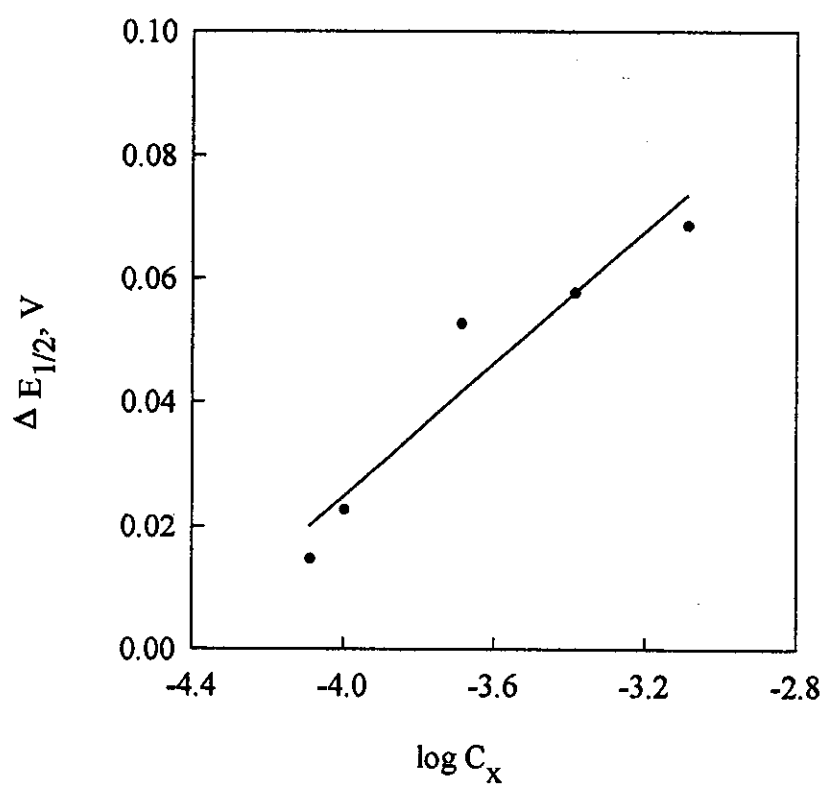


Fig. 41 E: $\Delta E_{1/2}$ - $\log C_x$ plot of Cd(II)-norfloxacin complex

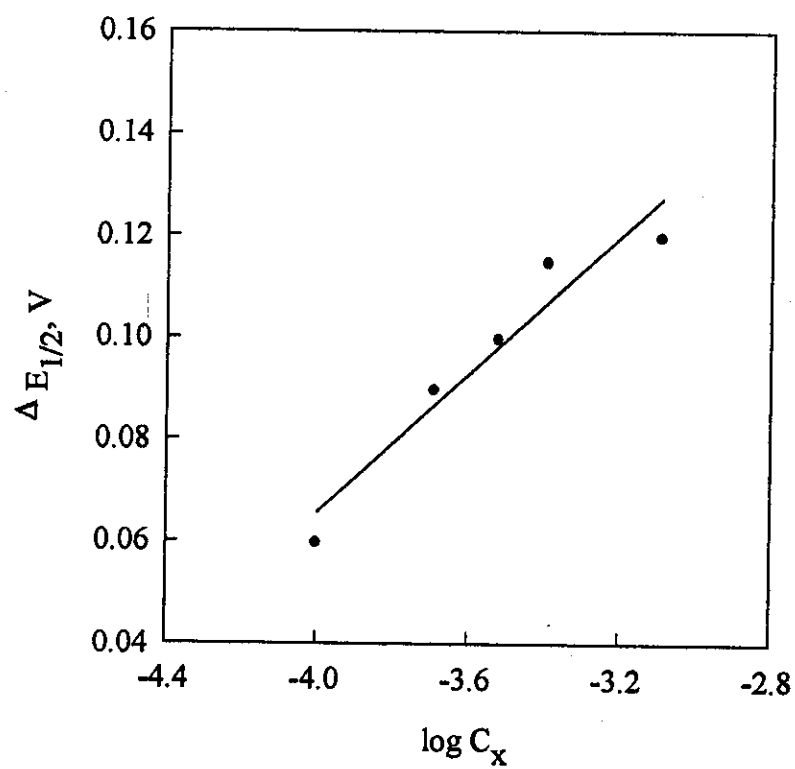


Fig. 41 F: $\Delta E_{1/2}$ - $\log C_x$ plot of Zn(II)-norfloxacin complex

Table 29:

Polarographic data obtained for Cd(II)-norfloxacin complex in 0.1 M NaClO₄

L.conc	i _d	ΔE _{1/2}	αn	Stoichiometry Metal : Drug
Zero	0.95	0.000	0.80	1:2
8 x 10 ⁻⁵	0.90	0.015	0.71	
1 x 10 ⁻⁴	0.82	0.023	0.70	
2 x 10 ⁻⁴	0.80	0.053	0.68	
4 x 10 ⁻⁴	0.68	0.056	0.66	
8 x 10 ⁻⁴	0.62	0.069	0.62	

Table 30:

Polarographic data obtained for Zn(II)-norfloxacin complex in 0.1 M NaClO₄

L.conc	i _d	ΔE _{1/2}	αn	Stoichiometry Metal: Drug
Zero	1.04	0.00	0.76	1:2
8 x 10 ⁻⁵	0.95	0.02	0.71	
1 x 10 ⁻⁴	0.80	0.06	0.70	
2 x 10 ⁻⁴	0.75	0.09	0.67	
3 x 10 ⁻⁴	0.67	0.10	0.64	
4 x 10 ⁻⁴	0.54	0.12	0.63	
8 x 10 ⁻⁴	0.49	0.13	0.61	

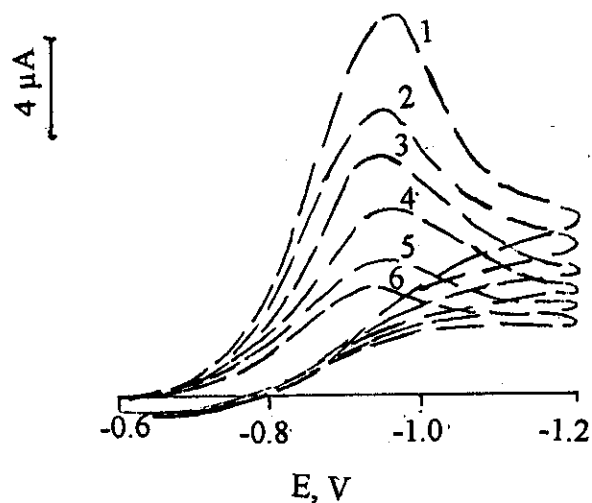
3.3.1.4. Cyclic Voltammetry

Cyclic voltammetric behaviour of 1×10^{-4} M norfloxacin was studied at glassy carbon electrode in B.R. buffer solutions of different pH values 4.6, 7.4 and 10.4 containing 20% ethanol. The voltammograms were recorded at different scan rates from 20 to 500 mV /sec, Fig. 42A. These voltammograms showed one cathodic peak within the studied pH range and at different scan rates. The peak potentials showed cathodic shift by increasing the scan rate which indicated the irreversible nature of the electrode reaction pathway.

The plots of i_p as a function of square root of scan rate $v^{1/2}$ is represented in Fig 42B. Linear correlations slightly deviating from the origin were obtained. This behaviour confirming that the electrode process of norfloxacin is controlled mainly by diffusion with some adsorption contribution⁽¹¹²⁾.

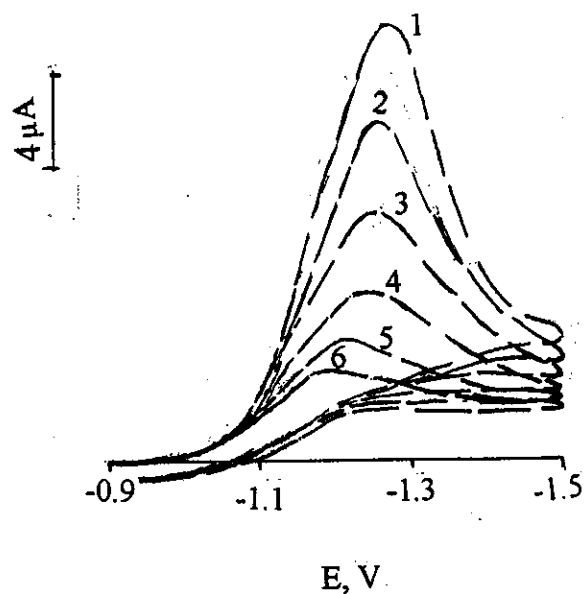
Plotting E_p versus $\ln v$ at the given pH values, showed linear correlations of slope values proportional to αn_a , Fig. 42C. From the slopes of this plot, the transfer co-efficient α values were calculated for the probable values of n_a , Table 31. This showed that n_a is equal to 2, i.e. the rate determining step of the electrode process may involve two electrons.

1- pH = 4.6



- 1- scan rate 500 mV/s
- 2- scan rate 300 mV/s
- 3- scan rate 200 mV/s
- 4- scan rate 100 mV/s
- 5- scan rate 50 mV/s
- 6- scan rate 20 mV/s

2- pH = 7.4



3- pH = 10.4

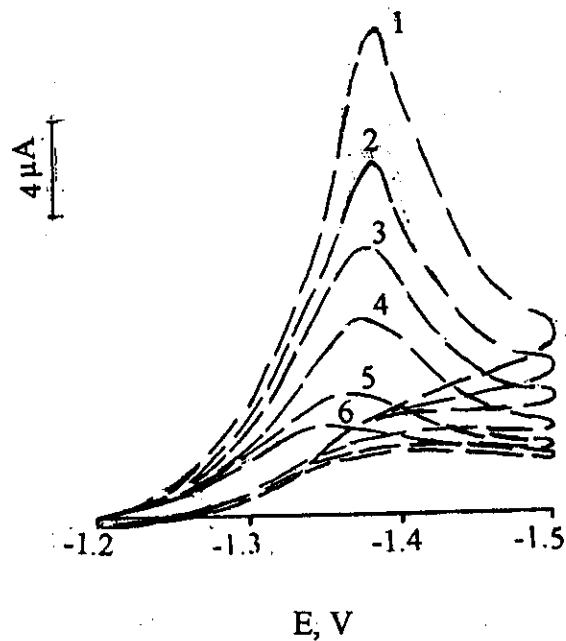


Fig. 42 A: Cyclic voltammetric behaviour of norfloxacin in B.R. buffer solutions of different pH values.

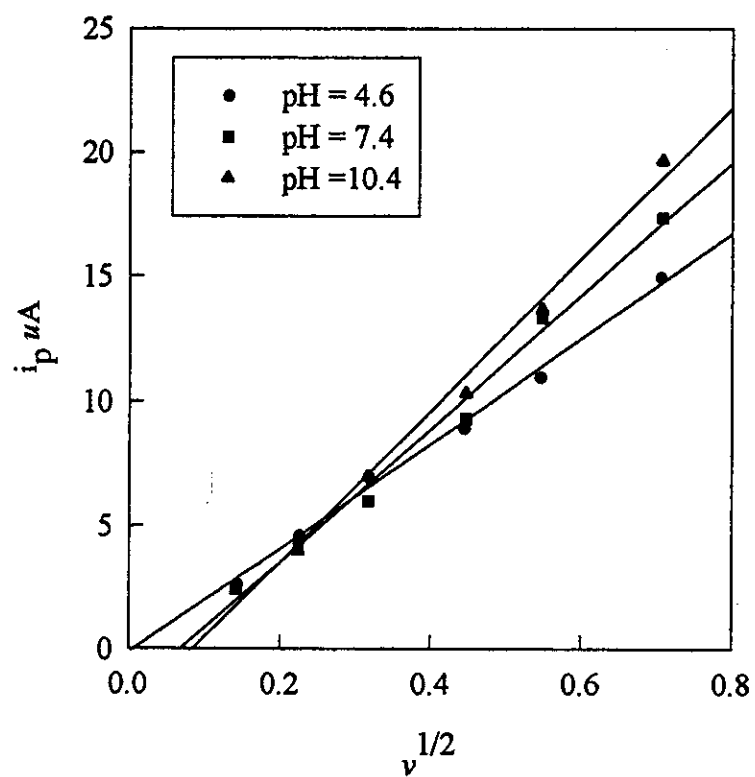


Fig. 42 B: $i_{p_c} - v^{1/2}$ plots of norfloxacin at different pH values.

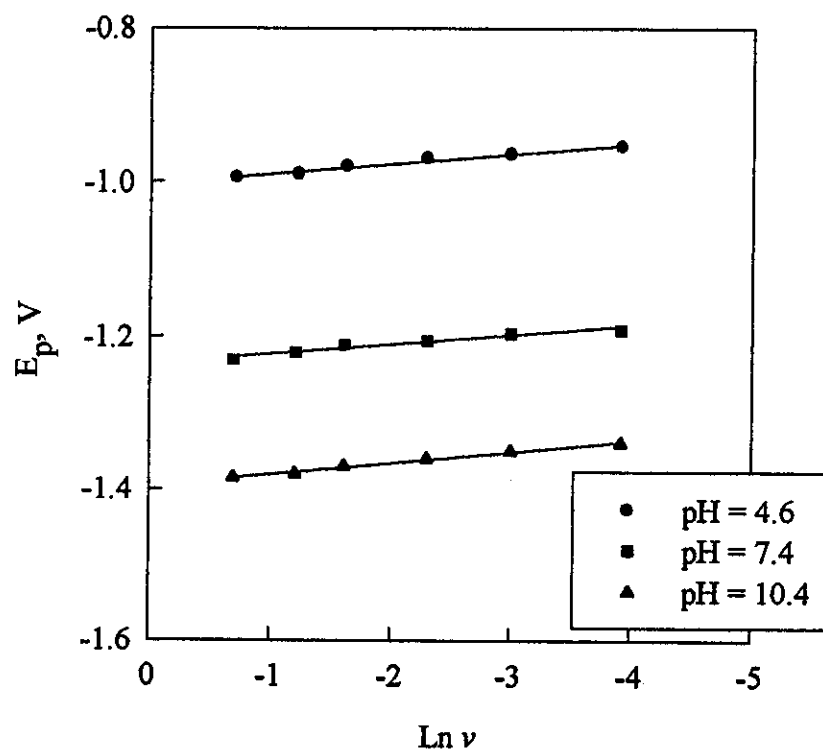


Fig.42C: $E_p - \ln v$ plots of norfloxacin at different pH values.

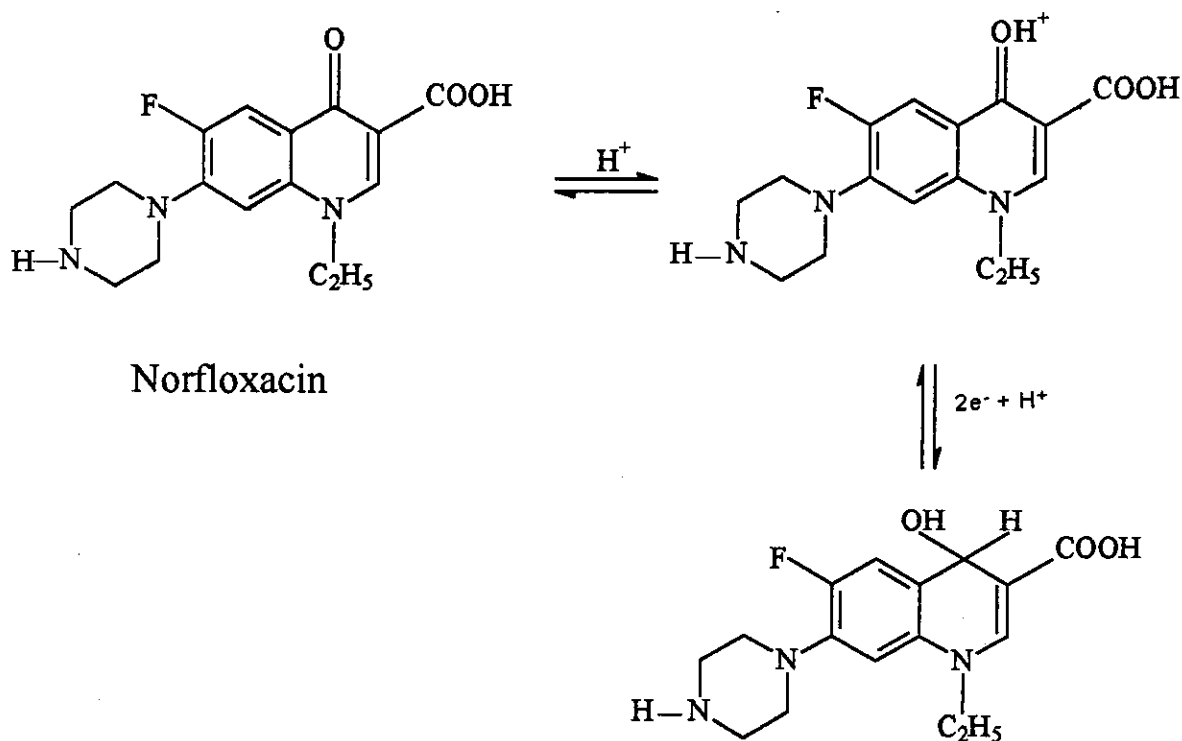
Table 31:

Cyclic voltammetric data for 1×10^{-4} M norfloxacin in B.R. buffer solutions of different pH values containing 20% (v/v) ethanol, at 25°C.

pH	Scan rate (mV/s)	i_p μA	$-E_p$ (V)	$\delta E_p / \delta \ln v$	α	
					na=1.0	na=2.0
4.60	500	15.00	0.995	0.0126	1.019	0.510
	300	11.00	0.990			
	200	9.00	0.980			
	100	7.00	0.970			
	50	4.67	0.965			
	20	3.67	0.955			
7.40	500	17.33	1.230	0.0123	1.045	0.522
	300	13.33	1.220			
	200	9.33	1.210			
	100	6.00	1.205			
	50	4.33	1.195			
	20	2.67	1.190			
10.40	500	19.67	1.385	0.0145	0.886	0.443
	300	13.67	1.380			
	200	10.33	1.370			
	100	7.00	1.360			
	50	4.00	1.350			
	20	2.67	1.340			

3.3.1.5. The Electrode Reaction

The electrochemical behaviour of norfloxacin indicated that there are two electrons and one proton involved in the rate determining step. The CPC electrolysis showed that the total number of electrons (n) amount to 2.0. Therefore, the electrode mechanism could take place as following:



3.3.1.6. Cathodic Adsorption Square Wave Stripping Voltammetry of norfloxacin

The results of DC-polarography and cyclic voltammetry indicated the weak adsorption and association of norfloxacin and the effective interfacial accumulation of the norfloxacin film on the surface of the glassy-carbon electrode. Square wave stripping voltammetry at the glassy carbon electrode is used for the electroanalytical determination of norfloxacin.

1. Optimization of the experimental and instrumental conditions

Both of the experimental and instrumental conditions were optimized here for the quantitative determination of norfloxacin.

1- Effect of pH on the cathodic adsorption stripping peak of norfloxacin

The cathodic adsorption stripping voltammetric peak current of 1.0×10^{-6} M/l norfloxacin was recorded as a function of potential in B. R. buffer solutions of different pH values from 2.0 to 11.5, Fig. 43. The obtained peaks were due to the reduction of the absorbed norfloxacin at the glassy carbon electrode surface. A well-developed peak was observed at pH equal to 9.2.

2. Effect of supporting electrolyte on the CAdSWSV peak of norfloxacin

The effect of some supporting electrolytes on the CAdSV peak was recorded in Fig. 44. The most suitable medium for the developing well peak current of norfloxacin was B. R. buffer solution of pH equal to 9.2.

3. Effect of deposition potential

The influence of deposition potential was studied over the potential range from -200 to -900 mV, Fig. 45. The most suitable deposition potential is -500 mV.

4. Effect of frequency

The effect of different values of frequency from 100 to 5000 Hz on the stripping peak current was recorded. The most suitable frequency value was 5000 Hz, Fig. 46.

5. Effect of pulse width

The effect of pulse width on the peak height was studied in the range from 20 to 200 mV, Fig. 47. The most suitable pulse width was 200 mV.

6. Effect of pulse height

The effect of pulse height on the peak height was studied in the range from 20 to 200 mV. The peak current formed is directly proportional to the pulse height, Fig. 48. In the present study, a sharp peak height was obtained at pulse height 200 mV.

7. Effect of deposition time

In the square wave stripping analysis of norfloxacin, the height of the formed peak is almost proportional to the deposition time t_d . On studying the effect of deposition time on norfloxacin, the most suitable t_d was 240 sec, after this value the peak current decreases again, Fig. 49.

8. Effect of scan rate

On studying the effect of different scan rates, a scan rate of 1.0 mV/s gave a maximum response, Fig. 50.

2. Quantitative determination of norfloxacin by CAdSWS voltammetry

The applicability of the cathodic adsorptive square wave stripping voltammetric technique as an analytical tool for the determination of

norfloxacin was tested by measuring the peak current as a function of concentration, Fig. 51.

Calibration graph

A stock solution of norfloxacin 1×10^{-3} M was prepared and different concentrations were obtained by accurate dilution. The stripping peaks of the final samples were recorded under the optimum experimental conditions. The variation of peak current with concentration was represented in Fig. 52. The slope of the calibration graph (a) was 18.1×10^4 , the intercept (b) was 0.0424 and the value of c is determined according to equation (12), Table 33.

The precision was determined from four repeated measurements of different concentrations of the norfloxacin. The mean recovery and the standard deviation of the method were calculated, Table 33.

Detection Limit

In the present study, the standard deviation of the blank (S.D.) is 2.16×10^{-5} and $a = 20.6 \times 10^4$, so the detection limit is 2.5×10^{-9} M (7.98×10^{-4} $\mu\text{g/ml}$).

Determination of norfloxacin in its dosage form:

The proposed procedure is successfully applied for the analysis of norfloxacin in its dosage form. The precision is determined from four repeated measurements of different concentrations, Table 34. The mean recovery of norfloxacin in norxin tablets is 99.94 ± 0.57 , Table 35. The agreement between the two procedures confirms the validity of the SWCAdSV technique in the analysis of norfloxacin in its dosage forms under the suitable experimental and instrumental conditions.

Table 33:

Assay of norfloxacin in B.R. buffer solution of pH 9.2 using CAdSWSV at: $E_d = -500$ mV, $t_d = 240$ sec, scan rate = 1.0 mV/sec, pulse height = 200 mV, pulse width = 200 mV and frequency = 5000 Hz.

Conc. Taken M	i_p μA	Conc. Found M	Recovery %R	Av. Conc. found M	Mean %R	S.D
1×10^{-6}	0.2257	1.008×10^{-6}	100.80	1.01×10^{-6}	100.78	0.17
	0.2255	1.007×10^{-6}	100.70			
	0.2253	1.006×10^{-6}	100.60			
	0.2261	1.010×10^{-6}	101.00			
8×10^{-7}	0.1840	8.053×10^{-7}	100.67	8.047×10^{-7}	100.59	0.12
	0.1841	8.058×10^{-7}	100.73			
	0.1837	8.039×10^{-7}	100.49			
	0.1837	8.039×10^{-7}	100.49			
7×10^{-7}	0.1619	6.981×10^{-7}	99.72	7.004×10^{-7}	100.05	0.29
	0.1625	7.009×10^{-7}	100.14			
	0.1622	6.995×10^{-7}	99.93			
	0.1629	7.029×10^{-7}	100.41			
5×10^{-7}	0.1222	5.053×10^{-7}	101.10	5.074×10^{-7}	101.49	0.33
	0.1228	5.083×10^{-7}	101.65			
	0.1230	5.092×10^{-7}	101.84			
	0.1225	5.068×10^{-7}	101.36			
The mean recovery = 100.05 ± 0.23						
Slope = 20.6×10^4						
Intercepte = 0.0181						
Corr. Coeff. = 0.9995						

Table 34:

Assay of norfloxacin tablet in B.R. buffer solution of pH 9.2 using CAdSWSV at: $E_d = -500$ mV, $t_d = 240$ sec, scan rate = 1.0 mV/sec, pulse height = 200 mV, pulse width = 200 mV and frequency = 500 Hz.

Name of tablets	Conc M	ip μ A	Conc. Found M	%R	Av. Conc found M	Mean %R	S.D.
Norxin	2.5×10^{-7}	0.0700	2.519×10^{-7}	100.76	2.50×10^{-7}	100.14	0.66
		0.0692	2.481×10^{-7}	99.22			
		0.0697	2.505×10^{-7}	100.19			
		0.0698	2.509×10^{-7}	100.40			
	3.5×10^{-7}	0.0900	3.490×10^{-7}	99.72	3.50×10^{-7}	100.14	0.53
		0.0908	3.529×10^{-7}	100.83			
		0.0900	3.490×10^{-7}	99.72			
		0.0904	3.510×10^{-7}	100.28			
	4.5×10^{-7}	0.1100	4.461×10^{-7}	99.14	4.48×10^{-7}	95.54	0.51
		0.1100	4.461×10^{-7}	99.14			
		0.1105	4.485×10^{-7}	99.68			
		0.1110	4.509×10^{-7}	100.21			
The mean recovery = 99.94 ± 0.57							
Slope = 20.6×10^4							
Intercept = 0.0181							
Corr. Coeff = 0.9995							

Table 35:

Assay of norfloxacin in its dosage forms B.R. buffer solution of pH 9.2 using CAdSWSV at: $E_d = -500$ mV, $t_d = 240$ sec, scan rate = 1.0 mV/sec, pulse height = 200 mV, pulse width = 200 mV and frequency = 500 Hz.

Brand Name (Producer)	Labelled Conc. (Drug)	%Recovery \pm S.D.	
		Proposed method	Reported method*
Norxin	400 mg/tablet	99.94 \pm 0.57 (n = 4)	100.00 \pm 3.74

* The official method⁽³¹⁾

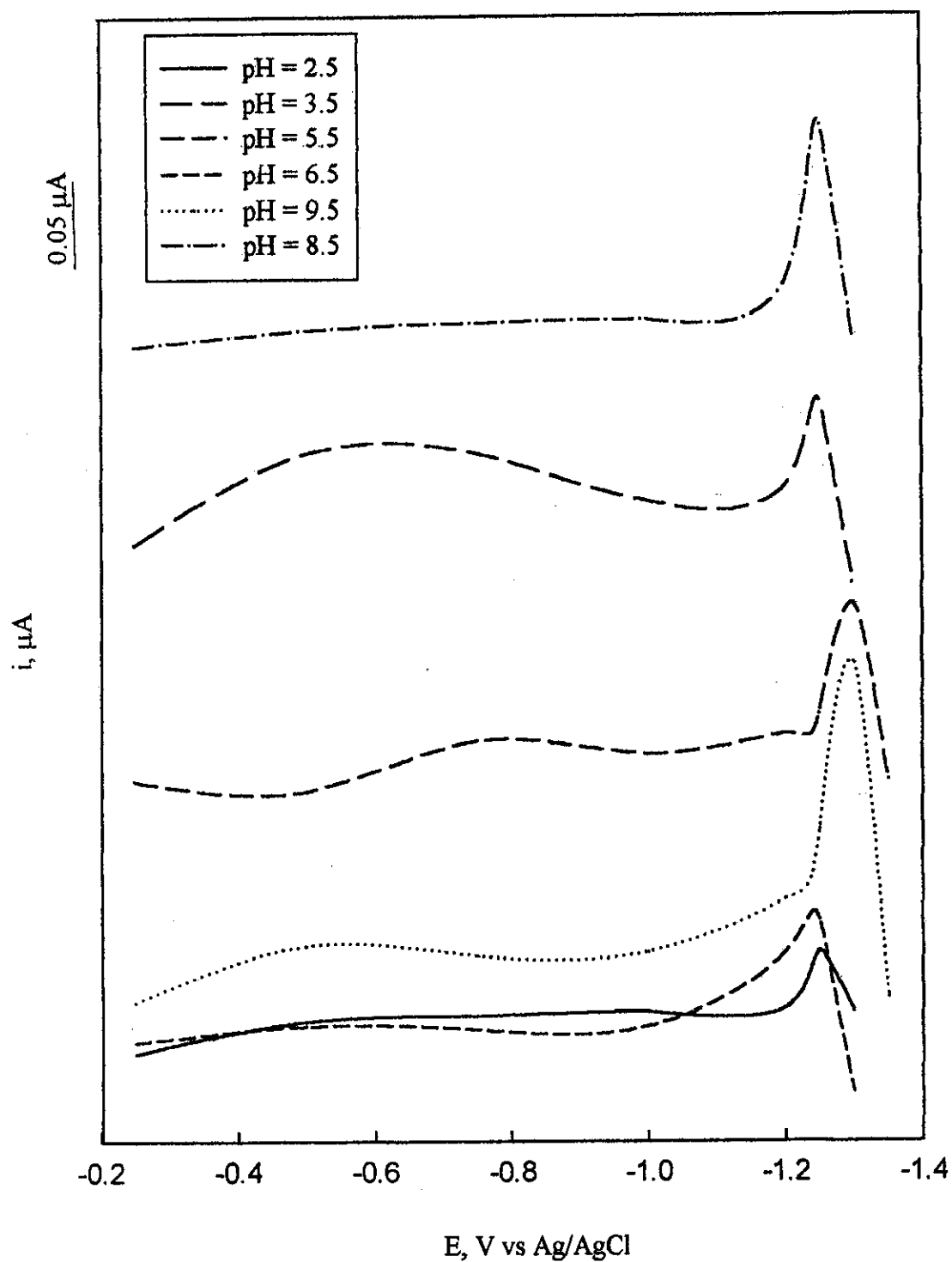


Fig. 43: Effect of pH on the CAdSWSV peak of 1×10^{-6} M of norfloxacin in B.R. buffer solution at; $t_d = 300$ sec, $E_d = -200$ mV, scan rate = 1.0 mV/sec, frequency = 5000 Hz, pulse height = 20 mV and pulse width = 50 mV.

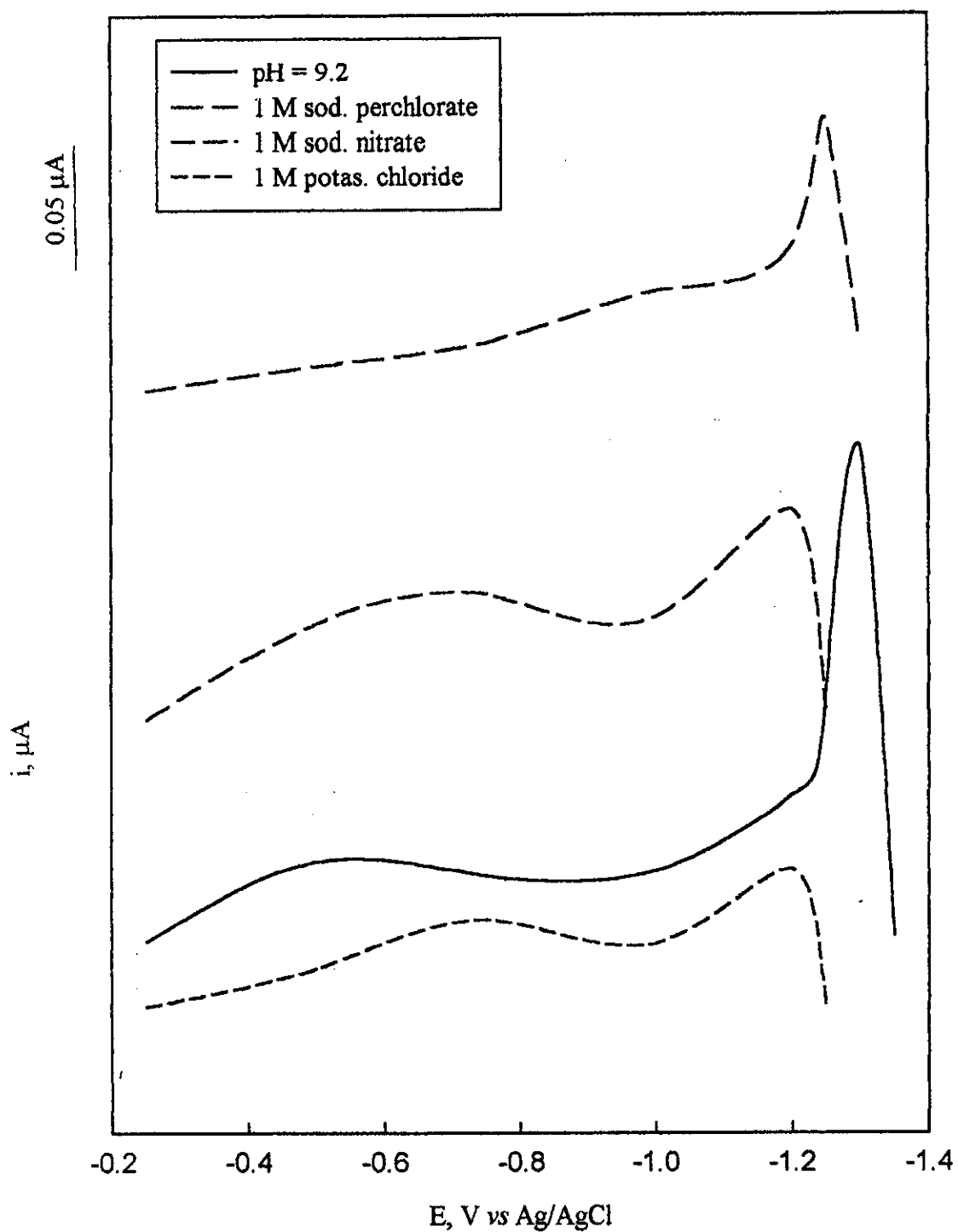


Fig. 44: Effect of supporting electrolyte solutions on the CAdSWSV peak of 1×10^{-6} M of norfloxacin in B.R. buffer solution at $t_d = 300$ sec, $E_d = -200$ mV, scan rate = 1.0 mV/sec, frequency = 5000 Hz, pulse height = 20 mV and pulse width = 50 mV.

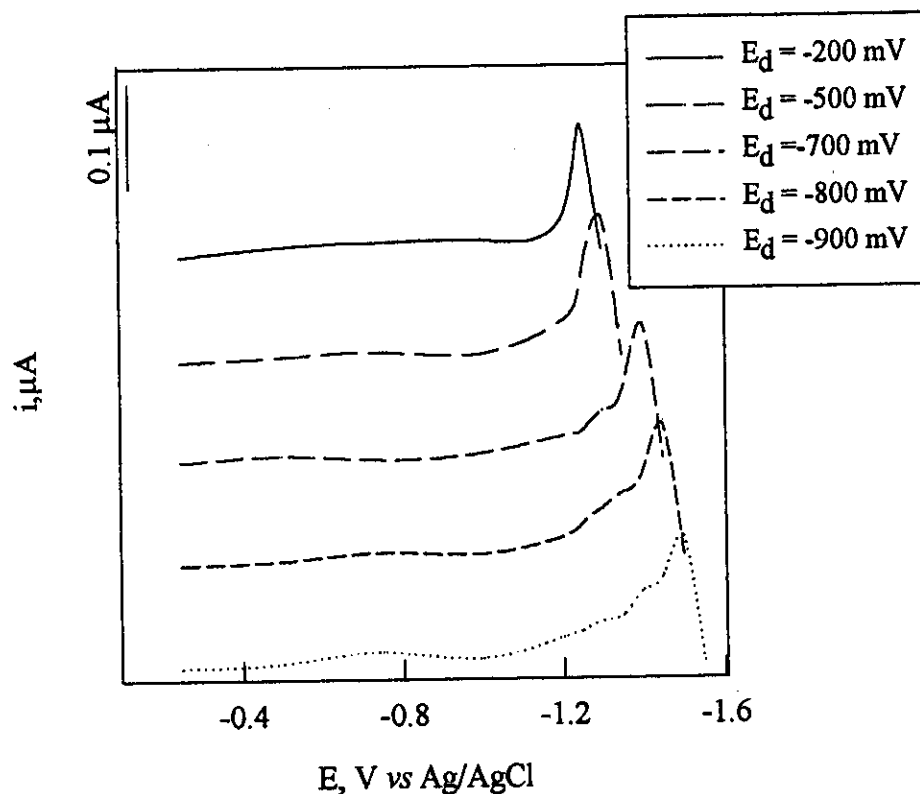


Fig. 45: Effect of E_d on 1×10^{-6} M of norfloxacin in B. R. buffer solution of pH = 9.2, scan rate = 10 mV/s, pulse height = 20 mV, pulse width = 50 mV, t_d = 300 sec and frequency = 5000 Hz

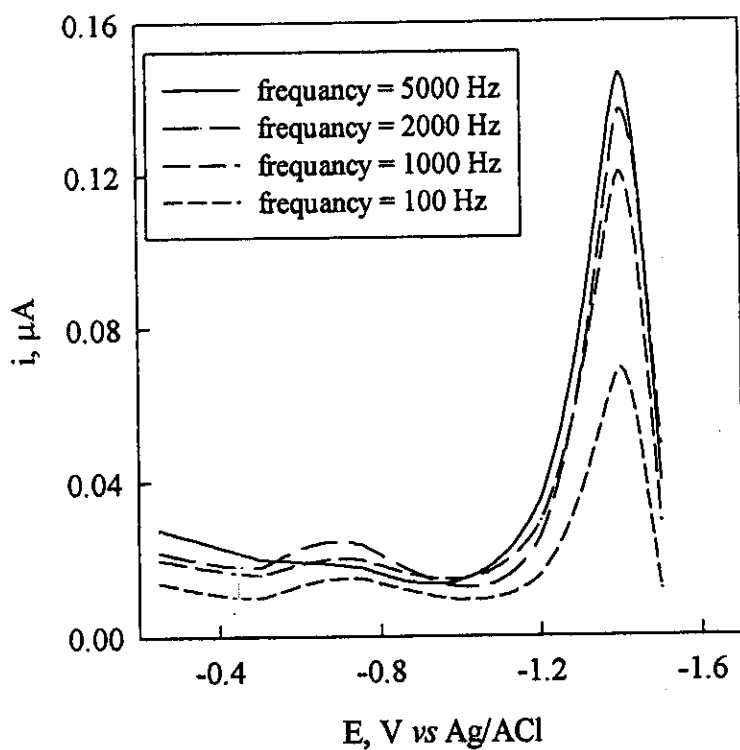


Fig. 46: Effect of frequency on 1×10^{-6} M of norfloxacin in B.R. buffer solution of pH 9.2, scan rate = 10 mV/s, E_d = -500 mV, pulse height = 20 mV, pulse width = 50 mV and t_d = 300 sec

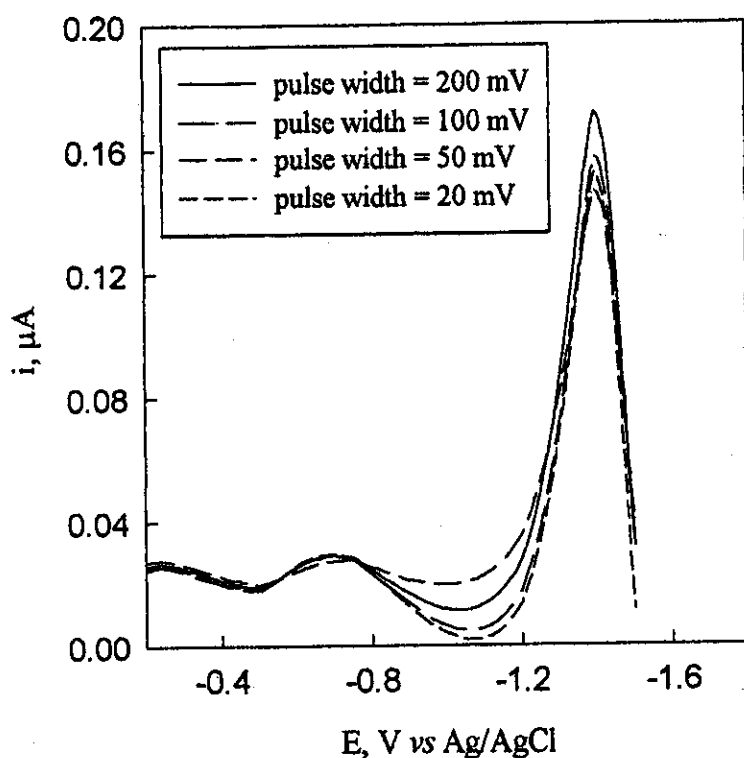


Fig. 47: Effect of pulse width of 1×10^{-6} M of norfloxacin in B.R. buffer solution of pH = 9.2, at $E_d = -500$ mV, scan rate = 1.0 mV/s and pulse height = 20 mV, $t_d = 300$ sec and frequency = 5000 Hz.

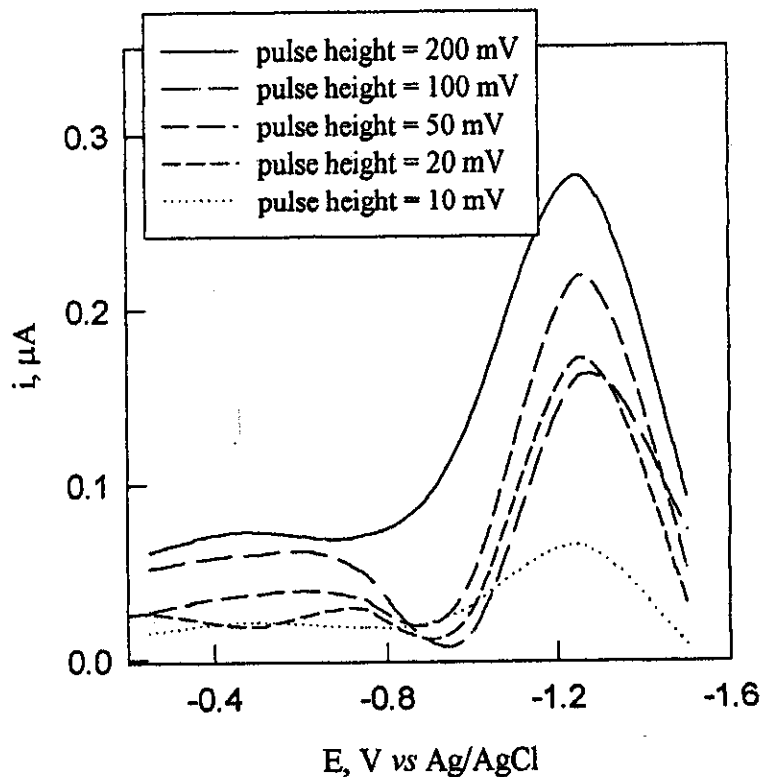


Fig. 48: Effect of pulse height of 1×10^{-6} M of norfloxacin in B. R. buffer solution of pH = 9.2, at $E_d = -500$ mV, scan rate = 1.0 mV/s and pulse width = 200 mV, $t_d = 300$ sec and frequency = 5000 Hz.

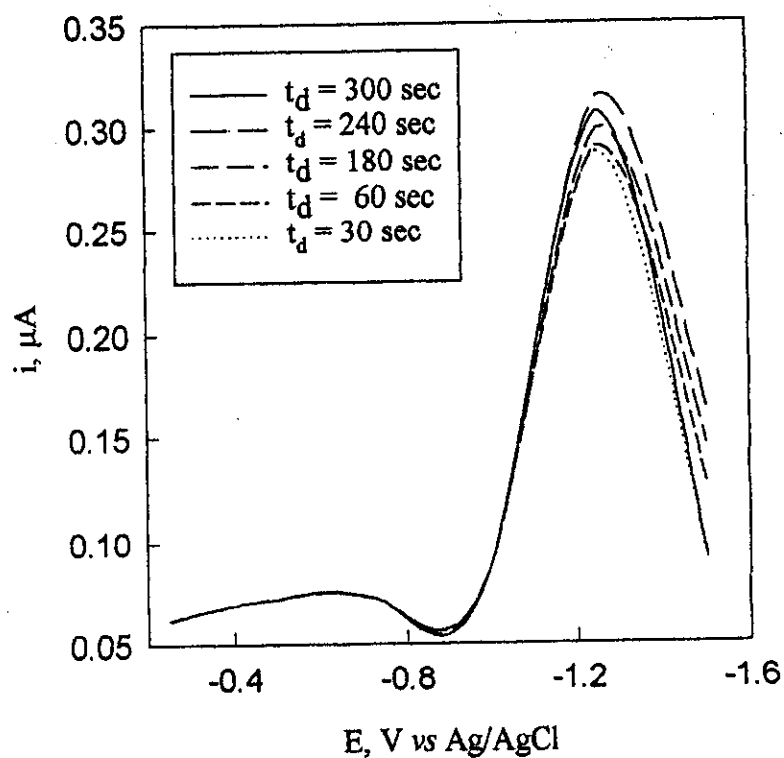


Fig. 49: Effect of t_d of 1×10^{-6} M of norfloxacin in B.R. buffer solution of pH = 9.2, at $E_d = -500$ mV, scan rate = 1.0 mV/sec and pulse height = 200 mV, pulse width = 200 mV and frequency = 5000 Hz

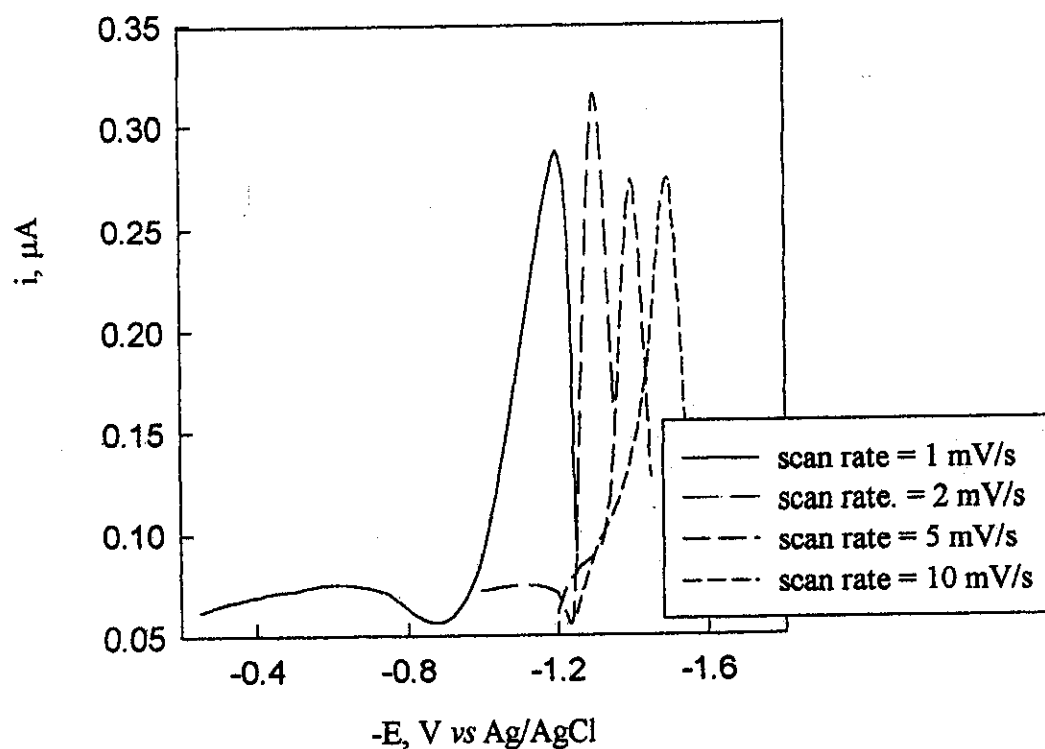


Fig. 53: Effect of scan rate of 1×10^{-6} M of norfloxacin in B.R. buffer solution of pH = 9.2, at $E_d = -500$ mV, $t_d = 240$ sec, pulse width = 200 mV, pulse height = 200 mV and frequency = 5000 Hz.

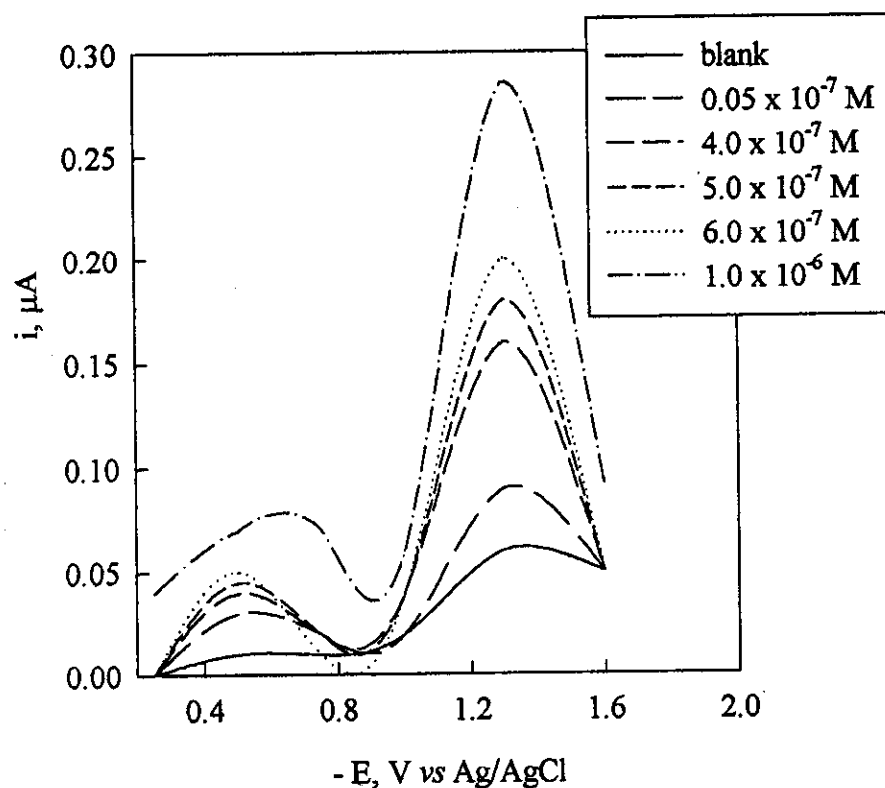


Fig. 51 A: Effect of concentration of norfloxacin in B.R. buffer solution of pH 9.2 at: $t_d = 240$ sec, $E_d = -500$ mV, scan rate = 2.0 mV/s, pulse width = 200 mV and pulse height = 200 mV.

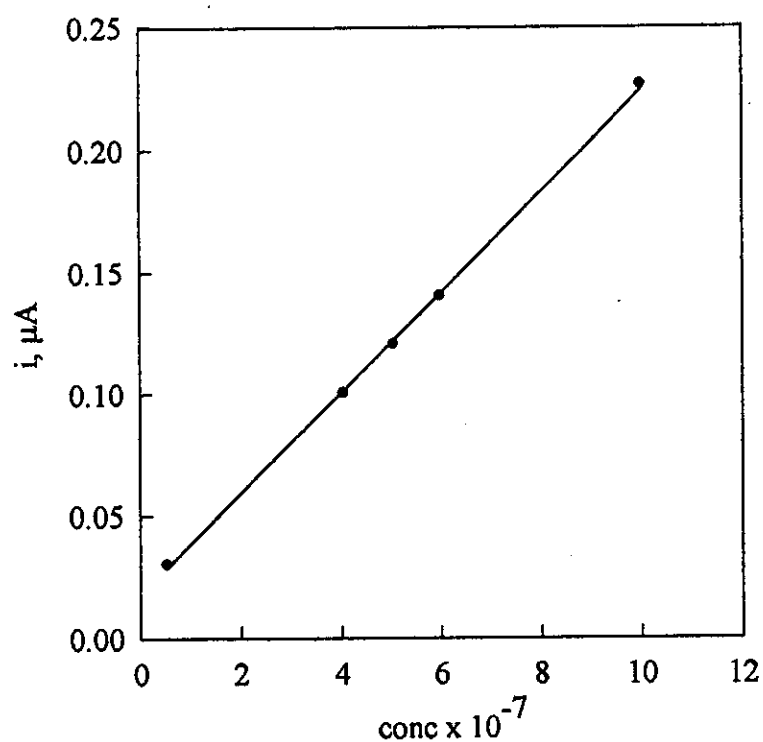


Fig. 52: Calibration curve of norfloxacin under the optimum conditions.

3.3.2. Spectrophotometric studies on drug complexes in solution

In order to investigate the optimum conditions for the formation of norfloxacin-reagent complexes, the experimental conditions were established by varying one parameter while the others were constant and observing its effect on the absorbance of the coloured species.

3.3.2.1. Determination of optimum conditions

1. Effect of pH:

In order to defined the optimum pH values at which the complexes between norfloxacin and reagents I, II, and III were formed following procedure was achieved, 5 ml of universal buffer solutions of pH range 2.5-11.5, 1.0 ml 1.0×10^{-3} M reagent I, II or III and 1.0 ml of 1.0×10^{-3} M of the drug were mixed. The volume was completed to 10 ml with distilled water. The absorption spectra were recorded against a blank solution prepared by the same way without drug at the same pH value, Fig. 53–55. The optimum pH were detected to be 3.5, 8.5 and 10.5 on using reagents I, II and III, respectively, Table 36.

2. Determination of λ_{\max} of the complex species:

The optimum λ_{\max} at which each complex species absorbed, the following sequence must be followed up:

- A) Spectrum of 1.0 ml 1×10^{-3} M of drug solution at the suitable pH using the same pH as a blank.
- B) Spectrum of 1.0 ml 1×10^{-3} M of pure reagent at the same suitable pH value using the same pH as a blank
- C) Spectrum of 1.0 ml 1×10^{-3} M of drug and 1.0 ml 1×10^{-3} M of reagent against 1.0 ml 1×10^{-3} M of reagent and buffer as blank.

The complexes were formed at λ_{max} equaled 550, 520 and 591 nm with the reagents I, II and III, respectively, Fig. 53-55.

3. Effect of time and temperature:

The effect of time and temperature on drug- reagent complexes was studied. The complexes were formed spontaneously after mixing the drug and reagents at room temperature and remain stable for 24 h.

4. Effect of sequence of additions:

On changing the sequence of additions of the drug, buffer and reagent, it found that the following sequence (reagent-drug-buffer) gave the best results for complexes of norfloxacin with all analytical reagents used in this study, other sequence gave lower absorbance values under the same experimental conditions.

5. Effect of reagent concentration:

Different concentrations of the reagents I, II and III were added to the constant volume of drug 1.0 ml of 1.0×10^{-3} M and the buffer solution of suitable pH. It is found that 1.0 ml of 1.0×10^{-3} M of reagents is sufficient to produce maximum absorbance value.

3.3.2.2. Molecular structure

1. Molar ratio method:

The molar ratio method was used to study the stoichiometry of the complexes between norfloxacin and reagents I, II and III. The obtained absorbance values were plotted against the molar ratio $[R]/[D]$, Fig 53-55. Experimental results showed that the ratio of all formed complexes was 1:1 (D: R).

2. Continuous variation method:

Continuous variation method was used for investigating the ratio of the drug and reagents in the formed complexes. The results obtained by this method revealed the formation of only 1:1 ion-pair complexes were formed.

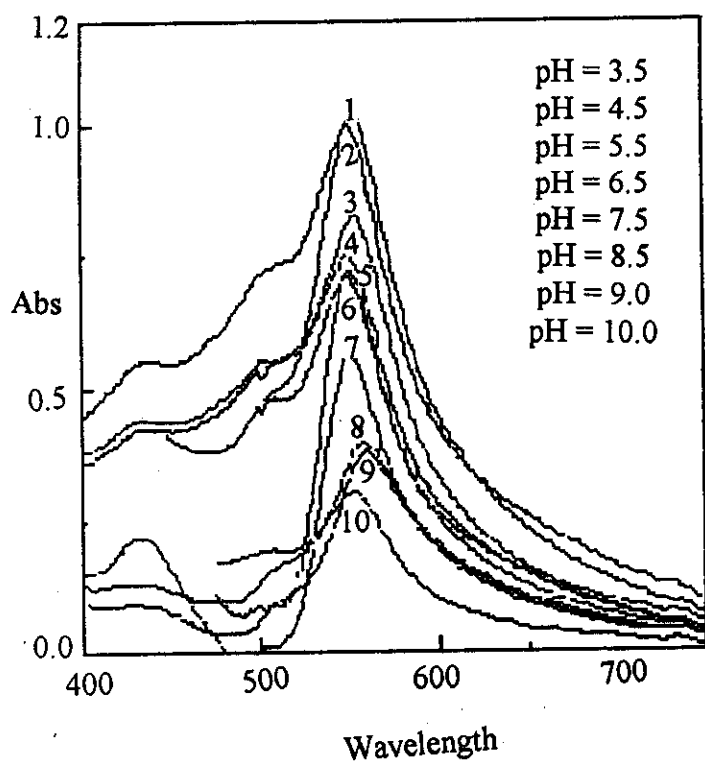
3.3.2.3. Stability constants of the formed complex:

The molar ratio and continuous variation methods used for the determination of the stability constant of the formed complex. The values of the stability constant showed that the norfloxacin-I is more stable than norfloxacin -III and norfloxacin -II, Table 36.

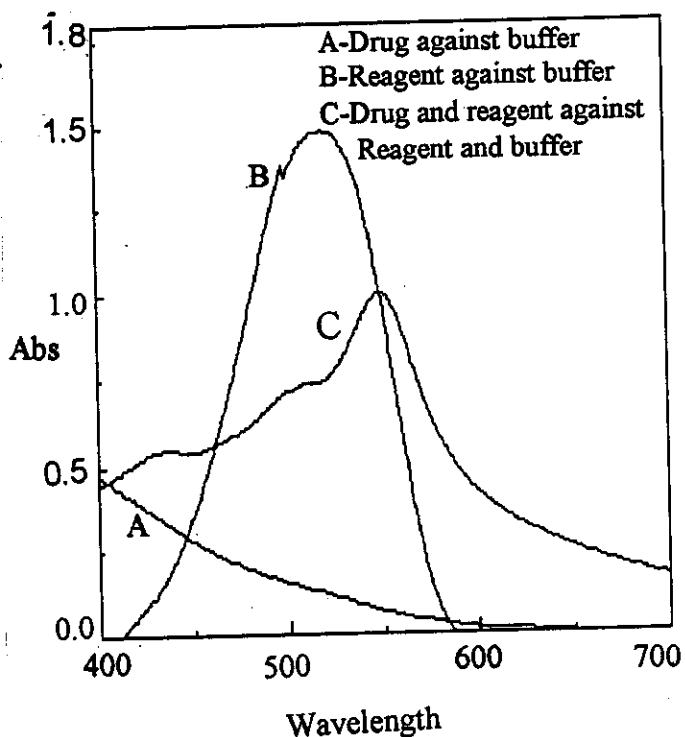
Table 36:

stiochiometry and stability constant of reagent complexes obtained from different spectrophotometric methods.

Complexes	pH	λ_{\max}	Molar ratio		Continous variation	
			R:D	Log K	R:D	Log K
Nor-I	3.5	550	1:1	8.69	1:1	8.32
Nor -II	8.5	520	1:1	7.06	1:1	7.01
Nor -III	10.5	591	1:1	8.61	1:1	8.24



Effect of pH on nor-I complex



Determination of wavelength

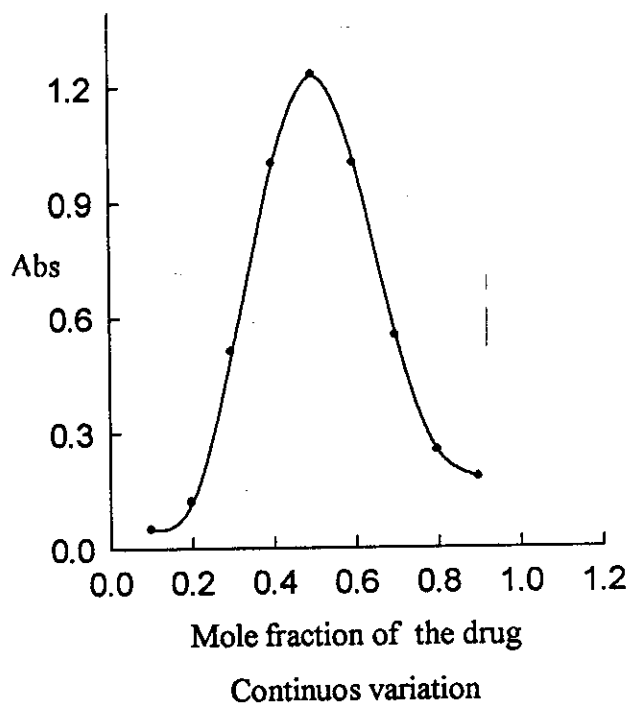
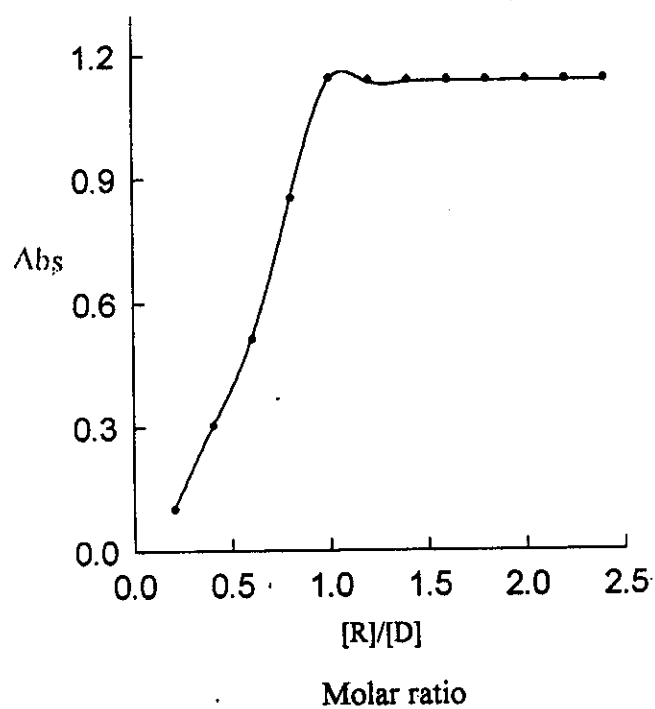
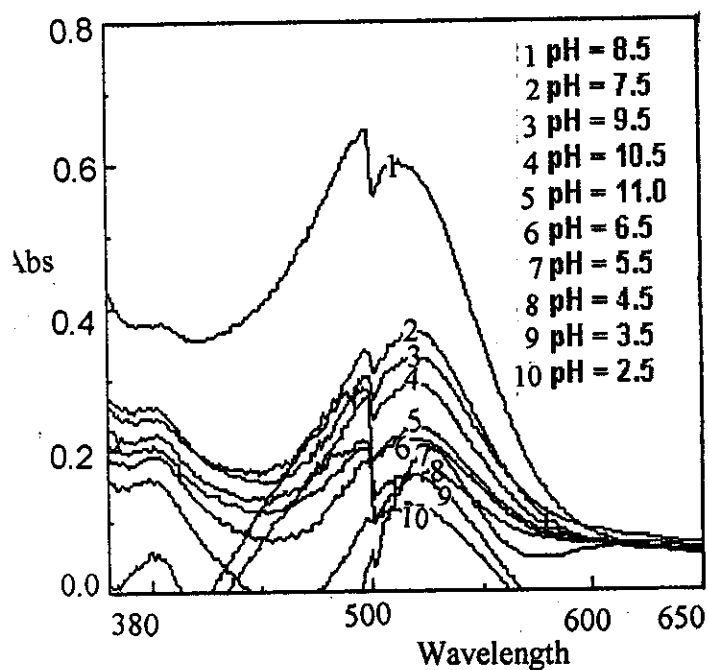
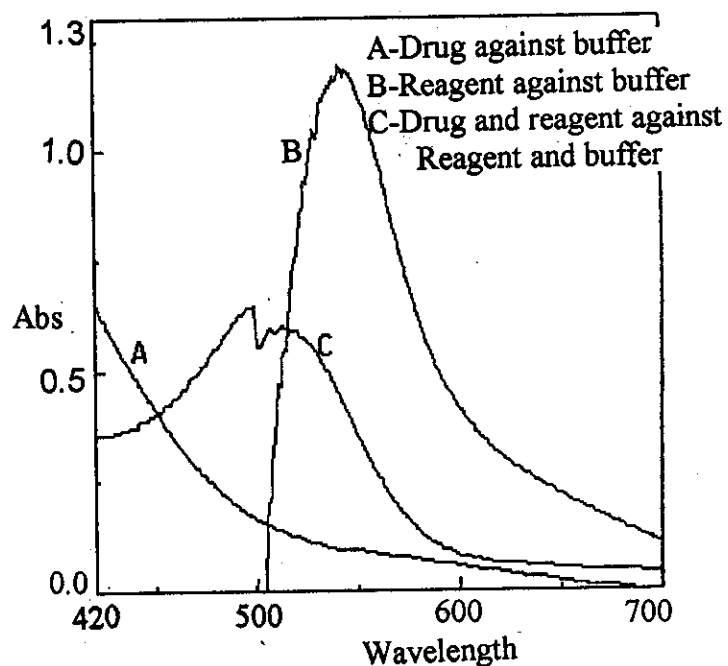


Fig. 53: Norfloxacin with sudan II



Effect of pH on Nor-II complex



Determination of wavelength

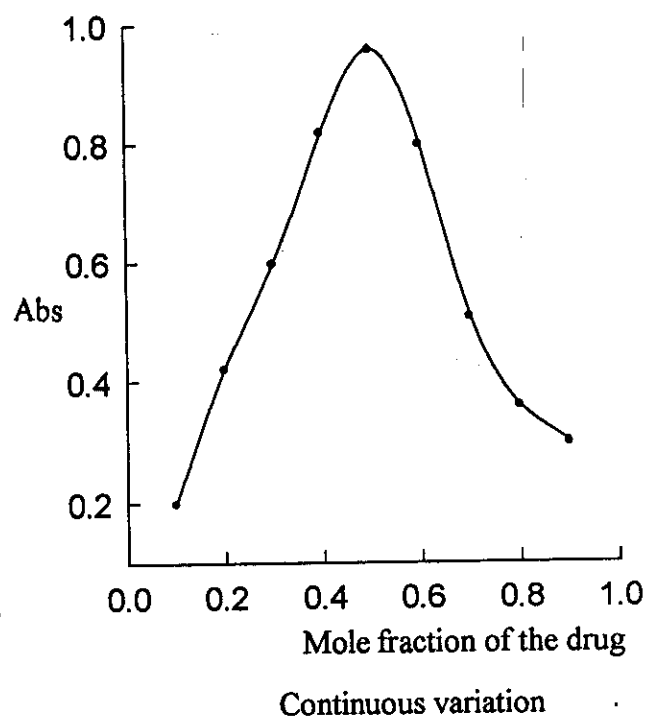
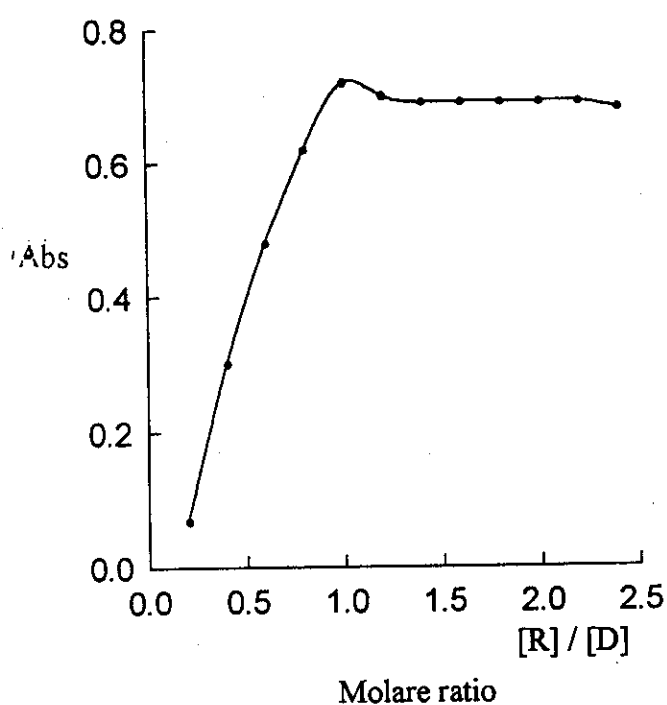
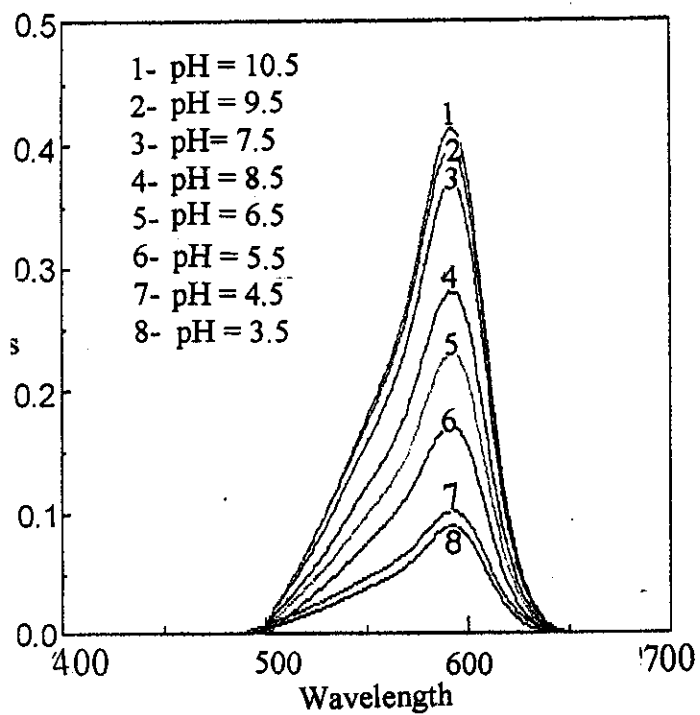
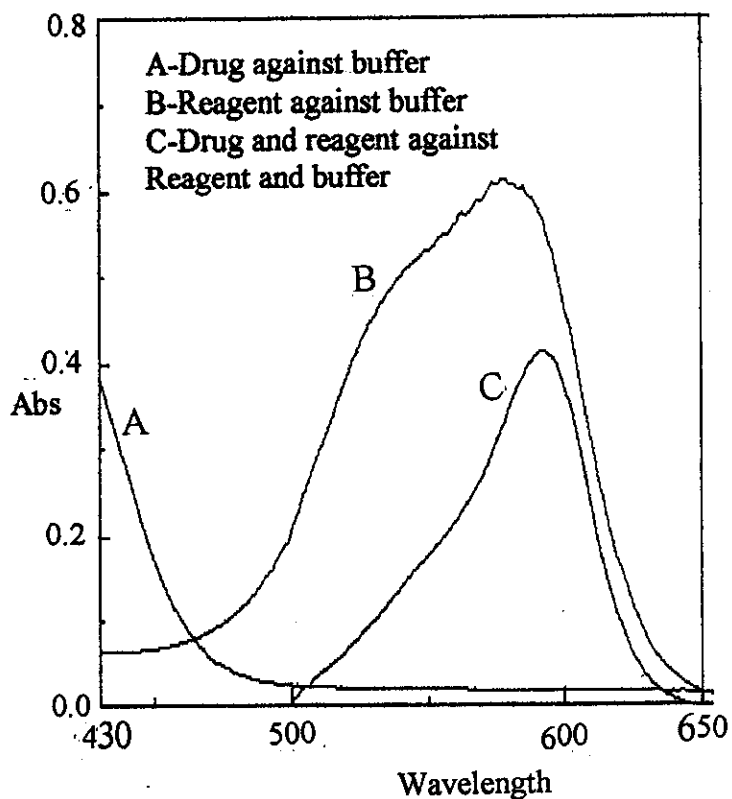


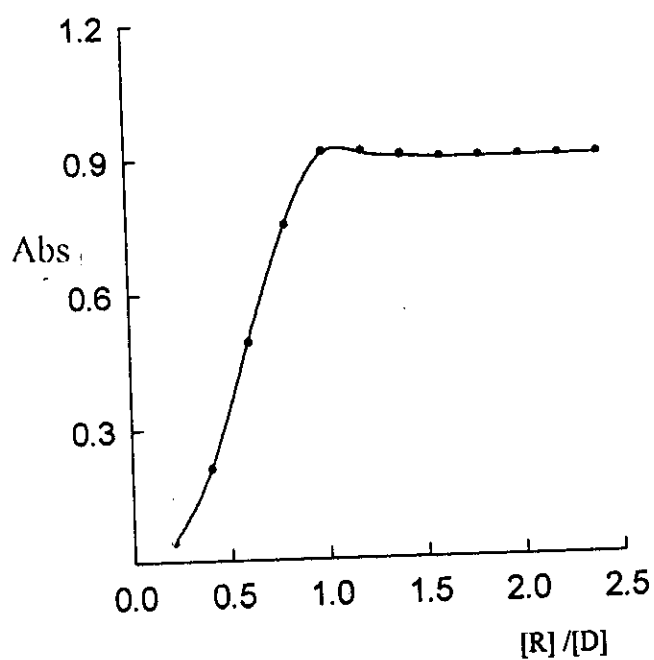
Fig. 54: Norfloxacin with congo-red



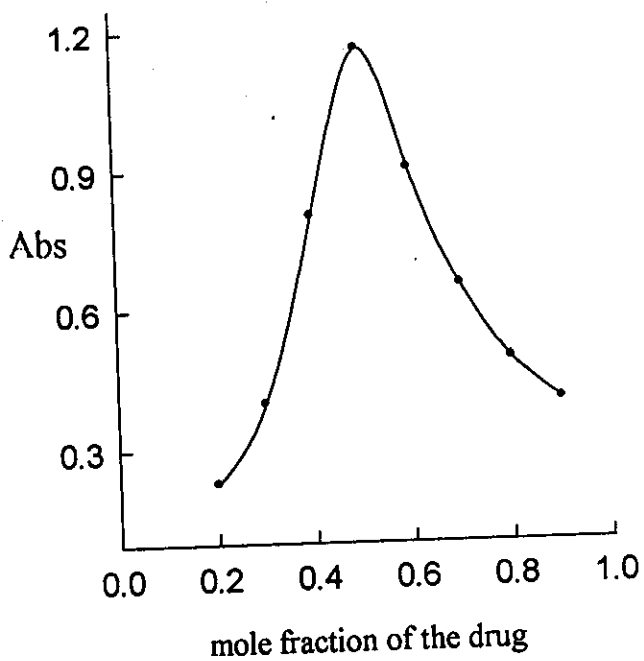
Effect of pH on nor-III



Determination of wavelength



Molar ratio



Continuous variation

Fig. 55: Norfloxacin with gentian violet

3.3.2.4. Validity of Beer's law:

After optimizing the experimental conditions at which the maximum absorbance was recorded, the absorbance of a series of different concentrations of the investigated drug in $\mu\text{g/ml}$ were measured at the recommended λ_{max} and plotted as a function of the drug concentration as in Fig. 56. The limits of concentration in which the drug obey Beer's law were listed in Table 37.

Ringbom optimum concentration range was determined, Fig. 57. The values of molar absorptivity and **Sandell** sensitivity were listed also in Table 37. The results indicate high sensitivity in the micro determination of norfloxacin.

3.3.2.5. Interference:

The interferences of co-existing additives were investigated under the optimum conditions. Experiments showed that all additives did not interfere in the determination of norfloxacin, indicating the high selectivity of the proposed method.

3.3.2.6. Analytical applications:

The proposed method for determination of norfloxacin using the analytical reagents I, II and III, was applied to norxin tablets. This pharmaceutical formulations containing norfloxacin tablet was analysed using the proposed reagents (six determinations). The obtained results Results were shown in Table 38 showing good agreement with those of the British Pharmacopoeia (1998) procedure which is based on HPLC method and so confirming that the proposed method is highly sensitive, therefore it could be used easily for the routine analysis of pure form and in its pharmaceutical preparations.

3.3.2.7. Accuracy and precision:

The accuracy of the proposed was appointed using different concentrations. This was checked during the work by running six replicate standard samples.

In order to determine the precision of the method, solutions containing different concentrations of drug were prepared and the absorbance of the prepared solution was measured and repeated for six times. The value of standard deviation was calculated as in Table 38.

The Students t-test and the variance ratio F-test values obtained at 95 % confidence level and five degrees of freedom did not exceed the theoretical tabulated value indicating no significant difference between the proposed and the official methods.

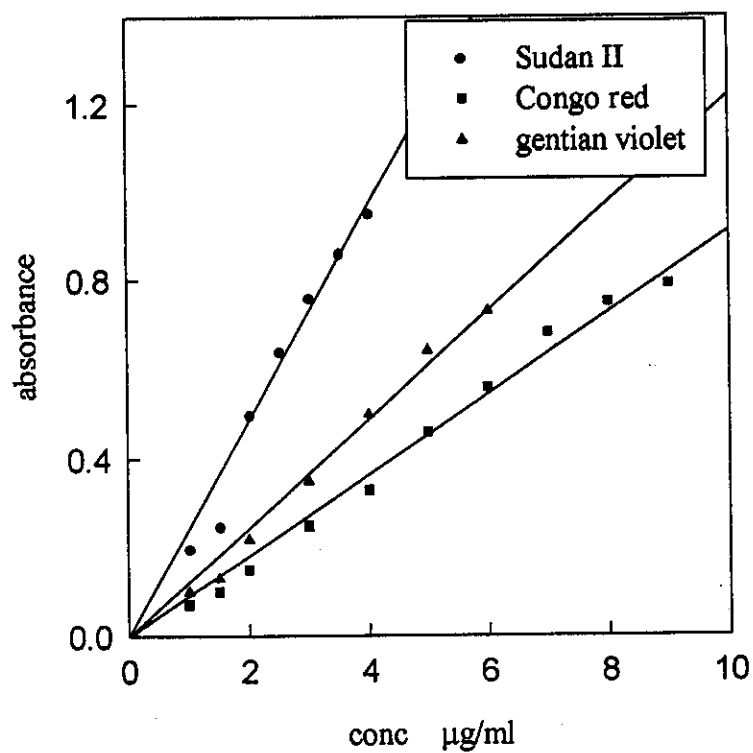


Fig. 56: Beer's law graph of the norfloxacin using reagents under consideration

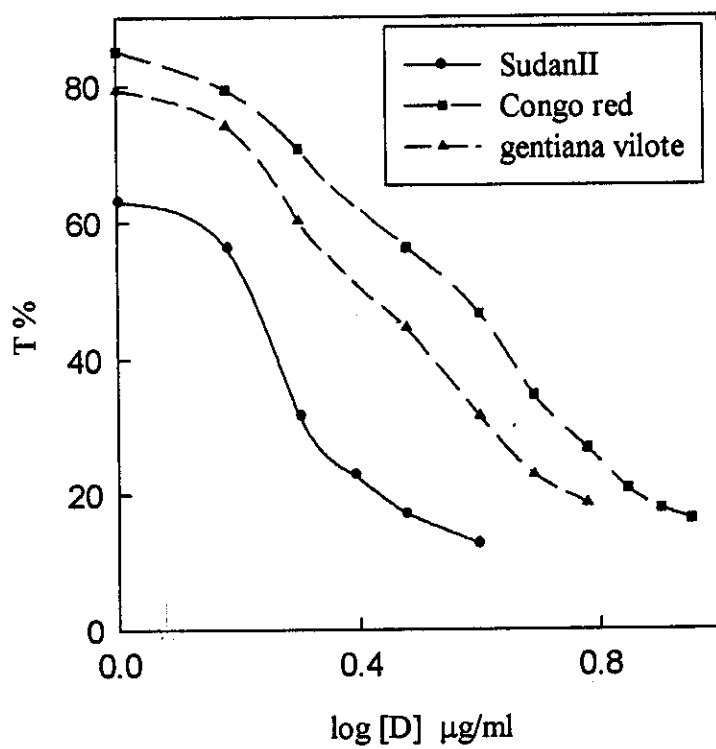


Fig. 57: Ringbom graph for norfloxacin

Table 37:

Cumulative data of norfloxacin with the reagent I, II and III.

Reagent	pH	λ_{\max}	Ringbom range $\mu\text{g/ml}$	Beer's range $\mu\text{g/ml}$	S.D	R.S.D %	Error %	S ng cm^{-2}	ϵ $\text{l mol}^{-1} \text{cm}^{-1}$
I	3.5	550	1.26-3.25	1.0-4.0	0.26	0.41	0.167	4.99	6.4×10^4
II	8.5	520	1.26-8.41	1.0-9.0	0.17	0.28	0.114	8.87	3.6×10^4
III	10.5	591	1.26-5.16	1.0-6.0	0.12	0.23	0.094	10.30	3.1×10^4

*S: Sandell sensitivity

* ϵ : Molar absorptivity

Table 38:

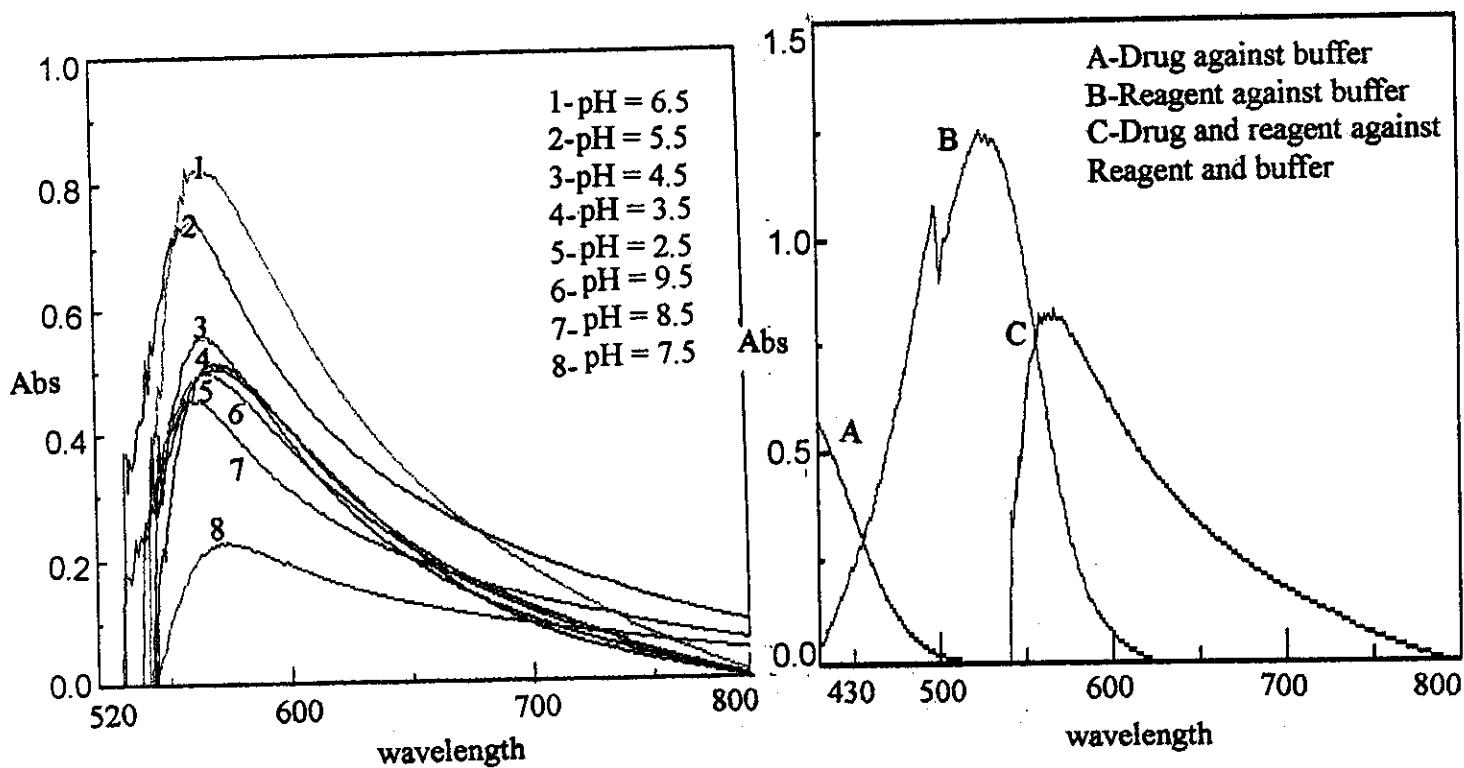
Evaluation of accuracy and precision of the proposed and official methods for norfloxacin determination in norxin tablets

Reagent	Content mg/tab	Found* (mg)		S.D	R.S.D %	Error %	Recovery %	F# value	t# value
		O	P						
I	400	392	398	0.244	0.264	0.108	99.5	1.718	0.35
II	400	392	399	0.316	0.356	0.145	99.8	1.024	0.76
III	400	392	393	0.250	0.270	0.110	98.3	1.636	0.16
t# Theoretical value = 2.57									
F# Theoretical value = 5.05									

*: Average of six determinations

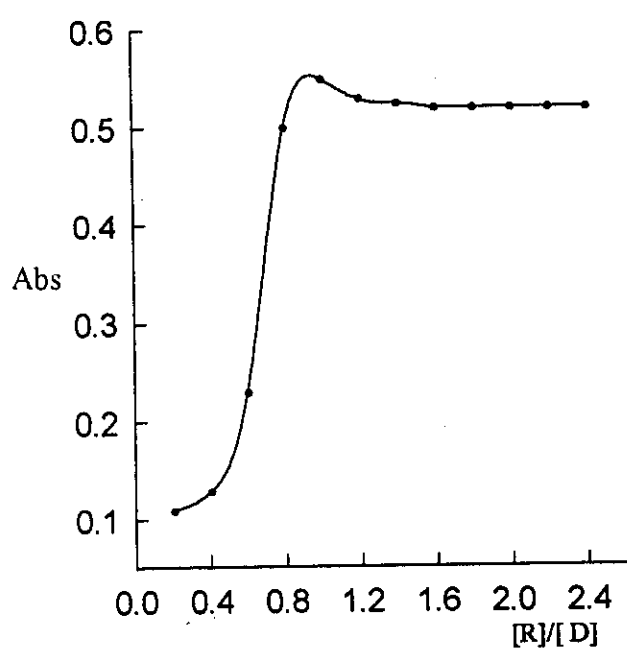
O: Official method

P: Proposed method

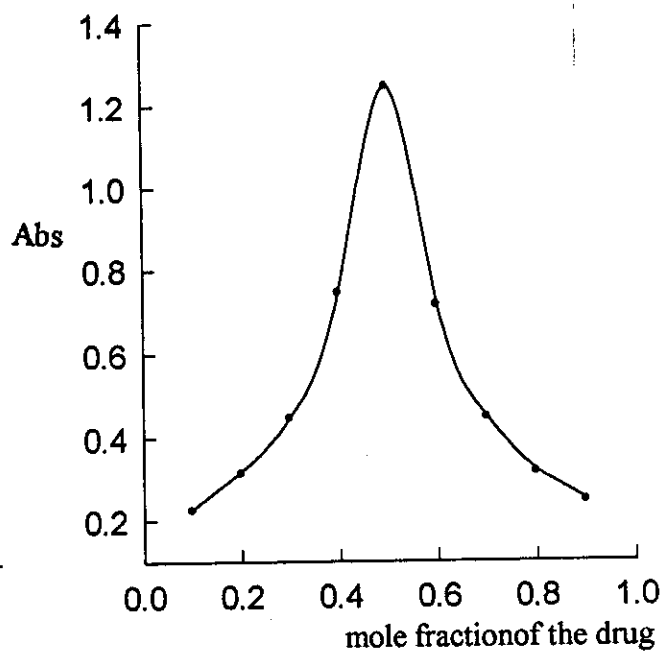


Effect of pH on ofl-I complex

Determination of wavelength



Molar ratio

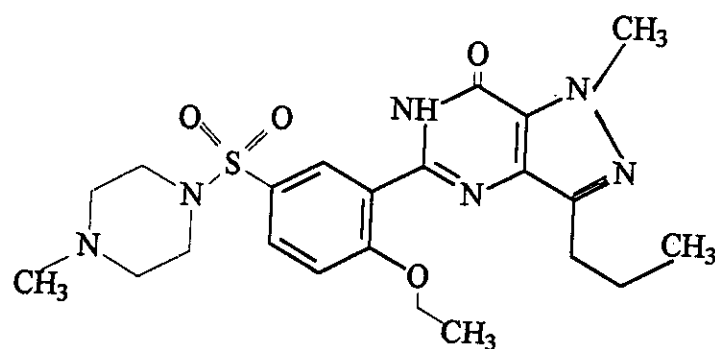


Continuous variation

Fig. 34: Ofloxacin with sudan II

3.4. Electrochemical and analytical behaviour of sildenafil citrate in B.R. solutions of different pH-values:

sildenafil citrate is 1-[[3- (6,7-dihydro-1-methyl-7-oxo-3-propyl-1 H-pyrazolo[4,3-d]-pyrimidin-5-yl)-4-ethoxyphenyl]sulfonyl]-4-methyl-piprazine citrate] is sexual stimulant⁽⁹⁹⁾.



Sildenafil citrate

The electrochemical studies of sildenafil citrate including the electrochemical behaviour at the mercury dropping electrode using DC-polarography technique and at glassy carbon electrode using cyclic voltammetry technique. Also it includes determination of sildenafil citrate in pure and pharmaceutical dosage form using square-wave adsorptive stripping voltammetric and spectrophotometric techniques.

3.4.1. Electrochemical behaviour of sildenafil citrate in B.R. solutions of different pH-values:

I- DC-Polarography:

Current-Potential Curves:

The polarographic reduction of 4×10^{-4} M of sildenafil citrate was investigated in B.R. buffer solutions of different pH values in the range from 3.5 to 10.0 containing 20% (v/v) ethanol. The recorded polarograms showed a single reduction wave in the entire pH range, Fig 58A. The wave height is slightly constant over the studied pH range, Fig. 58B.

$E_{1/2}$ of the polarographic waves displayed shift to more negative potentials on increasing the alkalinity of the electrolysis medium. This indicates that the H^+ ions were participating in the electrode process.

Effect of Mercury Height:

The plots of $\log i_l$ against $\log h$ for sildenafil citrate in B. R. buffer solutions of different pH-values containing 20% (v/v) ethanol were recorded and represented in Fig. 58C. Calculation of the exponent x , was found to vary from 0.559 to 0.700. These values indicated that the reduction process is mainly controlled by diffusion with some adsorption contribution, Table 39.

Analysis of the Polarographic Waves:

Plotting of $\log [i/i_d - i]$ against $E_{d.e}$ of the polarographic waves gives linear correlations, Fig 58D. The slope values S_1 amounting from 50.1 to 63.1 mV indicating the irreversibility of the electrode process, Table 39. The values of the transfer co-efficient α can be calculated for probable values of n_a . The most probable values of α indicated that, within the studied pH range n_a was equal to two for sildenafil citrate.

Half-Wave Potential –pH Curves:

Plotting of $E_{1/2}$ against pH for the recorded waves gives a straight line with two segments with slope value S_2 , Fig. 58E. The number of hydrogen ions Z^+_H for sildenafil citrate were calculated at different pH values, Table 39. Furthermore, the most probable values of α parameter indicated that, the ratio $Z^+_H/n_a = 0.5$. This means that the number of protons and electrons n_a involved in the rate-determining step equal to one and two, respectively.

Table 39:

Polarographic data and parameters for the reduction of 4×10^{-4} M sildenafil citrate in buffer solutions of various pH values containing 20% ethanol, at 25°C.

pH	i_d μA	$-E_{1/2}$ V	$\log i_1$ /log h	S_1 mV	αna	\underline{g}		S_2 mV	Z^+_{H}
						$n_a=1.0$	$n_a=2$		
3.5	1.09	1.08		55.2	1.071	1.071	0.535	38	0.688
4.5	1.04	1.12		59.3	0.996	0.996	0.498	38	0.641
5.5	1.04	1.16	0.56	61.0	0.968	0.968	0.484	38	0.623
6.5	0.97	1.19		56.6	1.045	1.045	0.522	38	0.671
7.0	0.95	1.22	0.63	60.9	0.969	0.969	0.485	73	1.198
7.5	0.94	1.27		53.7	1.101	1.101	0.551	73	1.359
8.0	0.91	1.32		63.1	0.936	0.936	0.468	73	1.157
8.5	0.88	1.35	0.70	50.3	1.174	1.174	0.587	73	1.451
9.0	0.83	1.38		51.9	1.138	1.138	0.569	73	1.129
10.0	0.86	1.44		50.1	1.179	1.179	1.179	73	1.457

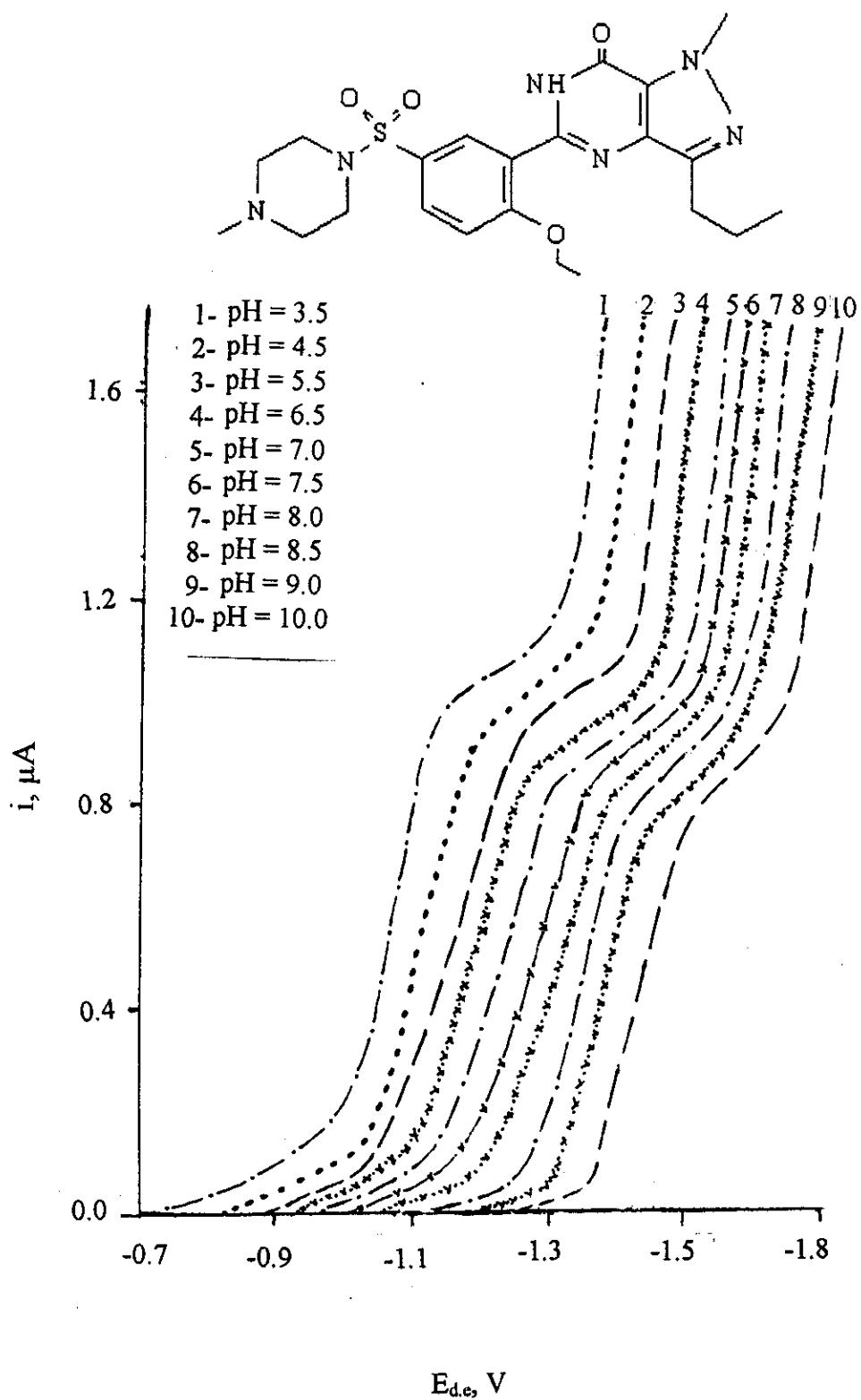


Fig. 58A: DC-polarograms of sildenafil citrate in B.R. buffer solutions of different pH values.

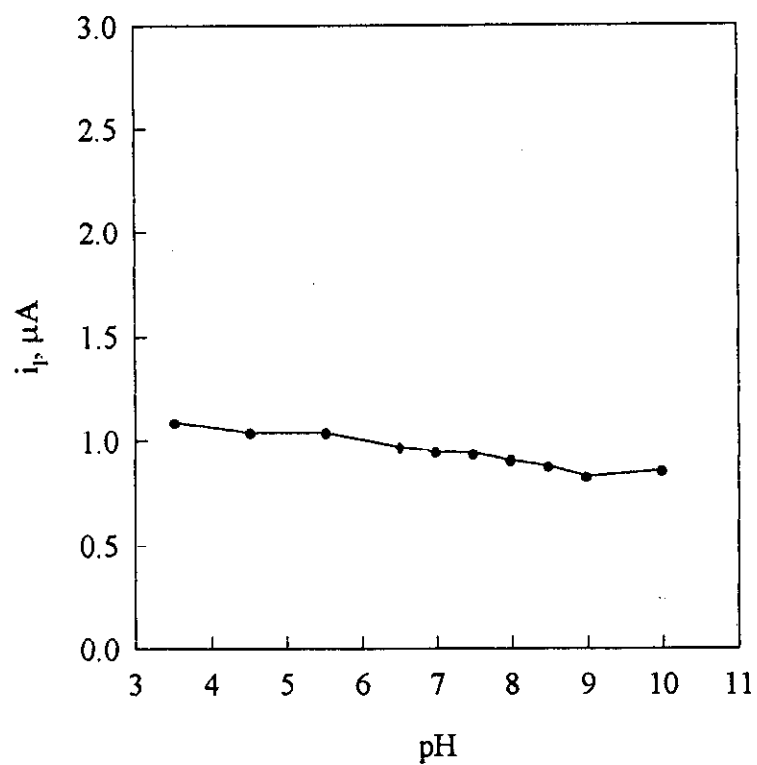


Fig. 58 B: i_l - pH plot of sildenafil citrate

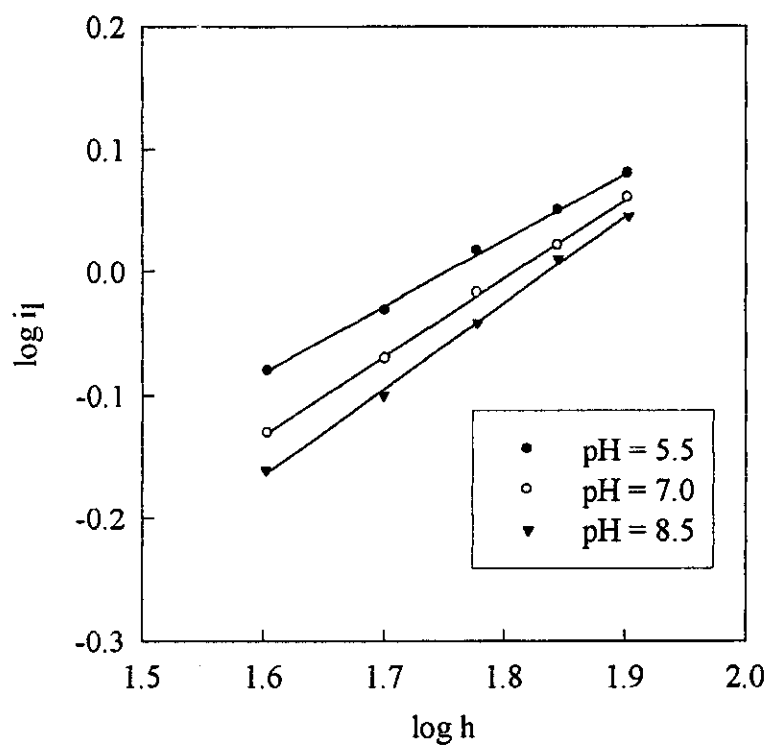


Fig. 58 C: $\log i_l$ - $\log h$ plots of sildenafil citrate at different pH values

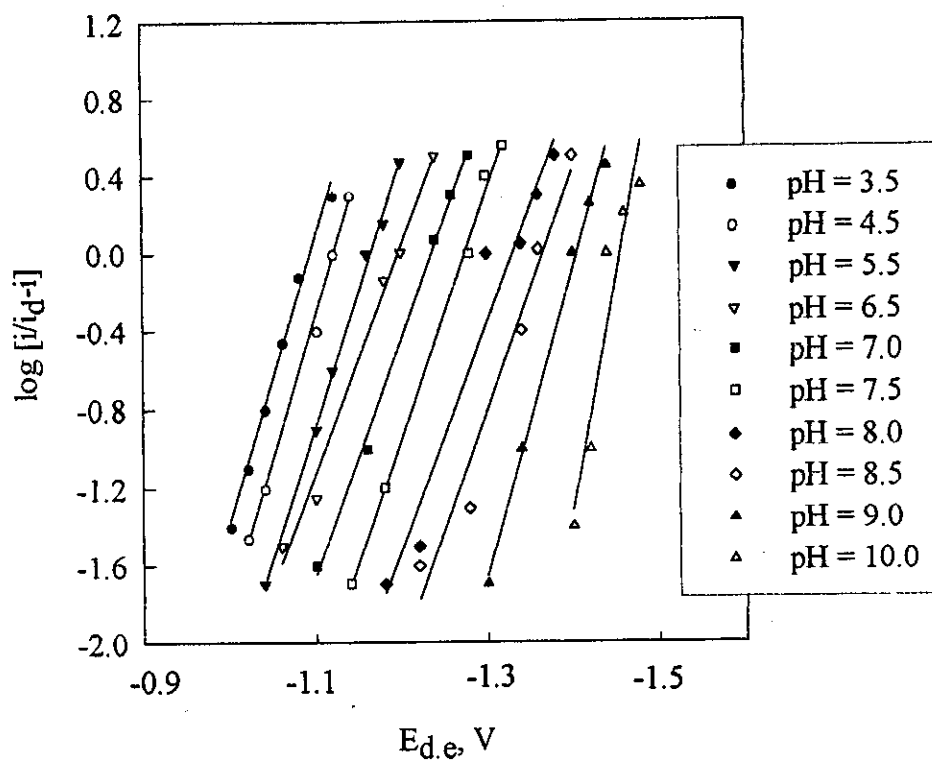


Fig. 58 D: $\log [i/i_d - i] - E_{d,e}$ plots of sildenafil citrate at different pH values

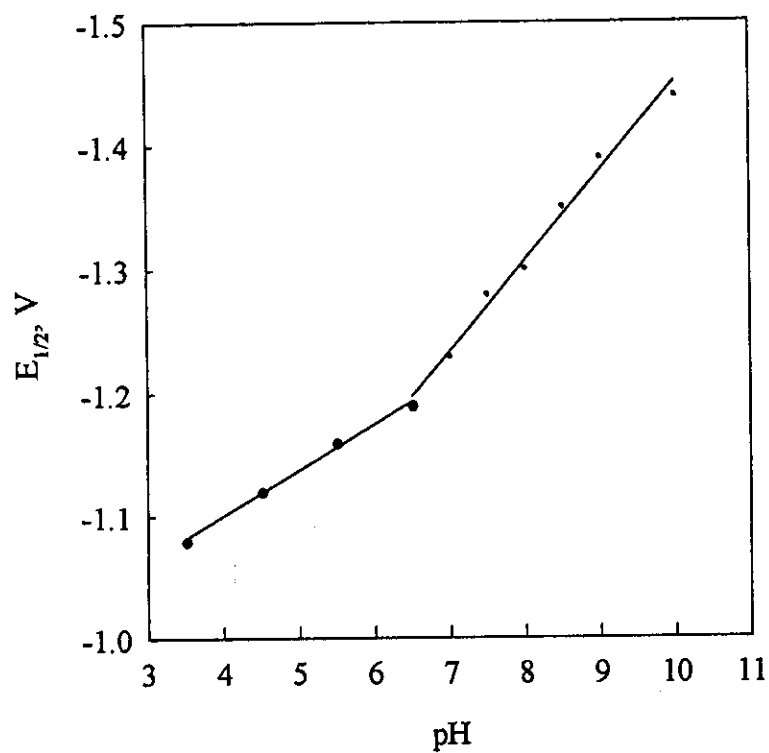


Fig. 58 E: $E_{1/2}$ -pH plots of sildenafil citrate

Determination of sildenafil citrate using DC-polarograph

Determination of sildenafil citrate was occurred in different media, sodium perchlorate, acetate buffer, B.R. buffer and phosphate buffer. The most obvious wave is shown in B.R. buffer pH 3.5. A stock solution of 1×10^{-3} M sildenafil citrate was prepared and different concentrations were obtained by accurate dilution. The polarograms of the final samples were recorded, Fig. 59 (A-B). The variation of wave current with concentration is represented in Table 40. The detection limit was found 1.0×10^{-5} M (4.45 $\mu\text{g/ml}$).

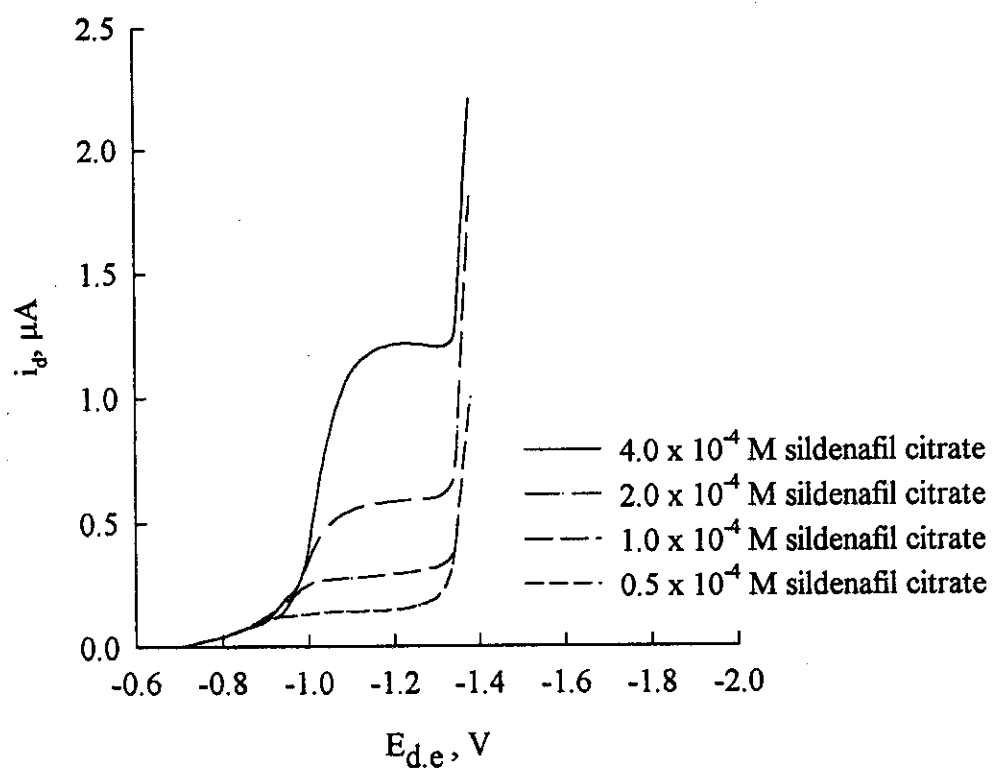


Fig. 59A: DC-polarograms of different concentration of sildenafil citrate

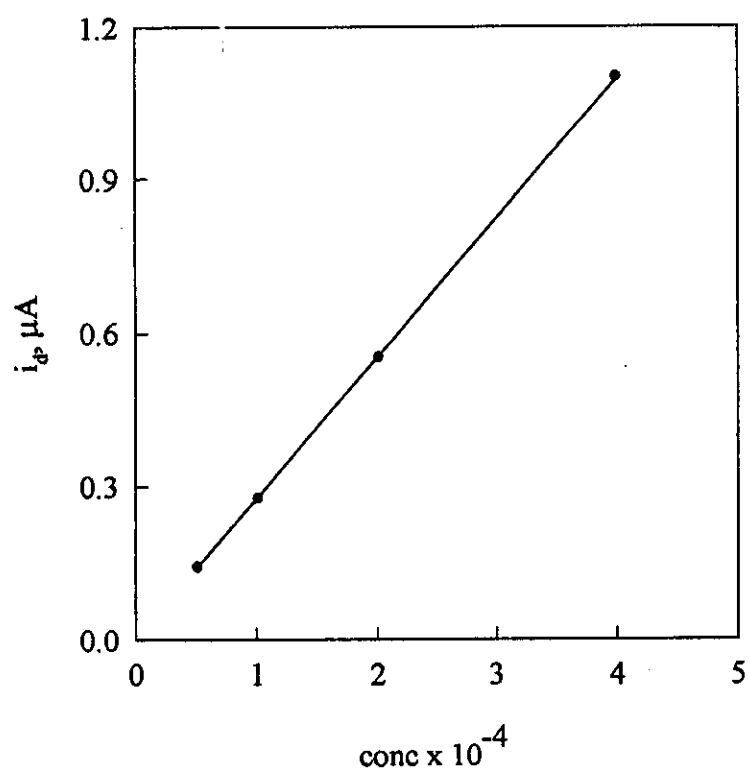


Fig. 59B: Calibration curve of sildenafil citrate

Table 40:

Assay of sildenafil citrate in B.R. buffer solution of pH 3.5 using DC polarography.

Compound Concentration M	Current (i) μA	Conc. Found	Recovery %	S.D
0.5×10^{-4}	0.137	4.970×10^{-5}	99.4	1.50
	0.136	4.890×10^{-5}	97.8	
	0.135	4.820×10^{-5}	96.4	
1.0×10^{-4}	0.273	1.000×10^{-4}	100.0	0.61
	0.271	9.880×10^{-4}	98.8	
	0.272	9.920×10^{-4}	99.2	
2.0×10^{-4}	0.545	1.990×10^{-4}	99.5	0.25
	0.543	1.980×10^{-4}	99.0	
	0.544	1.985×10^{-4}	99.3	
4.0×10^{-4}	1.090	4.000×10^{-4}	100.0	0.26
	1.091	4.001×10^{-4}	100.1	
	1.088	3.980×10^{-4}	99.6	
Recovery % = 99.1 ± 0.66				

3.4.1.2. Cyclic Voltammetry :

Cyclic voltammetric behaviour of 1×10^{-4} M of sildenafil citrate was studied at the surface of glassy carbon electrode in B.R. buffer solutions of pH = 3.6, 7.0, 9.6 containing 20% ethanol at different scan rates ranging from 20 to 500 mV /sec, Fig. 60A. These voltammograms showed only one cathodic peak within the scan rate range. The peak potential showed a cathodic shift by increasing the scan rate that indicated the irreversible nature of the electrode reaction pathway.

Plotting of i_p against $v^{1/2}$, linear correlations deviating from the origin were obtained as represented in Fig. 60B. This confirming that the electrode process of sildenafil citrate is controlled mainly by diffusion with some adsorption contribution.

Plotting E_p against $\ln v$, linear correlations of slope values proportional to αn_a were obtained, Fig. 60C. Calculation of (α) for the probable values of (n_a) , shows that n_a is equal to two, Table 41. This reveals that the rate determining step of the electrode process involve two electrons.

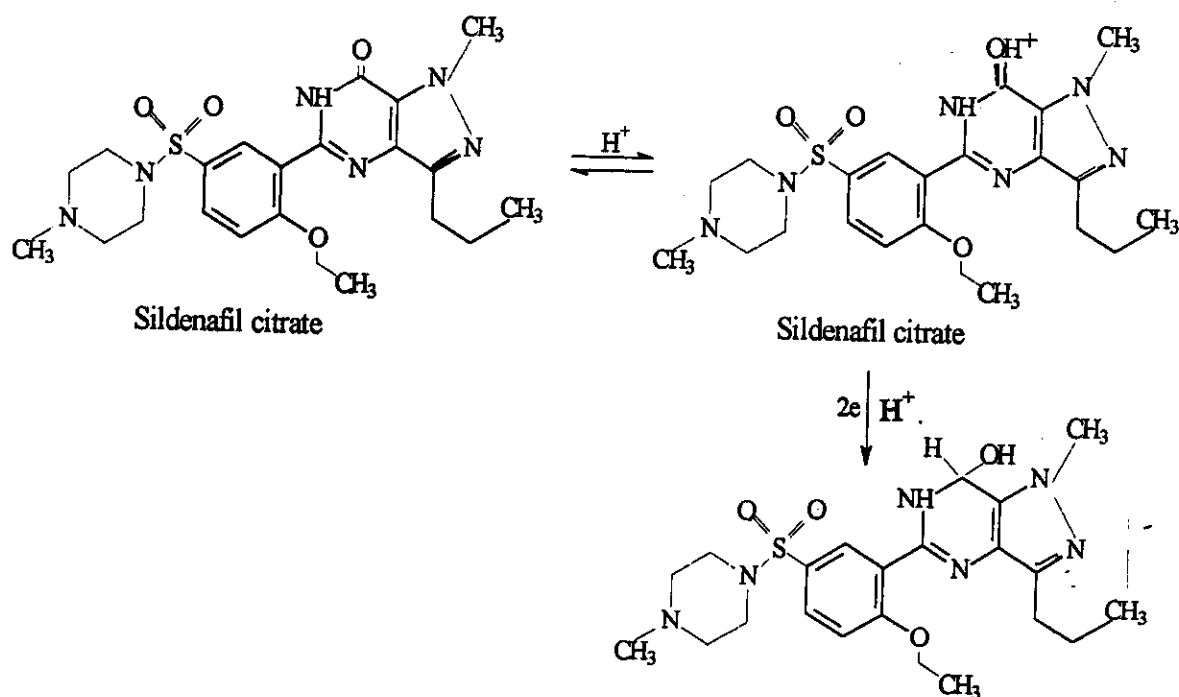
Table 41:

Cyclic voltammetric data for 1×10^{-4} M sildenafil citrate in aqueous B.R. buffer solution of different pH values containing 20% (v/v) ethanol, at 25°C.

pH	Scan rate (mV/s)	i_p μA	$-E_p$ V	$\delta E_p / \delta \ln v$	α	
					na=1.0	na=2.0
3.6	500	12.33	0.660	0.0124	1.036	0.518
	300	7.67	0.653			
	200	5.67	0.645			
	100	4.67	0.630			
	50	3.67	0.623			
	20	3.00	0.615			
7.0	500	20.83	0.760	0.0118	1.089	0.544
	300	13.33	0.740			
	200	10.83	0.720			
	100	7.50	0.700			
	50	5.83	0.680			
	20	4.17	0.660			
9.6	500	22.30	1.075	0.0105	1.224	0.612
	300	13.85	1.000			
	200	10.77	0.975			
	100	6.69	0.950			
	50	6.92	0.925			
	20	5.38	0.900			

The Electrode Reaction:

From DC-polarographic data shown in Table (39), the number of electrons at the rate determining step was found to be two. From controlled potential coulometry (CPC) n was determined to be 2.0 electrons. The number of Z_H^+ at the rate determining step was found to be unity. The reduction process of sildenafil citrate was achieved by consuming one proton and two electrons as following:



3.4.1. Cathodic Adsorption Square Wave Stripping Voltammetry of sildenafil citrate

The electroanalytical determination of sildenafil citrate in pure and pharmaceutical dosage forms was performed using square wave stripping voltammetry technique at the surface of the glassy-carbon electrode. The method of determination was optimized by conditioning the instrument as well as the suitable media.

I. Optimization of the experimental and instrumental conditions

Both of the experimental and instrumental conditions were optimized for the electroanalytical determinations of sildenafil citrate using square wave stripping voltammetry by studying the following effects:

1. Effect of pH on the cathodic adsorption stripping peak current of sildenafil citrate

The cathodic adsorption stripping voltammetric current of 1.0×10^{-6} M sildenafil citrate was recorded as a function of potential in B.R. buffer solutions of different pH values 2.0-11.5 and represented in Fig. 61. The obtained peaks were due to the reduction of the adsorbed drug at the glassy-carbon electrode surface. A well-developed peak was observed at pH equal 7.5.

2. Effect of supporting electrolyte on the CAdSWSV peak of sildenafil citrate

The effect of some supporting electrolytes on the CAdSWSV peak was studied and represented in Fig. 62. The most suitable medium for electrolysis and developing well peak current of sildenafil citrate was B.R. buffer solution of pH 7.5.

3. Effect of deposition potential

The influence of deposition potential was recorded over the potential range from -200 to -900 mV, Fig. 63. The most suitable deposition potential is -400 mV.

4. Effect of frequency

The effect of variation of the frequency on the electrochemical response was recorded at values ranging from 100 to 5000 Hz. The current of the formed peak was found to increase on increasing the frequency, Fig. 64. The most suitable value of frequency was found 5000 Hz.

5. Effect of pulse width

The effect of pulse width on the peak height was studied in the range from 20 to 200 mV, Fig. 65. The most suitable pulse width was 200 mV.

6. Effect of pulse height

The effect of pulse height on the stripping peak current was studied in the range from 20 to 200 mV. The peak current formed was directly proportional to the pulse height, Fig. 66. In the present study, a sharp peak height was obtained at pulse height equal to 200 mV.

7. Effect of deposition time

The effect of deposition time on the CAdSWSV peak height was studied at different time intervals. The most suitable t_d was 300 sec, Fig. 67.

8. Effect of scan rate

On studying the effect of different scan rates from 1.0 to 10.0 mV/s. The maximum response was found at scan rate equal to 10.0 mV/s, Fig. 68.

2. Quantitative determination of sildenafil citrate by CAdSWSV

The applicability of the cathodic adsorptive square wave stripping voltammetric technique as an analytical method for the determination of sildenafil citrate was tested by measuring the peak current as a function of concentration, Fig. 69.

Calibration graph

A stock solution of sildenafil citrate 1×10^{-3} M was prepared and different concentrations were obtained by accurate dilutions. The peaks of the final samples were recorded under the optimum conditions in quarter replicate measurements. The variation of peak current versus concentration was represented Fig. 70. The slope of the calibration graph (a) was 12.2×10^4 and the intercept (b) was 0.0115 and the value of c is determined and listed in Table 43.

The precision was determined from four repeated measurements of different concentrations of the compound under the optimum conditions. The mean recovery and the standard deviation were calculated, Table 43.

Detection Limit

In the present study, the standard deviation of the blank S.D. is 1.5×10^{-4} and $a = 12.2 \times 10^4$, so the detection limit is 3.7×10^{-9} M (1.65×10^{-3} μ g/ml).

Determination of sildenafil citrate in its dosage form:

The mean recovery of sildenafil citrate in viagra tablets 100.8 ± 0.66 , Table 44. The proposed procedure is successfully applied for the analysis of sildenafil citrate in its dosage in comparing with the HPLC official method, Table 45.

Table 42:

Cathodic adsorptive square wave stripping peak current (i_p) of 1.0×10^{-6} M sildenafil citrate in B.R. buffer solution of pH 7.5 at different conditions.

Deposition time t_d , Sec	Deposition potential $-E_d$, V	Scan rate mV/s	Pulse height mV	Pulse width mV	i_p μA
Effect of E_d					
300	200	10.0	20	50	0.1054
	400				0.1163
	600				0.1075
	900				0.117
Effect of pulse width					
300	400	10.0	20	200	0.1183
				100	0.1175
				50	0.1163
				20	0.0953
Effect of pulse height					
300	400	1.0	200	200	0.1358
			100		0.1200
			50		0.1190
			20		0.1183
Effect of t_d					
300	400	10.0	200	200	0.1358
240					0.1321
120					0.1315
60					0.1301
Effect of scan rate					
300	400	1.0	200	200	0.1315
		2.0			0.1333
		5.0			0.1340
		10.0			0.1358

Table 43:

Assay of sildenafil citrate in B.R. buffer solution of pH 7.5 using CAdSWSV at: $E_d = -400$ mV, $t_d = 300$ sec, scan rate = 10.0 mV/sec, pulse height = 200 mV pulse width = 200 mV and frequency 5000 Hz.

Conc. Taken M	i _p μA	Conc. Found M	Recovery (%R)	Av. Conc. (found) M	Mean %R	S.D
9 x 10 ⁻⁷	0.1220	9.057 x 10 ⁻⁷	100.6	9.07 x 10 ⁻⁷	100.73	0.19
	0.1221	9.066 x 10 ⁻⁷	100.7			
	0.1220	9.057 x 10 ⁻⁷	100.6			
	0.1224	9.090 x 10 ⁻⁷	101.0			
8 x 10 ⁻⁷	0.1080	7.909 x 10 ⁻⁷	98.87	7.96 x 10 ⁻⁷	99.50	0.52
	0.1085	7.951 x 10 ⁻⁷	99.39			
	0.1088	7.975 x 10 ⁻⁷	99.69			
	0.1092	8.008 x 10 ⁻⁷	100.10			
6 x 10 ⁻⁷	0.0844	5.981 x 10 ⁻⁷	99.6	6.02 x 10 ⁻⁷	100.38	0.66
	0.0848	6.008 x 10 ⁻⁷	100.1			
	0.0852	6.040 x 10 ⁻⁷	100.7			
	0.0855	6.066 x 10 ⁻⁷	101.1			
5 x 10 ⁻⁷	0.0720	4.959 x 10 ⁻⁸	99.2	4.99 x 10 ⁻⁷	99.98	0.56
	0.0725	5.000 x 10 ⁻⁸	100.0			
	0.0726	5.008 x 10 ⁻⁸	100.2			
	0.0728	5.025 x 10 ⁻⁸	100.5			
The mean recovery = 100.15 ± 0.48						
Slope = 12.2 x 10 ⁴						
Intercept = 0.0115						
Corr. Coeff. = 0.9965						

Table 44:

Assay of sildenafil citrate tablet in B.R. buffer solution of pH 7.5 using CAdSWSV at: $E_d = -400$ mV, $t_d = 300$ sec, scan rate = 10.0 mV/sec, pulse height = 200 mV and pulse width = 200 mV.

Name of tablets	Conc taken M	ip (μA)	Conc. found M	%R	Av. Conc found M	Mean %R	S.D.
viagra	1.0 x 10 ⁻⁷	0.0238	1.008 x 10 ⁻⁷	100.8	1.01 x 10 ⁻⁷	101.0	0.82
		0.0290	1.026 x 10 ⁻⁷	102.5			
		0.0237	1.000 x 10 ⁻⁷	100.0			
		0.0238	1.008 x 10 ⁻⁷	100.8			
	3.0 x 10 ⁻⁷	0.0484	3.025 x 10 ⁻⁷	100.8	3.02 x 10 ⁻⁷	100.6	0.71
		0.0480	2.992 x 10 ⁻⁷	99.7			
		0.0484	3.025 x 10 ⁻⁷	100.8			
		0.0486	3.041 x 10 ⁻⁷	101.4			
	4.0 x 10 ⁻⁷	0.0608	4.041 x 10 ⁻⁷	101.0	4.03 x 10 ⁻⁷	100.8	0.44
		0.0608	4.041 x 10 ⁻⁷	101.0			
		0.0609	4.049 x 10 ⁻⁷	101.2			
		0.0604	4.008 x 10 ⁻⁷	100.2			
The mean recovery = 100.8 ± 0.66							
Slope = 12.2 x 10 ⁴							
Intercept = 0.0115							
Corr. Coeff = 0.9965							

Table 45:

Assay of sildenafil citrate in its dosage forms B.R. buffer solution of pH 7.5 using CAdSWSV at: $E_d = -400$ mV, $t_d = 300$ sec, scan rate = 10.0 mV/sec, pulse height = 200 mV pulse width = 200 mV.

Brand Name (Producer)	Labelled Conc. (Drug)	%Recovery \pm S.D.	
		Proposed Method	Reported method*
Viagra	200 mg/tablet	100.8 ± 0.66 (n = 4)	99.0 ± 2.7 (n = 6)

* The official method HPLC⁽¹¹⁹⁾

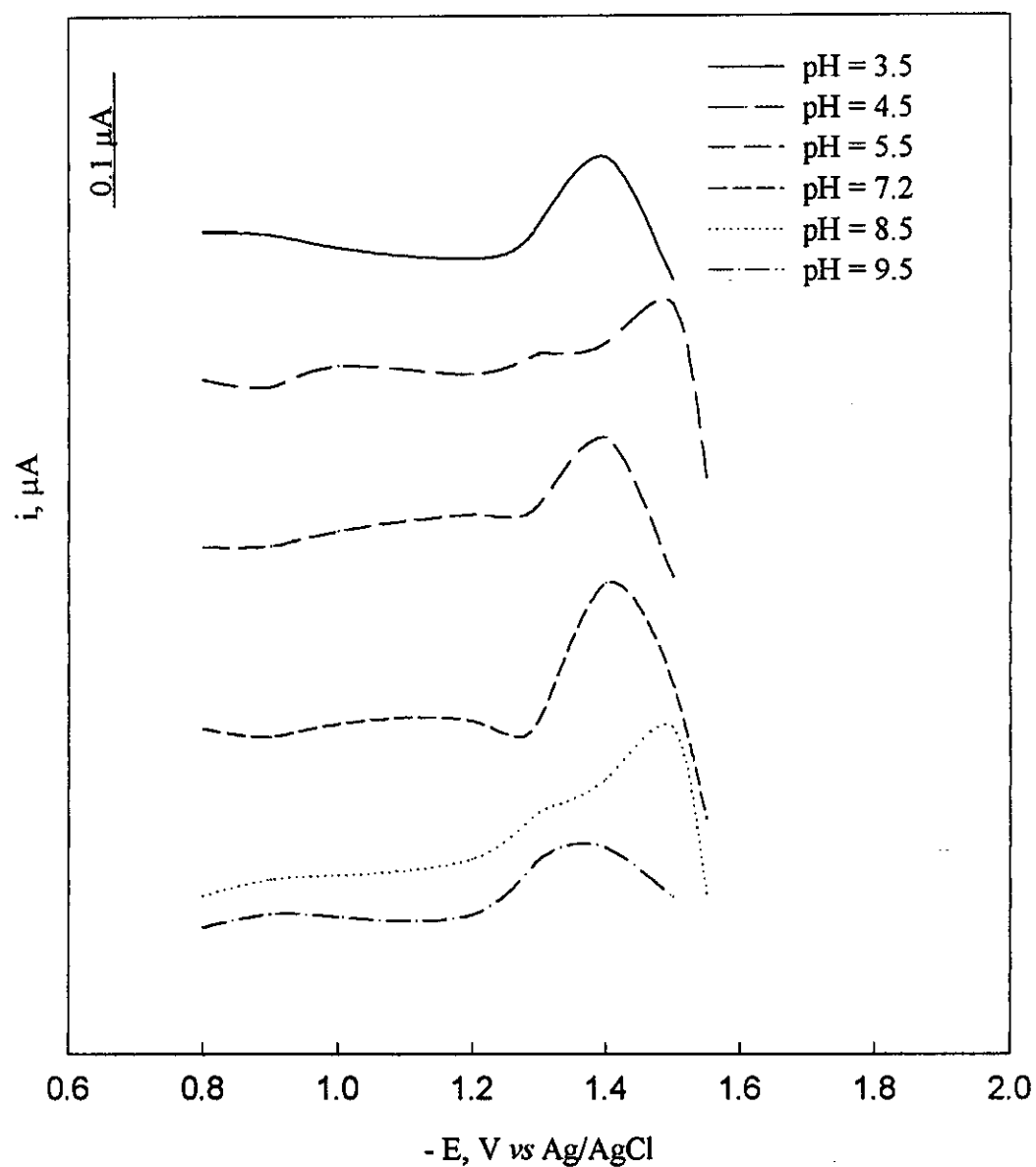


Fig. 61: Effect of pH on the CAdSWSV peak of 1×10^{-6} M of sildenafil citrate in B.R. buffer solution at: $t_d = 300$ sec, $E_d = -200$ mV, scan rate = 10 mV/s, frequency = 5000 Hz, pulse height = 20 mV and pulse width = 50 mV.

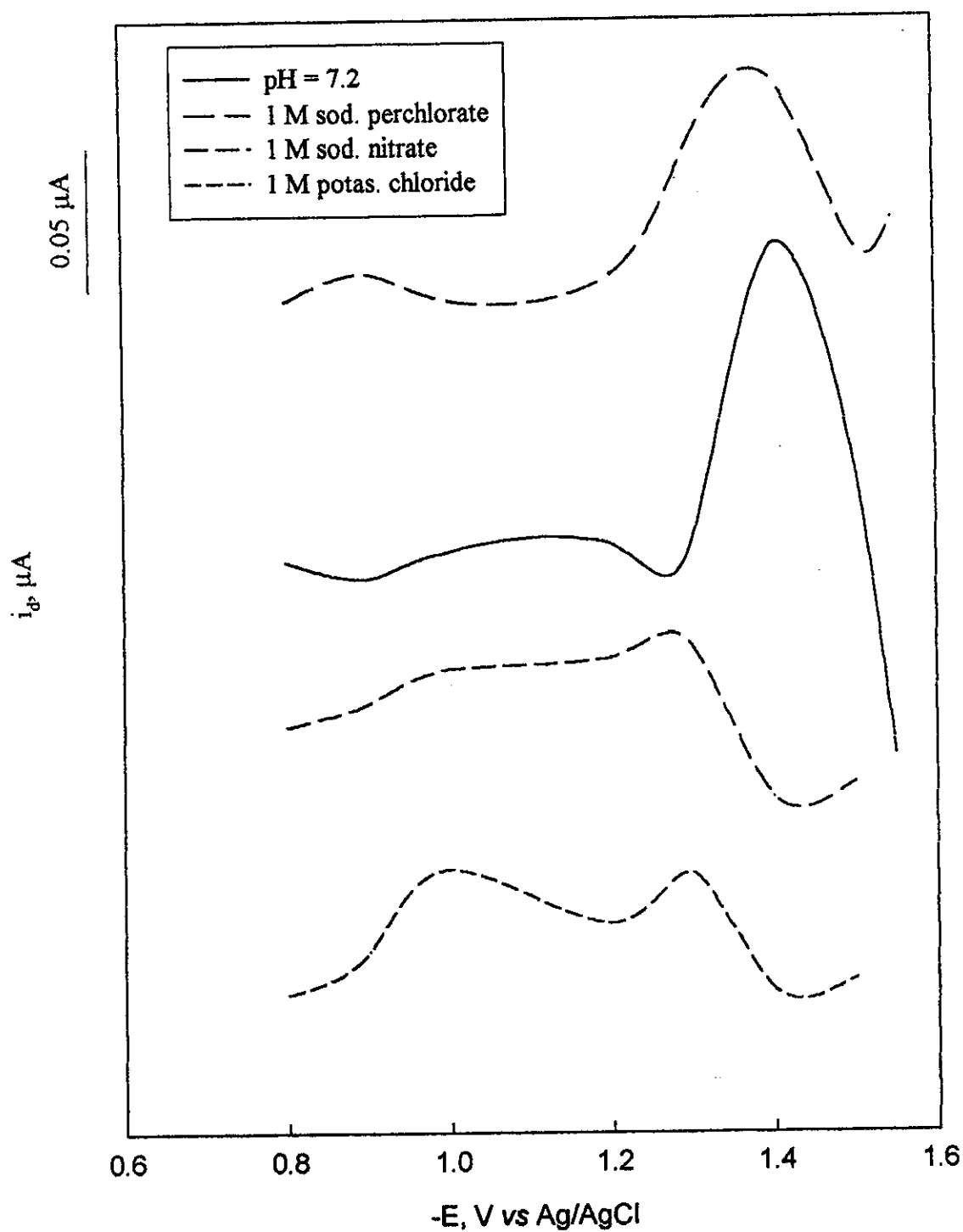


Fig. 62: Effect of supporting electrolyte solution on the CAAdSWSV peak of 1×10^{-6} M of sildenafil citrate in B.R. buffer solution at $t_d = 300$ sec, $E_d = -200$ mV, scan rate = 10 mV/s, frequency = 5000 Hz, pulse height = 20 mV and pulse width = 50 mV.

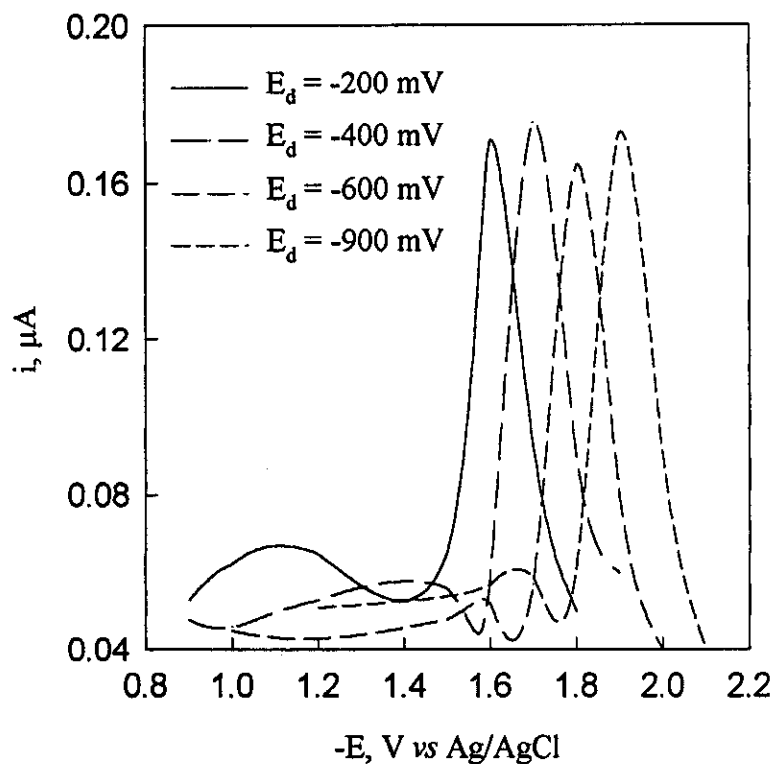


Fig. 63: Effect of E_d on 1×10^{-6} M of sildenafil citrate in B.R. buffer solution of pH 7.2 at $t_d = 300$ sec, pulse width = 50 mV, pulse height = 20 mV and scan rate = 10 mV/s

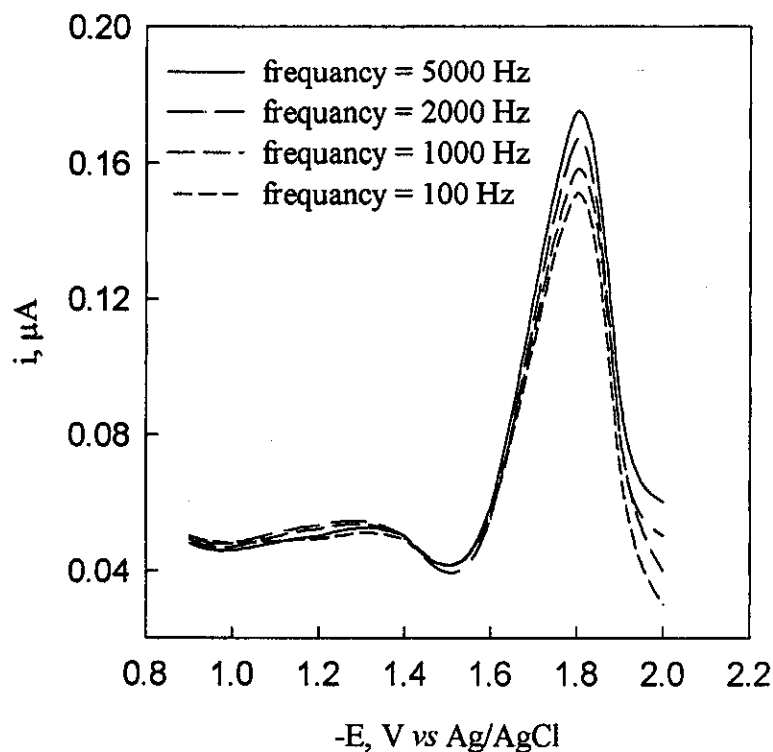


Fig. 64: Effect of frequency on 1×10^{-6} M of sildenafil citrate in B.R. buffer solution of pH 7.2 at $E_d = -400$ mV, $t_d = 300$ sec, pulse width = 50 mV, pulse height = 20 mV and scan rate = 10 mV/s

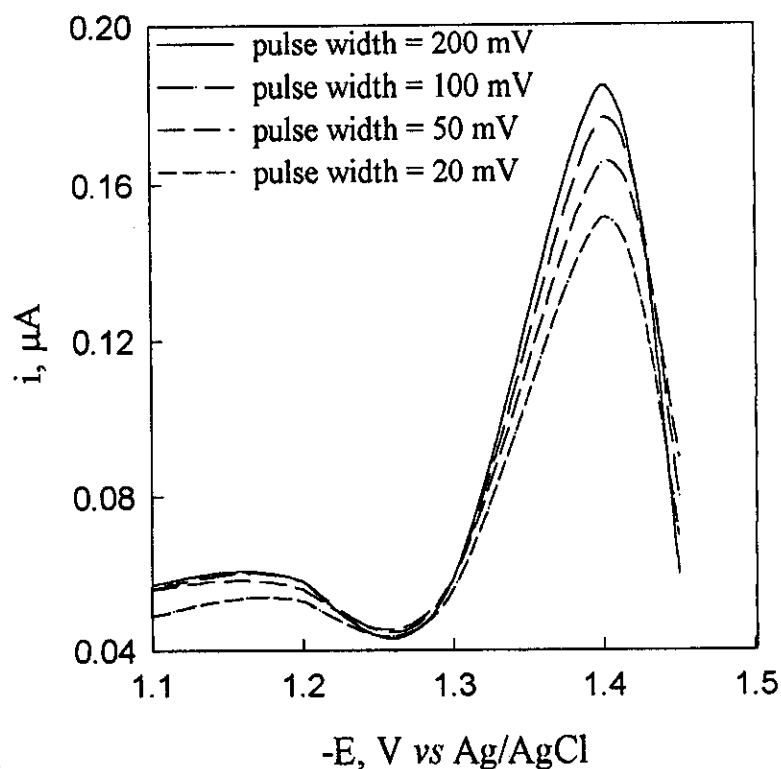


Fig. 65: Effect of pulse width of 1×10^{-6} M of sildenafil citrate in B.R. buffer solution at: $t_d = 300$ sec, $E_d = -400$ mV, scan rate = 10 mV/s, frequency = 5000 Hz, and pulse height = 20 mV.

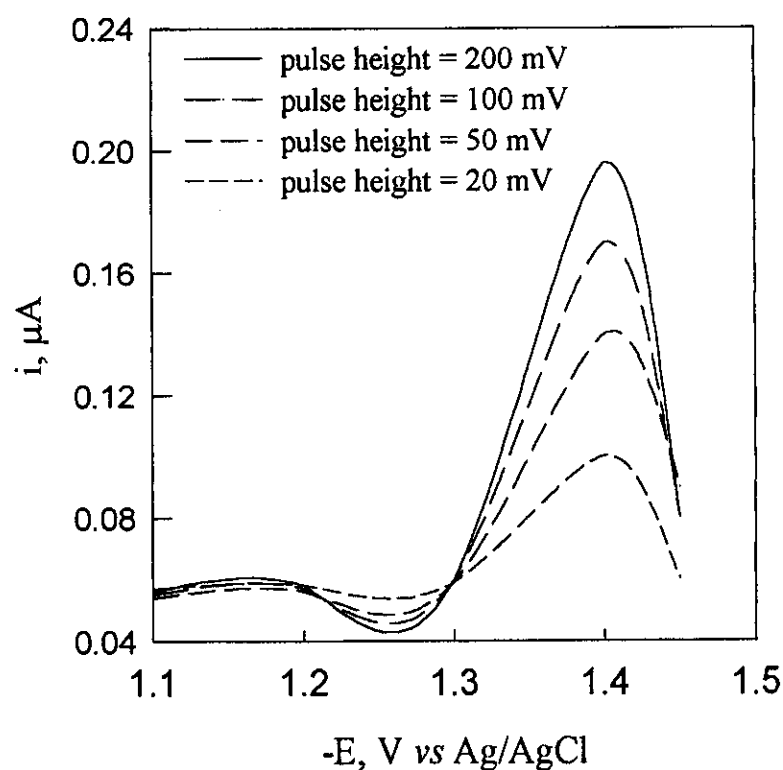


Fig. 66: Effect of pulse height of 1×10^{-6} M of sildenafil citrate in B.R. buffer solution at: $t_d = 300$ sec, $E_d = -400$ mV, scan rate = 10 mV/s, frequency = 5000 Hz, and pulse width = 200 mV.

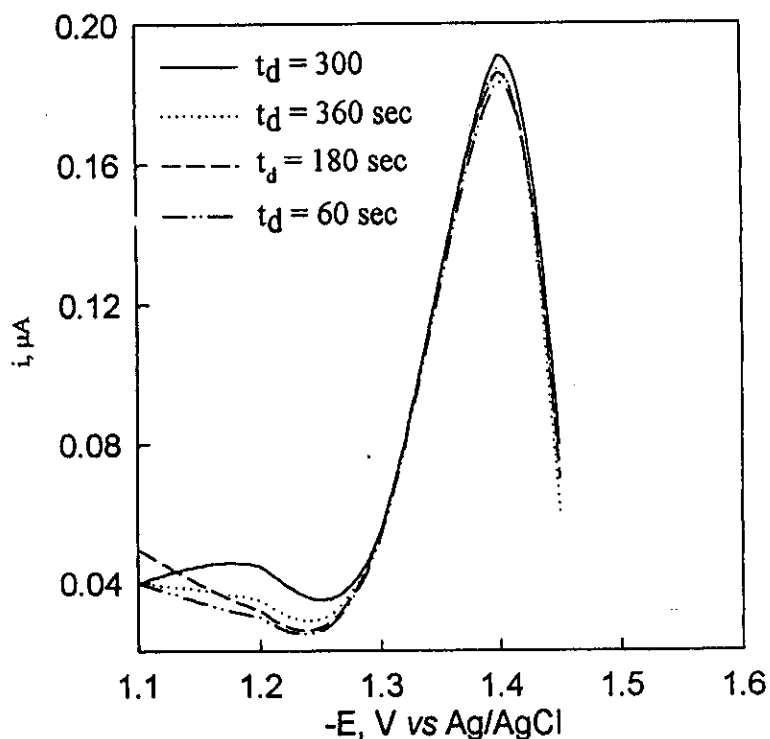


Fig. 67: Effect of t_d of 1×10^{-6} M sildenafil citrate in B.R. buffer solution of pH 7.5 at $E_d = -400$ mV, pulse height of 200 mV, pulse width of 200 mV, scan rate 10 mV/s and frequency of 5000 Hz.

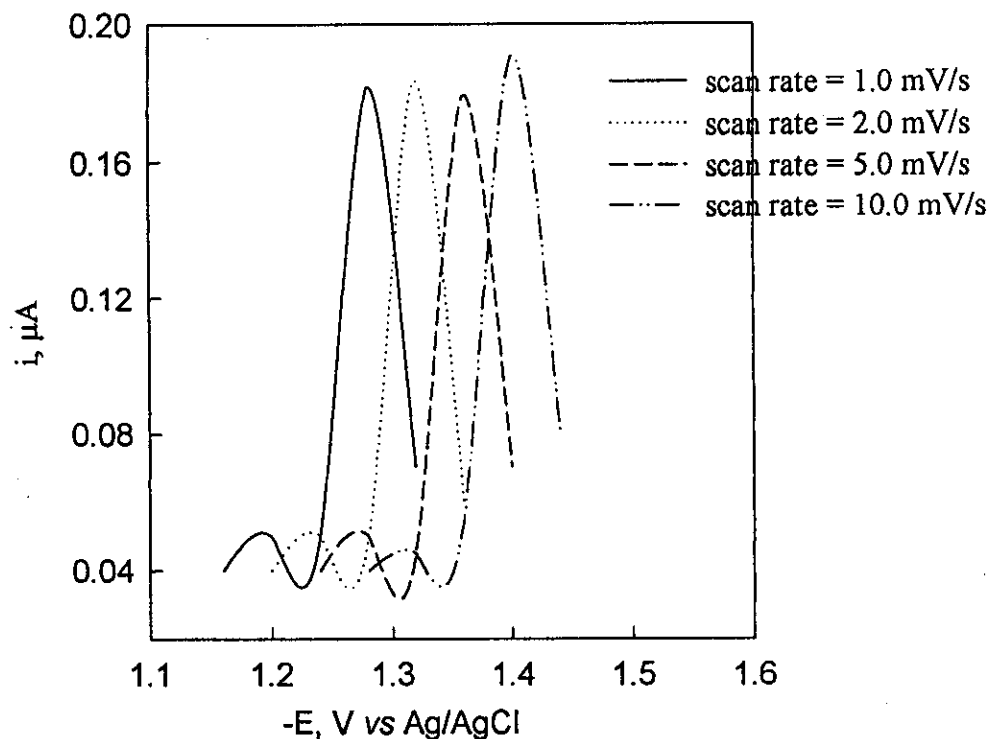


Fig. 68: Effect of scan rate on 1×10^{-6} M sildenafil citrate in B.R. buffer solution of pH 7.5 at $E_d = -400$ mV, pulse height of 200 mV, pulse width of 200 mV, $t_d = 300$ sec and frequency of 5000 Hz.

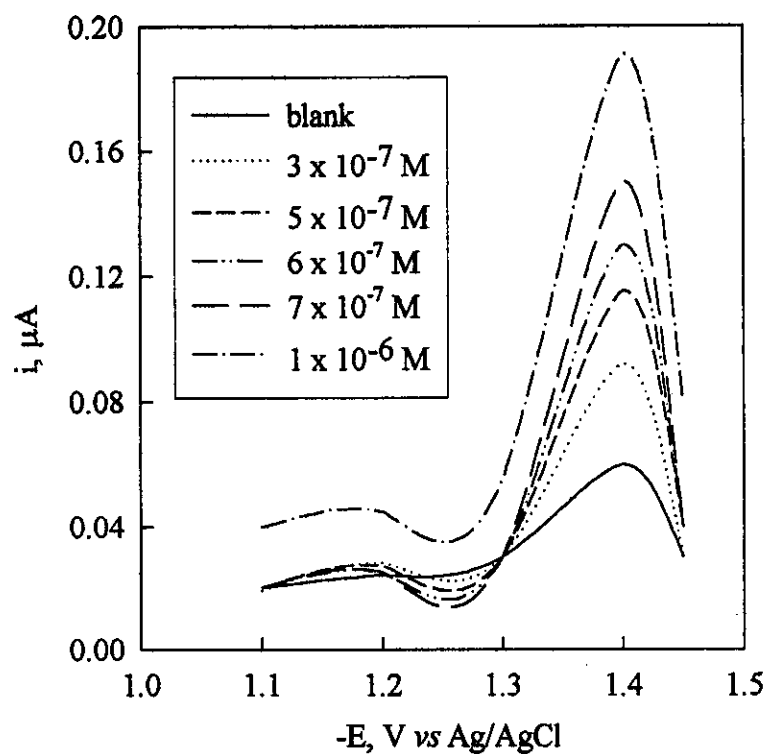


Fig. 69: Different concentrations of sildenafil citrate in B.R. buffer solution of pH 7.5; at $E_d = -400$ mV, $t_d = 300$ sec pulse height of 200 mV, pulse width of 200 mV, scan rate 10 mV/s and frequency of 5000 Hz.

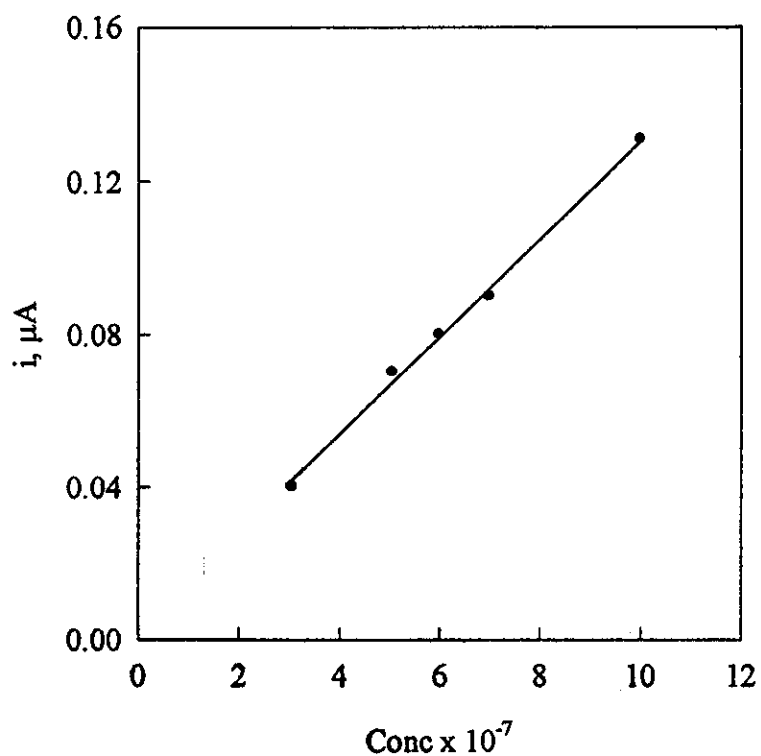


Fig.70: Calibration curve of sildenafil citrate

3.4.2. Spectrophotometric studies on sildenafil citrate with reagents I, II and III:

To establish the optimum conditions for the formation of drug - reagent complexes, the effects of several experimental variables were recorded.

3.4.2.1. Determination of optimum conditions

1. Effect of pH:

The effect of pH on the formation of drug-reagent complex between sildenafil citrate and reagents, I, II, and III was studied in universal buffer solutions of pH range 2.5-11.5. The optimum pH values recommended for subsequent studies of drug-reagent complexes with the drug were 6.5, 2.5 and 11.0 on using reagents I, II and III, respectively, Fig. (71-73).

2. Determination of λ_{\max} of the complex species:

The following sequence was done for determination of the optimum λ_{\max} for the formed complexes:

- A) Spectrum of 1.0 ml 1.0×10^{-3} M of drug solution at the suitable pH using the same pH as a blank.
- B) Spectrum of 1.0 ml 1.0×10^{-3} M of reagent solution at the same suitable pH value using the same pH as a blank
- C) Spectrum of 1.0 ml 1.0×10^{-3} M drug solution and 1.0 ml 1.0×10^{-3} M reagent solution against 1.0 ml (1.0×10^{-3}) M of reagent and buffer as blank.

The maximum wavelength at which the complexes formed were 554, 523 and 569 nm with the reagents I, II and III, respectively, Fig. (71-73).

3. Effect of time and temperature:

On studying of the influence of time and temperature on drug- reagent complexes it was found that the complexes were formed spontaneously after mixing the drug and reagents at room temperature and still constant for 24 h.

4. Effect of sequence of additions:

Different sequence of additions affected on the absorbance value of the complex. Experiments showed that (reagent-drug-buffer) gave the best results for sildenafil citrate I, II and III complexes, other sequence gave lower absorbance values.

5. Effect of reagent concentrations:

On studying the effect of reagents concentration , it is found that 1.0 ml 1.0×10^{-3} M was sufficient for all reagents to produce maximum absorbance.

3.4.2.2. Molecular structure

1. Molar ratio method:

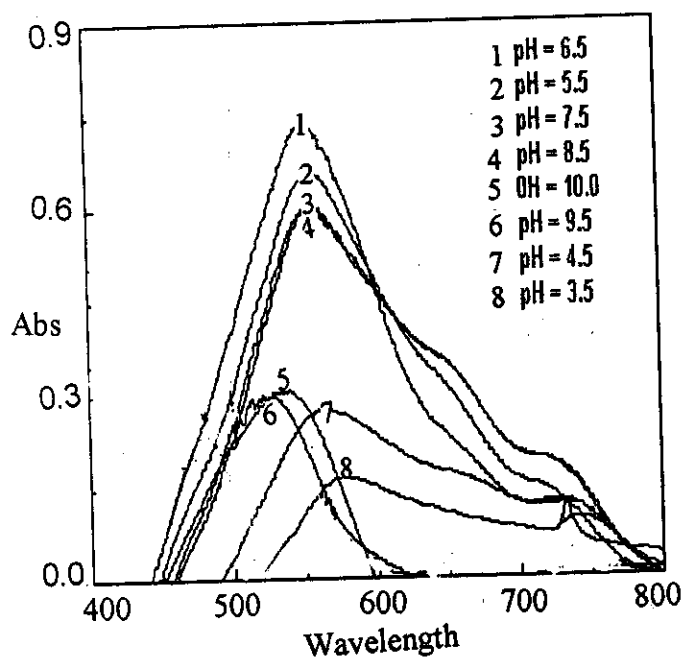
The molar ratio method was used to study the stoichiometry of the complexes between sildenafil citrate and reagents I, II and III. Experiments showed that the complex is formed as 1:1 (R:D) ratio, Fig. (71-73).

2. Continuous variation method:

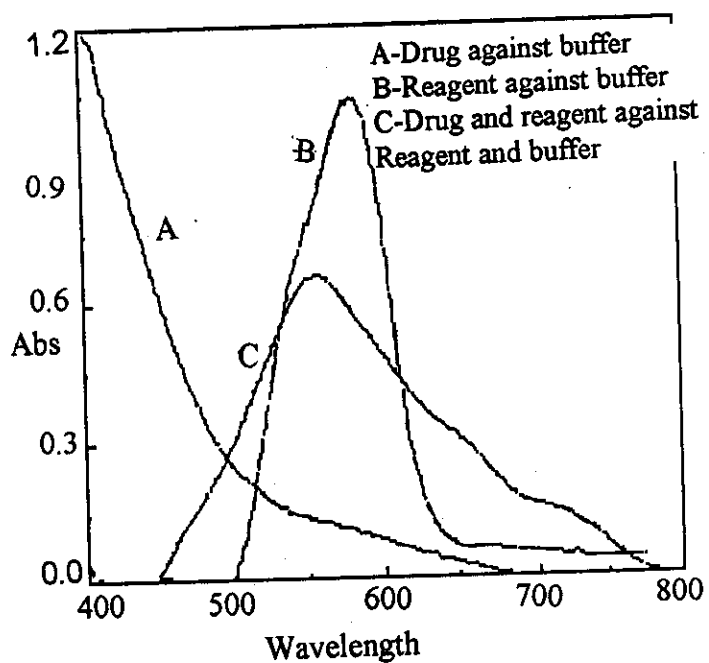
The modification continuous variation method was applied to investigate the stoichiometry between the drug and reagents, Fig. (71-73). Results revealed the formation of 1:1 (R:D) complex. This showed that the interaction between sildenafil citrate and reagents occurred through ion-pair association in ratio of (1:1).

3.4.2.3. Stability constants of the formed complex:

The above spectrophotometric methods were usually applied to determine the stability constant of the formed complex. Table 46. Inspection of the data revealed that the sildenafil citrate-II is more stable than sildenafil citrate-I and sildenafil citrate-III.



Effect of pH on sild-I



Determination of wavelength

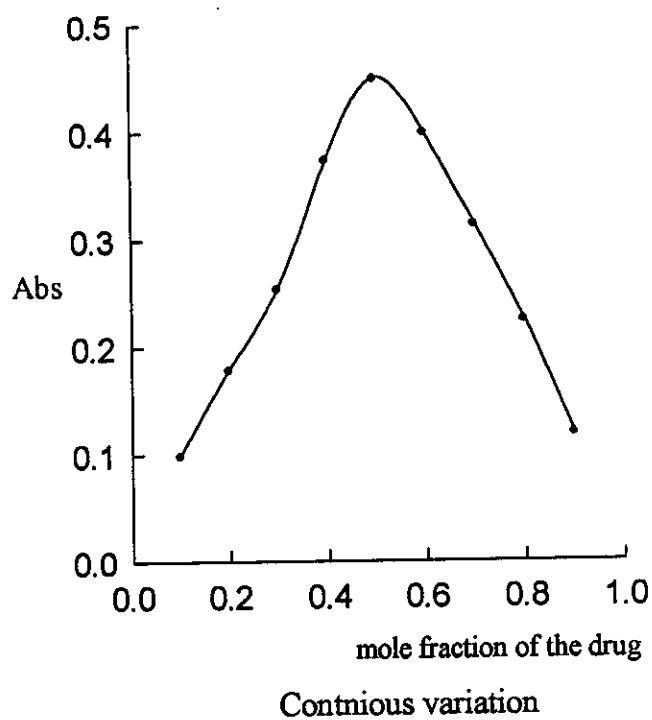
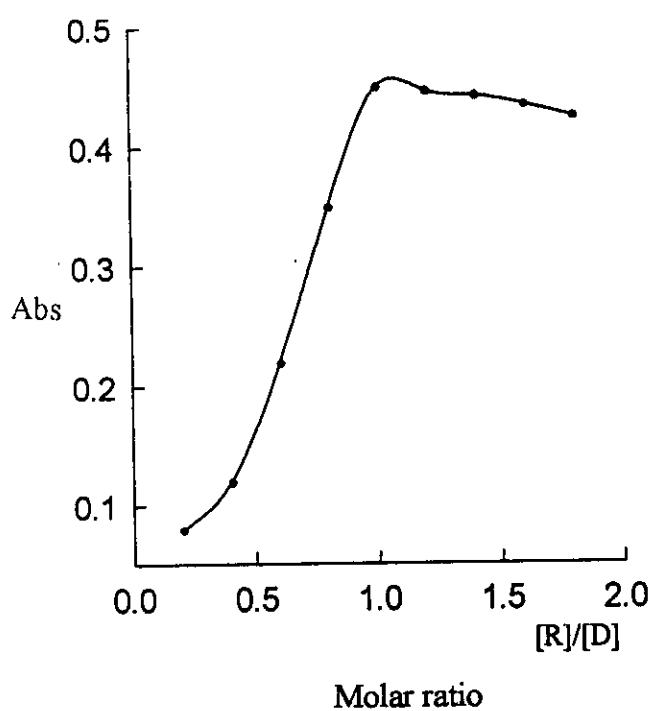
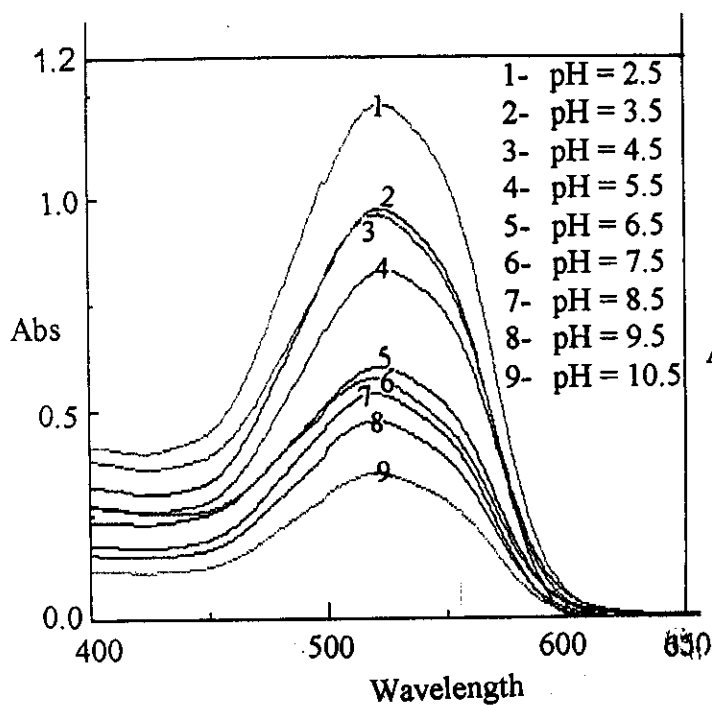
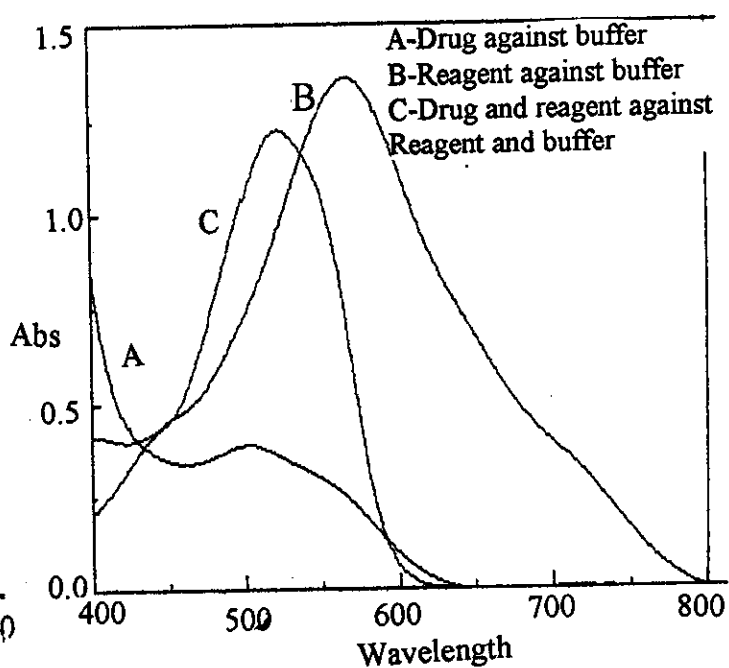


Fig. 71: Sildenafil citrate with sudan II



Effect of pH on sildenafil-II complex



Determination of wavelength

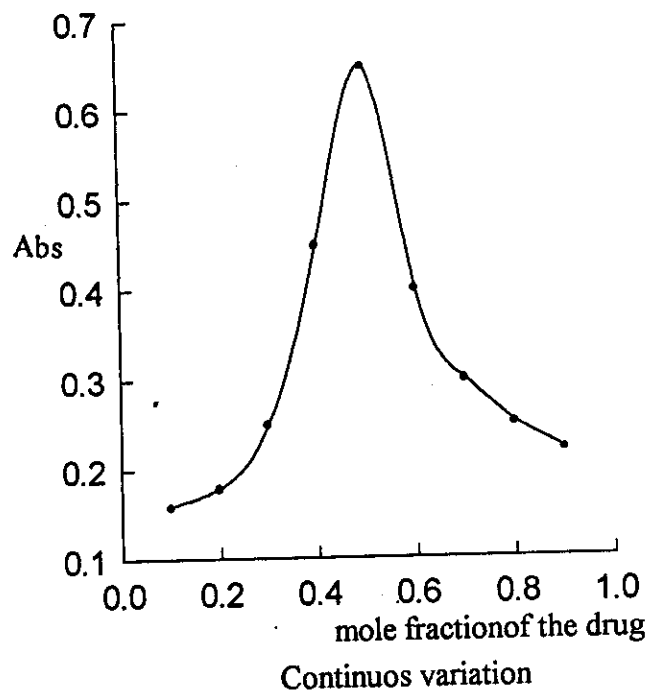
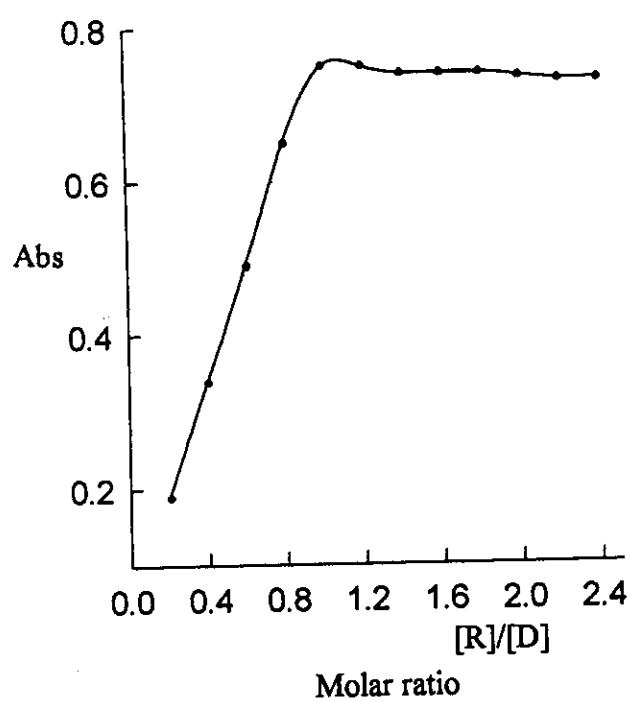
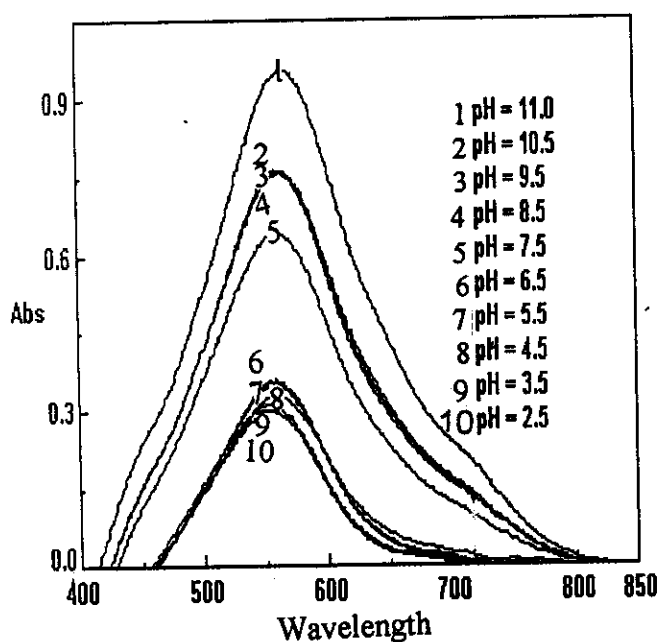
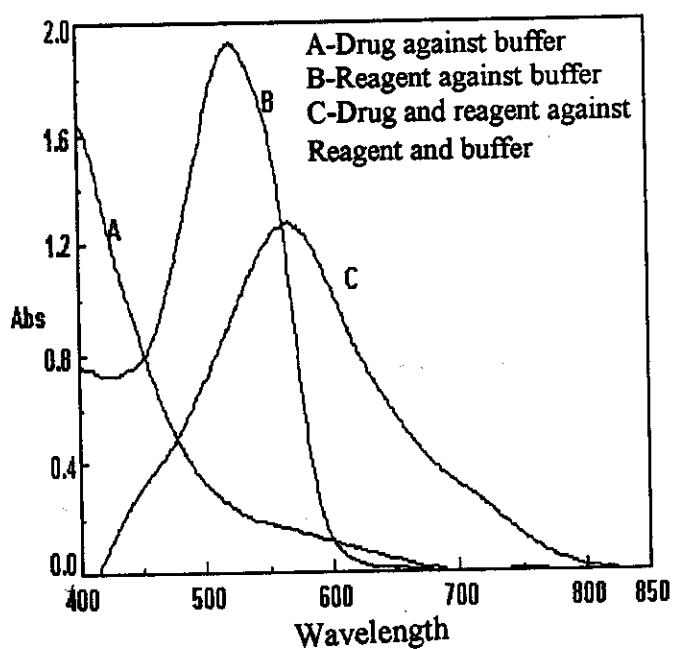


Fig. 72: Sildenafil citrate with congo red



Effect of pH on sildenafil-III complex



Determination of wavelength

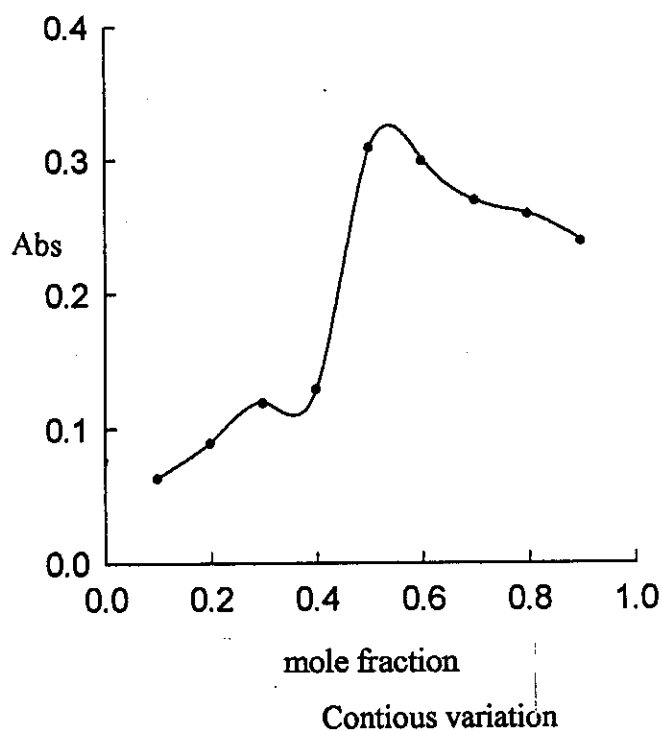
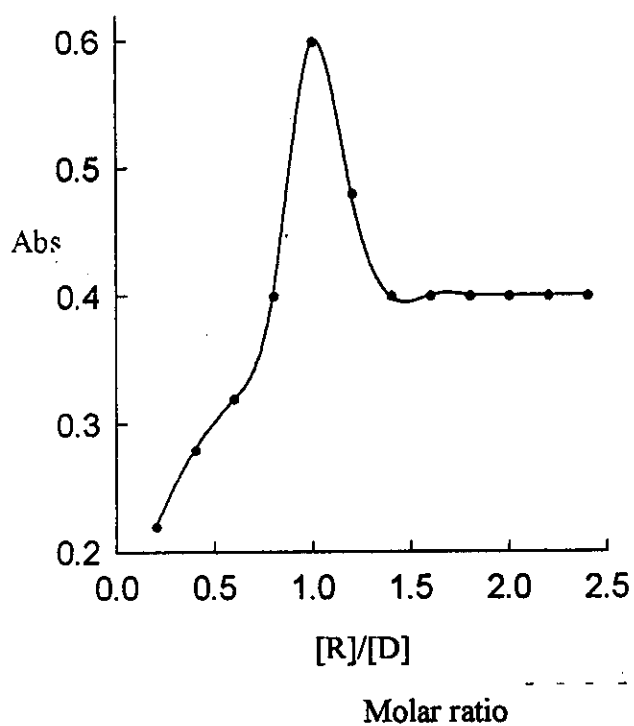


Fig. 73: Sildenafil citrate with gentian violet

Table 46:

stiochiometry and stability constant of the complexes obtained from different spectrophotometric methods.

complexes	pH	λ_{\max}	Molar ratio		Cont. variation	
			M:L	Log K_n	M:L	Log K_n
Sildenafil-I	6.5	554	1:1	7.94	1:1	7.64
Sildenafil -II	2.5	523	1:1	8.52	1:1	8.50
Sildenafil -III	11.0	569	1:1	5.72	1:1	5.44

3.4.2.4. Validity of Beer's law:

The limits of concentrations in which the drug obeys Beer's law were recorded under the optimum experimental conditions for each of the formed complexes, these concentration limits were listed in Table 47, Fig.74.

Ringbom optimum concentration range was determined, Fig 75. The molar absorptivity and **Sandell** sensitivity were listed also in Table 47. Inspection of the data indicates high sensitivity in the micro determination of sildenafil citrate with the investigated reagents.

3.4.2.5. Interference:

The interferences of co-existing additives were investigated under the optimum conditions. Experiments showed that all additives did not interfere in the determination of sildenafil citrate, indicating the high selectivity of the proposed method.

3.4.2.6. Analytical applications:

The proposed method for determination of sildenafil citrate using the analytical reagents under investigation was performed to its tablet form such as *viagra*. These pharmaceutical preparation was analysed by the proposed method under the optimum conditions. Results were shown confirming that the proposed method is highly sensitive, therefore it could be used easily for the routine analysis of pure form and in its pharmaceutical preparations as recorded in Table 48. Results of analysis of sildenafil citrate tablets by proposed method show a good agreement with the HPLC⁽¹¹³⁾ procedure. recoveries of the proposed and the official procedures were recorded in Table 48.

3.4.2.7. Accuracy and precision:

The accuracy of the proposed method for the determination of sildenafil citrate using reagents I,II and III, were assessed using different concentrations. This was checked during the work by running six replicate standard samples.

In order to determine the precision of the method, solutions containing different concentrations of drug were prepared and the absorbance of the prepared solution was measured and repeated for six times. The value of standard deviation was calculated.

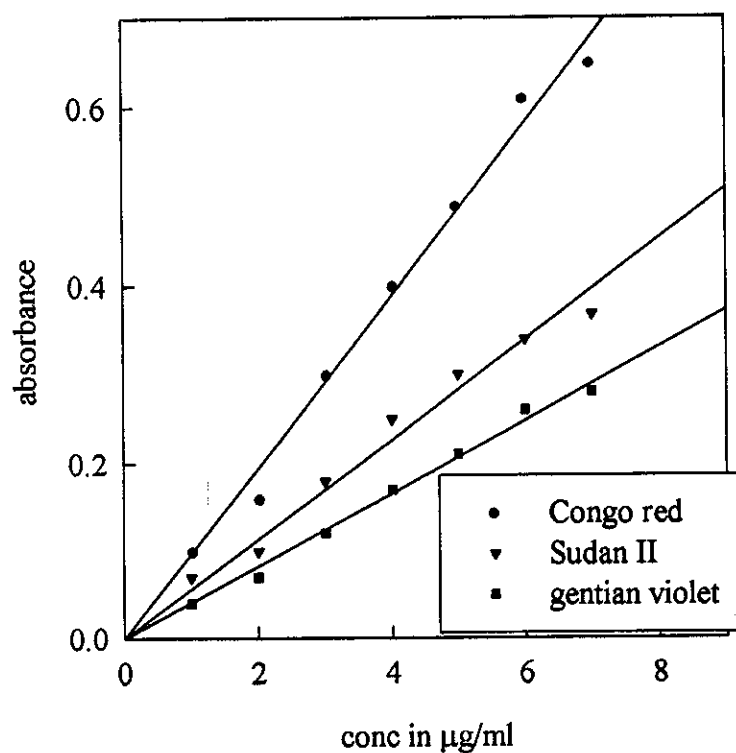


Fig. 74: Beer's law graph of sildenafil citrate using reagents under consideration

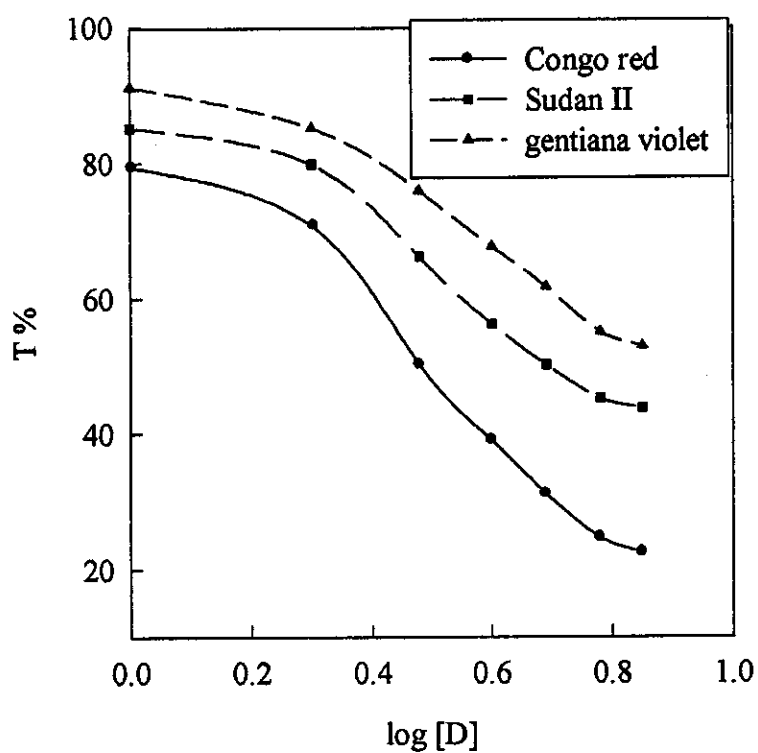


Fig. 75: Ringbom plot for sildenafil citrate

Table 47

Cumulative data of sildenafil citrate with the reagents (I, II and III) under investigation

Reagent	pH	λ_{\max}	Ringb. optim. range $\mu\text{g/ml}$	Beer's range $\mu\text{g/ml}$	S.D	R.S.D %	E%	S ng cm^{-2}	$\epsilon \text{ l mol}^{-1} \text{ cm}^{-1}$
I	6.5	554	1.9-6.31	1.0-7.0	0.40	0.58	0.24	27.81	1.6×10^4
II	2.5	523	1.9-6.31	1.0-7.0	0.22	0.56	0.23	17.00	2.6×10^4
III	11.0	569	1.9-6.31	1.0-7.0	0.41	0.69	0.28	9.61	4.6×10^4

*S: Sandell sensitivity

* ϵ : Molar absorptivity

Table 48:

Evaluation of accuracy and precision of the proposed and official method for sildenafil citrate determination in viagra tablets

Reagent	Cont. mg/tab	Found* (mg)	S.D	R.S. D %	Error %	Recov. %	F [#] value	t [#] value
I	200	195	1.449	1.62	0.665	97.5	3.470	0.65
II	200	199	1.229	1.43	0.584	99.5	4.826	0.86
III	200	198	1.293	1.34	0.547	99.0	4.360	0.76
t [#] Theoretical value = 2.57								
F [#] Theoretical value = 5.05								

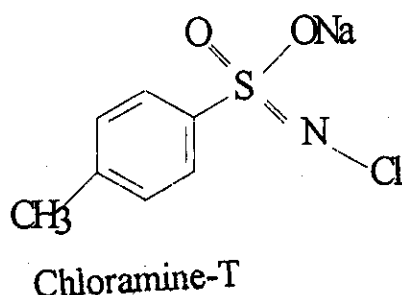
*: Average of six determinations

O: Official method

P: Proposed method

3.5.1. Electrochemical behaviour of chloramine-T in B.R. solutions of different pH-values containing 20% (v/v) DMF:

Chloramine-T [sodium N-chlorotoluene P-sulphonimide Trihydrate] is a disinfectant and uses as antiseptic and has the following chemical structure⁽¹²⁰⁾.



The electrochemical behaviour of chloramine-T was recorded using DC-polarographic and cyclic voltammetric techniques to throw the light on the reduction mechanism. Also, the quantitative determination of chloramine-T in pure form was studied using square wave stripping voltammetry. The electroanalytical determination was performed after optimizing both the instrumental and experimental conditions.

I- DC-Polarography:

Current-Potential Curves:

The polarographic reduction of 4×10^{-4} M of chloramine-T was investigated in B.R. buffer solutions of different pH values from 2.9 to 11.2 containing 20% (v/v) DMF. The recorded polarograms showed only a single reduction wave in the entire pH range, Fig 76A. The half wave potential of the polarographic waves of chloramine-T is pH dependent and showed cathodic shift on increasing the pH values of the electrolysis solutions. This behaviour indicated that the H^+ ions are participating in the rate determining step and the transfer of protons precedes the electron transfer process.

The limiting current i_l is nearly constant at $\text{pH} \leq 6.9$ and decreased to its half value at pH values greater than 7.0, Fig. 76B. This behaviour may be due to the formation of hardly reducible species in the alkaline medium⁽¹²¹⁾.

Effect of Mercury Height:

The plots of $\log i_l$ as a function of $\log h$ for chloramine-T in B.R. buffer solutions of different pH values containing 20% (v/v) DMF, is shown in Fig. 76C. Slope x has values from 0.61 and 0.75 which indicating that the reduction process is mainly controlled by diffusion with some adsorption contribution appeared in alkaline media, Table 49.

Analysis of the Polarographic Waves:

Plotting of $\log [i/(i_d-i)]$ against $E_{d,e}$ for chloramine-T in B.R. buffer solution of different pH-values containing 20% (v/v) DMF gave linear correlations as represented in Fig. 76D. Slope values S_1 amounting between 50.1 and 63.9 mV indicating the irreversibility of the electrode process.

Values of the transfer co-efficient α were calculated for the probable values of n_a . The most probable α values indicated that, within the entire pH range n_a is equal to two for the investigated compound.

Half-Wave Potential – pH Curves:

Plotting of $E_{1/2}$ against pH for the reduction waves gave a straight line consists of one segment, Fig. 76E. From the value of S_2 and S_1 , Z_H^+ was determined, Table 49. Inspection of the obtained data indicated that, the ratio Z_H^+/n_a is equal to 0.5. This means that the number of protons Z_H^+ and electrons n_a involved in the rate-determining step equal to one and two, respectively.

Table 49

Polarographic data and parameters for the reduction of 4×10^{-4} M chloramine-T in buffer solutions of various pH values containing 20% DMF at 25°C.

pH	i_d μA	$-E_{1/2}$ V	$\log i_i$ /log h	Slope mV	$\alpha n a$	$\frac{\alpha}{n_a=1}$	$\frac{\alpha}{n_a=2}$	S2	Z^+_{H}
2.9	0.91	1.15		54.3	1.088	1.088	0.544	28	0.516
3.7	0.90	1.18	0.61	51.4	1.149	1.149	0.575	28	0.545
4.7	0.86	1.20		50.1	1.180	1.180	0.590	28	0.559
5.7	0.81	1.25		55.7	1.061	1.061	0.531	28	0.503
6.9	0.77	1.28	0.75	50.0	1.182	1.182	0.591	28	0.560
7.7	0.37	1.29		55.5	1.065	1.065	0.532	28	0.505
8.3	0.38	1.32		58.8	1.005	1.005	0.502	28	0.476
9.5	0.36	1.34	0.68	62.1	0.952	0.952	0.476	28	0.451
10.5	0.34	1.36		56.8	1.040	1.040	0.520	28	0.493
11.2	0.32	1.39		63.9	0.926	0.926	0.463	28	0.438

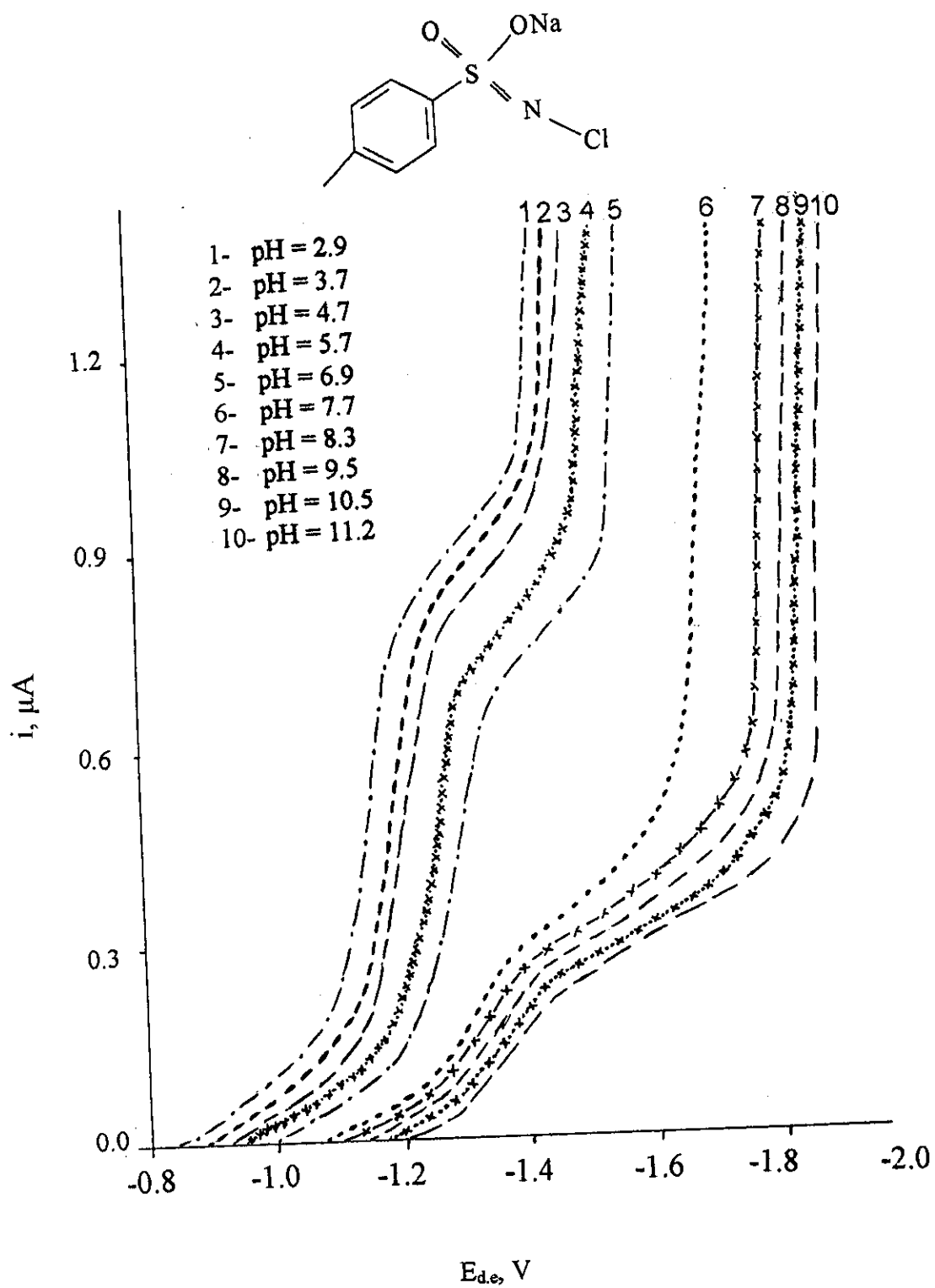


Fig. 76A: DC-polarograms of chloramine-T in B.R. buffer solutions of different pH values.

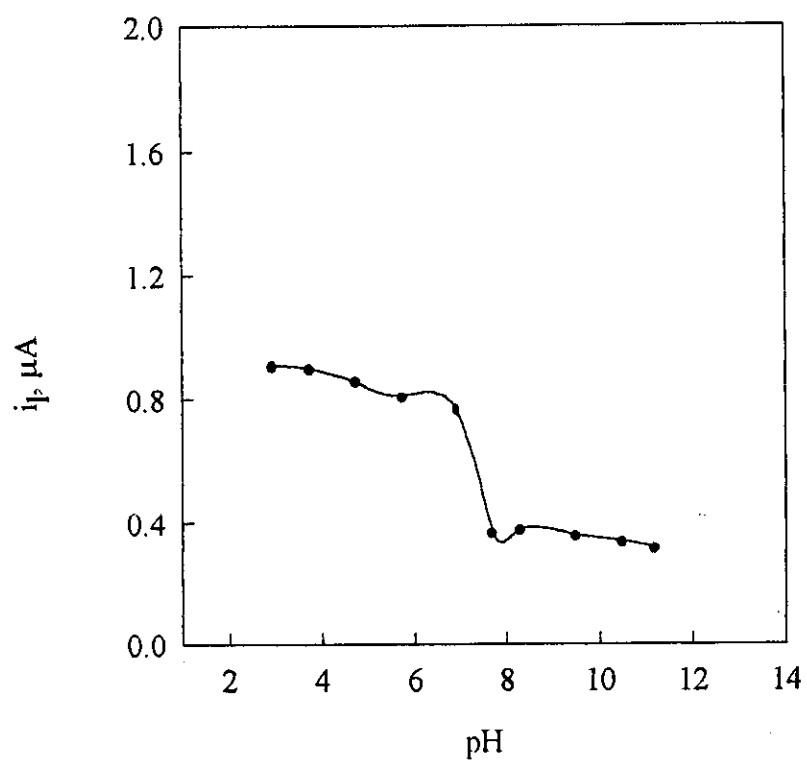


Fig. 76 B: i_l -pH plot of Chloramine-T

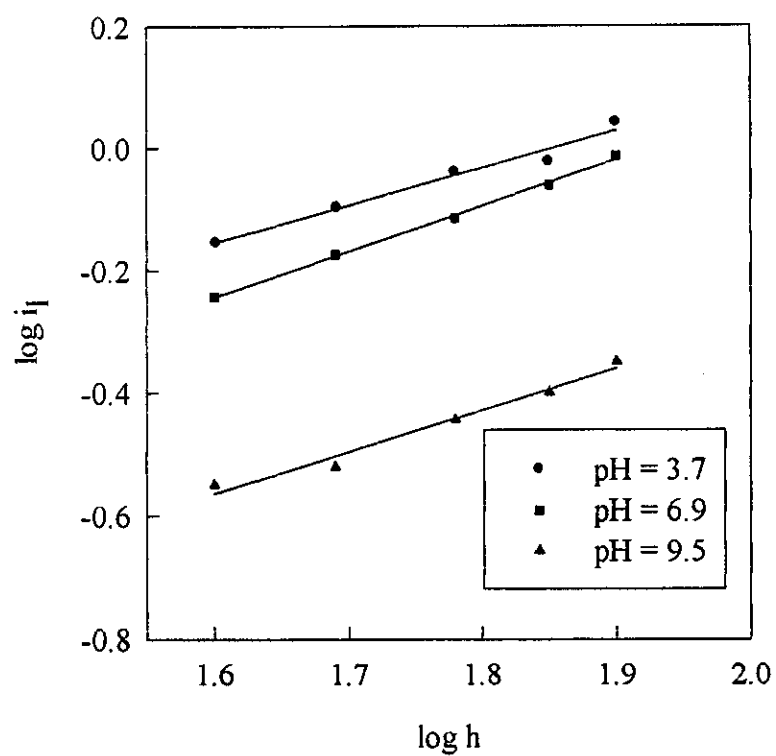


Fig. 76 C: $\log i_l$ - $\log h$ plots of chloramine-T at different pH values

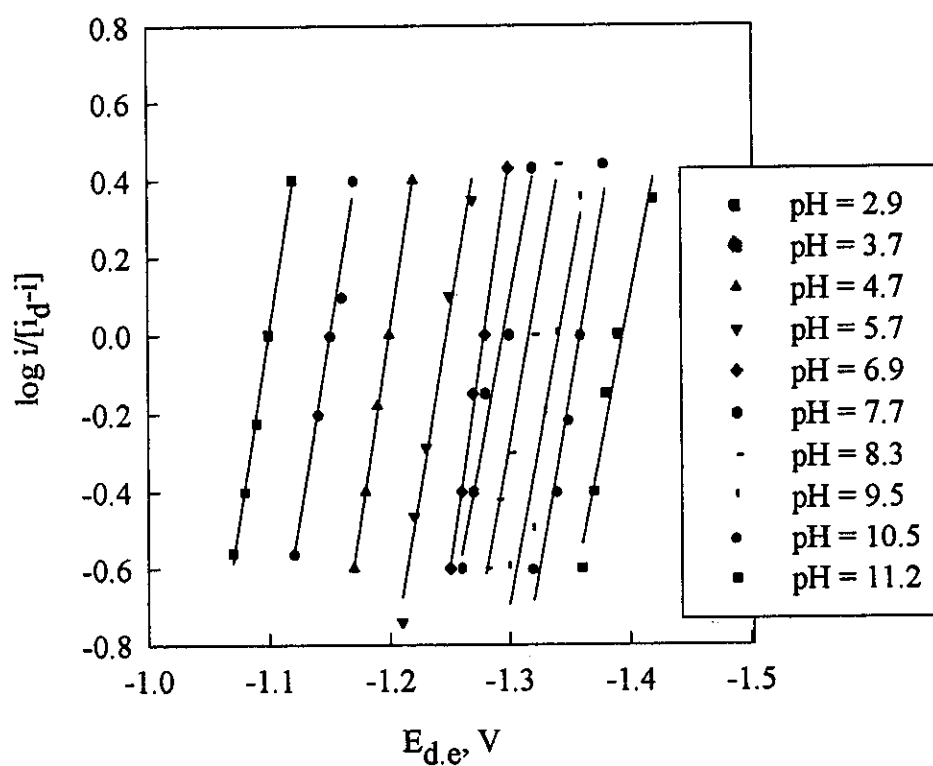


Fig. 76 D: $\log i/[i_d-i]$ - $E_{d,e}$ plots of Chloramine-T at different pH values

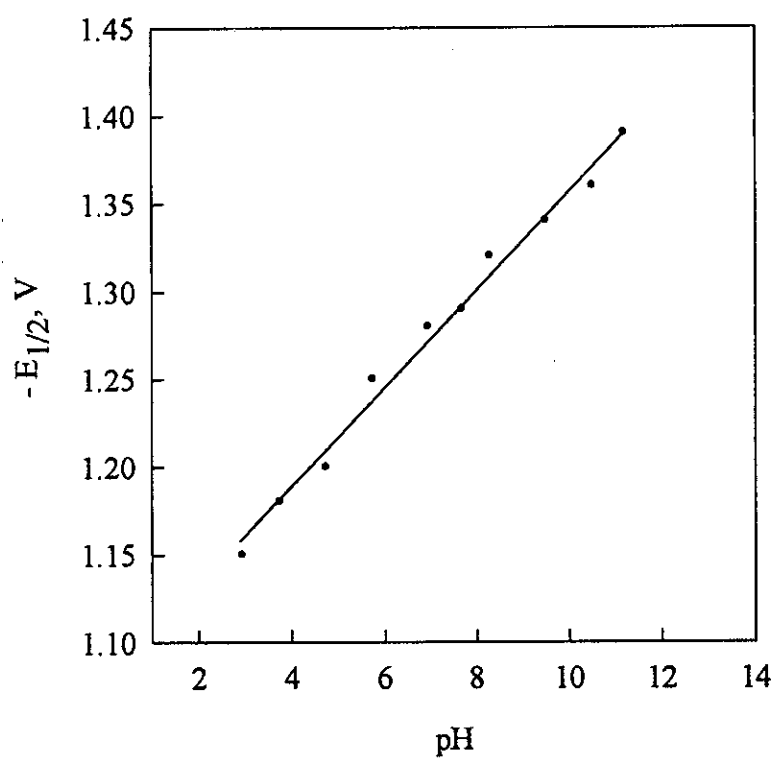


Fig. 76 E: $E_{1/2}$ - pH plot of Chloramine-T

3.5.1.2. Determination of Chloramine T

Chloramine-T was studied in different media such as phosphate buffer, acetate buffer and 1.0 M sodium perchlorate. The most obvious polarographic wave was showed in B.R. buffer pH 2.9 in 20% (v/v) DMF. On decreasing the concentration of the drug, the diffusion current is also decreases till the polarographic wave is completely disappeared, Fig. 77 A. Calibration graph of chloramine-T was represented in Fig. 77 B. The detection limit was calculated from the three repeated value to be 0.3×10^{-4} M (8.45 $\mu\text{g/ml}$). Table 52. shows the polarographic waves of different concentration of Chloramine-T.

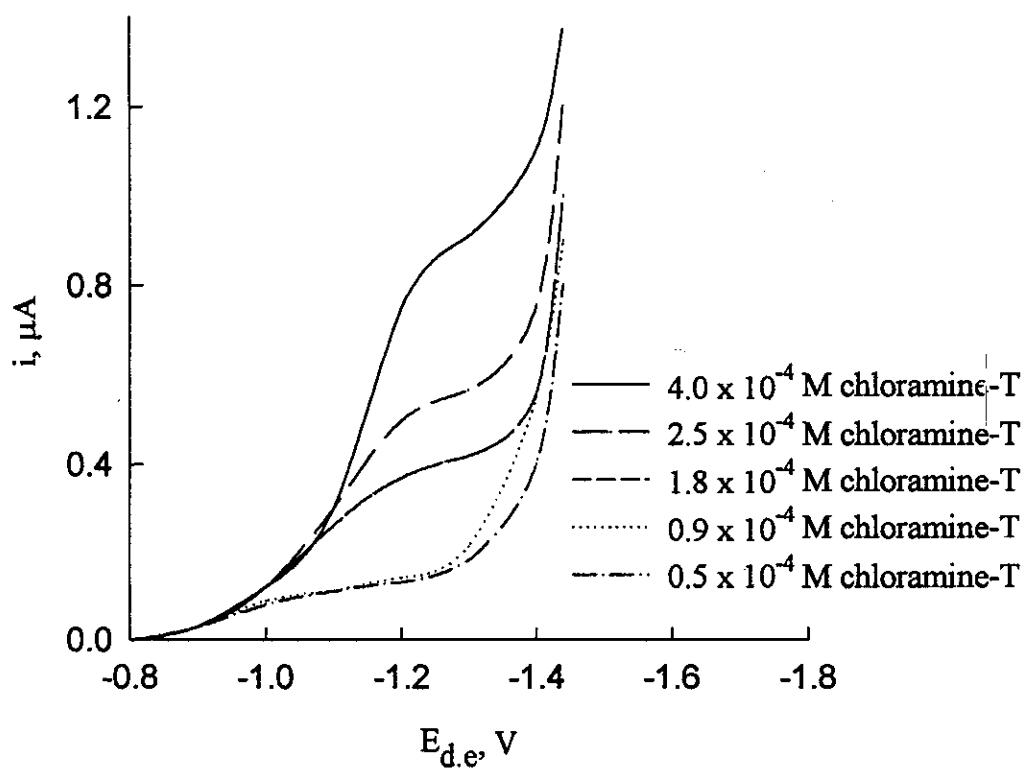


Fig. 77A: DC polarograms at different concentrations of chloramine-T

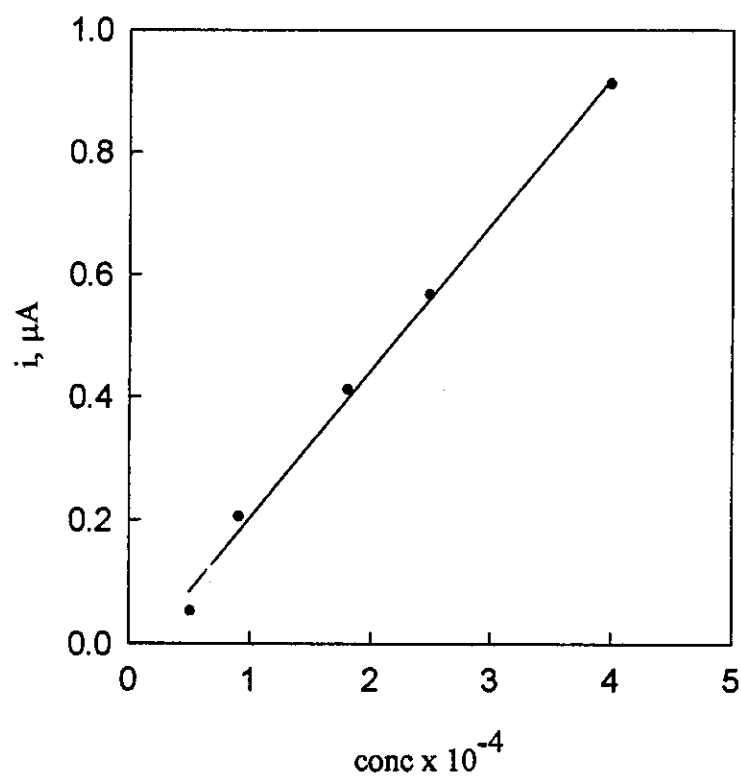


Fig. 77B: Calibration curve of chloramine-T

Table 50:

Assay of different concentration of chloramine-T in B.R. buffer solution of pH 2.9 using DC-polarography.

Compound Conc M	Current i μA	Conc found	Recovery %	S.D
0.5 x 10 ⁻⁴	0.050	5.00 x 10 ⁻⁵	100.0	0.611
	0.049	4.96 x 10 ⁻⁵	99.2	
	0.048	4.94 x 10 ⁻⁵	98.8	
0.9 x 10 ⁻⁴	0.089	8.94 x 10 ⁻⁵	99.3	0.557
	0.289	8.90 x 10 ⁻⁵	98.9	
	0.088	8.84 x 10 ⁻⁵	98.2	
1.8 x 10 ⁻⁴	0.410	1.80 x 10 ⁻⁴	100.1	0.603
	0.407	1.78 x 10 ⁻⁴	98.9	
	0.408	1.79 x 10 ⁻⁴	99.4	
2.5 x 10 ⁻⁴	0.571	2.50 x 10 ⁻⁴	100.3	0.404
	0.566	2.48 x 10 ⁻⁴	99.5	
	0.568	2.49 x 10 ⁻⁴	99.8	
4.0 x 10 ⁻⁴	0.910	3.97 x 10 ⁻⁴	99.3	0.250
	0.911	3.98 x 10 ⁻⁴	99.5	
	0.909	3.98 x 10 ⁻⁴	99.8	
Recovery % = 99.4 ± 0.48				

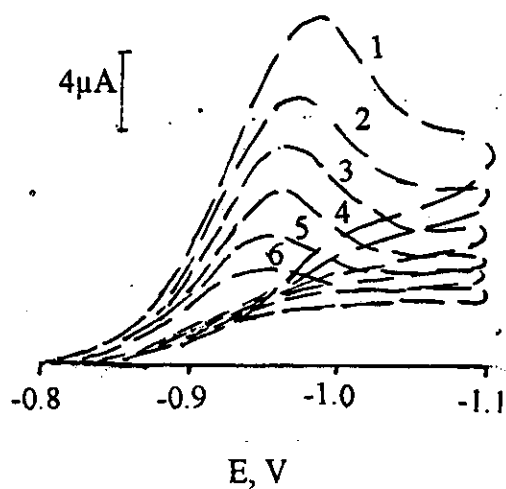
3.5.2. Cyclic Voltammetry:

Cyclic voltammetric behaviour of 1×10^{-4} M chloramine-T was investigated at the glassy carbon electrode surface in B.R. buffer solutions of pH 3.3, 7.5, 10.4 containing 20% (v/v) DMF. The voltammograms were recorded at different scan rates varying from 20 to 500 mV /sec, Fig. 78A. The voltammograms showed one cathodic peak within the entire pH range.

Plotting of i_p against square root of scan rate $v^{1/2}$, linear correlations slightly deviating from the origin were obtained, Fig. 78A. This behaviour confirmed that the electrode process of chloramine-T is controlled mainly by diffusion with some adsorption contribution.

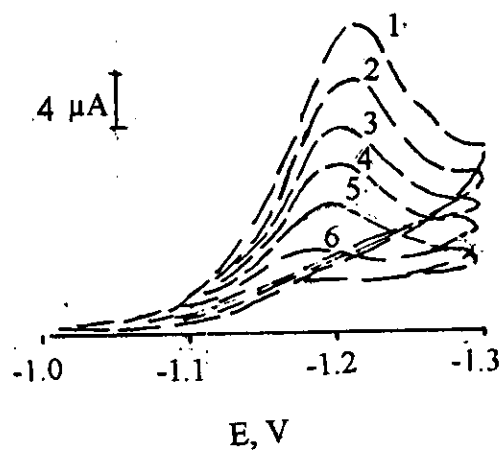
Plotting E_p against $\ln v$ at the given pH showed linear correlations of slope values proportional to αn_a were obtained, Fig. 78C. The values of transfer co-efficient α were calculated for the probable values of n_a , Table 51. The listed data showed that n_a is equal to two this revealed that the rate determining step of the electrode process involves two electrons.

1- pH = 3.3



1- scan rate 500 mV/s
2- scan rate 300 mV/s
3- scan rate 200 mV/s
4- scan rate 100 mV/s
5- scan rate 50 mV/s
6- scan rate 20 mV/s

2- pH = 7.5



3- pH = 10.4

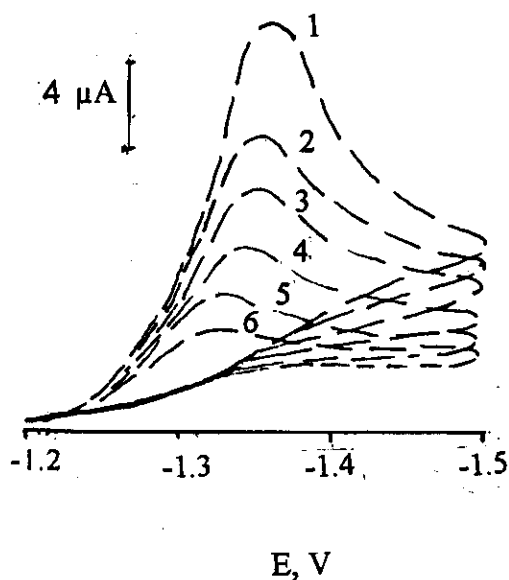


Fig. 78A: Cyclic voltammetric behaviour of chloramin-T in B.R. buffer solutions of different pH values.

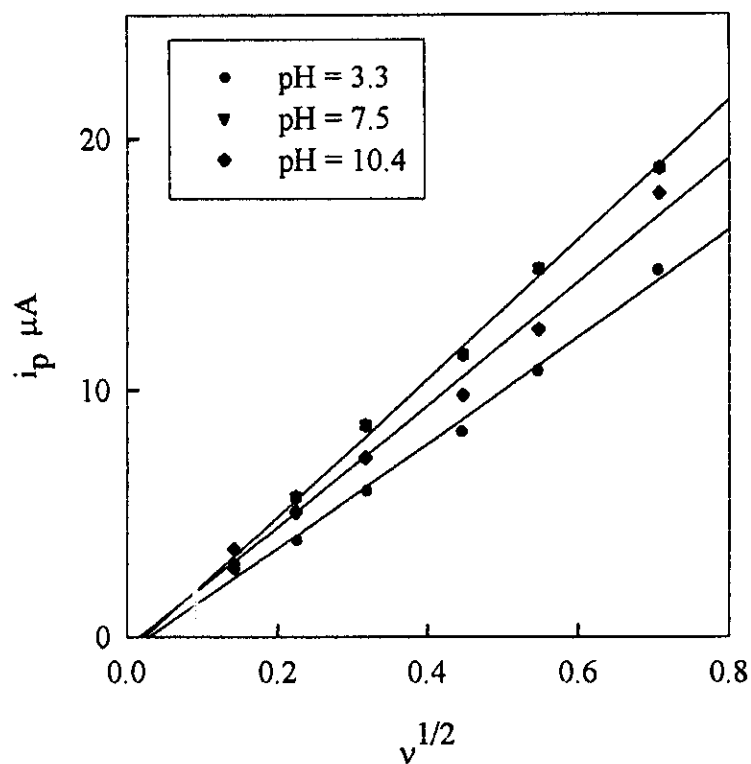


Fig.78 B: i_p - $v^{1/2}$ plots of Chloramine -T at different pH values.

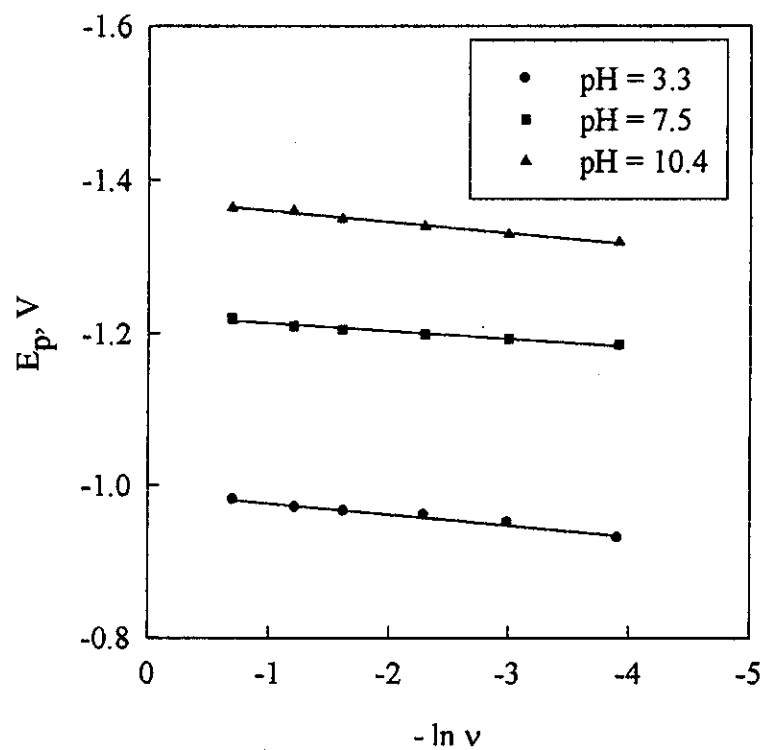


Fig.78 C: E_p - $\ln v$ plots of chloramine-T at different pH values.

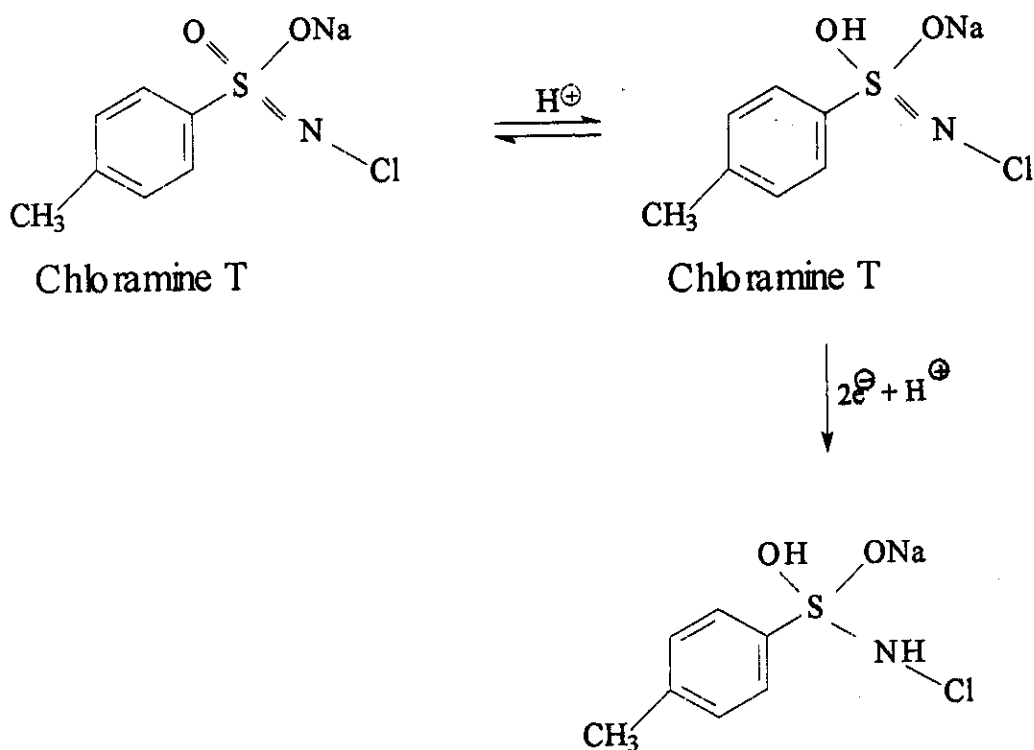
Table 51:

Cyclic voltammetric data for 1×10^{-4} M Chloramine-T in buffer solution B.R. of different pH values containing 20% (v/v) DMF, at 25°C.

pH	Scan rate mV/s	i_p μA	$-E_p$ V	$\delta E_p / \delta \ln v$	α	
					na=1.0	na=2.0
3.3	500	14.8	0.980	0.0144	0.892	0.446
	300	10.8	0.970			
	200	8.4	0.965			
	100	6.0	0.960			
	50	4.0	0.950			
	20	2.8	0.930			
7.5	500	18.8	1.220	0.0103	1.248	0.624
	300	14.8	1.210			
	200	11.4	1.205			
	100	8.6	1.199			
	50	5.7	1.193			
	20	2.9	1.185			
10.4	500	17.8	1.365	0.0145	0.886	0.443
	300	12.4	1.360			
	200	9.8	1.350			
	100	7.3	1.341			
	50	5.1	1.330			
	20	3.6	1.320			

3.5.1.3. The electrode reaction:

The electroactive behaviour of chloramine-T using Dc polarographic and cyclic voltammetric techniques showed that one proton and two electrons were involved in the rate determining step. The CPC electrolysis showed that the total number of electrons was two. The reduction process could take place as following:



3.5.1.4. Cathodic Adsorption Square Wave Stripping Voltammetry (CAdSWSV) of Chloramine-T

Chloramine-T was determined in its pure form electroanalytically using square wave stripping voltammetric technique after optimizing both experimental and instrumental conditions at the glassy carbon electrode.

3.5.1.1. Optimization of the experimental and instrumental conditions

Both of the experimental and instrumental conditions were optimized here for the quantitative determination of chloramine-T using CAdSWSV, Table 54.

1- Effect of pH on the cathodic adsorptive stripping peak of chloramine-T

The cathodic adsorptive stripping voltammetric current of 1×10^{-6} M/l chloramine-T was recorded as a function of potential in Britton Robinson buffer solution of pH ranging from 2.0 to 11.5, Fig. 79. The obtained peaks were due to the reduction of the absorbed compound at the glassy carbon electrode surface. A well developed peak was observed at pH equal 7.2.

2- Effect of supporting electrolyte on the CAdSWSV peak current of chloramine-T

The effect of some supporting electrolytes on the CAdSWSV peak of chloramine-T was studied. Figure 80 showed that pH 7.2 is the most suitable medium for the developing well-defined peak current of chloramine-T.

3- Effect of deposition potential

The influence of deposition potential was studied over the potential range from -100 to -800 mV, Fig. 81. The most suitable deposition potential is -400 mV.

4- Effect of frequency

The effect of frequency on the stripping peak current was recorded within the rang from 100 to 5000 Hz. The most suitable frequency was found at 5000 Hz, Fig. 82.

5- Effect of pulse width

The stripping voltammograms were recorded at different pulse widths, this displayed that the most suitable value for the analytical determination obtained at 200 mV, Fig. 83.

6- Effect of pulse height

The effect of pulse height on the CAdSWSV peak height was studied. The peak current formed is directly proportional to the pulse height, Fig. 84. In the present study, a sharp peak height was obtained at pulse height equals to 200 mV.

7- Effect of deposition time

In the stripping analysis, the height of the formed peak is almost proportional directly to the deposition time t_d till 360 sec, then the current decreases again, this may due to the complet coverage of the electrode surface. On studying the effect of deposition time on the investigated compound, the most suitable t_d equals to 300 sec, Fig. 85.

8- Effect of scan rate

On studying the effect of different scan rates, a scan rate of 1.0 mV/s gave a maximum response, Fig. 86.

3.5.1.2 Quantitative determination of chloramine-T by CAdSWSV

The applicability of the square wave cathodic adsorptive stripping voltammetric technique as an analytical method for the determination of chloramine-T is tested by measuring the CAdSWSV peak current as a function of concentration, Fig. 87.

Calibration graph

A stock solution of chloramine-T 1×10^{-3} M was prepared and different concentrations were obtained by accurate dilution. The CAdSWSV peaks of the final samples were recorded under the optimum experimental conditions. The variation of peak current with concentration is represented Fig. 88. A straight line with slope equal to 7.9×10^4 , intercept equal to 0.0453 and the value of the taken concentration c is determined, Table 53.

The precision was determined from four repeated measurements for different concentrations of the compound under investigation, the mean recovery is 98.98 and the standard deviation were calculated to be ± 0.42

Detection Limit

In the present study, S.D. of the blank is 1.5×10^{-4} and the slope of the calibration graph is 7.9×10^4 , so the detection limit is found to be 5.7×10^{-9} M (1.6×10^{-3} $\mu\text{g/ml}$).

Table 52:

Cathodic adsorptive stripping peak current (i_p) of 1×10^{-6} M chloramine-T in B.R. buffer solution of pH 7.2 at different conditions.

Deposition time t_d , Sec	Deposition potential $-E_d$, mV	Scan rate mV/s	Pulse Height mV	Pulse width mV	i_p μA
Effect of E_d					
300	200	1.0	20	50	0.1437
	400				0.1613
	500				0.1044
	600				0.0540
	800				0.0430
Effect of pulse width					
300	400	1.0	20	200	0.1692
				100	0.1621
				50	0.1613
				20	0.1324
				10	0.1060
Effect of pulse height					
300	400	1.0	200	200	0.1881
			100		0.1805
			50		0.1755
			20		0.1692
			10		0.1212
Effect of t_d					
360	400	1.0	200	200	0.1750
300					0.1881
240					0.1850
120					0.1810
60					0.1779
Effect of scan rate					
300	400	1.0	200	200	0.1881
		2.0			0.1751
		5.0			0.1695
		10.0			0.1691

Table 53:

Assay of chloramine-T in B.R. buffer solution of pH 7.2 using CAdSWSV at:
 $E_d = -400$ mV, $t_d = 300$ sec, scan rate = 1.0 mV/sec, pulse height = 200 mV,
 pulse width = 200 mV and frequency = 5000 Hz.

Conc. Taken M	i _p μA	Conc. Found M	% Recovery %R	Av. Conc. (found) M	Mean %R	S.D
1.0 x 10 ⁻⁶	0.1241	9.975 x 10 ⁻⁶	99.8	1.000 x10 ⁻⁷	99.9	0.12
	0.1241	9.975 x 10 ⁻⁶	99.8			
	0.1243	1.000 x 10 ⁻⁶	100.0			
	0.1243	1.000 x 10 ⁻⁶	100.0			
7.5 x 10 ⁻⁷	0.1048	7.532 x 10 ⁻⁷	100.4	7.509 x 10 ⁻⁷	100.1	0.36
	0.1045	7.494 x 10 ⁻⁷	99.9			
	0.1044	7.481 x 10 ⁻⁷	99.7			
	0.1048	7.532 x 10 ⁻⁷	100.4			
6.0 x 10 ⁻⁷	0.0920	5.911 x 10 ⁻⁷	98.5	5.968 x 10 ⁻⁷	99.5	0.67
	0.0927	6.000 x 10 ⁻⁷	100.0			
	0.0925	5.975 x 10 ⁻⁷	99.6			
	0.0926	5.987 x 10 ⁻⁷	99.8			
3.0 x 10 ⁻⁷	0.0685	2.937 x 10 ⁻⁷	97.9	2.956 x 10 ⁻⁸	98.6	0.75
	0.0688	2.975 x 10 ⁻⁷	99.2			
	0.0688	2.975 x 10 ⁻⁷	99.2			
	0.0685	2.937 x 10 ⁻⁷	97.9			
The mean recovery = 99.53 ± 0.48						
Slope = 7.9 x 10 ⁴						
Intercept = 0.0453						
Corr. Coeff. = 0.9936						

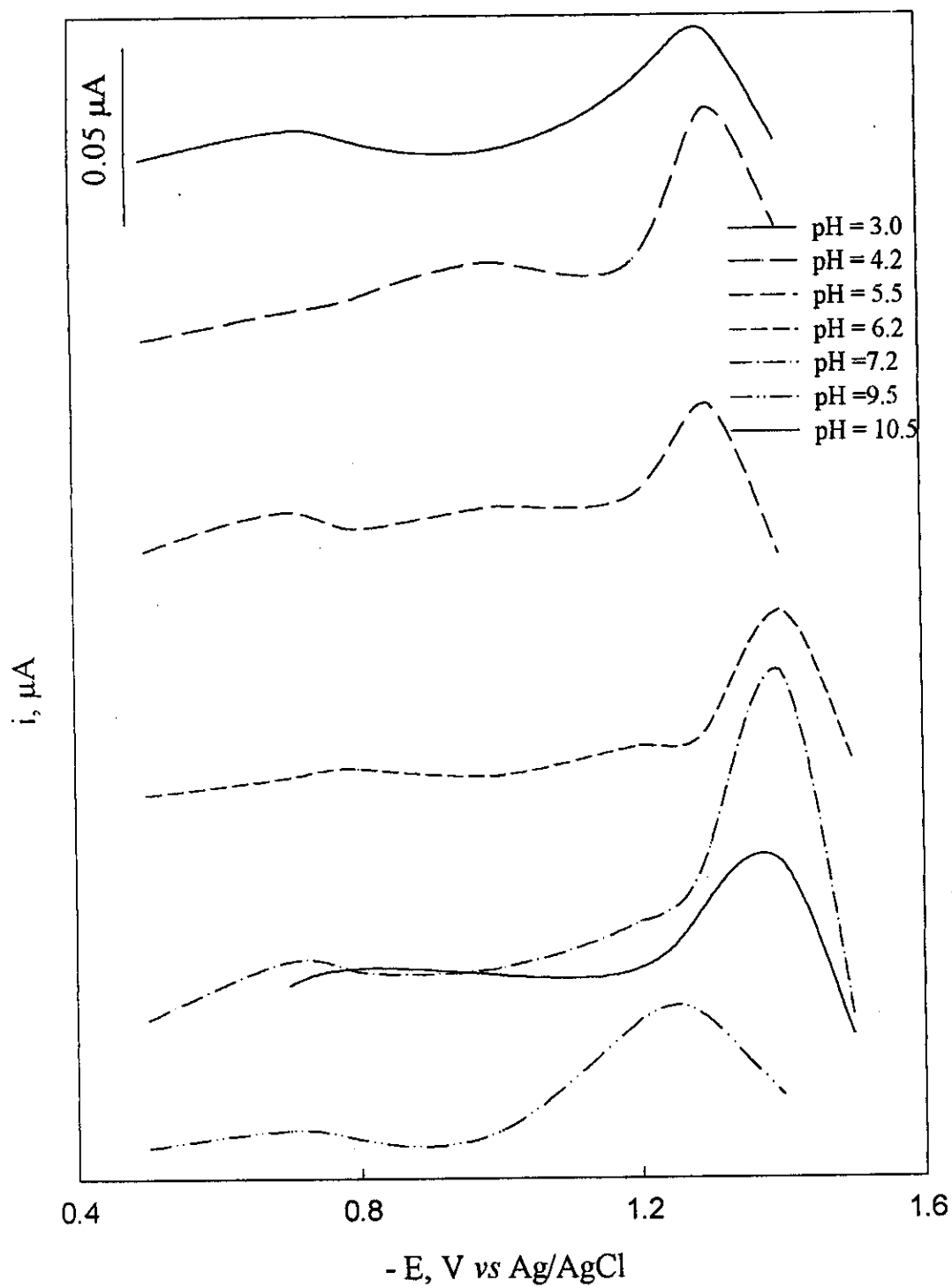


Fig. 79: Effect of pH of B.R. buffer solution on the CAdSWSV of 1×10^{-6} M of chloramine-T; at $E_d = -100$ mV, $t_d = 300$ sec, pulse height = 20 mV, pulse width = 50 mV and frequency = 5000 Hz.

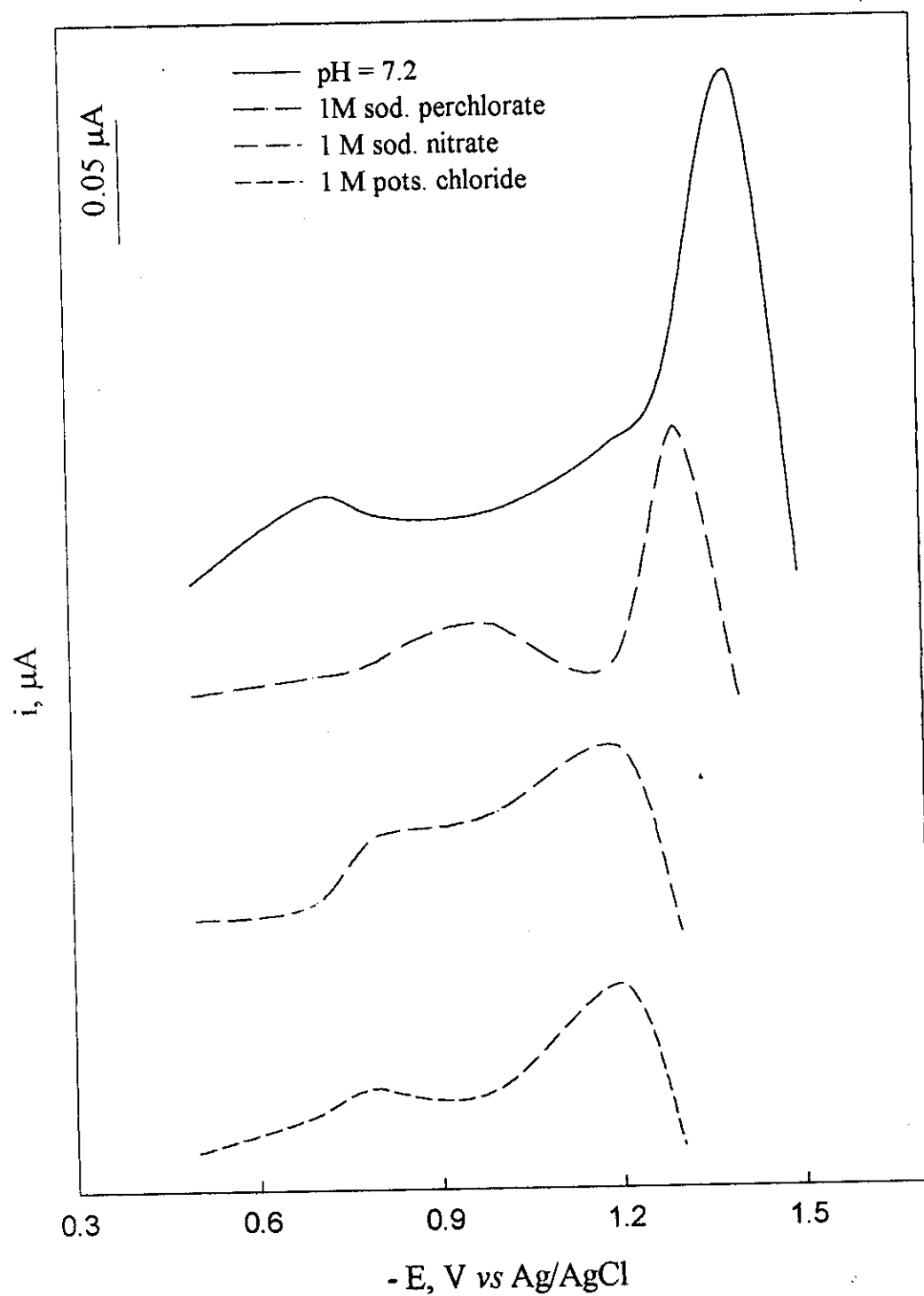


Fig. 80: Effect of supporting electrolyte solutions on the CAdSWSV peak of $1 \times 10^{-6} \text{ M}$ o-chloramin-T at, $E_d = -100 \text{ mV}$, $t_d = 300 \text{ sec}$, scan rate = 1.0 mV/s , pulse width = 50 mV , pulse height = 20 mV and frequency = 5000 Hz .

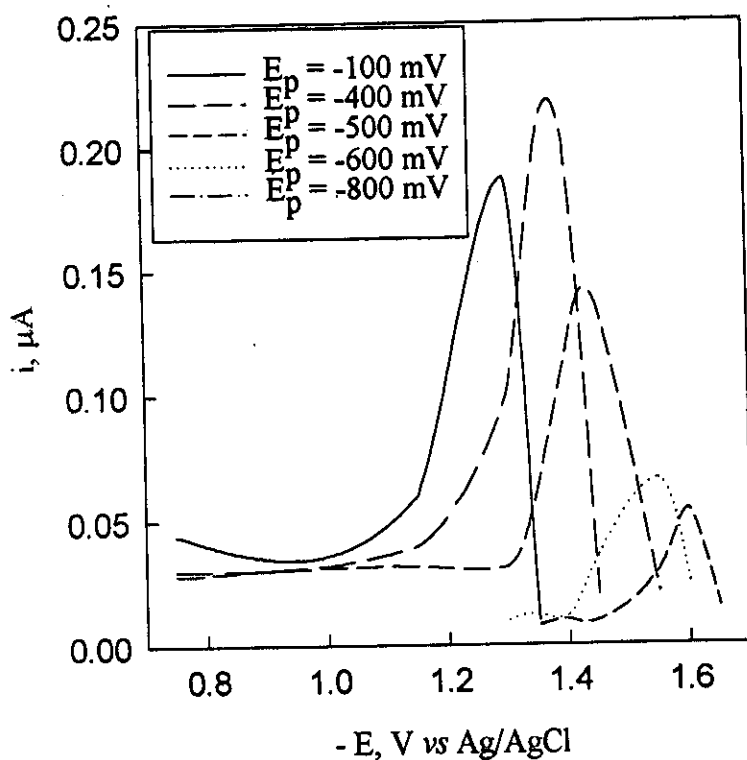


Fig. 81: Effect of E_d on the CAAdSWSV of 1×10^{-6} M of chloramine-T in B.R. buffer solution of pH 7.2 at: $t_d = 300$ sec, scan rate = 1.0 mV/s, pulse width = 50 mV, pulse height = 20 mV and frequency = 5000 Hz.

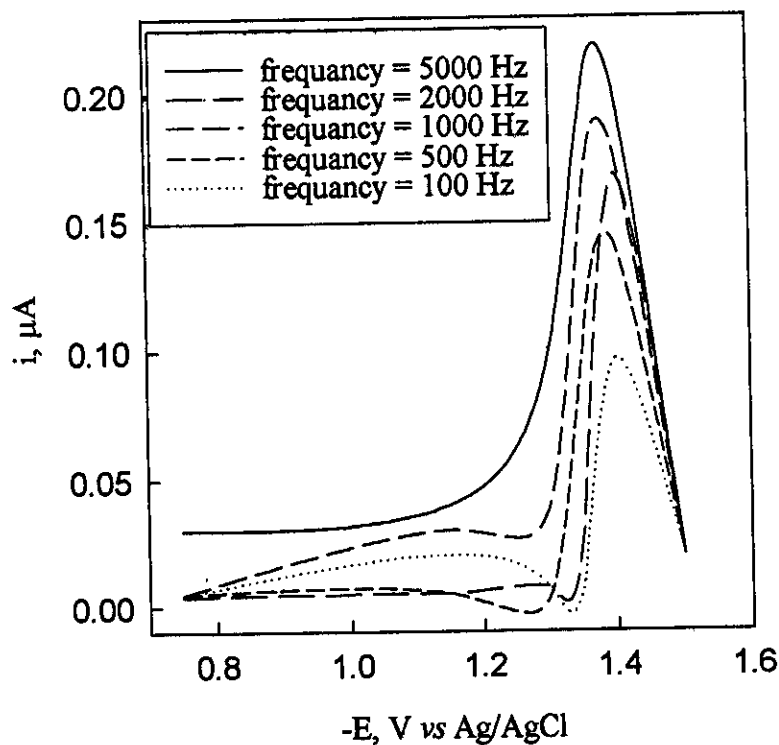


Fig. 82: Effect of E_d on the CAAdSWSV of 1×10^{-6} M of chloramine-T in B.R. buffer solution of pH 7.2 at: $t_d = 300$ sec, scan rate = 1.0 mV/s, pulse width = 50 mV, pulse height = 20 mV and frequency = 5000 Hz.

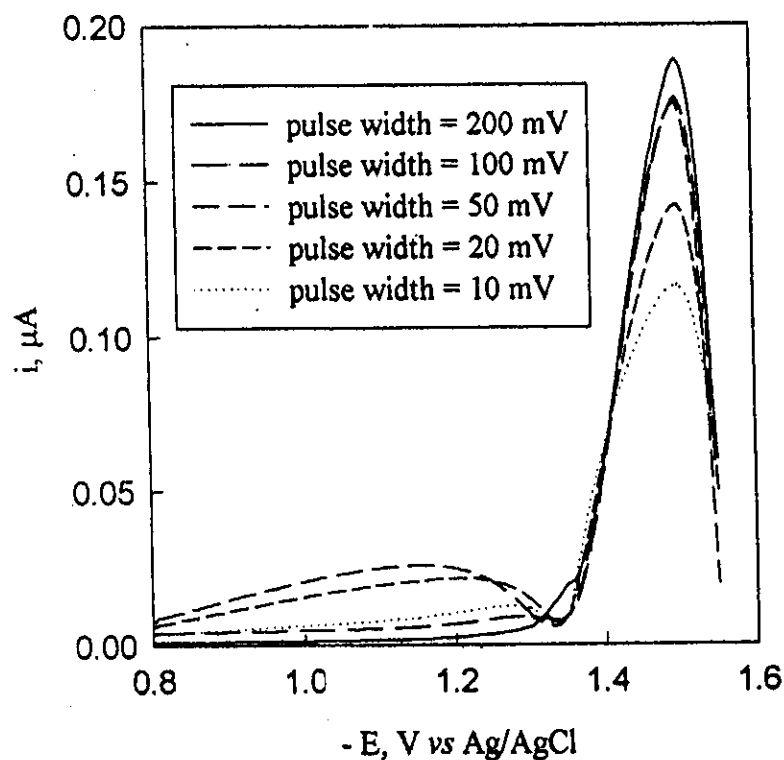


Fig. 83: Effect of pulse width on the CAdSWSV peak of 1×10^{-6} M of chloramine-T in B.R. buffer solution of pH = 7.2, at $E_d = -400$ mV, $t_d = 300$ sec and pulse height = 20 mV.

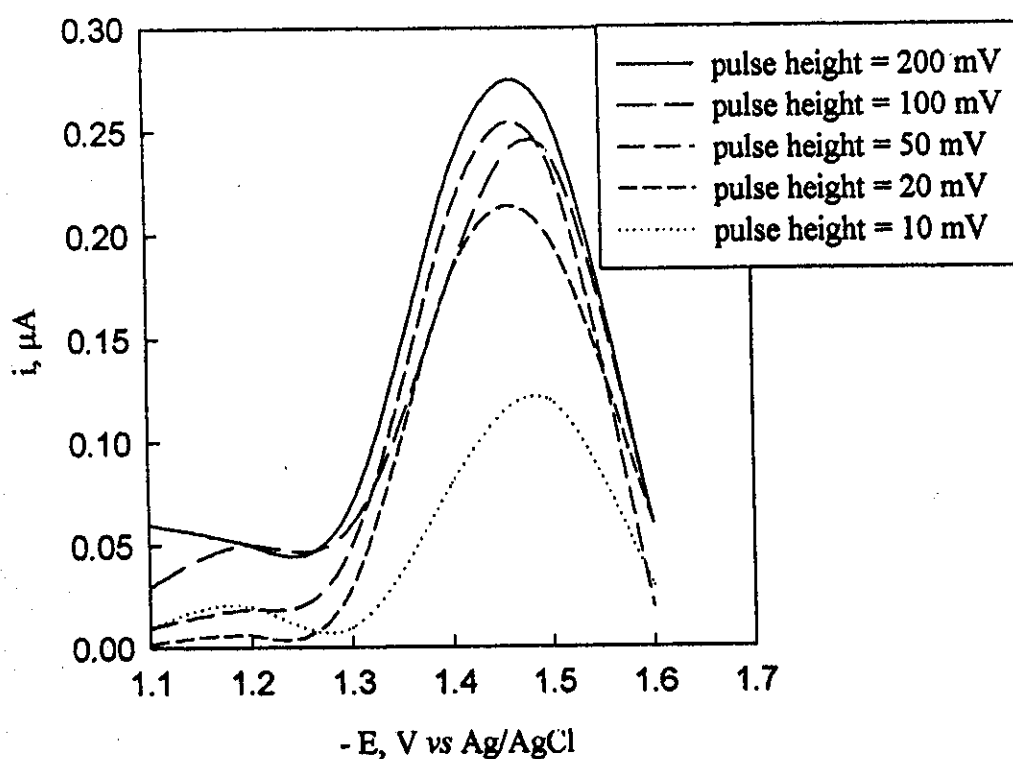


Fig. 84: Effect of pulse height of 1×10^{-6} M of chloramine-T in buffer solution of pH 7.2, at $E_d = -400$ mV, $t_d = 300$ sec, scan rate = 1.0 mV/s, pulse width = 100 mV, and frequency = 5000 Hz.

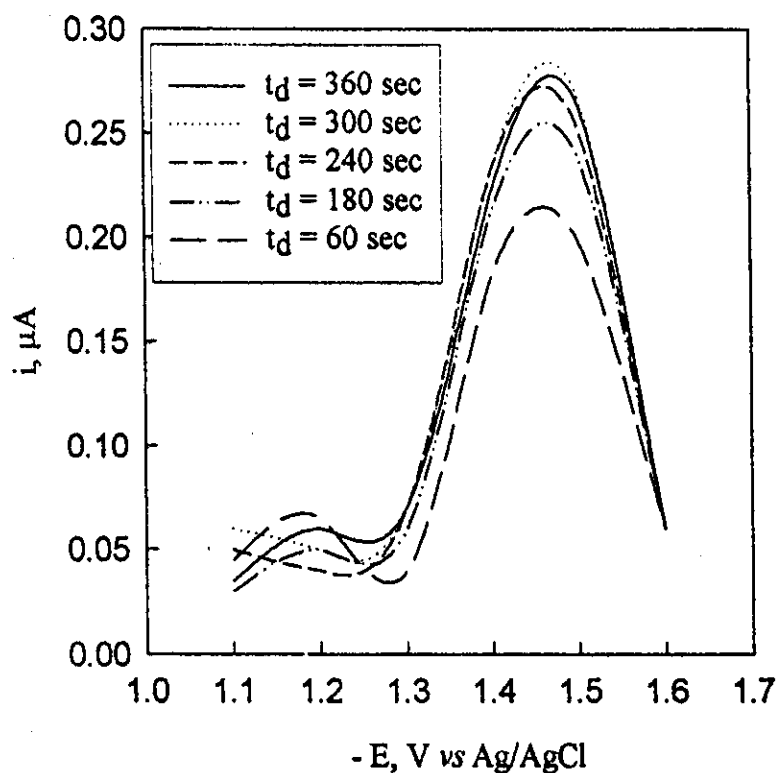


Fig. 85: Effect of t_d on the CAdSWSV peak of 1×10^{-6} M of chloramine-T in B.R. buffer solution of pH 7.2, at $E_d = -400$ mV, scan rate = 1.0 mV/s pulse width = 200 mV and pulse height = 200 mV.

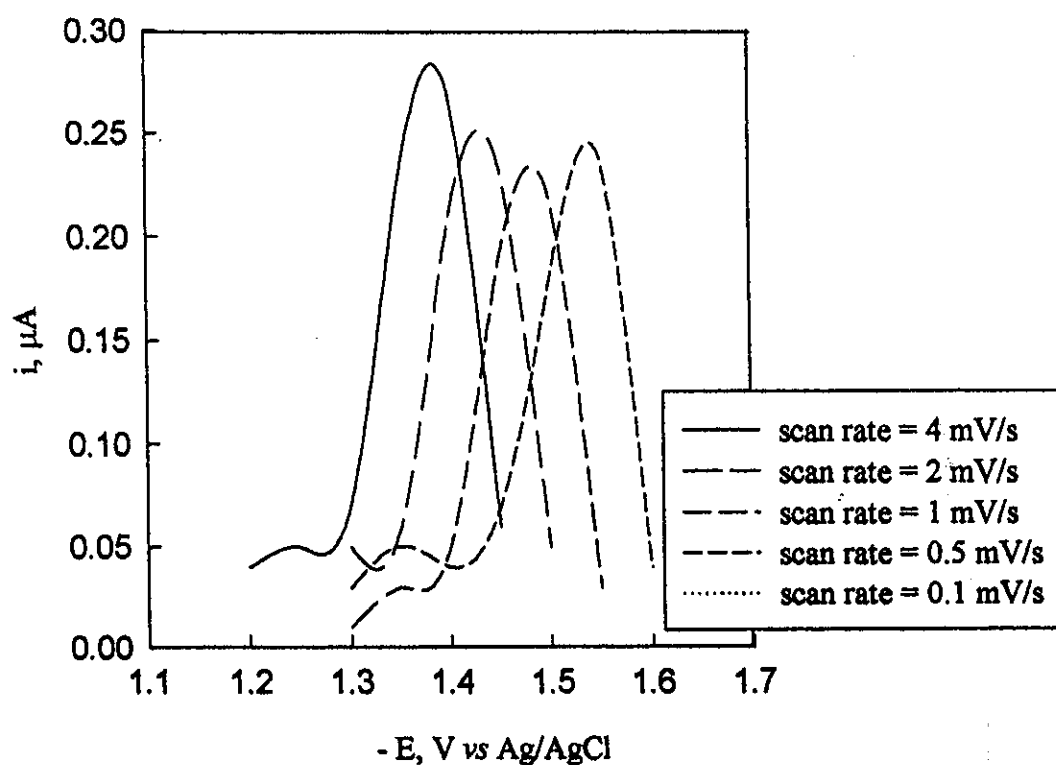


Fig. 86: Effect of scan rate on the CAdSWSV peak of 1×10^{-6} M of chloramine-T in B.R. buffer solution of pH 7.2, at $E_d = -400$ mV, $t_d = 300$ sec, pulse width = 200 mV and pulse height = 200 mV.

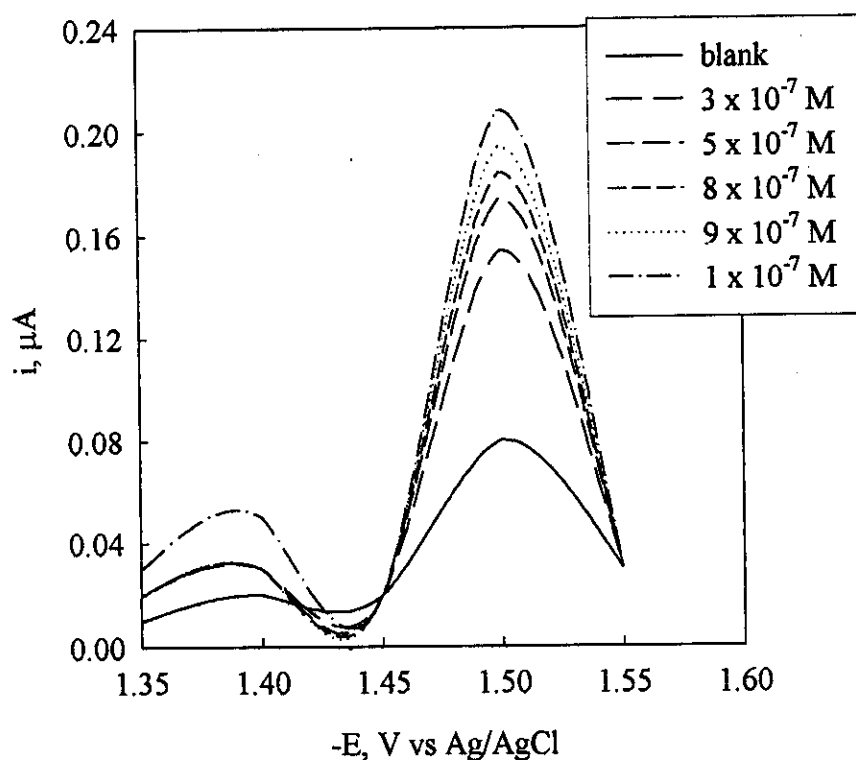


Fig. 87: Different concentrations of chloramine-T in B.R. buffer solution of pH 7.2 at $E_d = -400 \text{ mV}$, $t_d = 300 \text{ sec}$, pulse height = 200 mV, pulse width = 200 mV/s, scan rate = 1.0 mV/s and frequency of 5000 Hz

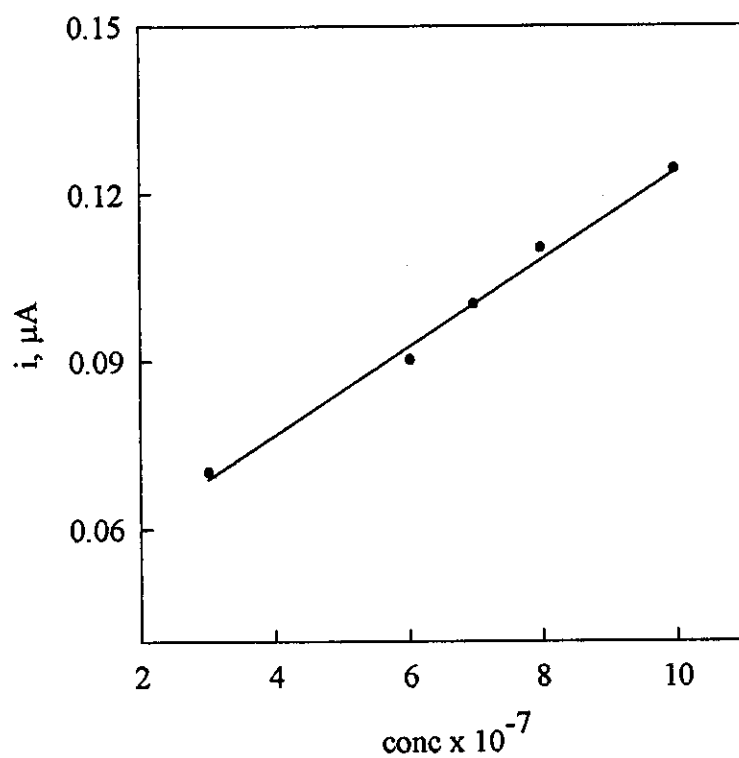


Fig. 88: Calibration curve of chloramine-T